ACS OMEGA

http://pubs.acs.org/journal/acsodf

Article

Highlighting Thermodynamic Coupling Effects in the Immersion Precipitation Process for Formation of Polymeric Membranes

Rajamani Krishna*

Cite This: *ACS Omega* 2020, 5, 2819−2828

Read Online

ACCESS | Metrics & More | Article Recommendations | Supporting Information

ABSTRACT: In the immersion precipitation process for membrane formation, a polymer casting film is placed in contact with a nonsolvent in a coagulation bath; an essential feature of the membrane formation process is the foray into the metastable region of the ternary phase diagram for the nonsolvent/solvent/polymer system. The primary objective of this article is to trace the origins of such forays. The Maxwell−Stefan diffusion formulation is combined with the Flory−Huggins description of phase equilibrium thermodynamics to set up a model for describing the transient equilibration trajectory that is followed in the polymer casting film. Four different systems are analyzed: water/acetone/CA, water/DMF/PVDF, water/NMP/PSF, and water/NMP/PEI (CA = cellulose acetate; PVDF = poly(vinylidene fluoride); PSF = polysulfone; PEI = polyetherimide, DMF = dimethyl formamide; NMP = *N*-methyl-2-pyrrolidone). The analysis shows that diffusional forays are mainly engendered due to thermodynamic coupling effects; such effects are quantified by the set of thermodynamic factors $\Gamma_{ij} = \frac{\phi_i}{\phi_j}\frac{\partial \ln a_i}{\partial \ln \phi_j}$, where a_i, the activity of species i, is dependent on the volume fractions, ϕ_i and ϕ_j, of both nonsolvent (i) and solvent (j). In regions close to phase transitions, the off-diagonal elements $\Gamma_{ij}(i \neq j)$ are often negative and may attain large magnitudes in relation to the diagonal elements Γ_{ii}. Strong thermodynamic coupling effects cause the transient equilibration trajectories to be strongly curvilinear, causing ingress into the metastable region. If thermodynamic coupling effects are ignored, no such ingress occurs. It is also shown that analogous diffusional forays may lead to emulsion formation in partially miscible liquid mixtures.

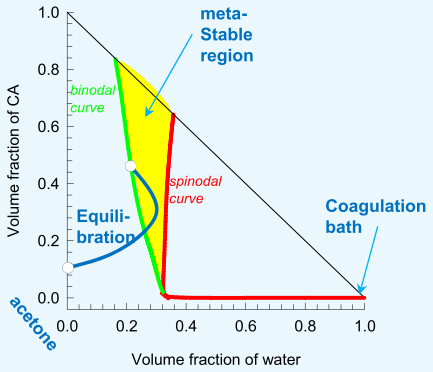

1. INTRODUCTION

The landmark discovery of the asymmetric cellulose acetate (CA) membrane by Loeb and Sourirajan[1] for water desalination has had a significant technological impact on the development of a wide variety of polymer membranes that have several practical applications.[2,3] To set the scene for this article and define its objectives, let us consider the basic principles of the immersion precipitation procedure that was originally used for preparing CA membranes.[3−13] The ternary phase diagram for ternary water/acetone/CA solutions, constructed on the basis of the volume fractions using the Flory−Huggins description of phase equilibrium thermodynamics, is shown in Figure 1. The binodal curve for this ternary mixture defines the limits of phase miscibility; the compositions at the end of a tie-line are in thermodynamic equilibrium requiring equality of component activities, a_i, in the two contiguous fluid phases. The spinodal curve defines the limit of phase stability. Along the spinodal curve, the determinant $|\Gamma| = 0$, where $|\Gamma|$ is a 2×2 dimensional matrix of thermodynamic correction factors with elements defined by

$$\Gamma_{ij} = \frac{\phi_i}{\phi_j}\frac{\partial \ln a_i}{\partial \ln \phi_j};\ i, j = 1, 2 \tag{1}$$

where ϕ_i and ϕ_j denote the volume fractions of water and acetone, respectively.[14,15]

The inset to Figure 1 is a schematic of the immersion precipitation process in which a thin layer of casting film of the acetone/CA mixture, placed on a support layer, is brought into contact with water in a coagulation bath. As illustrated, the transient equilibration trajectory when a 10% solution of CA in acetone is immersed in the coagulation bath is indicated by the solid blue line connecting A and A*. With increasing immersion contact times, the compositions within the polymer casting film will get progressively richer in water and impoverished in acetone.[3,5,6,12,13] Consequently, the equilibration trajectories get progressively closer to the binodal curve. Figure 1 plots the

Received: October 27, 2019
Accepted: January 27, 2020
Published: February 10, 2020

https://dx.doi.org/10.1021/acsomega.9b03609
ACS Omega 2020, 5, 2819−2828

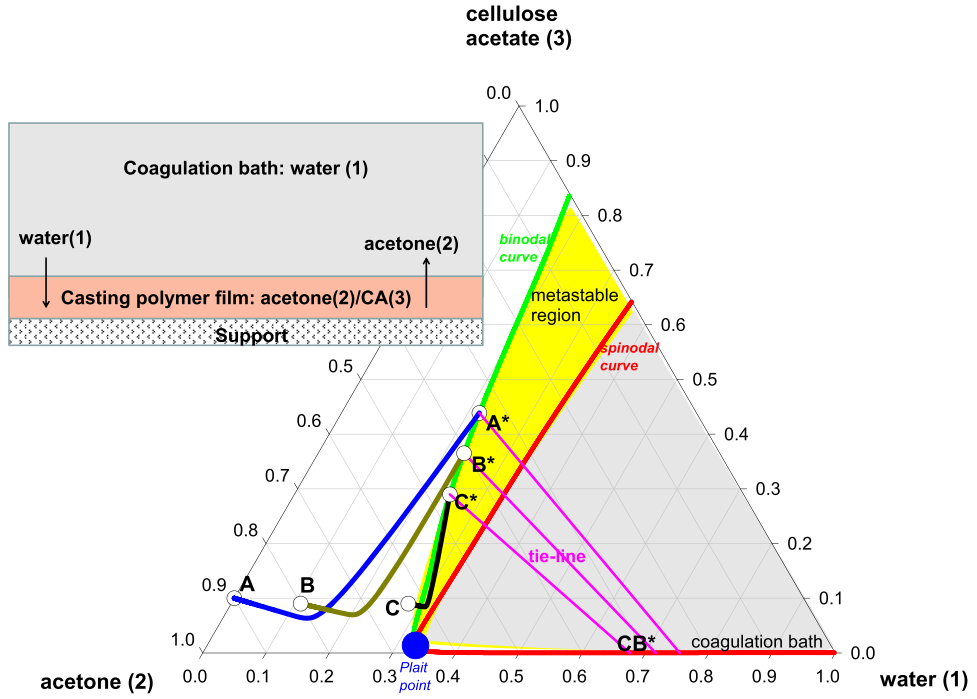

Figure 1. Transient equilibration trajectories A−A*, B−B*, and C−C* during the immersion precipitation process for membrane preparation. These trajectories were determined from simulations using the starting compositions A, B, and C in the polymer casting film. Further calculation details and data inputs are provided in the Supporting Information (SI) accompanying this publication.

progression in the equilibration trajectories A−A*, B−B*, and C−C* with increasing immersion times. All three trajectories are strongly curvilinear. Particularly noteworthy is that the trajectory C−C* has penetrated into the metastable region between the binodal and spinodal curves. This foray into the metastable region causes precipitation of polymer in the casting film. Experimental evidence of such forays is provided by McHugh and Tsay.[16]

The primary objective of this article is to trace the theoretical origins of the diffusional foray into the metastable region as witnessed for the trajectory C−C*. For this purpose, we set up a model to describe the equilibration trajectories by combining the Flory−Huggins description of phase equilibrium with the Maxwell−Stefan formulations for diffusion.[17−21] By detailed analysis of four different systems: water/acetone/CA, water/DMF/PVDF, water/NMP/PSF, and water/NMP/PEI (CA = cellulose acetate; PVDF = poly(vinylidene fluoride); PSF = polysulfone; PEI = polyetherimide; DMF = dimethyl formamide; NMP = *N*-methyl-2-pyrrolidone), we aim to show that the diffusional forays into metastable regions are primarily engendered by thermodynamic coupling effects that are quantified by the off-diagonal elements $\Gamma_{ij}(i \neq j)$. The secondary objective of this article is to demonstrate that the same concepts and modeling approaches are applicable to describe diffusion-induced ingress into metastable regions, resulting in emulsification[22−24] and production of nanospheres and nanoparticles by the exploitation of the "Ouzo effect".[25−27]

2. RESULTS AND DISCUSSIONS

2.1. Maxwell−Stefan Formulation for Diffusion in Ternary Polymer Solutions. For a description of diffusion in ternary nonsolvent (1)/solvent (2)/polymer (m) solutions, it is convenient to use volume fractions, ϕ_i, as composition measures because this facilitates combination with the Flory−Huggins description of phase equilibrium. Let us define the volumetric diffusion fluxes J_i^V, relative to the volume average velocity of the mixture $u^V = \phi_1 u_1 + \phi_2 u_2 + \phi_m u_m$.

$$J_i^V = \phi_i(u_1 - u^V);\ \ i = 1, 2$$
$$J_m^V = \phi_m(u_m - u^V) = -J_1^V - J_2^V \tag{2}$$

The volume fractions are related to the molar concentrations, $\phi_i = c_i \bar{V}_i$, where $\bar{V}_i$ is the partial molar volume of species *i*. The use of u^V as a reference velocity is particularly convenient for polymeric solutions because $\bar{V}_i$ is practically composition independent.

In the Maxwell−Stefan (M−S) formulation, the volumetric diffusion fluxes, J_i^V, expressed in the units $m^3\ m^{-2}\ s^{-1}$, are related to the chemical potential gradients as follows[17,18,20]

$$-\phi_1 \frac{1}{RT}\frac{\partial \mu_1}{\partial z} = \frac{(\phi_2 J_1^V - \phi_1 J_2^V)}{Đ_{12}^V} + \frac{(\phi_m J_1^V - \phi_1 J_m^V)}{Đ_{1m}^V}$$
$$-\phi_2 \frac{1}{RT}\frac{\partial \mu_2}{\partial z} = \frac{(\phi_1 J_2^V - \phi_2 J_1^V)}{Đ_{21}^V} + \frac{(\phi_m J_2^V - \phi_2 J_m^V)}{Đ_{2m}^V} \tag{3}$$

The M−S diffusivities, $Đ_{1m}^V$ and $Đ_{2m}^V$, quantifying interactions ("friction") between species 1 and 2 with the polymer chains are relatable to the self-diffusivities in polymer solutions, for which estimation procedures using the free-volume theory are well established.[28−30] The M−S diffusivities $Đ_{12}^V$ and $Đ_{21}^V$, appearing in the first right members of eq 3, quantify the 1−2 friction. The symmetry constraint demanded by the Onsager reciprocal relations is

$$\frac{Đ_{21}^V}{\bar{V}_1} = \frac{Đ_{12}^V}{\bar{V}_2} \tag{4}$$

The M−S diffusivities $Đ_{12}^V$ and $Đ_{21}^V$ are relatable to the M−S diffusivities in binary nonsolvent/solvent solutions for which reliable estimation procedures are available in the litera-

https://dx.doi.org/10.1021/acsomega.9b03609
ACS Omega 2020, 5, 2819−2828

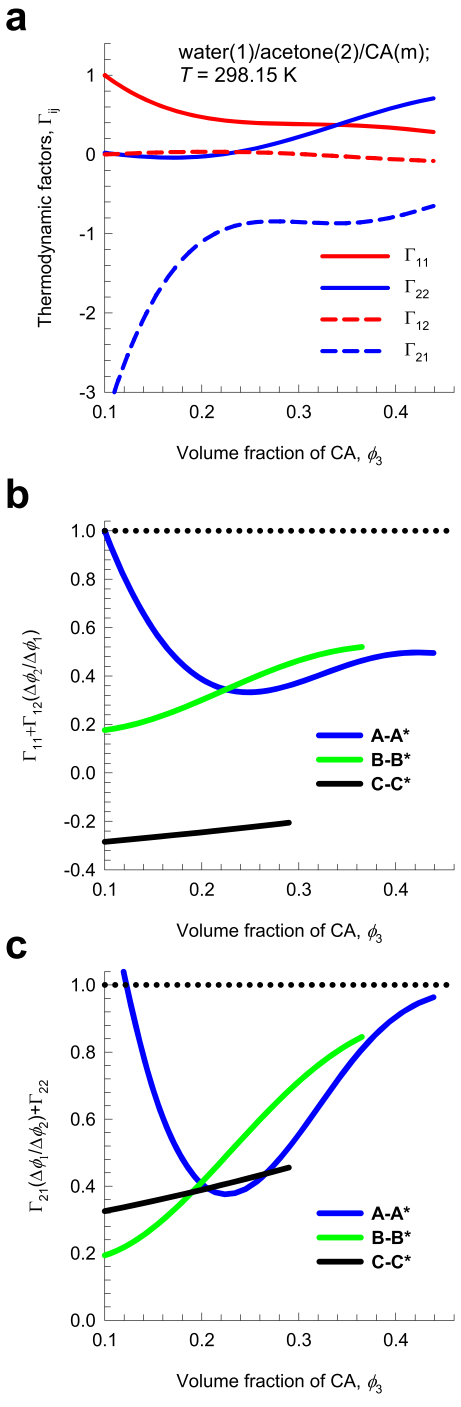

Figure 2. (a) Calculations for the matrix of thermodynamic correction factors, Γ_{ij}. (b, c) Calculations of (b) $\Gamma_{11} + \Gamma_{12}$ $(\Delta\phi_2/\Delta\phi_1)$ and (c) Γ_{21} $(\Delta\phi_1/\Delta\phi_2)$ for volume fractions along a straight line connecting A−A*, B−B*, and C−C* in Figure 1. Further calculation details and data inputs are provided in the Supporting Information accompanying this publication.

ture.[14,15,31,32] Detailed derivations of eq 3, including comparison with the equivalent Bearman friction formulation,[28,30,33,34] along with step-by-step procedures for estimation of the set of M−S diffusivities are provided in the Supporting Information (SI) accompanying this publication.

In view of eq 1, the left members of eq 3 can be expressed in terms of the gradients in the volume fractions

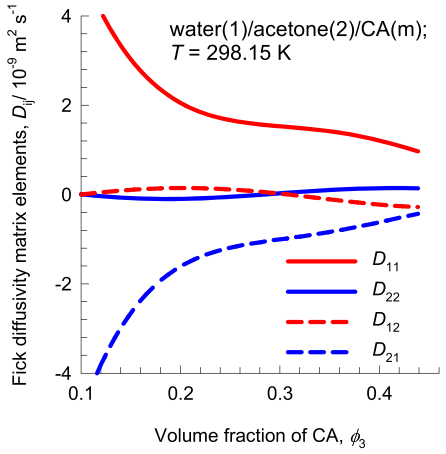

Figure 3. Elements of the Fick diffusivity matrix $[D]$, for water (1)/acetone (2)/CA (m) at T = 298.15 K. Further calculation details and data inputs are provided in the Supporting Information accompanying this publication.

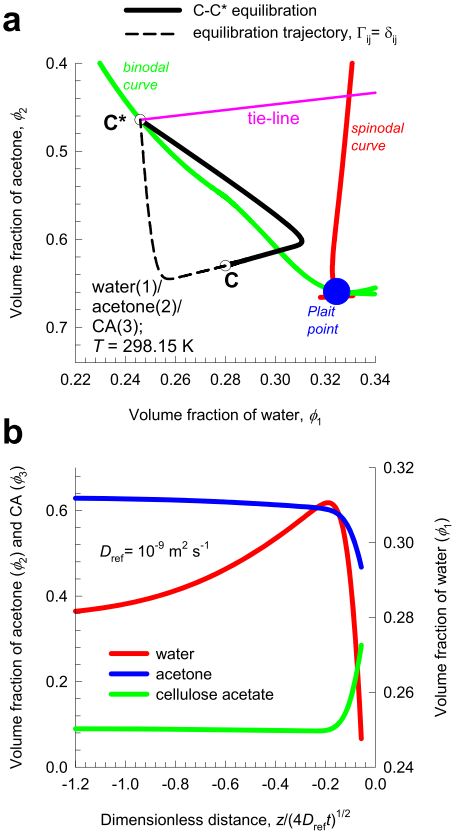

Figure 4. (a) Transient equilibration trajectory C−C* in the water/acetone/casting film. The dashed lines represent simulation results when the simplification $\Gamma_{ij} = \delta_{ij}$, the Kronecker delta, is invoked. (b) Transient volume fraction profiles in the casting solution, as a function of the dimensionless distance coordinate $z/\sqrt{4D_{ref}t}$. Further calculation details and data inputs are provided in the Supporting Information accompanying this publication.

$$\frac{\phi_i}{RT}\frac{\partial \mu_i}{\partial z} = \phi_i \frac{\partial \ln a_i}{\partial z} = \sum_{j=1}^{2} \Gamma_{ij}\frac{\partial \phi_j}{\partial z};\ i, j = 1, 2 \tag{5}$$

For the system water (1)/acetone (2)/CA (3), Figure 2a shows calculations of the four elements Γ_{ij} as a function of the volume

https://dx.doi.org/10.1021/acsomega.9b03609
ACS Omega 2020, 5, 2819−2828

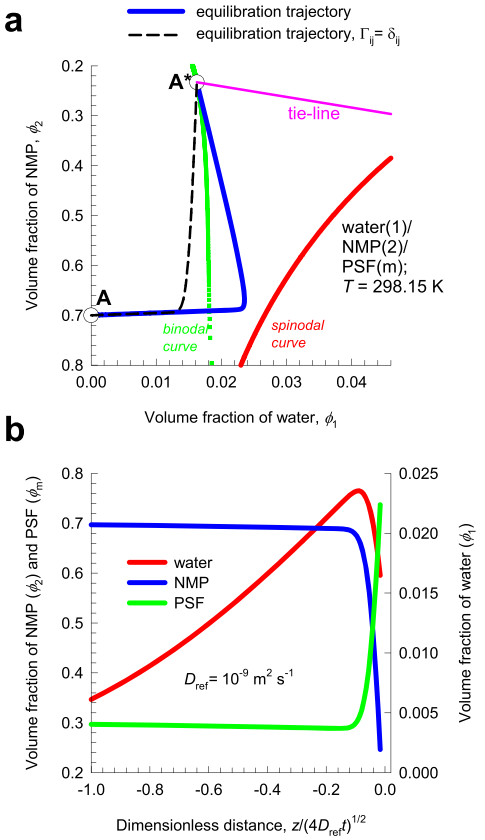

Figure 5. (a) Transient equilibration trajectory A−A* water/NMP/PSF casting film. (b) Transient volume fraction profiles in the casting solution, as a function of the dimensionless distance coordinate $z/\sqrt{4D_{ref}t}$. Further calculation details and data inputs are provided in the Supporting Information accompanying this publication.

fractions of CA that lie on a straight line connecting A ($\phi_{10} = 0.2181$; $\phi_{20} = 0.34308$) with A* ($\phi_{1I} = 0.2181$; $\phi_{2I} = 0.34308$) in Figure 1. Particularly noteworthy are the large negative values of Γ_{21}. Γ_{ij} factors have the effect of influencing the driving forces for the transport of water (1) and acetone (2), into and away from the casting film. Thermodynamic coupling effects on the driving forces for water and acetone transport may be quantified by the factors $\Gamma_{11} + \Gamma_{12}\,(\Delta\phi_2/\Delta\phi_1)$ and $\Gamma_{21}\,(\Delta\phi_1/\Delta\phi_2) + \Gamma_{22}$, where $\Delta\phi_i$ denotes the difference between the interfacial volume fractions, ϕ_{iI}, and those at the start of the equilibration process, ϕ_{i0}

$$\Delta\phi_1 = \phi_{1I} - \phi_{10};\quad \Delta\phi_2 = \phi_{2I} - \phi_{20} \tag{6}$$

These terms are plotted in Figure 2b,c for volume fractions along straight lines connecting A−A*, B−B*, and C−C*. In all three cases, the influence of thermodynamic coupling is to suppress both the driving forces of water and acetone. If thermodynamic coupling effects are ignored by invoking the assumption $\Gamma_{ij} = \delta_{ij}$, the Kronecker delta, both these factors should be unity. Remarkably, we note that for C−C* equilibration, thermodynamic coupling serves not only to reduce the magnitude of the driving force for water transport but also to reverse its sign. The precise consequences of such sign reversals will be elaborated in a later section.

Combining eqs 3 and 5 and casting into matrix notation, we obtain

$$-[\Gamma]\frac{\partial}{\partial z}\begin{pmatrix}\phi_1\\ \phi_2\end{pmatrix} = \begin{bmatrix}\dfrac{\phi_1}{\mathcal{D}_{1m}^{V}} + \dfrac{\phi_2}{\mathcal{D}_{12}^{V}} + \dfrac{\phi_m}{\mathcal{D}_{1m}^{V}} & -\phi_1\left(\dfrac{1}{\mathcal{D}_{12}^{V}} - \dfrac{1}{\mathcal{D}_{1m}^{V}}\right)\\ -\phi_2\left(\dfrac{1}{\mathcal{D}_{21}^{V}} - \dfrac{1}{\mathcal{D}_{2m}^{V}}\right) & \dfrac{\phi_1}{\mathcal{D}_{21}^{V}} + \dfrac{\phi_2}{\mathcal{D}_{2m}^{V}} + \dfrac{\phi_m}{\mathcal{D}_{2m}^{V}}\end{bmatrix}\begin{pmatrix}J_1^{V}\\ J_2^{V}\end{pmatrix} = [B]\begin{pmatrix}J_1^{V}\\ J_2^{V}\end{pmatrix} \tag{7}$$

Premultiplying eq 7 by $[B]^{-1}$, we can explicitly relate the diffusion fluxes to the gradients in the volume fractions

$$\begin{pmatrix}J_1^{V}\\ J_2^{V}\end{pmatrix} = -[D]\frac{\partial}{\partial z}\begin{pmatrix}\phi_1\\ \phi_2\end{pmatrix};\quad [D] = [B]^{-1}[\Gamma] \tag{8}$$

Equation 8 also serves to define the 2 × 2 dimensional square matrix of Fick diffusivities $[D]$, which is a product of two square matrices $[B]^{-1}$ and $[\Gamma]$. Generally speaking, the off-diagonal contributions of each of the two matrices, $[B]^{-1}$ and $[\Gamma]$ are non-negligible; consequently, molecular diffusion in ternary polymer solutions is a strongly coupled process.

Figure 3 shows calculations of the elements of the Fick diffusivity matrix $[D]$ for volume fractions that lie on a straight line connecting A with A* in Figure 1. The variation of the four elements of $[D]$ with the volume fraction of CA shows approximately the same trends as the corresponding elements of the matrix of thermodynamic factors $[\Gamma]$ in Figure 2a. The large negative value of the off-diagonal element D_{21} is largely engendered by the corresponding negative off-diagonal element Γ_{21}.

2.2. Modeling Transient Diffusion in the Immersion Precipitation Process. To meet the objectives of this article, we seek an analytic solution to describe the immersion precipitation transience and essentially follow the model of Tsay and McHugh.[13] The diffusion process is considered to be essentially uni-(z)-directional; the position $z = 0$ corresponds to the position of the interface at the start of the equilibration process. The contiguous immiscible phases, coagulation bath and polymer casting film, are both considered to be semi-infinite. At the position $z = +\infty$, the composition corresponds to that of the bulk coagulation bath that is time-invariant. At the position $z = -\infty$, the composition corresponds to that of the polymer casting film that is in contact with the support layer; this composition is also time-invariant. At any time t, during the immersion precipitation process, we have thermodynamic equilibrium at the interface between the two immiscible phases, at compositions A* and CB*. The volume fractions ϕ_{iI} and ϕ_{1bI} are determined by the thermodynamic equilibrium constraints

$$a_{1I} = a_{1bI};\quad a_{2I} = a_{2bI} \tag{9}$$

The Flory−Huggins (F−H) description of phase equilibrium thermodynamics[17−19,35−37] is used to solve the set of eq 9; calculation details and F−H input parameters for all investigated systems are provided in the SI.

The transient ternary diffusion within the polymer casting film is described by a set of two coupled partial differential equations

https://dx.doi.org/10.1021/acsomega.9b03609
ACS Omega 2020, 5, 2819−2828

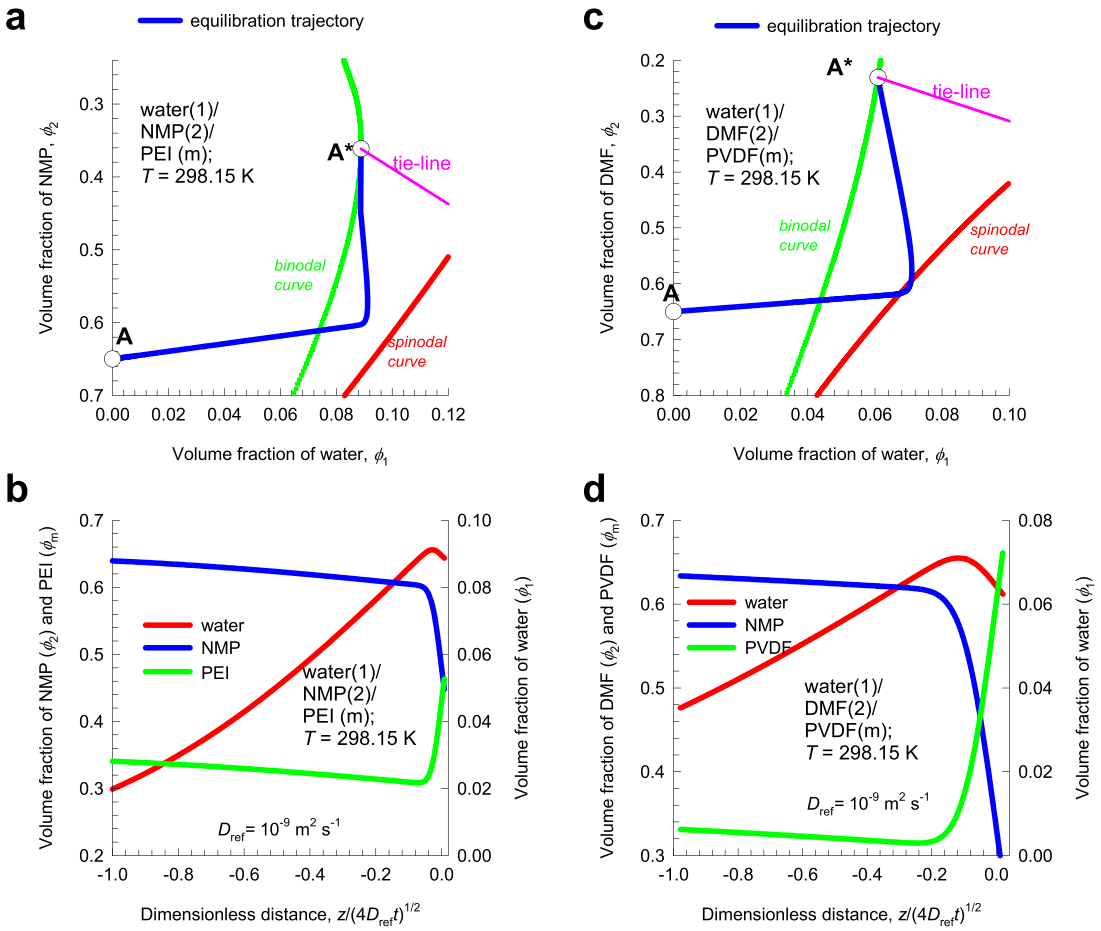

Figure 6. (a, b) Transient equilibration in the water/NMP/PEI casting film. (c, d) Transient equilibration in the water/DMF/PVDF casting film. Further calculation details and data inputs are provided in the Supporting Information accompanying this publication.

$$\frac{\partial\begin{pmatrix}\phi_1\\ \phi_2\end{pmatrix}}{\partial t} = -\frac{\partial\begin{pmatrix}J_1^V\\ J_2^V\end{pmatrix}}{\partial z} \tag{10}$$

Inserting eq 8 for the volumetric fluxes results in

$$\frac{\partial\begin{pmatrix}\phi_1\\ \phi_2\end{pmatrix}}{\partial t} = [D]\frac{\partial^2\begin{pmatrix}\phi_1\\ \phi_2\end{pmatrix}}{\partial z^2} \tag{11}$$

Commonly, the coagulation bath consists of a binary mixture of nonsolvent (1) and solvent (2). As a good approximation, the composition of the coagulation bath may be assumed to be polymer-free. The corresponding relation for the transient diffusion process in the coagulation bath is described by

$$\frac{\partial\phi_{1b}}{\partial t} = D_b\frac{\partial^2\phi_{1b}}{\partial z^2} \tag{12}$$

The subscript b in eq 12 refers to the coagulation bath, and D_b represents the Fick diffusivity in the binary solution in the bath.

The initial conditions for eqs 11 and 12 are

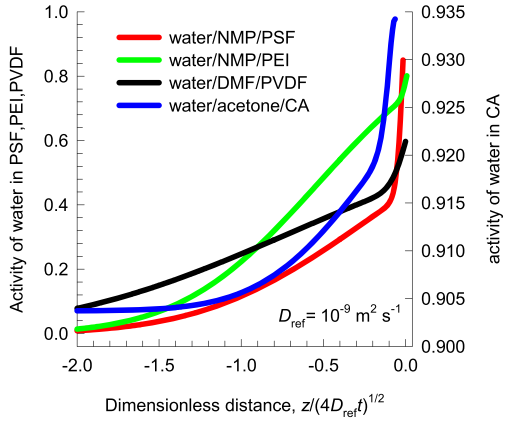

Figure 7. Transient profiles of water activity in the casting solution for water/acetone/CA, water/NMP/PSF, water/NMP/PEI, and water/DMF/PVDF plotted as a function of the dimensionless distance coordinate $z/\sqrt{4D_{ref}t}$.

$$z \geq 0,\ t = 0, \quad \begin{pmatrix}\phi_1(z,0)\\ \phi_2(z,0)\end{pmatrix} = \begin{pmatrix}\phi_{10}\\ \phi_{20}\end{pmatrix}$$

$$z \leq 0,\ t = 0, \quad \phi_{1b}(z,0) = \phi_{1b0} \tag{13}$$

where ϕ_{i0} and ϕ_{1b0} are the initial compositions of the polymer casting film and bath, respectively.

https://dx.doi.org/10.1021/acsomega.9b03609
ACS Omega 2020, 5, 2819−2828

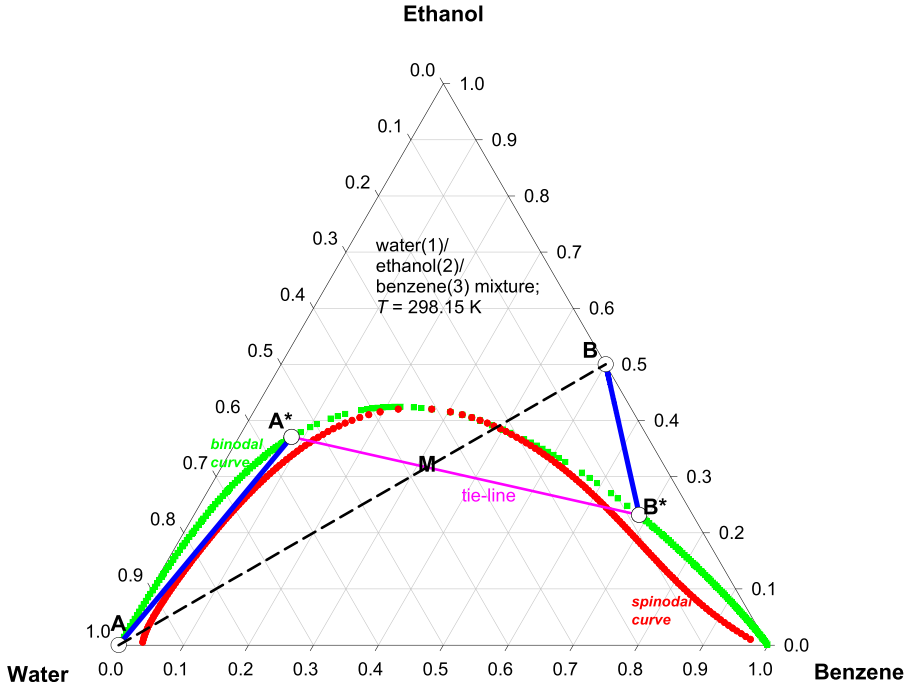

Figure 8. Transient equilibration trajectories A−A* and B−B* for the water/ethanol/benzene mixture at 298 K, demonstrating foray into the metastable region in the water-rich region of the phase diagram. The solid blue lines represent the trajectories calculated using the Ruschak−Miller model. Further calculation details and data inputs are provided in the Supporting Information accompanying this publication.

The boundary conditions are

$$z = -\infty, \quad t \geq 0, \quad \begin{pmatrix} \phi_1(-\infty, t) \\ \phi_2(-\infty, t) \end{pmatrix} = \begin{pmatrix} \phi_{10} \\ \phi_{20} \end{pmatrix}$$

$$z = +\infty, \quad t \geq 0, \quad \phi_{1b}(+\infty, t) = \phi_{1b0} \tag{14}$$

An analytic solution for the transient volume fractions in the bath is obtained if the Fick diffusivity D_b is assumed to be composition independent[13,38]

$$\phi_{1b}(z, t) = \phi_{1b0} + \frac{\text{erfc}\left(\frac{z}{\sqrt{4D_b t}}\right)}{\text{erfc}\left(\frac{r}{\sqrt{4D_b}}\right)}(\phi_{1bI} - \phi_{1b0}) \tag{15}$$

The corresponding analytic expression for the volume fractions in the polymer casting film is also derivable if the Fick diffusivity matrix $[D] = [B]^{-1}[\Gamma]$ is also assumed to be composition independent; see Taylor and Krishna.[31] In all of the calculations presented in this article, the Fick $[D]$ is evaluated at the average volume fractions $\frac{1}{2}\begin{pmatrix} \phi_{10} + \phi_{1I} \\ \phi_{20} + \phi_{2I} \end{pmatrix}$; this linearization procedure has been established to yield results of good accuracy.[18] The transient volume fractions in the polymer film can be written as 2 × 2 dimensional matrix generalization of eq 15; see Taylor and Krishna[31] for further theoretical background on matrix generalization procedures

$$\begin{pmatrix} \phi_1(z, t) \\ \phi_2(z, t) \end{pmatrix} = \begin{pmatrix} \phi_{10} \\ \phi_{20} \end{pmatrix} + \left[\text{erfc}\left(-\frac{z}{\sqrt{4t}}[D]^{-1/2}\right)\right] \left[\text{erfc}\left(-\frac{r}{2}[D]^{-1/2}\right)\right]^{-1} \begin{pmatrix} \phi_{1I} - \phi_{10} \\ \phi_{2I} - \phi_{20} \end{pmatrix} \tag{16}$$

Due to interchange of nonsolvent and solvent between the polymer casting film and the bath, the position of the interface, $\varepsilon(t) = r\sqrt{t}$, will shift with time

$$\begin{pmatrix} \phi_1(\varepsilon(t), t) \\ \phi_2(\varepsilon(t), t) \end{pmatrix} = \begin{pmatrix} \phi_{1I} \\ \phi_{2I} \end{pmatrix}; \quad \phi_{3I} = 1 - \phi_{1I} - \phi_{2I}$$

$$\phi_{1b}(\varepsilon(t), t) = \phi_{1bI} = 1 - \phi_{2bI} \tag{17}$$

In eq 17, $\varepsilon(t) = r\sqrt{t}$ is the position of the moving interface, and r is a constant with units of m $s^{-1/2}$, which is determinable from the continuity of component fluxes at either side of the moving interface

$$J_i^V|_{z=\varepsilon(t)} - J_{ib}^V|_{z=\varepsilon(t)} = (\phi_{iI} - \phi_{ibI})\frac{d\varepsilon(t)}{dt} = (\phi_{iI} - \phi_{ibI})\frac{r}{2\sqrt{t}}; \quad i = 1, 2 \tag{18}$$

The simultaneous solution of the set of four nonlinear eqs 9 and 18 allows calculation of the interfacial compositions ϕ_{1I}, ϕ_{2I}, ϕ_{1bI}, and r.

2.3. Simulations of Four Immersion Precipitation Processes. First, we investigate in detail the C−C* equilibration trajectory followed in the water/acetone/CA casting film when the initial volume fractions in the casting film are chosen as $\phi_{10} = 0.28$; $\phi_{20} = 0.63$; $\phi_{1b0} = 0.75$; and $\phi_{2b0} = 0.25$; corresponding to the position C indicated in Figure 1. The simultaneous solution of the equations describing thermodynamic equilibrium at the interface (eq 9) and the flux continuity relations (eq 18) results in the interfacial volume fractions $\phi_{1I} = 0.24596$; $\phi_{2I} = 0.46422$; and $\phi_{1bI} = 0.6753$; these correspond to C* and CB*. The value of $r = -3.46302 \times 10^{-6}$ is negative because of the shrinkage of the polymer casting film due to the impoverishment of acetone. Evaluated at the arithmetic average volume fractions between the initial and final equilibrated

https://dx.doi.org/10.1021/acsomega.9b03609
ACS Omega 2020, 5, 2819−2828

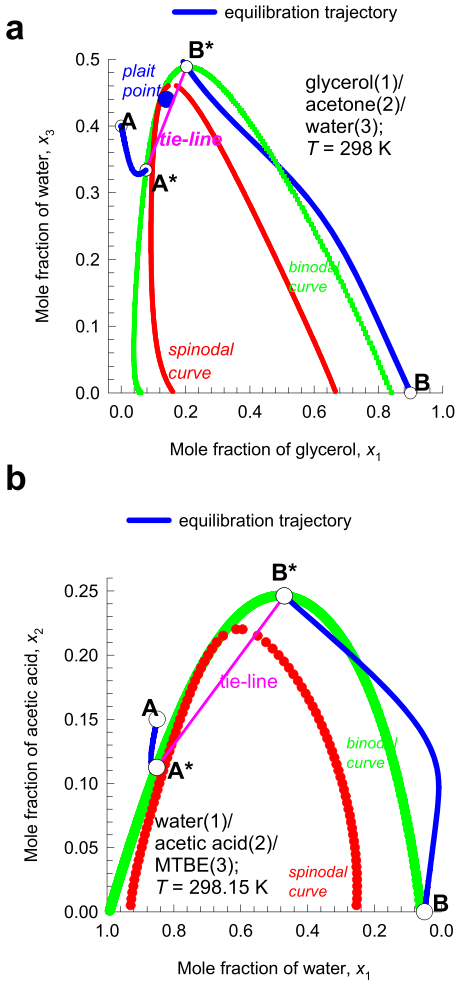

Figure 9. (a) Transient equilibration trajectories for the glycerol (1)/acetone (2)/water (3) mixture at 298 K, demonstrating foray into the meta-region in the glycerol-rich phase. (b) Transient equilibration trajectories for the system water (1)/acetic acid (2)/MTBE (3) at 298 K, demonstrating forays into the metastable region in the MTBE-rich phase. Further calculation details and data inputs are provided in the Supporting Information accompanying this publication.

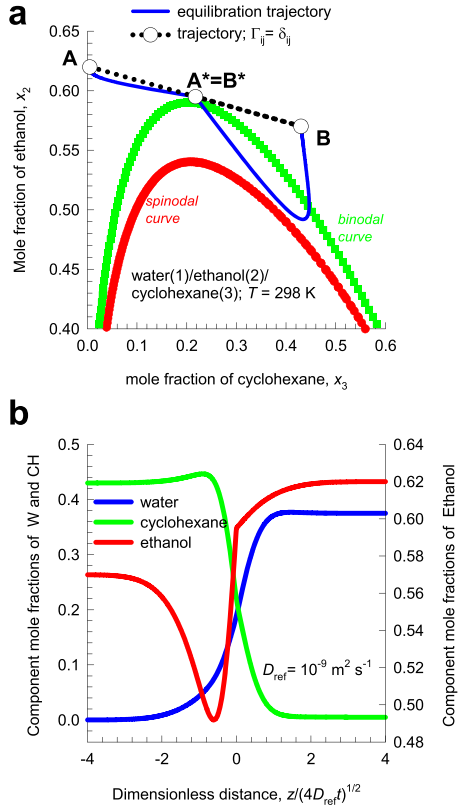

Figure 10. (a) Trajectories followed during transient equilibration of homogenous mixtures of two different compositions A and B for the system water (1)/ethanol (2)/cyclohexane (3) at 298 K. (b) Transient composition profiles plotted as a function of the dimensionless distance coordinate $z/\sqrt{4D_{ref}t}$. Further calculation details and data inputs are provided in the Supporting Information accompanying this publication.

compositions, $\frac{1}{2}\begin{pmatrix}\phi_{10}+\phi_{1I}\\ \phi_{2I}+\phi_{2I}\end{pmatrix}$, the elements of the matrix of thermodynamic factors, and the Fick diffusivity matrix are: $[\Gamma] = \begin{bmatrix}0.15393 & -0.08279\\ -0.53829 & 0.49255\end{bmatrix}$ and $[D] = \begin{bmatrix}0.46829 & -0.25204\\ -0.36327 & 0.21014\end{bmatrix} \times 10^{-9}$ m^2 s^{-1}. Noteworthy are the large negative values of both off-diagonal elements Γ_{12} and Γ_{21}. Both off-diagonal elements D_{12} and D_{21} are also negative, primarily because of the corresponding negative values of Γ_{12} and Γ_{21}.

The equilibration trajectory calculated using eq 16 is plotted in Figure 4a composition space; we note that the C−C* is strongly curvilinear and has penetrated into the metastable region.

The volume fractions of the three components are plotted in Figure 4b as a function of the dimensionless distance coordinate $z/\sqrt{4D_{ref}t}$ in the casting film, where we take the value of the reference diffusivity $D_{ref} = 1 \times 10^{-9}$ m^2 s^{-1}. There is a significantly higher volume fraction of the polymer near the surface of the casting film, $z \approx 0$. This implies that the polymer distributes asymmetrically across the membrane thickness, resulting in an asymmetric polymer membrane. Also noteworthy is that the volume fraction of water shows a pronounced overshoot at $z/\sqrt{4D_{ref}t} \approx -0.2$; this overshoot signifies uphill diffusion.[14,32,39] The overshoot in water is a direct result of the influence of thermodynamic coupling on the driving force of water, causing the effective driving force to undergo sign reversal, as witnessed in Figure 2b.

To delineate the influence of thermodynamic coupling, we repeated the simulations by invoking the assumption $\Gamma_{ij} = \delta_{ij}$ and calculating the Fick matrix using $[D] = [B]^{-1}$; this results in C−C* trajectory indicated by the dashed line in Figure 4a. No ingress into the metastable region is experienced, and the trajectory tends to veer away from the binodal curve in its approach to C*. The inescapable conclusion is that the influence of the thermodynamic correction factors is to draw the trajectories into the metastable region, leading eventually to polymer precipitation.

Next, we analyze the transient equilibration trajectory followed in the ternary water/NMP/PSF solutions in which the initial volume fractions in the polymer casting film and coagulation bath are chosen as $\phi_{10} = 0$; $\phi_{20} = 0.7$; $\phi_{1b0} = 0.3$; $\phi_{2b0} = 0.7$, corresponding to the position A indicated in Figure 5a. The simultaneous solution of the equations describing thermodynamic equilibrium at the interface (eq 9) and the flux continuity relations (eq 18) results in the interfacial volume fractions $\phi_{1I} = 0.01623$; $\phi_{2I} = 0.23293$; and $\phi_{1bI} = 0.25625$. Both

https://dx.doi.org/10.1021/acsomega.9b03609
ACS Omega 2020, 5, 2819−2828

the off-diagonal elements of $[\Gamma] = \begin{bmatrix} 0.93085 & -0.01965 \\ -5.36896 & 0.46328 \end{bmatrix}$ and $[D] = \begin{bmatrix} 1.39456 & -0.02938 \\ -0.6735 & 0.01775 \end{bmatrix} \times 10^{-9}$ m^2 s^{-1} are negative. The strong coupling effects cause the A−A* equilibration trajectory to exhibit a foray into the metastable region. The dashed line in Figure 5a represents the trajectory followed by invoking the assumption $\Gamma_{ij} = \delta_{ij}$ and ignoring thermodynamic correction factors; in this scenario, the A−A* does not cross the binodal curve.

The volume fractions of the three components are plotted in Figure 5a as a function of the dimensionless distance coordinate $z/\sqrt{4D_{ref}t}$ in the casting film. The polymer composition is significantly higher near the surface of the casting film, $z \approx 0$, resulting eventually in an asymmetric PSF membrane. The transient overshoot of water signifies uphill transport.

The analyses of the A−A* equilibration trajectories for water/NMP/PEI and water/DMF/PVDF solutions proceed along precisely analogous lines; the results are summarized in Figure 6a−d. Incursions into the metastable regions, induced by off-diagonal elements $\Gamma_{ij} (i \neq j)$, are experienced in both cases. Uphill diffusion causes overshoots in water compositions near the surface of the casting films, and the congregation of PEI and PVDF polymers near the surface of the casting film, $z \approx 0$, is also evident in Figure 6b,d.

The phenomena of uphill diffusion resulting in transient overshoots of water experienced in the four examples above are, however, not in violation of the second law of thermodynamics.[32,39] As verification, the corresponding transient profiles of the activity of water are plotted in Figure 7; in all four cases, the variation of activity along the dimensionless distance is monotonic. Put another way, water transport is down the activity hill.

2.4. Emulsion Formation in Partially Miscible Liquid/Liquid Mixtures. We now demonstrate analogies between the immersion precipitation process with emulsion formation. According to Miller,[22] "If the two bulk liquids are not initially at equilibrium, it is conceivable that dynamic processes such as diffusion could produce emulsification when the two liquids are brought into contact without stirring." The necessary conditions for spontaneous emulsification are derived by Ruschak and Miller[23] in terms of diffusion equilibration composition trajectories that must necessarily enter the metastable regions. These authors adopted the Fickian formulation in which the diffusion flux of each species i is considered to be linearly dependent on its own composition gradient, with the Fickian diffusivities of each component equal to one another.

As illustrated, Figure 8 shows the phase diagram for the partially miscible water (1)/ethanol (2)/benzene (3) mixtures at 298 K. Bringing pure water (indicated by A) in contact with a 50:50 ethanol/benzene mixture (indicated by B) results in a mixture composition (indicated by M) that ends up in the two-phase region of the phase diagram. This mixture will separate into two liquid phases of compositions A* and B* that lie on the binodal curve at either end of the tie-line. The phase A will equilibrate to the composition A*, while phase B will equilibrate to B*. Using the model of Ruschak and Miller,[23] wherein all of the component diffusivities in the ternary mixture are equal to one another, the diffusion equilibration trajectories A−A* and B−B* will both be straight lines in ternary composition space. We note that the A−A* trajectory lies in the metastable region between the binodal and spinodal curves. This foray into the metastable region is a necessary condition for emulsification to occur. Vitale and Katz[27] have coined the generic term Ouzo effect to describe such a process of creating metastable liquid−liquid dispersions. Since no input of mechanical energy is involved, this offers an energy-efficient method of producing nanospheres and nanoparticles.[25]

The Ruschak−Miller model is overly simplistic because the linear equilibration trajectories are only realized if the thermodynamic correction factors are ignored, $\Gamma_{ij} = \delta_{ij}$, and the Fick diffusivity matrix $[D]$, in either contiguous fluid phase, degenerates to a scalar diffusivity times the identity matrix.[14,15] Detailed analysis of the published experimental data on diffusivities in several partially miscible ternary liquid mixtures reveals that the interdiffusion process is strongly coupled due to thermodynamic correction factors close to regions of phase transitions, and the off-diagonal elements of the Fick diffusivity matrix $[D]$ exert significant influences on the equilibration trajectories.[14,15,32,39]

The model for the immersion precipitation process is amenable to the straight-forward extension to cater for interdiffusion between two partially miscible liquid phases (A, B), with two different Fick diffusivity matrices $[D_A]$ and $[D_B]$; the detailed derivations are available in the SI.

Figure 9a shows the simulation results for A−A* and B−B* equilibration trajectories for glycerol/acetone/water mixtures; both trajectories are both strongly curvilinear in composition space; in the glycerol-rich phase, the B−B* exhibits a foray into the metastable region with the potential for emulsification. Similarly, for water/acetic acid/MTBE mixtures, the ingress of B−B* into the metastable region (see Figure 9b) in the MTBE-rich phase may result in emulsion formation. Analogous results are obtained for water/chloroform/acetic acid, water/acetone/ethyl-acetate, water/ethanol/ethyl-acetate, and water/acetic acid/1-hexanol mixtures; see simulation results in Figures S24, S25, S27, and S29. It is noteworthy that the Ruschak−Miller model with straight-line equilibration would also have anticipated the possibilities of emulsification for all of the aforementioned six mixtures.

We now demonstrate scenarios in which forays into metastable regions can occur under conditions that are not anticipated using the model of Ruschak and Miller.[23] For water (1)/ethanol (2)/cyclohexane (3) mixtures, we choose the set of starting compositions for the ethanol-rich phase (A) and cyclohexane-rich phase (B) as $x_{1A0} = 0.375$; $x_{2A0} = 0.62$; $x_{1B0} = 0$; $x_{2B0} = 0.57$; see Figure 10a. The composition of the A−B mixture, A* = B* = $x_{1I} = 0.1875$; $x_{2I} = 0.595$, lies in the homogeneous single-phase region, but close to the binodal curve. According to the Ruschak−Miller analysis, no entry into the metastable regions is possible. Calculations of the A−A* and B−B* trajectories with reliable estimates of the Maxwell−Stefan diffusivities, along with proper accounting of thermodynamic correction factors (using the NRTL equation for phase equilibrium), lead to curvilinear trajectories. The B−B* penetrates the metastable zone in the cyclohexane-rich phase. The composition profiles of the three components are plotted in Figure 10b as a function of the dimensionless distance coordinate $z/\sqrt{4D_{ref}t}$. We note that ethanol experiences a pronounced undershoot during the transient equilibration process. Concomitantly, cyclohexane displays a slight overshoot. The overshoot/undershoot phenomena, along with the entry into the metastable zone, are engendered by the significant off-diagonal elements of $[\Gamma_B] = \begin{bmatrix} 0.59141 & -0.19602 \\ -0.70702 & 0.3644 \end{bmatrix}$ in the cyclohexane-rich phase. Indeed, if thermodynamic coupling

https://dx.doi.org/10.1021/acsomega.9b03609
ACS Omega 2020, 5, 2819−2828

effects are completely ignored by invoking the assumption $\Gamma_{ij} = \delta_{ij}$, the equilibration trajectory (shown by the dotted line in Figure 10a) shows no entry into the metastable region.

Analyses of transient equilibration in glycerol/acetone/water, water/acetone/ethyl-acetate, water/acetic acid/1-hexanol, and water/acrylonitrile/toluene mixtures yield results that are precisely analogous to those in Figure 10; see Figures S23, S26, S29, S32, and S33. In all cases, thermodynamic coupling induces entry into metastable zones, while the Ruschak–Miller model calculations do not anticipate such incursions.

The crystal formation and growth as a consequence of diffusional foray into supersaturated regions is also a consequence of thermodynamic coupling.[32,40]

3. CONCLUSIONS

For partially miscible ternary fluid mixtures, diffusivities in regions close to phase transitions are strongly influenced by phase equilibrium thermodynamics. These influences are quantified by thermodynamic correction factors Γ_{ij}, whose off-diagonal elements Γ_{12} and Γ_{21} are often significantly large in relation to the Γ_{11} and Γ_{22}. Consequently, interphase diffusion is a strongly coupled process that results in strongly curvilinear equilibration trajectories during transient equilibration. Such trajectories often signify uphill diffusion phenomena, and cause forays into the metastable regions, lying between the binodal and spinodal curves. Such forays are essential in the immersion precipitation process for the preparation of CA, PSF, PEI, and PVDF membranes, with asymmetry in the polymer distribution along the thickness. In all cases, if the off-diagonal elements Γ_{12} and Γ_{21} are set to zero, no polymer precipitation is realized. The transient development of volume fractions of water in the polymer casting film exhibits overshoots in all of the four cases; such overshoots are signatures of uphill diffusion. The theoretical model developed in this work should provide guidelines to the polymer chemist for choosing a set of operating conditions, and mixture compositions in the casting film and coagulation bath to prepare asymmetric polymeric membranes.

The exploitation of the Ouzo effect for the formation of metastable emulsions in liquid/liquid mixtures is also crucially dependent on thermodynamic coupling effects.

■ ASSOCIATED CONTENT

Supporting Information

The Supporting Information is available free of charge at https://pubs.acs.org/doi/10.1021/acsomega.9b03609.

(1) Detailed development of the Maxwell–Stefan (M–S) diffusion equations for multicomponent fluid mixtures; (2) comparison of the M–S formulation with the Bearman friction formulation; (3) procedures for estimation of the M–S diffusivities; (4) description of phase equilibrium using the Flory–Huggins relations; (5) development of the analytic model to describe equilibration in the immersion precipitation process; (6) detailed development of the model to describe emulsification in ternary fluid mixtures, and (7) data inputs and simulation details for all investigated mixtures (PDF)

■ AUTHOR INFORMATION

Corresponding Author

Rajamani Krishna − *Van 't Hoff Institute for Molecular Sciences, University of Amsterdam 1098 XH Amsterdam, The Netherlands;* orcid.org/0000-0002-4784-8530; Email: r.krishna@contact.uva.nl

Complete contact information is available at: https://pubs.acs.org/10.1021/acsomega.9b03609

Notes

The author declares no competing financial interest.

■ ACKNOWLEDGMENTS

The author acknowledges the contribution of Dr J. M. van Baten for providing codes for calculation of phase equilibria.

■ NOMENCLATURE

Latin Alphabet

a_i	component activity, dimensionless
$[B]$	matrix of inverse M–S coefficients, m^{-2} s
c_i	molar concentration of species i, mol m^{-3}
$Đ_{ij}^{V}$	M–S diffusivity for binary pair i–j, m^2 s^{-1}
$[D]$	Fick diffusivity matrix, m^2 s^{-1}
$[I]$	identity matrix, dimensionless
J_i^{V}	volumetric diffusion fluxes with respect to u^{V}, m^3 m^{-2} s^{-1}
n	number of species in the mixture, dimensionless
R	gas constant, 8.314 J mol^{-1} K^{-1}
t	time, s
T	absolute temperature, K
x_i	mole fraction of component i in bulk fluid phase, dimensionless
u^{V}	volume average mixture velocity, m s^{-1}
$\overline{V}_i$	partial molar volume of species i, m^3 mol^{-1}
z	direction coordinate, m

■ GREEK ALPHABET

γ_i	activity coefficient of component i, dimensionless
δ_{ij}	Kronecker delta, dimensionless
$\varepsilon(t)$	position of moving boundary, m
Γ_{ij}	thermodynamic correction factors, dimensionless
μ_i	molar chemical potential, J mol^{-1}
ϕ_i	volume fraction of species i, dimensionless

■ SUBSCRIPT

i	referring to component i
I	referring to the interface
m	refers to polymer
n	referring to component n
t	referring to the total mixture

■ SUPERSCRIPT

V volume average reference velocity frame

■ MATRIX NOTATION

()	column matrix
[]	square matrix

■ REFERENCES

(1) Loeb, S.; Sourirajan, S. Sea Water Demineralization by Means of an Osmotic Membrane. In *Saline Water Conversion II*; Gould, R. F., Ed.; Advances in Chemistry Series; American Chemical Society, 1963; Chapter 9, pp 117–132.

(2) Ulbricht, M. Advanced Functional Polymer Membranes. *Polymer* **2006**, *47*, 2217–2262.

(3) van de Witte, P.; Dijkstra, P. J.; van den Berg, J. W. A.; Feijen, J. Phase separation processes in polymer solutions in relation to membrane formation. *J. Membr. Sci.* **1996**, *117*, 1−31.
(4) van den Berg, G. B.; Smolders, C. A. Diffusional phenomena in membrane separation processes. *J. Membr. Sci.* **1992**, *73*, 103−118.
(5) Reuvers, A. J.; Smolders, C. A. Formation of membranes by means of immersion precipitation Part II. The mechanism of formation of membranes prepared from the system cellulose acetate - acetone - water. *J. Membr. Sci.* **1987**, *34*, 67−86.
(6) Reuvers, A. J.; van den Berg, J. W. A.; Smolders, C. A. Formation of membranes by means of immersion precipitation Part II. The mechanism of formation of membranes prepared from the system cellulose acetate - acetone - water. *J. Membr. Sci.* **1987**, *34*, 45−65.
(7) Radovanovic, P.; Thiel, S. W.; Hwang, S.-T. Formation of asymmetric polysulfone membranes by immersion precipitation. Part I. Modelling mass transport during gelation. *J. Membr. Sci.* **1992**, *65*, 213−229.
(8) Radovanovic, P.; Thiel, S. W.; Hwang, S.-T. Formation of asymmetric polysulfone membranes by immersion precipitation. Part II. The effects of casting solution and gelation bath compositions on membrane structure and skin formation. *J. Membr. Sci.* **1992**, *65*, 231−246.
(9) Strathmann, H.; Kock, K. The Formation Mechanism of Phase Inversion Membranes. *Desalination* **1977**, *21*, 2411−2255.
(10) Guillen, G. R.; Yinjin Pan, Y.; Li, M.; Hoek, E. V. Preparation and Characterization of Membranes Formed by Nonsolvent Induced Phase Separation: A Review. *Ind. Eng. Chem. Res.* **2011**, *50*, 3798−3817.
(11) Wang, D.-M.; Lai, J.-Y. Recent advances in preparation and morphology control of polymeric membranes formed by nonsolvent induced phase separation. *Curr. Opin. Chem. Eng.* **2013**, *2*, 229−237.
(12) Tsay, C. S.; McHugh, A. J. Mass Transfer Modeling of Asymmetric Membrane Formation by Phase Inversion. *J. Polym. Sci., Part B: Polym. Phys.* **1990**, *28*, 1327−1365.
(13) Tsay, C. S.; McHugh, A. J. An Improved Numerical Algorithm for Ternary Diffusion with a Moving Interface. *Chem. Eng. Sci.* **1991**, *46*, 1179−1187.
(14) Krishna, R. Serpentine Diffusion Trajectories and the Ouzo Effect in Partially Miscible Ternary Liquid Mixtures. *Phys. Chem. Chem. Phys.* **2015**, *17*, 27428−27436.
(15) Krishna, R. Highlighting Diffusional Coupling Effects in Ternary Liquid Extraction and Comparisons with Distillation. *Ind. Eng. Chem. Res.* **2016**, *55*, 1053−1063.
(16) McHugh, A. J.; Tsay, C. S. Dynamics of the Phase Inversion Process. *J. Appl. Polym. Sci.* **1992**, *46*, 2011−2021.
(17) Krishna, R. Describing Mixture Permeation across Polymeric Membranes by a Combination of Maxwell-Stefan and Flory-Huggins Models. *Polymer* **2016**, *103*, 124−131.
(18) Krishna, R. Using the Maxwell-Stefan formulation for Highlighting the Influence of Interspecies (1-2) Friction on Binary Mixture Permeation across Microporous and Polymeric Membranes. *J. Membr. Sci.* **2017**, *540*, 261−276.
(19) Krishna, R. Highlighting Thermodynamic Coupling Effects in Alcohol/Water Pervaporation across Polymeric Membranes. *ACS Omega* **2019**, *4*, 15255−15264.
(20) Ribeiro, C. P.; Freeman, B. D.; Paul, D. R. Modeling of Multicomponent Mass Transfer across Polymer Films using a Thermodynamically Consistent Formulation of the Maxwell-Stefan Equations in terms of Volume Fractions. *Polymer* **2011**, *52*, 3970−3983.
(21) Fornasiero, F.; Prausnitz, J. M.; Radke, C. J. Multicomponent Diffusion in Highly Asymmetric Systems. An Extended Maxwell-Stefan Model for Starkly Different-Sized, Segment-Accessible Chain Molecules. *Macromolecules* **2005**, *38*, 1364−1370.
(22) Miller, C. A. Spontaneous Emulsification Produced by Diffusion - A Review. *Colloids Surf.* **1988**, *29*, 89−102.
(23) Ruschak, K. J.; Miller, C. A. Spontaneous Emulsification in Ternary Systems with Muss Transfer. *Ind. Eng. Chem. Fundam.* **1972**, *11*, 534−540.
(24) Jackson, R. Diffusion in Ternary Mixtures with and without Phase Boundaries. *Ind. Eng. Chem. Fundam.* **1977**, *16*, 304−306.
(25) Ganachaud, F.; Katz, J. L. Nanoparticles and Nanocapsules Created Using the Ouzo Effect: Spontaneous Emulsification as an Alternative to Ultrasonic and High-Shear Devices. *ChemPhysChem* **2005**, *6*, 209−216.
(26) Sitnikova, N. L.; Sprik, R.; Wegdam, G.; Eiser, E. Spontaneously Formed trans-Anethol/Water/Alcohol Emulsions: Mechanism of Formation and Stability. *Langmuir* **2005**, *21*, 7083−7089.
(27) Vitale, S. A.; Katz, J. L. Liquid Droplet Dispersions Formed by Homogeneous Liquid-Liquid Nucleation: "The Ouzo Effect". *Langmuir* **2003**, *19*, 4105−4110.
(28) Alsoy, S.; Duda, J. L. Modeling of Multicomponent Drying of Polymer Films. *AIChE J.* **1999**, *45*, 896−905.
(29) Zielinski, J. M.; Hanley, B. F. Practical Friction-Based Approach to Modeling Multicomponent Diffusion. *AIChE J.* **1999**, *45*, 1−12.
(30) Price, P. E.; Romdhane, I. H. Multicomponent Diffusion Theory and Its Applications to Polymer-Solvent Systems. *AIChE J.* **2003**, *49*, 309−322.
(31) Taylor, R.; Krishna, R. *Multicomponent Mass Transfer*; John Wiley & Sons: New York, 1993.
(32) Krishna, R. Diffusing Uphill with James Clerk Maxwell and Josef Stefan. *Chem. Eng. Sci.* **2019**, *195*, 851−880.
(33) Bearman, R. J. On the Molecular Basis of some Current Theories of Diffusion. *J. Phys. Chem. A.* **1961**, *65*, 1961−1968.
(34) Vrentas, J. S.; Duda, J. L. Molecular diffusion in polymer solutions. *AIChE J.* **1979**, *25*, 1−24.
(35) Mulder, M. H. V.; Franken, A. C. M.; Smolders, C. A. Preferential Sorpton versus Preferential Permeability in Pervaporation. *J. Membr. Sci.* **1985**, *22*, 155−178.
(36) Yang, T.-H.; Lue, S. J. Modeling Sorption Behavior for Ethanol/Water Mixtures in a Cross-linked Polydimethylsiloxane Membrane Using the Flory-Huggins Equation. *J. Macromol. Sci., Part B: Phys.* **2013**, *52*, 1009−1029.
(37) Varady, M. J.; Pearl, T. P.; Stevenson, S. M.; Mantooth, B. A. Decontamination of VX from Silicone: Characterization of Multicomponent Diffusion Effects. *Ind. Eng. Chem. Res.* **2016**, *55*, 3139−3149.
(38) Crank, J. *The Mathematics of Diffusion*, 2nd ed.; Clarendon Press: Oxford, 1975.
(39) Krishna, R. Uphill Diffusion in Multicomponent Mixtures. *Chem. Soc. Rev.* **2015**, *44*, 2812−2836.
(40) Myerson, A. S.; Lo, P. Y. Cluster Formation and Diffusion in Supersaturated Binary and Ternary Acid Solutions. *J. Cryst. Growth* **1991**, *110*, 26−33.

https://dx.doi.org/10.1021/acsomega.9b03609
ACS Omega 2020, 5, 2819−2828

Highlighting Thermodynamic Coupling Effects in the Immersion Precipitation Process for Formation of Polymeric Membranes

Rajamani Krishna*

Van 't Hoff Institute for Molecular Sciences

University of Amsterdam

Science Park 904

1098 XH Amsterdam, The Netherlands

email: r.krishna@contact.uva.nl

Table of Contents

1 Preamble

The Supporting Information accompanying our article *Highlighting Thermodynamic Coupling Effects in the Immersion Precipitation Process for Formation of Polymeric Membranes* provides: (1) detailed development of the Maxwell-Stefan (M-S) diffusion equations for multicomponent fluid mixtures, (2) comparison of the M-S formulation with the Bearman friction formulation, (3) procedures for estimation of the M-S diffusivities, (4) description of phase equilibrium using the Flory-Huggins relations, (5) development of the analytic model to describe equilibration in the immersion precipitation process, (6) detailed development of the model to describe emulsification in ternary fluid mixtures, (7) data inputs and simulation details for all investigated mixtures.

All the calculations and simulations reported in this article were performed using MathCad 15.[1] For ease of reading, this Supporting Information is written as a stand-alone document; as a consequence, there is some overlap of material with the main manuscript.

2 Phenomenological relations for *n*-component diffusion

Before setting up the proper phenomenological relations between the diffusion fluxes and the driving forces, we first consider the various choices of concentration measures, and reference velocities. The treatment below is essentially a summary of Chapter 1 of Taylor and Krishna.[2]

2.1 Concentration measures

A summary of the wide variety of concentration measures for *n*-component mixtures that are encountered in practice is provided in Table S1.

2.2 Diffusion fluxes and reference velocities

If u_i denotes the ensemble average velocity of component *i* with respect to a laboratory-fixed (i.e. stationary) coordinate reference frame, the molar flux of component i in the laboratory-fixed reference frame is $N_i = c_i u_i$ and the molar flux of the mixture is $N_t = \sum_{i=1}^{n} N_i$. The modelling and design of separation and reaction equipment requires calculation of the diffusion fluxes, J_i; these are defined with respect to an arbitrarily chosen reference velocity of the fluid mixture, u:

$$J_i \equiv c_i(u_i - u); \quad i = 1,2,..n \tag{S1}$$

Most commonly, we choose u as the molar average velocity of the mixture

$$u = \sum_{i=1}^{n} x_i u_i = x_1 u_1 + x_2 u_2 + \cdots x_n u_n \tag{S2}$$

Only *n*-1 of the fluxes J_i are independent because the diffusion fluxes sum to zero

$$\sum_{i=1}^{n} J_i = 0 \tag{S3}$$

The molar fluxes N_i in the laboratory fixed reference frame are related to the diffusion fluxes J_i by

$$N_i \equiv c_i u_i = J_i + x_i N_t; \quad N_t = \sum_{i=1}^{n} N_i \tag{S4}$$

The molar diffusion flux can also be defined with respect to other reference velocities; some commonly used ones are summarized in Table S2.

For ideal gas mixtures, the molar average mixture velocity equals the volume average mixture velocity. The mass average reference velocity frame is convenient to use when the equations of conservation of mass need to be solved in conjunction with the momentum balance relations. The volume average mixture velocity is convenient for liquid mixtures. For diffusion of ions in dilute aqueous solutions, it is convenient to define the diffusion fluxes with respect to water (the *n*th component).

2.3 The Generalized Fick's law for *n*-component diffusion

Choosing the mole fraction gradients as the driving forces, the diffusion fluxes $J_i \equiv c_i \left(u_i - u\right); \quad i = 1, 2, ..n$ with respect to the molar average reference velocity may expressed as linear functions of the (n-1) independent driving forces, by defining a (n-1) × (n-1) dimensional Fick diffusivity matrix $[D]$

$$(J) = -c_t [D] \frac{d(x)}{dz} = -\frac{1}{\overline{V}} [D] \frac{d(x)}{dz} \tag{S5}$$

where $\overline{V} = \sum_{k=1}^{n} x_k \overline{V_k}$ is the mean molar volume of the mixture.

2.4 Other choices of reference velocities in the definition of [*D*]

The Fick diffusivity matrix $[D]$ is defined in eq (S5) in terms of molar diffusion fluxes, J_i, that are, in turn, defined with respect to the molar average reference velocity frame u. Other choice of fluxes and

reference velocities are encountered in the chemical engineering literature; see Section 3.2.2 of Taylor and Krishna.[2] See also Table S2.

For mass diffusion fluxes, $j_i \equiv \rho_i \left(u_i - v\right); \quad i = 1,2,..n; \quad \sum_{i=1}^{n} j_i = 0$ defined with respect the mass average mixture velocity $v = \sum_{i=1}^{n} \omega_i u_i$, we write $(j) = -\rho_t \left[D^{mass}\right] \frac{d(\omega)}{dz}$.

The mass fractions are related to the mole fractions x_i

$\omega_i = \frac{\rho_i}{\rho_t} = \frac{x_i M_i}{\sum_{i=1}^{n} x_i M_i} = \frac{x_i M_i}{\overline{M}}; \quad x_i = \frac{c_i}{c_t} = \frac{\frac{\omega_i}{M_i}}{\sum_{i=1}^{n} \frac{\omega_i}{M_i}} = \frac{\omega_i}{M_i}\overline{M}$, where M_i is the molar mass of species *i*, with the units kg mol^{-1}, and $\overline{M}$ is the mean molar mass of the mixture is $\overline{M} = \sum_{i=1}^{n} x_i M_i = \frac{1}{\sum_{i=1}^{n} \frac{\omega_i}{M_i}}$. The mixture mass density is related to the total molar concentration of the mixture $\rho_t = c_t \overline{M} = \frac{1}{\overline{V}} \overline{M}$.

For molar diffusion fluxes, $J_i^V \equiv c_i \left(u_i - u^V\right); \quad i = 1,2,..n; \quad \sum_{i=1}^{n} \overline{V}_i J_i^V = 0$. defined with respect the volume average mixture velocity $u^V = \sum_{i=1}^{n} c_i \overline{V}_i u_i$, we write $(J^V) = -\left[D^V\right] \frac{d(c)}{dz}$. This is a common choice in the experimental determination of diffusivities.

For *n*-component mixtures, the numerical values of the elements of $[D]$, $\left[D^{mass}\right]$, and $\left[D^V\right]$ are different. However, the determinants of the corresponding matrices are equal to one another.[2]

$$\left|D\right| = \left|D^{mass}\right| = \left|D^V\right| \tag{S6}$$

For the special case of a binary mixture, *n* = 2, $dx_1 = \frac{\frac{1}{M_1 M_2}}{\left(\frac{\omega_1}{M_1} + \frac{\omega_2}{M_2}\right)^2} d\omega_1; \quad d\omega_1 = \frac{M_1 M_2}{\left(x_1 M_1 + x_2 M_2\right)^2} dx_1$,

and the Fick diffusivity is the same for the three different choice of reference velocity frames[2]

Phenomenological relations for n-component diffusion

$$j_1 \equiv \rho_1 \left(u_1 - v\right) = -\rho_t D_{12} \frac{d\omega_1}{dz}$$
$$J_1 \equiv c_1 \left(u_1 - u\right) = -c_t D_{12} \frac{dx_1}{dz} \tag{S7}$$
$$J_1^V \equiv c_i \left(u_1 - u^V\right) = -D_{12} \frac{dc_1}{dz}$$

The inter-relationship between J_1 and j_1 is summarized in Table S3.

The formulae for transformation of the Fick diffusivity matrix from one reference frame to another are provided in Section 3.2.4 of Taylor and Krishna.[2] For example, for a ternary mixture, n = 3, the transformation between $[D]$, and $[D^{mass}]$ is

$$[D^{mass}] = [A][D][A]^{-1}; \quad [D] = [A]^{-1}[D^{mass}][A];$$
$$[A] \equiv \begin{bmatrix} 1-\omega_1\left(1-\dfrac{\omega_3 x_1}{x_3\omega_1}\right) & -\omega_1\left(1-\dfrac{\omega_3 x_2}{x_3\omega_2}\right) \\ -\omega_2\left(1-\dfrac{\omega_3 x_1}{x_3\omega_1}\right) & 1-\omega_2\left(1-\dfrac{\omega_3 x_2}{x_3\omega_2}\right) \end{bmatrix} \begin{bmatrix} \omega_1 & 0 \\ 0 & \omega_2 \end{bmatrix} \begin{bmatrix} x_1 & 0 \\ 0 & x_2 \end{bmatrix}^{-1} \tag{S8}$$

For the ternary mixture of nC_8H_{18}(1)/$nC_{10}H_{22}$(2)/1-methylnapthalene(3) with mass fractions $\omega_1 = \omega_2 = \omega_3 = 0.3333$ at 295.65 K, Leahy-Dios et al.[3] report experimental data on the Fick diffusivity matrix in the mass average reference velocity frame: $[D^{mass}] = \begin{bmatrix} 1.99 & -0.93 \\ -0.42 & 2.4 \end{bmatrix} \times 10^{-9}$ m^{2}s^{-1}; the large magnitudes of the off-diagonal elements are particular noteworthy. The corresponding mole fractions of the three components are x_1 = 0.384, x_2 = 0.308, x_3 = 0.308. On transformation using eq (S8), we obtain the matrix of Fick diffusivities in the molar average reference velocity frame $[D] = \begin{bmatrix} 1.92 & -1.07 \\ -0.333 & 2.47 \end{bmatrix} \times 10^{-9}$ m^{2}s^{-1}.

For a ternary mixture, n = 3, the transformation between $[D]$, and $[D^V]$ is given by eq (S9).

$$\left[D^V\right]=[A][D][A]^{-1};\quad [D]=[A]^{-1}\left[D^V\right][A];$$
$$[A]\equiv\begin{bmatrix}1-\frac{x_1}{\overline{V}}\left(\overline{V_1}-\overline{V_3}\right) & -\frac{x_1}{\overline{V}}\left(\overline{V_2}-\overline{V_3}\right)\\ -\frac{x_2}{\overline{V}}\left(\overline{V_1}-\overline{V_3}\right) & 1-\frac{x_2}{\overline{V}}\left(\overline{V_2}-\overline{V_3}\right)\end{bmatrix};\quad \overline{V}=\sum_{k=1}^{3}x_k\overline{V_k} \tag{S9}$$

Alimadadian and Colver;[4] report the elements of the Fick matrix $\left[D^V\right]$ in the volume average reference velocity frame for acetone(1)/benzene(2)/methanol(3) mixtures at 9 different compositions. At $x_1 = 0.350$, $x_2 = 0.302$, $x_3 = 0.348$, $\left[D^V\right]=\begin{bmatrix}3.819 & 0.42\\ -0.561 & 2.133\end{bmatrix}\times10^{-9}$ m^{2}s^{-1}. The partial molar volumes are $\overline{V_1}=74.1\times10^{-6};\quad \overline{V_2}=89.4\times10^{-6};\quad \overline{V_3}=40.7\times10^{-6}$ m^3 mol^{-1}. Using equation (S9), we can convert to the molar average reference velocity frame to obtain $[D]=\begin{bmatrix}3.651 & -0.069\\ -0.300 & 2.303\end{bmatrix}\times10^{-9}$ m^{2}s^{-1}; see Example 3.2.1 of Taylor and Krishna[2] for further calculation details.

2.5 The Maxwell-Stefan formulation for *n*-component diffusion

The Maxwell-Stefan approach, that we adopt in this article, has its origins in the pioneering works of James Clerk Maxwell[5] and Josef Stefan[6] who analyzed diffusion in *ideal gas mixtures*. The Maxwell-Stefan (M-S) formulation is best understood by considering *z*-directional diffusion in a binary gas mixture consisting of species 1 and 2, contained within the control volume shown schematically in Figure S1. The cross-sectional area available for diffusion is 1 m^2 and the length of the diffusion path is dz. If the change in the partial pressure of component *i* across the diffusion distance dz is $-dp_i$, the force acting on species *i* per m^3 is $-\frac{dp_i}{dz}$. The number of moles of species *i* per m^3, $c_i=\frac{p_i}{RT}$, and therefore the force acting per mole of species *i* is $-\frac{RT}{p_i}\frac{dp_i}{dz}$ which for an ideal gas mixture at constant temperature also equals the chemical potential gradient $-\frac{d\mu_i}{dz}$. This force is balanced by friction between the diffusing species 1 and 2, each diffusing with a velocity u_i (cf. Figure S2). We may expect

that the frictional drag to be proportional to the velocity difference $(u_1 - u_2)$, and we write $-\frac{d\mu_1}{dz} = \frac{RT}{Đ_{12}} x_2 (u_1 - u_2)$ where the term $\frac{RT}{Đ_{12}}$ is to be interpreted as the drag coefficient. The multiplier x_2 in the right member represents the mole fraction of component 2; this factor is introduced because we expect the friction to be dependent on the number of molecules of component 2 relative to that of component 1. The Maxwell-Stefan diffusivity $Đ_{12}$ has the units $m^2\ s^{-1}$ and the physical significance of an inverse drag coefficient. The extension to *n*-component mixtures is intuitively obvious and can be written for component 1, for example as follows

$$-\frac{d\mu_1}{dz} = \frac{RT}{Đ_{12}} x_2 (u_1 - u_2) + \frac{RT}{Đ_{13}} x_3 (u_1 - u_3) + ... + \frac{RT}{Đ_{1n}} x_n (u_1 - u_n) \tag{S10}$$

The corresponding relations for components 2, 3, ..*n* are written down in an analogous manner. The left member of eq (S10) is the negative of the gradient of the chemical potential, with the units N mol^{-1}; it represents the driving force acting per mole of species 1. The term $RT/Đ_{ij}$ is interpreted as the drag coefficient for the *i-j* pair. The multiplier x_j in each of the right members represents the mole fraction of component *j*; this factor is introduced because we expect the 1-*j* friction to be dependent on the number of molecules of *j* relative to that of component 1. The M-S diffusivity $Đ_{ij}$ has the units $m^2\ s^{-1}$ and the physical significance of an *inverse* drag coefficient. The magnitudes of the M-S diffusivities $Đ_{ij}$ do not depend on the choice of the mixture reference velocity because eq (S10) is set up in terms of velocity differences. Equation (S10) may be re-written as

$$-\frac{1}{RT}\frac{d\mu_i}{dz} = \sum_{\substack{j=1 \\ j\neq i}}^{n} \frac{x_j (u_i - u_j)}{Đ_{ij}} \tag{S11}$$

Multiplying both sides of equation (S11) by x_i we get

$$-\frac{x_i}{RT}\frac{d\mu_i}{dz} = \sum_{\substack{j=1 \\ j\neq i}}^{n} \frac{x_i x_j (u_i - u_j)}{Đ_{ij}} = \sum_{\substack{j=1 \\ j\neq i}}^{n} \frac{(x_j x_i u_i - x_i x_j u_j)}{Đ_{ij}} = \sum_{\substack{j=1 \\ j\neq i}}^{n} \frac{(x_j c_i u_i - x_i c_j u_j)}{c_t Đ_{ij}} \tag{S12}$$

Introducing the expressions for fluxes $N_i = c_i u_i = c_t x_i u_i$ and $J_i = N_i - x_i N_t$ in eq (S12), we get

Phenomenological relations for n-component diffusion

$$-\frac{x_i}{RT}\frac{d\mu_i}{dz}=\sum_{\substack{j=1\\ j\neq i}}^{n}\frac{x_j N_i - x_i N_j}{c_t Đ_{ij}}=\sum_{\substack{j=1\\ j\neq i}}^{n}\frac{x_j J_i - x_i J_j}{c_t Đ_{ij}};\quad i=1,2,\ldots n \tag{S13}$$

The Maxwell-Stefan diffusion formulation (S13) is consistent with the Onsager formulation; the Onsager Reciprocal Relations (ORR) imply that the M-S pair diffusivities are symmetric

$$Đ_{ij}=Đ_{ji};\quad i,j=1,2...n \tag{S14}$$

The second law of thermodynamics dictates that the rate of entropy production must be positive

$$\sigma=-\frac{1}{T}\sum_{i=1}^{n}\frac{d\mu_i}{dz}J_i=-\frac{1}{T}\sum_{i=1}^{n-1}\frac{d(\mu_i-\mu_n)}{dz}J_i\geq 0 \tag{S15}$$

Insertion of the Maxwell-Stefan eq (S13) into eq (S15) we obtain on re-arrangement[7]

$$\sigma=\frac{1}{2}c_t R\sum_{i=1}^{n}\sum_{j=1}^{n}\frac{x_i x_j}{Đ_{ij}}\left|u_i-u_j\right|^2\geq 0 \tag{S16}$$

The term $\frac{x_i}{RT}\frac{d\mu_i}{dz}$ on the left hand member of eq (S13) is the generalization of the mole fraction gradients, used as driving forces for ideal gas mixtures.

For non-ideal liquid mixtures, the chemical potential of component *i*, μ_i are related to the gradients of the component activities, $a_i=\gamma_i x_i$, where γ_i is the activity coefficient:

$$\mu_i=\mu_i^0+RT\ln(a_i)=\mu_i^0+RT\ln(\gamma_i x_i) \tag{S17}$$

For gaseous mixtures at high pressure, the chemical potential of component *i*, μ_i are related to the gradients of the component fugacities, $f_i=\phi_i p_i=\phi_i x_i p$:

$$\mu_i=\mu_i^0+RT\ln(f_i)=\mu_i^0+RT\ln(\phi_i x_i p_t) \tag{S18}$$

where ϕ_i is the fugacity coefficient and p_t is the total gas pressure.

In proceeding further, it is convenient to express the left member of eq (S13) in terms of the mole fraction gradients by introducing an (n-1) × (n-1) matrix of thermodynamic correction factors $[\Gamma]$:

Phenomenological relations for n-component diffusion

$$\frac{x_i}{RT}\frac{d\mu_i}{dz} = x_i\frac{d\ln a_i}{dz} = \sum_{j=1}^{n-1}\Gamma_{ij}\frac{dx_j}{dz};\quad \Gamma_{ij} = \delta_{ij} + x_i\frac{\partial \ln \gamma_i}{\partial x_j};\quad i,j = 1,2\ldots n-1 \tag{S19}$$

For non-ideal ternary liquid mixtures, the elements of $[\Gamma]$ can be calculated from Van Laar, Wilson, UNIQUAC or NRTL models describing phase equilibrium thermodynamics.[2, 8] The analogous expression for high pressure gaseous mixtures is

$$\frac{x_i}{RT}\frac{d\mu_i}{dz} = x_i\frac{d\ln f_i}{dz} = \sum_{j=1}^{n-1}\Gamma_{ij}\frac{dx_j}{dz};\quad \Gamma_{ij} = \delta_{ij} + x_i\frac{\partial \ln \phi_i}{\partial x_j};\quad i,j = 1,2\ldots n-1 \tag{S20}$$

In this case, the elements of $[\Gamma]$ can be calculated by analytic differentiation of an Equation of State (EOS) such as the Peng-Robinson (PR) EOS; for further details see Krishna and van Baten.[9] For binary mixtures, explicit analytic expressions for $\Gamma = x_1\frac{\partial \ln f_1}{\partial x_1} = \delta_{ij} + x_1\frac{\partial \ln \phi_1}{\partial x_1}$ for PR EOS are provided in the paper by Tuan et al.[10]

We also define a (n-1) × (n-1) matrix of inverse M-S diffusivities $[B]$ whose elements are given by

$$B_{ii} = \frac{x_i}{Đ_{in}} + \sum_{\substack{k=1\\k\neq i}}^{n}\frac{x_k}{Đ_{ik}};\quad B_{ij(i\neq j)} = -x_i\left(\frac{1}{Đ_{ij}} - \frac{1}{Đ_{in}}\right);\quad i,j = 1,2\ldots n-1 \tag{S21}$$

Combining eqs (S13), (S19), (S20), and (S21), we can re-cast eq (S13) into (n-1) dimensional matrix notation

$$-[\Gamma]\frac{d(x)}{dz} = \frac{1}{c_t}[B](J);\quad (J) = -c_t[B]^{-1}[\Gamma]\frac{d(x)}{dz} = -c_t[\Lambda][\Gamma]\frac{d(x)}{dz} = -\frac{1}{\overline{\overline{V}}}[\Lambda][\Gamma]\frac{d(x)}{dz} \tag{S22}$$

where we have additionally defined

$$[\Lambda] = [B]^{-1} \tag{S23}$$

The inter-relationships between the Fick, and the Maxwell-Stefan diffusivities is

$$\begin{aligned}&[D] = [B]^{-1}[\Gamma] = [\Lambda][\Gamma];\\ &(J) = -\frac{1}{\overline{\overline{V}}}[D]\frac{d(x)}{dz} = -\frac{1}{\overline{\overline{V}}}[\Lambda][\Gamma]\frac{d(x)}{dz}\end{aligned} \tag{S24}$$

Equation (S24) underscores the direct influence of mixture thermodynamics on the elements D_{ij} of the matrix of Fick diffusivities $[D]$.

For an ideal gas mixture, the thermodynamic correction factors $\Gamma_{ij} = \delta_{ij}$ and eq (S24) reduces to

$$[\Lambda] = [B]^{-1} = [D]; \quad \text{ideal gas mixture} \tag{S25}$$

For a binary mixture, $n = 2$, eq (S13) simplifies to

$$-\frac{x_1}{RT}\frac{d\mu_1}{dz} = \frac{(x_2 J_1 - x_1 J_2)}{c_t Đ_{12}} \tag{S26}$$

Introducing the constraints $J_2 = -J_1$, and $x_2 = 1 - x_1$, eq (S26) yields

$$J_1 = -c_t Đ_{12}\frac{x_1}{RT}\frac{d\mu_1}{dz} = -c_t Đ_{12}\Gamma\frac{dx_1}{dz} = -c_t D_{12}\frac{dx_1}{dz} \tag{S27}$$

in which the Fick diffusivity for binary mixture is

$$D_{12} = Đ_{12}\Gamma \tag{S28}$$

For a ternary mixture, $n = 3$, eq (S24) gives the following explicit expression for the four elements of the Fick diffusivity matrix

$$\begin{bmatrix} D_{11} & D_{12} \\ D_{21} & D_{22} \end{bmatrix} = \begin{bmatrix} \frac{x_2}{Đ_{23}} + \frac{x_1}{Đ_{12}} + \frac{x_3}{Đ_{23}} & x_1\left(\frac{1}{Đ_{12}} - \frac{1}{Đ_{13}}\right) \\ x_2\left(\frac{1}{Đ_{12}} - \frac{1}{Đ_{23}}\right) & \frac{x_1}{Đ_{13}} + \frac{x_2}{Đ_{12}} + \frac{x_3}{Đ_{13}} \end{bmatrix}^{-1} \begin{bmatrix} \Gamma_{11} & \Gamma_{12} \\ \Gamma_{21} & \Gamma_{22} \end{bmatrix} \tag{S29}$$

The matrix inversion in eq (S29) can performed explicitly and we obtain

$$\begin{bmatrix} D_{11} & D_{12} \\ D_{21} & D_{22} \end{bmatrix} = \begin{bmatrix} \Lambda_{11} & \Lambda_{12} \\ \Lambda_{21} & \Lambda_{22} \end{bmatrix}\begin{bmatrix} \Gamma_{11} & \Gamma_{12} \\ \Gamma_{21} & \Gamma_{22} \end{bmatrix};$$

$$\begin{bmatrix} \Lambda_{11} & \Lambda_{12} \\ \Lambda_{21} & \Lambda_{22} \end{bmatrix} = \frac{\begin{bmatrix} Đ_{13}\left(x_1 Đ_{23} + (1-x_1)Đ_{12}\right) & x_1 Đ_{23}\left(Đ_{13} - Đ_{12}\right) \\ x_2 Đ_{13}\left(Đ_{23} - Đ_{12}\right) & Đ_{23}\left(x_2 Đ_{13} + (1-x_2)Đ_{12}\right) \end{bmatrix}}{x_1 Đ_{23} + x_2 Đ_{13} + x_3 Đ_{12}} \tag{S30}$$

The determinant of $[B]$ for a ternary mixture is

$$|B| = \frac{x_1}{Đ_{12}Đ_{13}} + \frac{x_2}{Đ_{12}Đ_{23}} + \frac{x_3}{Đ_{13}Đ_{23}} = \frac{1}{|\Lambda|}; \quad |\Lambda| = \frac{Đ_{12}Đ_{13}Đ_{23}}{x_1Đ_{23}+x_2Đ_{13}+x_3Đ_{12}} \tag{S31}$$

The quantity $|\Lambda|^{1/2} = \sqrt{\frac{Đ_{12}Đ_{13}Đ_{23}}{x_1Đ_{23}+x_2Đ_{13}+x_3Đ_{12}}}$ can be interpreted as a measure of the "average" magnitude of M-S diffusivity in the ternary mixture.

For stable single phase fluid mixtures, we must have $|\Gamma| \geq 0$. In view of eq (S24) the condition of phase stability translates to

$$|D| \geq 0; \quad |\Gamma| \geq 0; \quad \text{phase stability} \tag{S32}$$

Equation (S32) implies that all the eigenvalues of the Fick matrix [D] are positive definite. It is interesting to note that thermodynamic stability considerations do not require the diagonal elements D_{ii} to be positive. If recourse is made to the kinetic theory of gases, it can be shown that the diagonal elements D_{ii} are individually positive for mixtures of ideal gases. The off-diagonal elements $D_{ij}(i \neq j)$ can be either positive or negative, even for ideal gas mixtures. Indeed, the sign of $D_{ij}(i \neq j)$ also depends on the component numbering.

The condition for phase stability in a binary fluid mixture is

$$D_{12} \geq 0; \quad \Gamma \geq 0; \quad \text{phase stability} \tag{S33}$$

The occurrence of $\Gamma < 0$ implies vapor/liquid or liquid/solid phase transitions.

2.6 Estimation procedures for the matrix [Λ]

For binary liquid mixtures, the Vignes interpolation[11, 12] is widely used to describe the composition dependence of the M-S diffusivity

$$Đ_{12} = \left(Đ_{12}^{x_1\to 1}\right)^{x_1}\left(Đ_{12}^{x_2\to 1}\right)^{x_2} \tag{S34}$$

where the limiting values of the M-S diffusivities are

$$D_{2,self}^{x_1\to 1} = Đ_{12}^{x_1\to 1}; \quad D_{1,self}^{x_2\to 1} = Đ_{12}^{x_2\to 1} \tag{S35}$$

Phenomenological relations for n-component diffusion

The infinite dilution self-diffusivities can be estimated using the Wilke-Chang, Tyn-Calus procedures that are described in detail by Taylor and Krishna.[2]

The description of the composition dependence of the M-S diffusivities $Đ_{ij}$ in liquid mixtures containing three or more species is much less developed. Krishna and van Baten[11] postulate that the M-S diffusivity of the *i-j* pair in the ternary *i-j-k* mixture depends on $D_{i,self}$ and $D_{j,self}$ in this mixture, but weighted with mole fractions on a *k*-free basis, i.e.

$$Đ_{ij} = \frac{x_i}{x_i + x_j} D_{j,self} + \frac{x_j}{x_i + x_j} D_{i,self} \tag{S36}$$

Each of the three M-S pair diffusivities $Đ_{ij}$ depends on six infinite dilution parameters

$$Đ_{12}^{x_1 \to 1}; \quad Đ_{12}^{x_2 \to 1}; \quad Đ_{13}^{x_1 \to 1}; \quad Đ_{13}^{x_3 \to 1}; \quad Đ_{23}^{x_2 \to 1}; \quad Đ_{23}^{x_3 \to 1} \tag{S37}$$

These limiting values of $Đ_{ij}$ at the edges of the ternary composition space are

$$\begin{aligned}
&Đ_{12}^{x_1 \to 1} = D_{2,self}^{x_1 \to 1}; \quad Đ_{12}^{x_2 \to 1} = D_{1,self}^{x_2 \to 1}; \quad Đ_{12}^{x_3 \to 1} = \frac{x_1}{x_1 + x_2} D_{2,self}^{x_3 \to 1} + \frac{x_2}{x_1 + x_2} D_{1,self}^{x_3 \to 1}; \\
&Đ_{13}^{x_1 \to 1} = D_{3,self}^{x_1 \to 1}; \quad Đ_{13}^{x_3 \to 1} = D_{1,self}^{x_3 \to 1}; \quad Đ_{13}^{x_2 \to 1} = \frac{x_1}{x_1 + x_3} D_{3,self}^{x_2 \to 1} + \frac{x_3}{x_1 + x_3} D_{1,self}^{x_2 \to 1}; \\
&Đ_{23}^{x_2 \to 1} = D_{3,self}^{x_2 \to 1}; \quad Đ_{23}^{x_3 \to 1} = D_{2,self}^{x_3 \to 1}; \quad Đ_{23}^{x_3 \to 1} = \frac{x_2}{x_2 + x_3} D_{3,self}^{x_1 \to 1} + \frac{x_3}{x_2 + x_3} D_{2,self}^{x_1 \to 1};
\end{aligned} \tag{S38}$$

Noting that the following limiting values hold

$$\begin{aligned}
&Đ_{12}^{x_1 \to 1} = D_{2,self}^{x_1 \to 1}; \quad Đ_{12}^{x_2 \to 1} = D_{1,self}^{x_2 \to 1}; \\
&Đ_{13}^{x_1 \to 1} = D_{3,self}^{x_1 \to 1}; \quad Đ_{13}^{x_3 \to 1} = D_{1,self}^{x_3 \to 1}; \\
&Đ_{23}^{x_2 \to 1} = D_{3,self}^{x_2 \to 1}; \quad Đ_{23}^{x_3 \to 1} = D_{2,self}^{x_3 \to 1};
\end{aligned} \tag{S39}$$

we derive

$$\begin{aligned}
&Đ_{12}^{x_1 \to 1} = D_{2,self}^{x_1 \to 1}; \quad Đ_{12}^{x_2 \to 1} = D_{1,self}^{x_2 \to 1}; \quad Đ_{12}^{x_3 \to 1} = \frac{x_1}{x_1 + x_2} Đ_{23}^{x_3 \to 1} + \frac{x_2}{x_1 + x_2} Đ_{13}^{x_3 \to 1}; \\
&Đ_{13}^{x_1 \to 1} = D_{3,self}^{x_1 \to 1}; \quad Đ_{13}^{x_3 \to 1} = D_{1,self}^{x_3 \to 1}; \quad Đ_{13}^{x_2 \to 1} = \frac{x_1}{x_1 + x_3} Đ_{23}^{x_2 \to 1} + \frac{x_3}{x_1 + x_3} Đ_{12}^{x_2 \to 1}; \\
&Đ_{23}^{x_2 \to 1} = D_{3,self}^{x_2 \to 1}; \quad Đ_{23}^{x_3 \to 1} = D_{2,self}^{x_3 \to 1}; \quad Đ_{23}^{x_3 \to 1} = \frac{x_2}{x_2 + x_3} Đ_{13}^{x_1 \to 1} + \frac{x_3}{x_2 + x_3} Đ_{12}^{x_1 \to 1};
\end{aligned} \tag{S40}$$

Equation (S40) is the proper estimation procedure for $Đ_{ij}^{x_j \to 1}$.

Phenomenological relations for n-component diffusion

For a ternary mixture, Wesselingh and Bollen[13] have suggested the following extension of the Vignes interpolation formula (S34)

$$Đ_{ij} = \left(Đ_{ij}^{x_i \to 1}\right)^{x_i} \left(Đ_{ij}^{x_j \to 1}\right)^{x_j} \left(Đ_{ij}^{x_k \to 1}\right)^{x_k} \tag{S41}$$

For the estimation of $Đ_{ij}^{x_k \to 1}$, the i - j pair diffusivity when both i and j are present in infinitely dilute concentrations. Krishna and van Baten[11] suggest the following extension of eq (S38)

$$\begin{aligned} Đ_{12}^{x_3 \to 1} &= \left(Đ_{13}^{x_3 \to 1}\right)^{x_1/(x_1+x_2)} \left(Đ_{23}^{x_3 \to 1}\right)^{x_2/(x_1+x_2)} \\ Đ_{13}^{x_2 \to 1} &= \left(Đ_{12}^{x_2 \to 1}\right)^{x_1/(x_1+x_3)} \left(Đ_{23}^{x_2 \to 1}\right)^{x_3/(x_1+x_3)} \\ Đ_{23}^{x_1 \to 1} &= \left(Đ_{12}^{x_1 \to 1}\right)^{x_2/(x_2+x_3)} \left(Đ_{13}^{x_1 \to 1}\right)^{x_3/(x_2+x_3)} \end{aligned} \tag{S42}$$

For the special case of an equimolar mixture we obtain

$$\begin{aligned} Đ_{12}^{x_3 \to 1} &= \sqrt{\left(Đ_{13}^{x_3 \to 1} Đ_{23}^{x_3 \to 1}\right)} \\ Đ_{13}^{x_2 \to 1} &= \sqrt{\left(Đ_{12}^{x_2 \to 1} Đ_{23}^{x_2 \to 1}\right)} \\ Đ_{23}^{x_3 \to 1} &= \sqrt{\left(Đ_{12}^{x_1 \to 1} Đ_{13}^{x_1 \to 1}\right)} \end{aligned} \tag{S43}$$

The simplified interpolation formula (S43) was proposed by Wesselingh and Bollen.[13]

The square root of the determinant $|\Lambda|^{1/2}$ may be viewed as a measure of the "magnitude" of the M-S diffusivity that characterizes diffusion in a ternary mixture.

$$|\Lambda|^{1/2} = \sqrt{\frac{Đ_{12} Đ_{13} Đ_{23}}{x_1 Đ_{23} + x_2 Đ_{13} + x_3 Đ_{12}}} \tag{S44}$$

Close to the regions of phase splitting, the thermodynamic coupling effects predominate and a simple procedure for the estimation of the Fick diffusivity matrix has been proposed[14]

$$[D] = |\Lambda|^{1/2} [\Gamma] \tag{S45}$$

The accuracy of the estimates using eq (S45) has been verified by comparison with a very wide range of MD simulations and experimental data. [14, 15]

2.7 List of Tables for Phenomenological relations for n-component diffusion

Table S1. Concentration measures

Concentration measure	units	Inter-relation, constraint
x_i, mole fraction of species i	-	$x_i = \frac{c_i}{c_t} = \frac{\frac{\omega_i}{M_i}}{\sum_{i=1}^{n} \frac{\omega_i}{M_i}} = \frac{\omega_i}{M_i}\overline{M}; \sum_{i=1}^{n} x_i = 1$
ω_i, mole fraction of species i	-	$\omega_i = \frac{\rho_i}{\rho_t} = \frac{x_i M_i}{\sum_{i=1}^{n} x_i M_i} = \frac{x_i M_i}{\overline{M}}; \sum_{i=1}^{n} \omega_i = 1$
c_i, molar density of species i	mol m^{-3}	$c_i = \frac{\rho_i}{M_i}; \sum_{i=1}^{n} c_i = c_t =$ mixture molar density$= \frac{1}{\overline{V}}$
ρ_i, mass density of species i	kg m^{-3}	$\rho_i = c_i M_i; \sum_{i=1}^{n} \rho_i = \rho_t =$ mixture mass density
M_i, molar mass of species i	kg mol^{-1}	$\overline{M} = \sum_{i=1}^{n} x_i M_i =$ mean molar mass of mixture
$\overline{V_i}$, partial molar volume of i	m^3 mol^{-1}	$\overline{V} = \sum_{i=1}^{n} x_i \overline{V_i} = \frac{1}{c_t} =$ mean molar volume of mixture
ϕ_i, volume fraction of species i	-	$\phi_i = c_i \overline{V_i}$
f_i, fugacity of species i	Pa	$\sum_{i=1}^{n} f_i = f_t =$ total mixture fugacity
μ_i, molar chemical potential of species i	J mol^{-1}	$\mu_i = \mu_i^0 + RT \ln f_i$

Table S2. Choice of reference velocity frame.

Reference velocity	Constraint on molar fluxes
$u = \sum_{i=1}^{n} x_i u_i =$ molar average mixture velocity	$\sum_{i=1}^{n} J_i = 0$
$v = \sum_{i=1}^{n} \omega_i u_i =$ mass average mixture velocity	$\sum_{i=1}^{n} \frac{\omega_i}{x_i} J_i = 0$
$u^V = \sum_{i=1}^{n} c_i \overline{V}_i u_i = \sum_{i=1}^{n} \phi_i u_i =$ volume average mixture velocity	$\sum_{i=1}^{n} \overline{V}_i J_i = 0$
$u_n = \sum_{i=1}^{n} \delta_{in} u_i =$ velocity of component n	$J_n = 0$

Table S3. Inter-relation between J_1 and j_1 for binary mixture

Molar fluxes	Mass fluxes
$J_1 = c_t x_1 (u_1 - u); u = x_1 u_1 + x_2 u_2$ $J_1 = c_t x_1 (u_1 - x_1 u_1 - x_2 u_2) = c_t x_1 x_2 (u_1 - u_2)$ $x_1 = \frac{\omega_1}{M_1}\overline{M}; x_2 = \frac{\omega_2}{M_2}\overline{M}; c_t = \frac{\rho_t}{\overline{M}}$ $J_1 = c_t x_1 x_2 (u_1 - u_2)$ $J_1 = \rho_t \omega_1 \omega_2 \frac{\overline{M}}{M_1 M_2}(u_1 - u_2) = \frac{\overline{M}}{M_1 M_2} j_1$	$j_1 = \rho_t \omega_1 (u_1 - v); v = \omega_1 u_1 + \omega_2 u_2$ $j_1 = \rho_t \omega_1 (u_1 - \omega_1 u_1 - \omega_2 u_2) = \rho_t \omega_1 \omega_2 (u_1 - u_2)$ $\omega_i = \frac{\rho_i}{\rho_t} = \frac{x_i M_i}{\sum_{i=1}^{n} x_i M_i} = \frac{x_i M_i}{\overline{M}}; \rho_t = c_t \overline{M}$ $j_1 = \rho_t \omega_1 \omega_2 (u_1 - u_2) = c_t x_1 x_2 (u_1 - u_2)$ $j_1 = c_t x_1 x_2 \frac{M_1 M_2}{\overline{M}}(u_1 - u_2) = \frac{M_1 M_2}{\overline{M}} J_1$
$dx_1 = \frac{\frac{1}{\overline{M_1 M_2}}}{\left(\frac{\omega_1}{M_1} + \frac{\omega_2}{M_2}\right)^2} d\omega_1; \quad d\omega_1 = \frac{M_1 M_2}{(x_1 M_1 + x_2 M_2)^2} dx_1$ $\frac{1}{\overline{M}} = \frac{\omega_1}{M_1} + \frac{\omega_2}{M_2}; \overline{M} = x_1 M_1 + x_2 M_2$ $dx_1 = \frac{\overline{M}^2}{M_1 M_2} d\omega_1; \quad d\omega_1 = \frac{M_1 M_2}{\overline{M}^2} dx_1$ $\frac{c_t}{\rho_t}\frac{x_1 x_2}{\omega_1 \omega_2} = \frac{\overline{M}}{M_1 M_2}$	
$J_1 = -c_t D_{12} \frac{dx_1}{dz};$ $dx_1 = \frac{\overline{M}^2}{M_1 M_2} d\omega_1; c_t = \frac{\rho_t}{\overline{M}}$ $J_1 = -\rho_t D_{12} \frac{\overline{M}}{M_1 M_2} \frac{d\omega_1}{dz}$ $\frac{M_1 M_2}{\overline{M}} J_1 = -\rho_t D_{12} \frac{d\omega_1}{dz} = j_1$	$j_1 = -\rho_t D_{12} \frac{d\omega_1}{dz}$ $d\omega_1 = \frac{M_1 M_2}{\overline{M}^2} dx_1; \rho_t = c_t \overline{M}$ $j_1 = -c_t D_{12} \frac{M_1 M_2}{\overline{M}} \frac{dx_1}{dz}$ $\frac{\overline{M}}{M_1 M_2} j_1 = -c_t D_{12} \frac{dx_1}{dz} = J_1$

2.1 List of Figures for Phenomenological relations for n-component diffusion

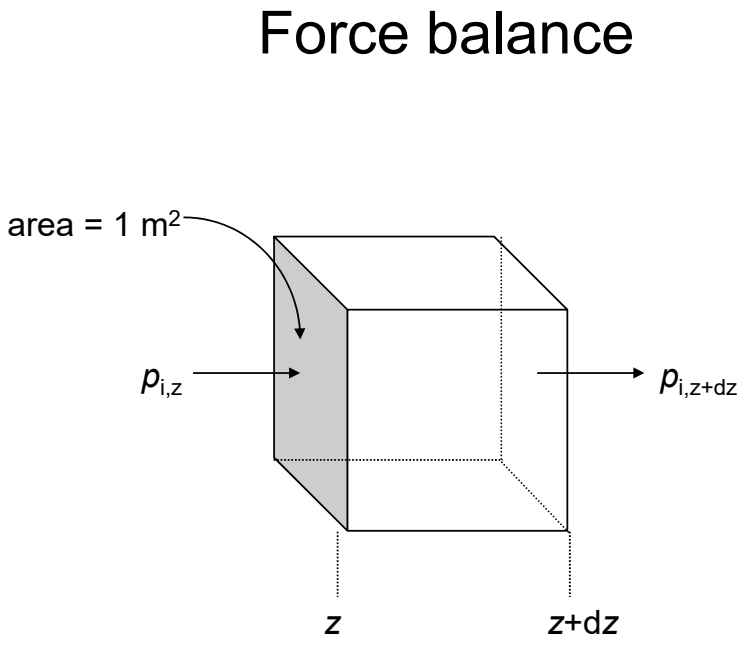

Figure S1. A force balance on a control volume containing an ideal gas mixture.

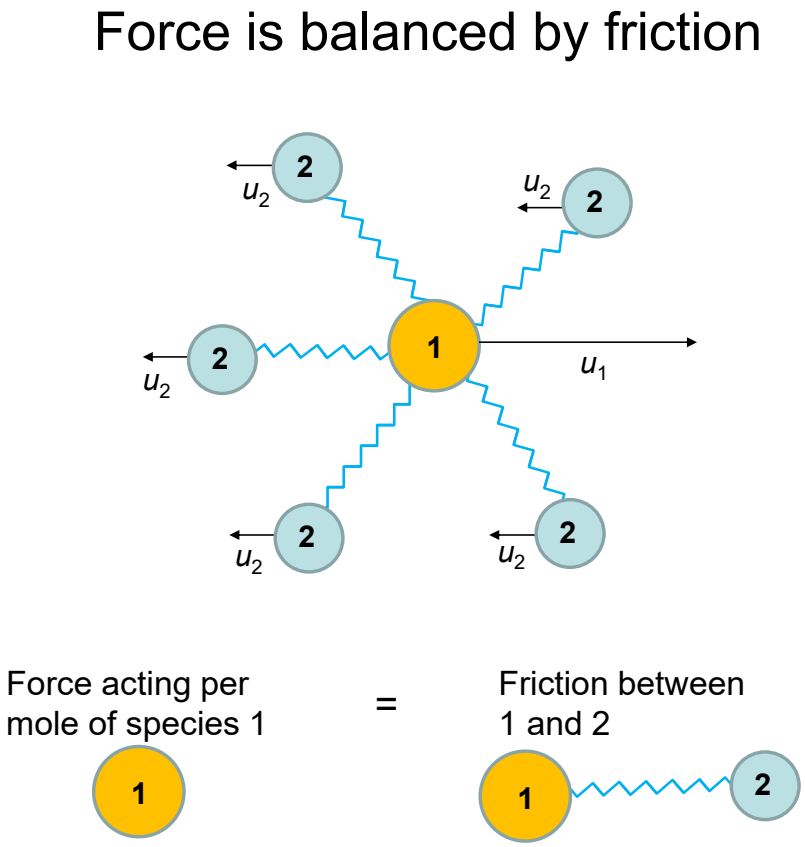

Figure S2. The force acting on each of the species in the diffusing binary mixture of species 1 and 2 is balanced by friction between the species 1 and 2.

3 Flory-Huggins description of polymer solution thermodynamics

The proper description of diffusion in polymer solutions is important in wide variety of contexts such as permeation across polymer membranes; for an introduction to this topic see Wesselingh and Krishna.[16] Diffusion in polymer solutions is strongly influenced by solution thermodynamics, that is most convenient described by the Flory-Huggins model. [16-18]

3.1 The Flory-Huggins model for polymer solutions

The Flory-Huggins equation in its simplest form deals with molecules that are similar chemically, but differ greatly in length. An example might be cross-linked polyethylene with the penetrant propane (C_3H_8). The Flory-Huggins model is based on the idea that the chain elements of the polymer arrange themselves randomly (but with the molecules remaining connected) on a three- dimensional lattice; see schematic in Figure S3. The guest species could be a solvent (e.g. acetone, toluene), or an anti-solvent such as water. The guest molecules are also termed "penetrants" in the context of polymer membrane permeation. In this article, we use the terms "solvent", "guest", and "penetrant" interchangeably, and referring to the same species.

The Flory-Huggins model does not take effects of crystallization or other inhomogeneities into account. The resulting equation for the activity of the penetrant is a simple function of the volume fraction of the penetrant in the membrane. We use ϕ_i to denote the volume fraction of the penetrant species *i*; the volume fraction of species *i* is $\phi_i = c_i \overline{V_i}$ where c_i is the molar concentration, and $\overline{V_i}$ is the partial molar volume of the penetrant species *i*. Other concentration measures are listed in Table S4. The use of mole fractions is not convenient for description of the thermodynamics of polymer solutions because the molar mass of the polymer chains are ill defined.[16]

The Flory-Huggins (F-H) model for binary mixture of solvent (1) and polymer (indicated by subscript m) is

$$\ln a_1 = \ln(\phi_1) + (1-\phi_1) - \phi_m \frac{\overline{V_1}}{\overline{V_m}} + \chi_{1m}\phi_m^2$$
$$\phi_m = 1-\phi_1 \qquad \text{(S46)}$$

Equation (S46) contains a non-ideality, or interaction parameter χ_{1m} that is assumed to be independent of the volume fraction. If $\chi_{1m} > 0$, the solvent and polymer repel, or dislike, each other. If $\chi_{1m} < 0$, the penetrant and polymer attract each other. If $\chi_{1m} = 0$, the solvent and polymer are similar in nature and there are no attractive or repulsive forces.

Figure S4 illustrates the influence of the interaction parameter χ_{1m} on the activity (a_1) and thermodynamic correction factor, $\Gamma = \frac{\partial \ln a_1}{\partial \ln \phi_1}$, that plays a pivotal role in diffusion. In these calculations, the ratio $\frac{\overline{V_1}}{\overline{V_m}} = 0$, i.e. the partial molar volume of the solvent is negligible in comparison to the molar volume of the polymer. If χ_{1m} is positive, the solution can split into two phases for a range of volume fractions, one rich in polymer and one rich in solvent; the demixing zone is indicated in cyan in Figure S4.

If the interaction parameter χ_{1m} is dependent on the volume fractions, the F-H model for unary systems needs to be extended as follows

$$\ln a_1 = \ln(\phi_1) + (1-\phi_1) - (1-\phi_1)\frac{\overline{V_1}}{\overline{V_m}} + \chi_{1m}(1-\phi_1)^2 + \phi_1(1-\phi_1)^2 \frac{\partial \chi_{1m}}{\partial \phi_1} \qquad \text{(S47)}$$

For ternary mixtures of two solvents (penetrants), 1 and 2, and the polymer (m), there are three interaction parameters in the F-H description of phase equilibrium: $\chi_{12}, \chi_{1m}, \chi_{2m}$. If each of the three interaction parameters $\chi_{12}, \chi_{1m}, \chi_{2m}$ are dependent on the volume fractions of the penetrants, ϕ_1, ϕ_2, the F-H model for the component activities a_1, a_2 of the penetrants in the polymer membrane (m) are

$$\begin{aligned}
\ln a_1 &= \ln(\phi_1) + (1-\phi_1) - \phi_2 \frac{\overline{V_1}}{\overline{V_2}} - \phi_m \frac{\overline{V_1}}{\overline{V_m}} + \left(\chi_{12}\phi_2 + \chi_{1m}\phi_m\right)\left(\phi_2 + \phi_m\right) - \chi_{2m}\frac{\overline{V_1}}{\overline{V_2}}\phi_2\phi_m - u_1u_2\phi_2\frac{\partial\chi_{12}}{\partial u_2} \\
&\quad - u_1u_2\phi_m\frac{\partial\chi_{1m}}{\partial u_2} - \phi_1\phi_m^2\frac{\partial\chi_{1m}}{\partial\phi_m} + \frac{\overline{V_1}}{\overline{V_2}}u_2^2\phi_m\frac{\partial\chi_{2m}}{\partial u_1} - \frac{\overline{V_1}}{\overline{V_2}}\phi_2\phi_m^2\frac{\partial\chi_{2m}}{\partial\phi_m} \\
\ln a_2 &= \ln(\phi_2) + (1-\phi_2) - \phi_1 \frac{\overline{V_2}}{\overline{V_1}} - \phi_m \frac{\overline{V_2}}{\overline{V_m}} + \left(\chi_{12}\phi_1\frac{\overline{V_2}}{\overline{V_1}} + \chi_{2m}\phi_m\right)\left(\phi_1 + \phi_m\right) - \chi_{1m}\frac{\overline{V_2}}{\overline{V_1}}\phi_1\phi_m + \frac{\overline{V_2}}{\overline{V_1}}u_1^2\phi_2\frac{\partial\chi_{12}}{\partial u_2} \\
&\quad + \frac{\overline{V_2}}{\overline{V_1}}u_1^2\phi_m\frac{\partial\chi_{1m}}{\partial u_2} - \frac{\overline{V_2}}{\overline{V_1}}\phi_1\phi_m^2\frac{\partial\chi_{1m}}{\partial\phi_m} - u_1u_2\phi_m\frac{\partial\chi_{2m}}{\partial u_1} - \phi_2\phi_m^2\frac{\partial\chi_{2m}}{\partial\phi_m}
\end{aligned} \tag{S48}$$

In eq (S48), we have defined $u_2 = \dfrac{\phi_2}{\phi_1+\phi_2}$; $\quad u_1 = 1-u_2 = \dfrac{\phi_1}{\phi_1+\phi_2}$; $\qquad \phi_m = 1-\left(\phi_1+\phi_2\right)$.

Equation (S48) corresponds precisely with equations (6) and (7) of Mulder et al.[19] The same set of extended equations are also given by Yang and Lue[20] and Varady et al.[21]

In the scenario in which the penetrant-polymer interaction parameters χ_{1m}, χ_{2m} are independent on the volume fractions of the penetrants, eq (S48) simplifies to yield

$$\begin{aligned}
\ln a_1 &= \ln(\phi_1) + (1-\phi_1) - \phi_2 \frac{\overline{V_1}}{\overline{V_2}} - \phi_m \frac{\overline{V_1}}{\overline{V_m}} + \left(\chi_{12}\phi_2 + \chi_{1m}\phi_m\right)\left(\phi_2 + \phi_m\right) - \chi_{2m}\frac{\overline{V_1}}{\overline{V_2}}\phi_2\phi_m - u_1u_2\phi_2\frac{\partial\chi_{12}}{\partial u_2} \\
\ln a_2 &= \ln(\phi_2) + (1-\phi_2) - \phi_1 \frac{\overline{V_2}}{\overline{V_1}} - \phi_m \frac{\overline{V_2}}{\overline{V_m}} + \left(\chi_{12}\phi_1\frac{\overline{V_2}}{\overline{V_1}} + \chi_{2m}\phi_m\right)\left(\phi_1 + \phi_m\right) - \chi_{1m}\frac{\overline{V_2}}{\overline{V_1}}\phi_1\phi_m + \frac{\overline{V_2}}{\overline{V_1}}u_1^2\phi_2\frac{\partial\chi_{12}}{\partial u_2}
\end{aligned} \tag{S49}$$

3.2 The Flory-Huggins model for liquid mixtures of two solvents

As a special (degenerate) case, eq (S48) can be applied to describe the component activities for binary *liquid phase* mixtures of two different solvents, 1 and 2. Let ϕ_1^L, ϕ_2^L represent the volume fractions of components 1 and 2 in the bulk liquid mixture. These volume fractions are related to the mass fractions ω_i^L in the bulk liquid mixture $\phi_i^L = \dfrac{\dfrac{\omega_i^L}{\rho_i^L}}{\displaystyle\sum_{i=1}^{n}\frac{\omega_i^L}{\rho_i^L}}$, where ρ_i^L is the liquid phase mass density of the penetrant species *i*. Other concentration measures, and inter-relations, are listed in Table S4. We also have the

constraint $\phi_1^L + \phi_2^L = 1$. The component activities in the liquid mixture are obtained from eq (S48) by omitting terms containing χ_{1m} and χ_{2m}, and setting $\phi_m = 0$; $\phi_1^L + \phi_2^L = 1$, and $u_2^L = \frac{\phi_2^L}{\phi_1^L + \phi_2^L} = \phi_2^L$:

$$\begin{aligned} \ln a_1^L &= \ln(\phi_1^L) + (1 - \frac{\overline{V_1}}{\overline{V_2}})\phi_2^L + \chi_{12}\left(\phi_2^L\right)^2 - \phi_1^L\left(\phi_2^L\right)^2 \frac{\partial \chi_{12}}{\partial \phi_2^L} \\ \ln a_2^L &= \ln(\phi_2^L) + (1 - \frac{\overline{V_2}}{\overline{V_1}})\phi_1^L + \frac{\overline{V_2}}{\overline{V_1}}\chi_{12}\left(\phi_1^L\right)^2 + \frac{\overline{V_2}}{\overline{V_1}}\phi_2^L\left(\phi_1^L\right)^2 \frac{\partial \chi_{12}}{\partial \phi_2^L} \end{aligned} \tag{S50}$$

Equation (S50) corresponds precisely with eqs (9), and (10) of Mulder et al.[19] The χ_{12} is related to the excess Gibbs free energy

$$\begin{aligned} \chi_{12} &= \frac{1}{x_1 \phi_2^L}\left[x_1 \ln(\frac{x_1}{\phi_1^L}) + x_2 \ln(\frac{x_2}{\phi_2^L}) + \frac{G^{excess}}{RT}\right] \\ \frac{G^{excess}}{RT} &= x_1 \ln(\gamma_1) + x_2 \ln(\gamma_2) \end{aligned} \tag{S51}$$

In eq (S51), x_1, x_2 are liquid phase mole fractions $x_i = \frac{c_i}{c_t} = \frac{\frac{\omega_i^L}{M_i}}{\sum_{i=1}^{n} \frac{\omega_i^L}{M_i}} = \frac{\omega_i^L}{M_i}\overline{M}$, where M_i is the molar mass of component *i* (units kg mol^{-1}), and $\overline{M} = \sum_{i=1}^{n} x_i M_i$ is the mean molar mass of the mixture; see Table S4.

The interaction parameter χ_{12} for mixtures such as water/ethanol are strongly dependent on the liquid mixture composition. The excess Gibbs free energy $\frac{G^{excess}}{RT} = x_1 \ln(\gamma_1) + x_2 \ln(\gamma_2)$ can be calculated from activity coefficient models such as that of Wilson, NRTL, and UNIQUAC.[19, 20] Mulder et al.[19] have also shown that the dependence of χ_{12} on the volume fractions of components in the bulk liquid mixture can be expressed as a fourth-order polynomial in $u_2^L = \frac{\phi_2^L}{\phi_1^L + \phi_2^L} = \phi_2^L$

$$\chi_{12} = a + b\left(u_2^L\right) + c\left(u_2^L\right)^2 + d\left(u_2^L\right)^3 + e\left(u_2^L\right)^4; \quad \text{bulk liquid mixture}$$
$$u_2^L = \frac{\phi_2^L}{\phi_1^L + \phi_2^L} = \phi_2^L; u_1^L = \frac{\phi_1^L}{\phi_1^L + \phi_2^L} = \phi_1^L = 1 - u_2^L = 1 - \phi_2^L \tag{S52}$$

The use of the fourth-order polynomial expression is particularly convenient for the evaluation of the derivative $\frac{\partial \chi_{12}}{\partial \phi_2^L}$ in eq (S50). The five coefficients, a, b, c, d, e can be determined by fitting of the Wilson, NRTL, and UNIQUAC models for $\frac{G^{excess}}{RT} = x_1 \ln(\gamma_1) + x_2 \ln(\gamma_2)$.

A significant contribution of Mulder et al.[19] is to demonstrate that the interaction parameter χ_{12} for the same two penetrants in the polymer matrix phase experiences the same composition dependence on the normalized volume fraction of component 2 within the polymeric solution: $u_2 = \frac{\phi_2}{\phi_1 + \phi_2}$, i.e.

$$\chi_{12} = a + b\left(u_2\right) + c\left(u_2\right)^2 + d\left(u_2\right)^3 + e\left(u_2\right)^4; \quad \text{polymer membrane phase}$$
$$u_2 = \frac{\phi_2}{\phi_1 + \phi_2}; u_1 = \frac{\phi_1}{\phi_1 + \phi_2} = 1 - u_2 \tag{S53}$$

3.3 List of Tables for Flory-Huggins description of polymer solution thermodynamics

Table S4. Concentration measures and inter-relationships.

Concentration measure	units	Inter-relation, constraint
x_i, mole fraction of species *i*	-	$x_i = \frac{c_i}{c_t} = \frac{\frac{\omega_i}{M_i}}{\sum_{i=1}^{n} \frac{\omega_i}{M_i}} = \frac{\omega_i}{M_i}\overline{M}; \sum_{i=1}^{n} x_i = 1$
ω_i, mole fraction of species *i*	-	$\omega_i = \frac{\rho_i}{\rho_t} = \frac{x_i M_i}{\sum_{i=1}^{n} x_i M_i} = \frac{x_i M_i}{\overline{M}}; \sum_{i=1}^{n} \omega_i = 1$
c_i, molar density of species *i*	mol m^{-3}	$c_i = \frac{\rho_i}{M_i}; \sum_{i=1}^{n} c_i = c_t = \text{mixture molar density} = \frac{1}{\overline{V}}$
ρ_i, mass density of species *i*	kg m^{-3}	$\rho_i = c_i M_i; \sum_{i=1}^{n} \rho_i = \rho_t = \text{mixture mass density}$
M_i, molar mass of species *i*	kg mol^{-1}	$\overline{M} = \sum_{i=1}^{n} x_i M_i = \text{mean molar mass of mixture}$
$\overline{V_i}$, partial molar volume of *i*	m^3 mol^{-1}	$\overline{V} = \sum_{i=1}^{n} x_i \overline{V_i} = \frac{1}{c_t} = \text{mean molar volume of mixture}$
ϕ_i, volume fraction of species *i*	-	$\phi_i = c_i \overline{V_i} = \frac{\frac{\omega_i}{\rho_i}}{\sum_{i=1}^{n} \frac{\omega_i}{\rho_i}}$

3.4 List of Figures for Flory-Huggins description of polymer solution thermodynamics

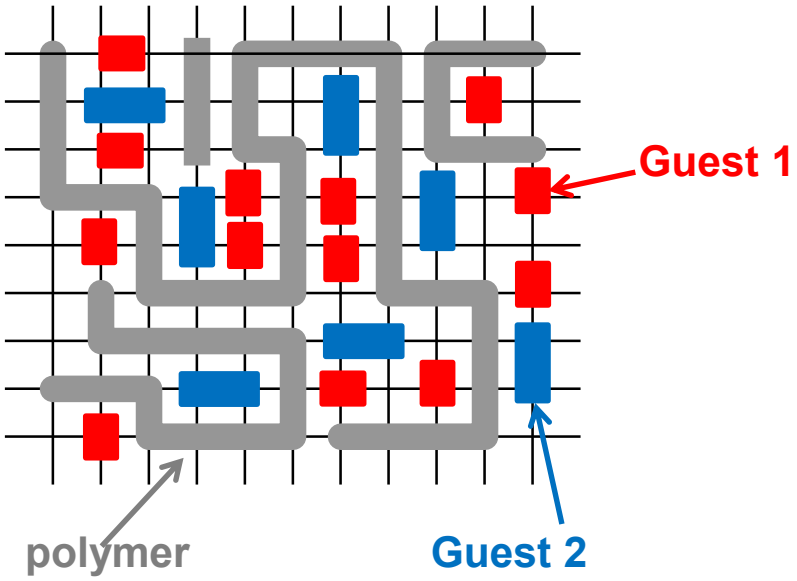

Figure S3. Schematic showing mixture permeation across polymeric membrane. The inset illustrates the Flory-Huggins lattice model.

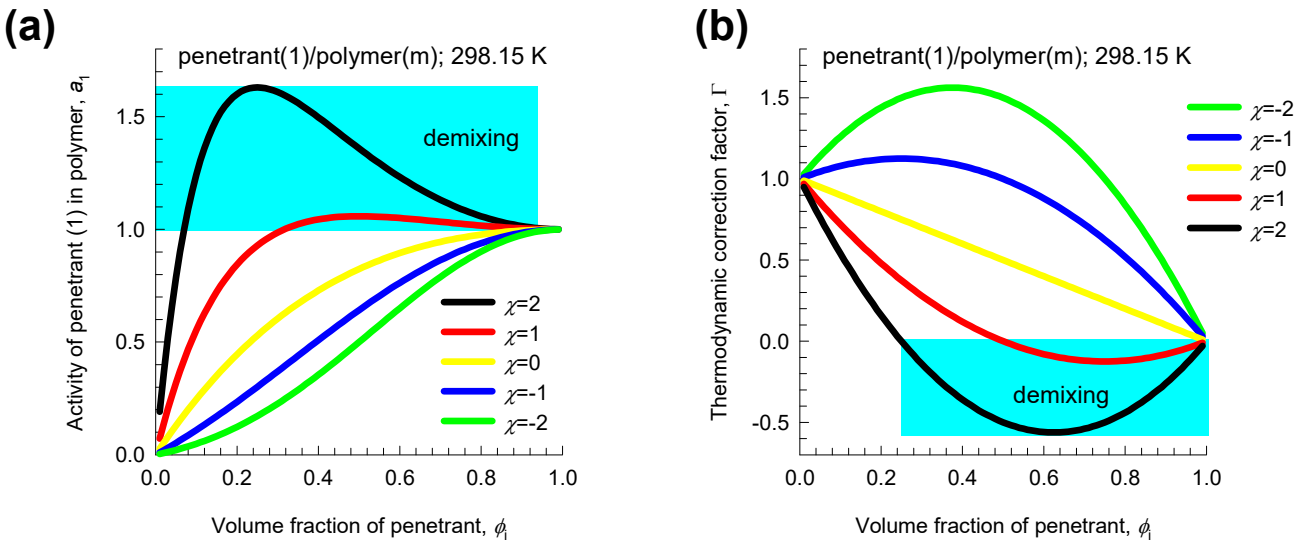

Figure S4. Influence of the interaction parameter on (a) the activity, a_1, and (b) thermodynamic correction factor, Γ. In these calculations, the ratio $\frac{\overline{V_1}}{V_m} = 0$, i.e. the molar volume of the penetrant is negligible in comparison to the molar volume of the polymer.

4 Diffusion in polymer solutions

4.1 The Maxwell-Stefan (M-S) description of diffusion in polymer solutions

We develop the Maxwell-Stefan (M-S) equations to describe the diffusion of *n* penetrants, 1, 2, 3,..*n* in a polymer matrix (m). The M-S equations represent a balance between the force exerted per mole of species *i* with the drag, or friction, experienced with each of the partner species in the mixture. We may expect that the frictional drag to be proportional to differences in the velocities of the diffusing species $(u_i - u_j)$, where u_i is the velocity of motion of the penetrant *i*. For diffusion in multicomponent polymer solutions such as acetone/cellulose acetate, $u_m \neq 0$, i.e. the polymer chains have a finite velocity of diffusion. For a mixture containing a total of *n* penetrants, 1, 2, 3,..*n* we write

$$
\begin{aligned}
-\frac{d\mu_1}{dz} &= \frac{RT}{Đ_{12}} X_2(u_1 - u_2) + \frac{RT}{Đ_{13}} X_3(u_1 - u_3) + \ldots + \frac{RT}{Đ_{1m}} X_m(u_1 - u_m) \\
-\frac{d\mu_2}{dz} &= \frac{RT}{Đ_{21}} X_1(u_2 - u_1) + \frac{RT}{Đ_{23}} X_3(u_2 - u_3) + \ldots + \frac{RT}{Đ_{2m}} X_m(u_2 - u_m) \\
&\cdots\cdots \\
-\frac{d\mu_n}{dz} &= \frac{RT}{Đ_{n1}} X_1(u_n - u_1) + \frac{RT}{Đ_{n2}} X_2(u_n - u_3) + \ldots + \frac{RT}{Đ_{nm}} X_m(u_n - u_m) \\
-\frac{d\mu_m}{dz} &= \frac{RT}{Đ_{m1}} X_1(u_m - u_1) + \frac{RT}{Đ_{m2}} X_2(u_m - u_3) + \ldots + \frac{RT}{Đ_{mn}} X_n(u_m - u_n)
\end{aligned}
\qquad \text{(S54)}
$$

The left members of eqs (S54) are the negative of the gradients of the chemical potentials, with the units N mol^{-1}; they represent the driving force acting per mole of species 1, and 2. The subscript m refers to the polymer chain, that is regarded as the (*n*+1)*th* component in the mixture. The term $RT/Đ_{im}$ is interpreted as the drag or friction coefficient between the penetrant *i* and the polymer. The term $RT/Đ_{ij}$ is interpreted as the friction coefficient for the *i-j* pair of penetrants. The multiplier X_j in each of the right members represents a measure of the composition of component *j* in the mixture because we expect the friction to be dependent on the number of molecules of *j* relative to that of component *i*.

There are many possible choices for composition measures X_i.

Mole fractions, x_i

Molar concentrations, c_i

Mass fractions, ω_i

Partial mass densities, ρ_i

Volume fractions, ϕ_i

The inter-relations between these concentration measures are provided in Table S4.

Written in terms of mole fractions, x_i, eqs (S54) are

$$
\begin{aligned}
-\frac{d\mu_1}{dz} &= \frac{RT}{Đ_{12}} x_2(u_1 - u_2) + \frac{RT}{Đ_{13}} x_3(u_1 - u_3) + \ldots + \frac{RT}{Đ_{1m}} x_m(u_1 - u_m) \\
-\frac{d\mu_2}{dz} &= \frac{RT}{Đ_{21}} x_1(u_2 - u_1) + \frac{RT}{Đ_{23}} x_3(u_2 - u_3) + \ldots + \frac{RT}{Đ_{2m}} x_m(u_2 - u_m) \\
&\cdots\cdots \\
-\frac{d\mu_n}{dz} &= \frac{RT}{Đ_{n1}} x_1(u_n - u_1) + \frac{RT}{Đ_{n2}} x_2(u_n - u_3) + \ldots + \frac{RT}{Đ_{nm}} x_m(u_n - u_m) \\
-\frac{d\mu_m}{dz} &= \frac{RT}{Đ_{m1}} x_1(u_m - u_1) + \frac{RT}{Đ_{m2}} x_2(u_m - u_3) + \ldots + \frac{RT}{Đ_{mn}} x_n(u_m - u_n)
\end{aligned}
\tag{S55}
$$

Only n of the chemical potential gradients $\frac{d\mu_i}{dz}$ are independent, because of the Gibbs-Duhem relationship

$$x_1 \frac{d\mu_1}{dz} + x_2 \frac{d\mu_2}{dz} + \cdots x_n \frac{d\mu_n}{dz} + x_m \frac{d\mu_m}{dz} = 0 \tag{S56}$$

The M-S formulation is consistent with the theory of irreversible thermodynamics. The Onsager Reciprocal Relations imply that the M-S pair diffusivities are symmetric

$$Đ_{ij} = Đ_{ji} \tag{S57}$$

Written in terms of volume fractions, the n independent chemical potential gradients are related to the velocity differences as follows

$$-\frac{1}{RT}\frac{d\mu_i}{dz}=\sum_{\substack{j=1\\ j\neq i}}^{n}\frac{\phi_j\left(u_i-u_j\right)}{Đ_{ij}^{V}}+\frac{\phi_m\left(u_i-u_m\right)}{Đ_{im}^{V}};\quad i=1,2,...n$$
$$-\phi_i\frac{1}{RT}\frac{d\mu_i}{dz}=\sum_{\substack{j=1\\ j\neq i}}^{n}\frac{\phi_i\phi_j\left(u_i-u_j\right)}{Đ_{ij}^{V}}+\frac{\phi_i\phi_m\left(u_i-u_m\right)}{Đ_{im}^{V}};\quad i=1,2,...n \tag{S58}$$

The modified M-S diffusivities $Đ_{ij}^{V}$ are related to the M-S diffusivities $Đ_{ij}=Đ_{ji}$, defined in terms of mole fractions, by: $c_t Đ_{ij}\overline{V_j}=\frac{Đ_{ij}\overline{V_j}}{\overline{V}}=Đ_{ij}^{V}$, and $c_t Đ_{im}\overline{V_m}=\frac{Đ_{im}\overline{V_m}}{\overline{V}}=Đ_{im}^{V}$. The symmetry constraint imposed by the Onsager Reciprocal Relations is

$$Đ_{ij}=\frac{Đ_{ij}^{V}}{\overline{V_j}}\overline{V}=Đ_{ji}=\frac{Đ_{ji}^{V}}{\overline{V_i}}\overline{V};\quad \frac{Đ_{ji}^{V}}{\overline{V_i}}=\frac{Đ_{ij}^{V}}{\overline{V_j}} \tag{S59}$$

It is important to note that the modified M-S diffusivities $Đ_{ij}^{V}$ are *not* symmetric. Specifically, for a ternary mixture of penetrants 1, 2, and polymer (m), the symmetry constraint demanded by the Onsager Reciprocal Relations is

$$\frac{Đ_{21}^{V}}{\overline{V_1}}=\frac{Đ_{12}^{V}}{\overline{V_2}} \tag{S60}$$

We define the *volumetric* flux of component *i* in a laboratory-fixed reference frame, expressed as m^3 m^{-2} s^{-1}

$$N_i^{V}=\phi_i u_i \tag{S61}$$

The corresponding *molar* flux of component *i*, in a laboratory-fixed reference frame, expressed as mol m^{-2} s^{-1} is $N_i=c_i u_i=\frac{\phi_i}{\overline{V_i}}u_i=\frac{N_i^{V}}{\overline{V_i}}$.

Let us define the volumetric diffusion fluxes J_i^{V} relative to the volume average velocity of the mixture u^{V},

$$
\begin{aligned}
&J_i^V = \phi_i\left(u_i - u^V\right); \quad \sum_{i=1}^{n} J_i^V + J_m^V = 0 \\
&J_m^V = \phi_m\left(u_m - u^V\right) = -J_1^V - J_2^V - \ldots - J_3^V; \\
&u^V = \phi_1 u_1 + \phi_2 u_2 \ldots + \phi_n u_n + \phi_m u_m
\end{aligned}
\tag{S62}
$$

Equation (S58) can be re-written in terms of the volumetric diffusion fluxes J_i^V

$$
-\phi_i \frac{1}{RT}\frac{d\mu_i}{dz} = \sum_{\substack{j=1 \\ j\neq i}}^{n} \frac{\left(\phi_j J_i^V - \phi_i J_j^V\right)}{Đ_{ij}^V} + \frac{\left(\phi_m J_i^V - \phi_i J_m^V\right)}{Đ_{im}^V}; \quad i = 1, 2, \ldots n \tag{S63}
$$

It is helpful to express the chemical potential gradients in terms of the volume fraction gradients by introducing an $n\times n$ dimensional matrix of thermodynamic factors $[\Gamma]$:

$$
\frac{\phi_i}{RT}\frac{d\mu_i}{dz} = \phi_i \frac{d\ln a_i}{dz} = \sum_{j=1}^{j=n} \Gamma_{ij}\frac{d\phi_j}{dz}; \qquad \Gamma_{ij} = \frac{\phi_i}{\phi_j}\frac{\partial \ln a_i}{\partial \ln \phi_j}; \quad i, j = 1, ,..n \tag{S64}
$$

Let us define an $n\times n$ dimensional square matrix $[B]$

$$
B_{ii} = \frac{\phi_i}{Đ_{im}^V} + \sum_{\substack{k=1 \\ k\neq i}}^{n} \frac{\phi_k}{Đ_{ik}^V} + \frac{\phi_m}{Đ_{im}^V}; \quad B_{ij(i\neq j)} = \phi_i\left(\frac{1}{Đ_{ij}^V} - \frac{1}{Đ_{im}^V}\right) \tag{S65}
$$

It is also convenient to define an $n\times n$ dimensional square matrix

$$
[\Lambda] = [B]^{-1} \tag{S66}
$$

Combining eqs (S63), (S64), and (S65) we may write an explicit expression for the volumetric diffusion fluxes J_i^V, expressed in n dimensional matrix notation

$$
\begin{aligned}
&\left(J^V\right) = -[B]^{-1}[\Gamma]\frac{d(\phi)}{dz}; \quad [\Lambda] = [B]^{-1}; \\
&\left(J^V\right) = -[\Lambda][\Gamma]\frac{d(\phi)}{dz}
\end{aligned}
\tag{S67}
$$

The $n\times n$ dimensional square matrix of Fick diffusivities $\left[D^V\right]$ may be defined

$$
\left[D^V\right] = [\Lambda][\Gamma] \tag{S68}
$$

4.2 Bearman friction formulation, and comparisons with M-S formulations

In the vast literature on diffusion in polymer solutions,[22, 23] it is customary to use the friction formulation for multicomponent diffusion in polymer solutions; this formulation, normally credited to Bearman,[24] is written in the following manner that is equivalent to equation (1) of Price and Romdhane[23]

$$
\begin{aligned}
&-\frac{d\mu_i}{dz} = \sum_{\substack{j=1 \\ j\neq i}}^{n} \frac{\rho_j}{M_j}\varsigma_{ij}\left(u_i - u_j\right) + \frac{\rho_m}{M_m}\varsigma_{im}\left(u_i - u_m\right); \quad i = 1\ldots\ldots n \\
&\frac{\rho_i}{M_i} = c_i; \quad i = 1\ldots\ldots n \\
&-\frac{d\mu_i}{dz} = \sum_{\substack{j=1 \\ j\neq i}}^{n} c_j\varsigma_{ij}\left(u_i - u_j\right) + c_m\varsigma_{im}\left(u_i - u_m\right); \quad i = 1\ldots\ldots n
\end{aligned}
\tag{S69}
$$

Comparing with the Maxwell-Stefan formulation (S58), we can derive the following inter-relations between the friction coefficients $\varsigma_{ij}, \varsigma_{im}$ in the Bearman eq (S69) and the modified M-S diffusivities $Đ_{ij}^{V}$

$$
\begin{aligned}
&\frac{\rho_j\varsigma_{ij}}{RTM_j} = \frac{\phi_j}{Đ_{ij}^{V}}; \quad \frac{\rho_m\varsigma_{im}}{RTM_m} = \frac{\phi_m}{Đ_{im}^{V}} \\
&\varsigma_{ij} = \frac{1}{c_j}\frac{RT\phi_j}{Đ_{ij}^{V}} = \frac{RT\overline{V}_j}{Đ_{ij}^{V}}; \quad \varsigma_{im} = \frac{1}{c_m}\frac{RT\phi_m}{Đ_{im}^{V}} = \frac{RT\overline{V}_m}{Đ_{im}^{V}}
\end{aligned}
\tag{S70}
$$

The symmetry constraint imposed by the Onsager Reciprocal Relations is

$$
\begin{aligned}
&\frac{Đ_{ji}^{V}}{\overline{V}_i} = \frac{Đ_{ij}^{V}}{\overline{V}_j}; \quad \varsigma_{ij} = \varsigma_{ji} \\
&\frac{Đ_{ij}^{V}}{RT\overline{V}_j} = \frac{\phi_j M_j}{\rho_j\overline{V}_j}\frac{1}{\varsigma_{ij}} = \frac{1}{\varsigma_{ij}} = \frac{Đ_{ji}^{V}}{RT\overline{V}_i} = \frac{\phi_i M_i}{\rho_i\overline{V}_i}\frac{1}{\varsigma_{ji}} = \frac{1}{\varsigma_{ji}}; \\
&\varsigma_{ij} = \frac{RT\overline{V}_j}{Đ_{ij}^{V}}\frac{\rho_j\overline{V}_j}{\phi_j M_j} = \frac{RT\overline{V}_j}{Đ_{ij}^{V}}; \quad \varsigma_{ji} = \frac{RT\overline{V}_i}{Đ_{ji}^{V}}\frac{\rho_i\overline{V}_i}{\phi_i M_i} = \frac{RT\overline{V}_i}{Đ_{ji}^{V}}
\end{aligned}
\tag{S71}
$$

For a binary solution consisting of solvent (1) and polymer (m), the Bearman eq (S69) reduces to

$$-\frac{d\mu_1}{dz}=\frac{\rho_m}{M_m}\varsigma_{1m}\left(u_1-u_m\right)=c_m\varsigma_{1m}\left(u_1-u_m\right)$$
$$\varsigma_{1m}=\frac{M_m}{\rho_m}\frac{RT\phi_m}{Đ_{1m}^V}=\frac{1}{c_m}\frac{RT\phi_m}{Đ_{1m}^V}=\frac{RT\overline{V}_m}{Đ_{1m}^V} \tag{S72}$$

4.3 Diffusion in binary polymer solutions

Let us start by considering a binary solution consisting of solvent (1) and polymer (m). Equation (S58) simplifies to yield

$$-\phi_1\frac{1}{RT}\frac{d\mu_1}{dz}=\frac{\left(\phi_1\phi_m u_1-\phi_1\phi_m u_m\right)}{Đ_{1m}^V}=\frac{\left(\phi_m N_1^V-\phi_1 N_m^V\right)}{Đ_{1m}^V}=\frac{\left(\phi_m J_1^V-\phi_1 J_m^V\right)}{Đ_{1m}^V} \tag{S73}$$

The J_1^V, J_m^V are the volumetric diffusion fluxes relative to the volume average velocity of the mixture

$$J_1^V=\phi_1\left(u_1-u^V\right);\quad J_m^V=\phi_m\left(u_m-u^V\right);\quad u^V=\phi_1u_1+\phi_m u_m;\quad J_1^V=-J_m^V;\quad \phi_1+\phi_m=1 \tag{S74}$$

In view of $J_1^V=-J_m^V;\quad \phi_1+\phi_m=1$, we may re-write eq (S73) as

$$J_1^V=-Đ_{1m}^V\phi_1\frac{1}{RT}\frac{d\mu_1}{dz}=-Đ_{1m}^V\left(\frac{\partial\ln a_1}{\partial\ln\phi_1}\right)\frac{d\phi_1}{dz}=-D_1^V\frac{d\phi_1}{dz} \tag{S75}$$

where $\Gamma=\dfrac{\partial\ln a_1}{\partial\ln\phi_1}$ is the thermodynamic correction factor, and $D_1^V=Đ_{1m}^V\dfrac{\partial\ln a_1}{\partial\ln\phi_1}$ is the Fick diffusivity.

An alternative flux expression is often used in the literature to describe for diffusion in polymer solutions: the mass fluxes, j_i^V, kg m^{-2} s^{-1}, relative to the volume average velocity of the mixture, are expressed as a linear function of the mass concentration gradients.[23] For the specific case of a binary solvent/polymer system

$$j_1^V=\rho_1\left(u_1-u^V\right)=\phi_1\frac{M_1}{\overline{V}_1}\left(u_1-u^V\right)=\frac{M_1}{\overline{V}_1}J_1^V=-D_1\frac{d\rho_1}{dz} \tag{S76}$$

Combining eqs (S72), (S75), and (S76) we obtain

$$
\begin{aligned}
&j_1^V = \frac{M_1}{\overline{V_1}} J_1^V = -Đ_{1m}^V \frac{M_1}{\overline{V_1}} \phi_1 \frac{1}{RT} \frac{d\mu_1}{dz}; \\
&Đ_{1m}^V = \overline{V_m} \frac{RT}{\varsigma_{1m}} \\
&j_1^V = -\overline{V_m} \frac{RT}{\varsigma_{1m}} \frac{M_1}{\overline{V_1}} \phi_1 \frac{1}{RT} \frac{d\mu_1}{dz} = -\overline{V_m} \frac{\rho_1}{\varsigma_{1m}} \frac{d\mu_1}{dz} = -\overline{V_m} \frac{\rho_1}{\varsigma_{1m}} \left(\frac{\partial \mu_1}{\partial \rho_1} \right) \frac{d\rho_1}{dz} = -D_1 \frac{d\rho_1}{dz}
\end{aligned}
\tag{S77}
$$

The Fick diffusivity, D_1, defined in eq (S75) is relatable to the Bearman friction coefficient, and the modified Maxwell-Stefan diffusivity:

$$
\begin{aligned}
&D_1 = \frac{\overline{V_m} \rho_1}{\varsigma_{1m}} \frac{\partial \mu_1}{\partial \rho_1} = \frac{\overline{V_m} RT}{\varsigma_{1m}} \left(\frac{\rho_1}{RT} \frac{\partial \mu_1}{\partial \rho_1} \right) = \frac{\overline{V_m} \rho_m}{\phi_m M_m} Đ_{1m}^V \left(\frac{\rho_1}{RT} \frac{\partial \mu_1}{\partial \rho_1} \right) = Đ_{1m}^V \left(\frac{\rho_1}{RT} \frac{\partial \mu_1}{\partial \rho_1} \right) \\
&\left(\frac{\rho_1}{RT} \frac{\partial \mu_1}{\partial \rho_1} \right) = \left(\frac{\partial \ln a_1}{\partial \ln \phi_1} \right) \left(\frac{\partial \ln \phi_1}{\partial \ln \rho_1} \right) \\
&D_1 = Đ_{1m}^V \left(\frac{\partial \ln a_1}{\partial \ln \phi_1} \right) \left(\frac{\partial \ln \phi_1}{\partial \ln \rho_1} \right)
\end{aligned}
\tag{S78}
$$

In eq (S78), we have used the equalities $\phi_m = c_m \overline{V_m} = \frac{\overline{V_m} \rho_m}{M_m}$. The thermodynamic correction factor $\left(\frac{\rho_1}{RT} \frac{\partial \mu_1}{\partial \rho_1} \right) = \left(\frac{\partial \ln a_1}{\partial \ln \phi_1} \right) \left(\frac{\partial \ln \phi_1}{\partial \ln \rho_1} \right)$ can be determined from the Flory-Huggins theory. From eqs (S75), and (S78), we note that the Fick diffusivities D_1^V and D_1 are defined in two different ways

$$
\begin{aligned}
&J_1^V = -Đ_{1m}^V \Gamma \frac{d\phi_1}{dz} = -D_1^V \frac{d\phi_1}{dz} \\
&j_1^V = -D_1 \frac{d\rho_1}{dz}
\end{aligned}
\tag{S79}
$$

The D_1^V and D_1 are not precisely identical but inter-related by $D_1 = \left(\frac{\partial \ln \phi_1}{\partial \ln \rho_1} \right) D_1^V$. Often, the simplification can be made that the correction factor $\left(\frac{\partial \ln \phi_1}{\partial \ln \rho_1} \right) \approx 1$.

4.4 Self-diffusivity in binary penetrant/polymer solutions

It is also common in the polymer diffusion literature, to relate the Fick diffusivity D_1 to the self-diffusivity, $D_{1,self}$. The rationale for this is that the free volume theory allows prediction of self-diffusivity, $D_{1,self}$.[16, 22, 25] The relation between D_1 and $D_{1,self}$ requires careful and rigorous derivation. We start with the Bearman eq (S69) and apply it to a ternary mixture containing species 1, tagged species 1*, and polymer (m). The tagged species 1* is identical to species 1 with respect to thermodynamics and diffusion. This results in the following expression for $D_{1,self}$

$$\frac{1}{D_{1,self}} = \frac{\rho_1}{RTM_1}\varsigma_{11} + \frac{\rho_m}{RTM_m}\varsigma_{1m} \tag{S80}$$

From eq (S72) we have the equalities $\frac{\rho_m}{RTM_m}\varsigma_{1m} = \frac{\phi_m}{Đ^V_{1m}}; \frac{\rho_1}{RTM_1}\varsigma_{11} = \frac{\phi_1}{Đ^V_{11}}$; so, we derive the following expression in terms of the M-S diffusivities

$$\frac{1}{D_{1,self}} = \frac{\phi_1}{Đ^V_{11}} + \frac{\phi_m}{Đ^V_{1m}} \tag{S81}$$

The $Đ^V_{11}$ is the self-exchange coefficient, and represents the self-diffusivity of pure 1; this can be estimated using the procedure such as Wilke-Chang.[9, 26, 27] In view of eq (S81) we find $Đ^V_{1m} = \phi_m D_{1,self}$ for the case of negligible 1-1 friction.

The corresponding expressions for the self-diffusivity of the polymer (m) are

$$\begin{aligned}
&\frac{1}{D_{m,self}} = \frac{\rho_m}{RTM_m}\varsigma_{mm} + \frac{\rho_1}{RTM_1}\varsigma_{1m} = \frac{\phi_m}{Đ^V_{mm}} + \frac{\phi_1}{Đ^V_{1m}} \\
&\frac{\rho_m}{RTM_m}\varsigma_{mm} = \frac{\phi_m}{Đ^V_{mm}}; \frac{\rho_1}{RTM_1}\varsigma_{1m} = \frac{\phi_1}{Đ^V_{1m}} \\
&\varsigma_{mm} = \frac{RT\overline{V_m}}{Đ^V_{mm}}; \varsigma_{1m} = \frac{RT\overline{V_1}}{Đ^V_{1m}}
\end{aligned} \tag{S82}$$

Combining eqs (S78) and (S80) we obtain

$$D_1 = Đ_{1m}^V \left(\frac{\rho_1}{RT} \frac{\partial \mu_1}{\partial \rho_1} \right) = \frac{\phi_m}{\left(\frac{1}{D_{1,self}} - \frac{\phi_1}{Đ_{11}^V} \right)} \left(\frac{\rho_1}{RT} \frac{\partial \mu_1}{\partial \rho_1} \right) \tag{S83}$$

Equation (S83) is precisely equivalent to equation (8) of Price and Romdhane;[23] Readers should note the differences in the notations used here and in the paper of Price and Romdhane:[23] the equivalence in

the notations are:
- Fick diffusivity $D_1 \equiv D_{11}$ of Price and Romdhane
- Self-diffusivity $D_{1,self} \equiv D_1$ of Price and Romdhane
- Self-exchange coefficient $\frac{Đ_{11}^V}{\phi_1} \equiv D_1^*$ of Price and Romdhane

For the limiting case of dilute solvent (species 1) in polymer (m) solutions, i.e. $\phi_1 << \phi_m$, we obtain

$$D_1 = Đ_{1m}^V \left(\frac{\rho_1}{RT} \frac{\partial \mu_1}{\partial \rho_1} \right) \approx \phi_m D_{1,self} \left(\frac{\rho_1}{RT} \frac{\partial \mu_1}{\partial \rho_1} \right) \tag{S84}$$

Equation (S84) is equivalent to equation (11) of Price and Romdhane.[23] The thermodynamic correction factor $\left(\frac{\rho_1}{RT} \frac{\partial \mu_1}{\partial \rho_1} \right) = \left(\frac{\partial \ln a_1}{\partial \ln \phi_1} \right) \left(\frac{\partial \ln \phi_1}{\partial \ln \rho_1} \right)$ can be determined from the Flory-Huggins theory. Often, the simplification can be made that the correction factor $\left(\frac{\partial \ln \phi_1}{\partial \ln \rho_1} \right) \approx 1$. We have the following inter-relations between the Bearman coefficients and M-S modified diffusivities

$$\begin{aligned}
&\varsigma_{1m} = \frac{\phi_m}{Đ_{1m}^V} \frac{RTM_m}{\rho_m} = \frac{RT\overline{V_m}}{Đ_{1m}^V}; \varsigma_{11} = \frac{\phi_1}{Đ_{11}^V} \frac{RTM_1}{\rho_1} = \frac{RT\overline{V_1}}{Đ_{11}^V} \\
&\varsigma_{mm} = \frac{\phi_m}{Đ_{mm}^V} \frac{RTM_m}{\rho_m} = \frac{RT\overline{V_m}}{Đ_{mm}^V}; \varsigma_{1m} = \frac{\phi_1}{Đ_{1m}^V} \frac{RTM_1}{\rho_1} = \frac{RT\overline{V_1}}{Đ_{1m}^V} \\
&\frac{\rho_m \varsigma_{1m}}{RTM_m} = \frac{\phi_m}{Đ_{1m}^V}; \frac{\rho_1 \varsigma_{11}}{RTM_1} = \frac{\phi_1}{Đ_{11}^V} \\
&\frac{\rho_m \varsigma_{mm}}{RTM_m} = \frac{\phi_m}{Đ_{mm}^V}; \frac{\rho_1 \varsigma_{1m}}{RTM_1} = \frac{\phi_1}{Đ_{1m}^V}
\end{aligned} \tag{S85}$$

From experiments, we can determine the Fick diffusivity D_1, along with the self-diffusivities $D_{1,self}$, and $D_{m,self}$ of solvent (1) and polymer (m). As illustration, Figure S5a shows the experimental data as reported in Figure 6 of Zielinski[28] for the self-diffusivities of toluene (1), and polystyrene (m) in polystyrene at 383 K as a function of the mass fraction of toluene. Also shown are the data for the Fick (mutual) diffusivity, D_1. The plotted data are those obtained from *five* different types of measurement techniques. There is a variation of about six orders of magnitude in the diffusivity values as a function of the mass fraction, ω_1. This strong variation renders the task of predicting, or estimating, diffusivities in polymer solutions an extremely difficult one.

A further point to note in the experimental data for $0.5 < \omega_1 < 1.0$ is that Fick diffusivity D_1 is lower than the self-diffusivity of toluene, $D_{1,self}$ by about 1-2 orders of magnitude. We calculate the thermodynamic correction factor, $\left(\frac{\rho_1}{RT}\frac{\partial \mu_1}{\partial \rho_1}\right)$, taking $\chi = 0.354$; see Figure S5b. There is a strong reduction in $\left(\frac{\rho_1}{RT}\frac{\partial \mu_1}{\partial \rho_1}\right)$, by about one to three orders of magnitude as $\omega_1 \to 1$.

Figure S5c compares the M-S diffusivity, calculated using $Đ_{1m}^{V} = D_1 \Big/ \left(\frac{\rho_1}{RT}\frac{\partial \mu_1}{\partial \rho_1}\right)$, with D_1, $D_{1,\text{self}}$, and $D_{2,\text{self}}$. We note that $Đ_{1m} \approx D_{1,self}$; this implies that the 1-1 friction is not of significant importance.

4.5 Free-volume theory for self-diffusivity in binary penetrant/polymer solutions

The free-volume theory[16, 22, 25] is commonly used for estimation of the self-diffusivity, $D_{1,self}$. The expression for the self-diffusivity for solvent(1)/polymer(2) system is commonly written as;

$$D_{1,self} = D_{1,self,0} \exp\left(\frac{-E}{RT}\right) \exp\left(-\frac{\left(\omega_1 V_1^* + \omega_2 \xi V_2^*\right)}{\hat{V}_{FH}/\gamma}\right)$$
$$\frac{\hat{V}_{FH}}{\gamma} = \omega_1\left(\frac{K_{11}}{\gamma}\right)\left(K_{21} - T_{g1} + T\right) + \omega_2\left(\frac{K_{12}}{\gamma}\right)\left(K_{22} - T_{g2} + T\right) \tag{S86}$$

Equation (S86) is the same as eqs (41), and (42) of Vrentas and Duda,[22] and eq (18) of Verros and Malamataris.[29] For detailed derivations, and theoretical background, see Vrentas and Duda.[22]

For the system toluene/polystyrene, the free-volume parameters are provided in Table 2 of Alsoy and Duda.[30] The continuous solid line in Figure S5c are the estimations of the self-diffusivity for toluene in polystyrene using Equation (S86). The excellent agreement is no surprise, because the free-volume parameters, totaling 12 in number, have been determined by fitting to experimental data on self-diffusivities.

Broadly speaking, self-diffusivities display an exponential increase with increasing volume fractions. This provides the rationale for the use of the exponential model for describing the composition dependence of the M-S diffusivity[31, 32]

$$Đ_{im}^{V} = Đ_{im,0}^{V} \exp\left[A_i\left(\phi_i + C_{ij}\phi_j\right)\right] \tag{S87}$$

Verros and Malamataris[29] provide a further illustration of use of the free-volume theory for estimation of the diffusivity of acetone (component 1) in cellulose acetate (indicated by subscript m) at T = 298.15 K. Calculations, using the input data provided in their paper, are presented in Figure S6. For this system, the penetrant (1) –membrane (m) interaction parameter is dependent on the volume fraction and the activities are calculated using eq (S47), taking $\frac{\overline{V_1}}{V_m} = 0.008$. The thermodynamic correction factor $\left(\frac{\rho_1}{RT}\frac{\partial \mu_1}{\partial \rho_1}\right)$ is a strongly decreasing function of the volume fraction, ϕ_1, and mass fraction ω_1; see Figure S6a,b. In these calculations the volume fractions, ϕ_1, are related to the mass fractions ω_1 by $\phi_1 = \frac{1}{1+\frac{\rho_{10}}{\rho_{20}}\frac{1-\omega_1}{\omega_1}}$, and $\omega_1 = \frac{1}{1+\frac{\rho_{20}}{\rho_{10}}\frac{1-\phi_1}{\phi_1}}$ where the ρ_{i0} are the mass densities of pure components.

The Fick diffusivity, calculated using the approximation $D_1 = \phi_m D_{1,self}\left(\frac{\rho_1}{RT}\frac{\partial \mu_1}{\partial \rho_1}\right)$, i.e. assuming negligible 1-1 friction, are presented in Figure S6b,d. With increasing volume, or mass, fractions of

acetone, we note that the Fick diffusivity falls increasing below the self-diffusivity due to the strong influence of the thermodynamic correction factor.

4.6 Diffusivities in ternary 1/2/polymer solutions

For diffusion in a ternary mixture consisting of two solvent species (1, 2) and polymer (m), eq (S63) reduces to

$$\begin{aligned} -\phi_1 \frac{1}{RT}\frac{d\mu_1}{dz} &= \frac{\left(\phi_2 J_1^V - \phi_1 J_2^V\right)}{Đ_{12}^V} + \frac{\left(\phi_m J_1^V - \phi_1\left(-J_1^V - J_2^V\right)\right)}{Đ_{1m}^V} \\ -\phi_2 \frac{1}{RT}\frac{d\mu_2}{dz} &= \frac{\left(\phi_1 J_2^V - \phi_2 J_1^V\right)}{Đ_{21}^V} + \frac{\left(\phi_m J_2^V - \phi_2\left(-J_1^V - J_2^V\right)\right)}{Đ_{2m}^V} \end{aligned} \tag{S88}$$

For the ternary 1/2/m mixture, eq (S65) simplifies to

$$[B] = \begin{bmatrix} \frac{\phi_1}{Đ_{1m}^V} + \frac{\phi_2}{Đ_{12}^V} + \frac{\phi_m}{Đ_{1m}^V} & -\phi_1\left(\frac{1}{Đ_{12}^V} - \frac{1}{Đ_{1m}^V}\right) \\ -\phi_2\left(\frac{1}{Đ_{21}^V} - \frac{1}{Đ_{2m}^V}\right) & \frac{\phi_1}{Đ_{21}^V} + \frac{\phi_2}{Đ_{2m}^V} + \frac{\phi_m}{Đ_{2m}^V} \end{bmatrix}; \quad [\Lambda] = [B]^{-1} \tag{S89}$$

The M-S diffusivity $Đ_{12}^V = \frac{Đ_{21}^V}{\overline{V_1}}\overline{V_2}$, and can be estimated from diffusivity data for the binary liquid phase mixtures of the two solvent species; we return to this estimation procedure later.

The Fick diffusivity matrix is

$$[D] = [\Lambda][\Gamma]; \quad [\Gamma] = \begin{bmatrix} \phi_1 \frac{\partial \ln a_1}{\partial \phi_1} & \phi_1 \frac{\partial \ln a_1}{\partial \phi_2} \\ \phi_2 \frac{\partial \ln a_2}{\partial \phi_1} & \phi_2 \frac{\partial \ln a_2}{\partial \phi_2} \end{bmatrix} \tag{S90}$$

For the case of negligible 1-2 friction, eq (S88) simplifies to

$$[B] = \begin{bmatrix} \frac{(1-\phi_2)}{Đ_{1m}^V} & \frac{\phi_1}{Đ_{1m}^V} \\ \frac{\phi_2}{Đ_{2m}^V} & \frac{(1-\phi_1)}{Đ_{2m}^V} \end{bmatrix}; \quad [\Lambda] = [B]^{-1} \tag{S91}$$

The matrix inversion in eq (S91) can be performed analytically, and we get the following explicit expression for the Fick diffusivity matrix for the scenario in which 1-2 friction is considered to be negligible

$$[D]=[\Lambda][\Gamma]=\frac{Đ_{1m}^{V}Đ_{2m}^{V}}{\phi_m}\begin{bmatrix}\frac{(1-\phi_1)}{Đ_{2m}^{V}} & -\frac{\phi_1}{Đ_{1m}^{V}}\\ -\frac{\phi_2}{Đ_{2m}^{V}} & \frac{(1-\phi_2)}{Đ_{1m}^{V}}\end{bmatrix}\begin{bmatrix}\phi_1\frac{\partial \ln a_1}{\partial \phi_1} & \phi_1\frac{\partial \ln a_1}{\partial \phi_2}\\ \phi_2\frac{\partial \ln a_2}{\partial \phi_1} & \phi_2\frac{\partial \ln a_2}{\partial \phi_2}\end{bmatrix}$$
$$=\frac{1}{\phi_m}\begin{bmatrix}(1-\phi_1)Đ_{1m}^{V} & -\phi_1 Đ_{2m}^{V}\\ -\phi_2 Đ_{1m}^{V} & (1-\phi_2)Đ_{2m}^{V}\end{bmatrix}\begin{bmatrix}\phi_1\frac{\partial \ln a_1}{\partial \phi_1} & \phi_1\frac{\partial \ln a_1}{\partial \phi_2}\\ \phi_2\frac{\partial \ln a_2}{\partial \phi_1} & \phi_2\frac{\partial \ln a_2}{\partial \phi_2}\end{bmatrix} \tag{S92}$$

The estimation of the four elements of the Fick diffusivities relies on the estimations of the self-diffusivities in the ternary mixture using the free-volume theory.

The volumetric fluxes are determined from

$$\begin{pmatrix}J_1^{V}\\ J_2^{V}\end{pmatrix}=-\frac{1}{\phi_m}\begin{bmatrix}(1-\phi_1)Đ_{1m}^{V} & -\phi_1 Đ_{2m}^{V}\\ -\phi_2 Đ_{1m}^{V} & (1-\phi_2)Đ_{2m}^{V}\end{bmatrix}\begin{bmatrix}\phi_1\frac{\partial \ln a_1}{\partial \phi_1} & \phi_1\frac{\partial \ln a_1}{\partial \phi_2}\\ \phi_2\frac{\partial \ln a_2}{\partial \phi_1} & \phi_2\frac{\partial \ln a_2}{\partial \phi_2}\end{bmatrix}\frac{d}{dz}\begin{pmatrix}\phi_1\\ \phi_2\end{pmatrix} \tag{S93}$$

Applying eq (S63) to quaternary 1/1*/2/m, and 1/2/2*/m mixtures, we can derive the following expressions for the self-diffusivities of the penetrants 1, and 2 in the 1/2m mixtures

$$\frac{1}{D_{1,self}} = \frac{\phi_1}{Đ_{11}^V} + \frac{\phi_2}{Đ_{12}^V} + \frac{\phi_m}{Đ_{1m}^V}; \quad \frac{1}{D_{2,self}} = \frac{\phi_2}{Đ_{22}^V} + \frac{\phi_1}{Đ_{21}^V} + \frac{\phi_m}{Đ_{2m}^V}$$

$$\frac{1}{D_{1,self}} = \frac{\rho_1 \varsigma_{11}}{RTM_1} + \frac{\rho_2 \varsigma_{12}}{RTM_2} + \frac{\rho_m \varsigma_{1m}}{RTM_m}; \quad \frac{1}{D_{2,self}} = \frac{\rho_2 \varsigma_{22}}{RTM_2} + \frac{\rho_1 \varsigma_{21}}{RTM_1} + \frac{\rho_m \varsigma_{2m}}{RTM_m}$$

$$Đ_{1m}^V = \phi_m \frac{RTM_m}{\rho_m \varsigma_{1m}}; Đ_{11}^V = \phi_1 \frac{RTM_1}{\rho_1 \varsigma_{11}}$$

$$Đ_{mm}^V = \phi_m \frac{RTM_m}{\rho_m \varsigma_{mm}}; Đ_{1m}^V = \phi_1 \frac{RTM_1}{\rho_1 \varsigma_{1m}} \tag{S94}$$

$$\frac{\rho_j \varsigma_{ij}}{RTM_j} = \frac{\phi_j}{Đ_{ij}^V}; \frac{\rho_2 \varsigma_{12}}{RTM_2} = \frac{\phi_2}{Đ_{12}^V}; \frac{\rho_1 \varsigma_{21}}{RTM_1} = \frac{\phi_1}{Đ_{21}^V}$$

$$\frac{\rho_m \varsigma_{1m}}{RTM_m} = \frac{\phi_m}{Đ_{1m}^V}; \frac{\rho_1 \varsigma_{11}}{RTM_1} = \frac{\phi_1}{Đ_{11}^V}$$

$$\frac{\rho_m \varsigma_{mm}}{RTM_m} = \frac{\phi_m}{Đ_{mm}^V}; \frac{\rho_1 \varsigma_{1m}}{RTM_1} = \frac{\phi_1}{Đ_{1m}^V}$$

Equation (S94) are precisely equivalent to equations (19), and (20) of Vrentas and Vrentas:[33]

$$\frac{1}{D_{1,self}} = \frac{\rho_1 \varsigma_{11}}{RTM_1} + \frac{\rho_2 \varsigma_{12}}{RTM_2} + \frac{\rho_m \varsigma_{1m}}{RTM_m}; \quad \frac{1}{D_{2,self}} = \frac{\rho_2 \varsigma_{22}}{RTM_2} + \frac{\rho_1 \varsigma_{21}}{RTM_1} + \frac{\rho_m \varsigma_{2m}}{RTM_m} \tag{S95}$$

For the case of negligible 1-1, 2-2, and 1-2 friction, eq (S94) simplifies to yield

$$Đ_{1m}^V = \phi_m D_{1,self}; \quad Đ_{2m}^V = \phi_m D_{2,self} \tag{S96}$$

Combining eq (S92), and (S96) allows estimation of the four elements of the Fick diffusivity matrix from information on the self-diffusivities of penetrants and the Flory-Huggins parameters to determine the matrix of thermodynamic correction factors.

Table 1 of Alsoy and Duda[30] provides four different scenarios (called Cases 1, 2, 3, and 4 in their paper) for estimation of the elements of the Fick diffusivity matrix; their expressions are expressed in terms of the self-diffusivities $D_{1,self}, D_{2,self}$ in the 1/2/m mixture. The combination of eqs (S92), and (S96), along with the simplification $\frac{\rho_i}{\rho_j}\frac{\partial \ln a_i}{\partial \ln \rho_j} \approx \frac{\phi_i}{\phi_j}\frac{\partial \ln a_i}{\partial \ln \phi_j}$, yields relations for the four elements of the Fick diffusivity matrix that are precisely equivalent to Case 4 in Table 1 of Alsoy and Duda.[30]

Diffusion in polymer solutions

The free-volume theory[16, 22, 25] is commonly used for estimation of the self-diffusivity, $D_{1,self}$, and $D_{2,self}$ in the 1/2/m mixture. The expression for the self-diffusivities for 1, and 2 in the solvent(1)/solvent(2)/polymer(3) system are given by equations (23), (24) and (25) of Zielinski and Hanley,[34] as reproduced below using their nomenclature

$$D_{1,self} = D_{1,self,0}\exp\left(\frac{-E}{RT}\right)\exp\left(-\frac{\left(\omega_1 V_1^* + \omega_2 \frac{\xi_{13}}{\xi_{23}} V_2^* + \omega_3 \xi_{13} V_3^*\right)}{\hat{V}_{FH}/\gamma}\right)$$

$$D_{2,self} = D_{2,self,0}\exp\left(\frac{-E}{RT}\right)\exp\left(-\frac{\left(\omega_1 V_1^* \frac{\xi_{23}}{\xi_{13}} + \omega_2 V_2^* + \omega_3 \xi_{23} V_3^*\right)}{\hat{V}_{FH}/\gamma}\right) \qquad \text{(S97)}$$

$$\frac{\hat{V}_{FH}}{\gamma} = \omega_1\left(\frac{K_{11}}{\gamma}\right)\left(K_{21} - T_{g1} + T\right) + \omega_2\left(\frac{K_{12}}{\gamma}\right)\left(K_{22} - T_{g2} + T\right) + \omega_3\left(\frac{K_{13}}{\gamma}\right)\left(K_{23} - T_{g3} + T\right)$$

We shall illustrate the estimations of the use of the free-volume theory by estimating the matrix of Fick diffusivities $[D]$, for methanol (component 1)/toluene (2)/poly(vinylacetate) (PVAc, subscript m) at T = 333.15 K. Figure S7a presents calculations for the matrix of thermodynamic correction factors, $[\Gamma] = \begin{bmatrix} \phi_1 \frac{\partial \ln a_1}{\partial \phi_1} & \phi_1 \frac{\partial \ln a_1}{\partial \phi_2} \\ \phi_2 \frac{\partial \ln a_2}{\partial \phi_1} & \phi_2 \frac{\partial \ln a_2}{\partial \phi_2} \end{bmatrix}$, using eq (S48), along with the Flory-Huggins parameters $\chi_{12} = 1; \chi_{1m} = 1.19; \chi_{2m} = 0.78$. In these calculations we take the sum of the volume fractions of methanol and toluene at a constant value $\phi_1 + \phi_2 = 0.4$. Particularly note-worthy are the negative values of the off-diagonal elements Γ_{12}, Γ_{21}. Figure S7b plots the ratios $-\frac{\Gamma_{12}}{\Gamma_{11}}$, and $-\frac{\Gamma_{21}}{\Gamma_{22}}$ as function of ϕ_1. We note that the off-diagonal elements are significantly larger in magnitude than the diagonal elements for a range of compositions.

Diffusion in polymer solutions

The self-diffusivities are estimated from eq (S97) using with free-volume parameters provided in Table 1 of Zielinski and Hanley.[34] The Fick diffusivity matrix $[D]$ can then be calculated by combination of eqs (S92), and (S96); the results are presented in Figure S7c. Both the off-diagonal elements D_{12}, D_{21} are negative. Figure S7d plots the ratios $-\frac{D_{12}}{D_{11}}$, and $-\frac{D_{21}}{D_{22}}$ as function of ϕ_1. We note that the off-diagonal elements are significantly larger in magnitude than the diagonal elements for a range of volume fractions. Comparison of Figure S7b,d clearly show that the large magnitudes of the ratios $-\frac{D_{12}}{D_{11}}$, and $-\frac{D_{21}}{D_{22}}$ have their origins in the corresponding ratios $-\frac{\Gamma_{12}}{\Gamma_{11}}$, and $-\frac{\Gamma_{21}}{\Gamma_{22}}$.

In their Table IV, Cussler and Lightfoot[35] report experimental data for the Fick diffusivity matrix $[D]$ for polystyrene(1)/cyclohexane(2)/toluene(3) mixtures. At composition mass fractions $\omega_1 = 0.05; \omega_2 = 0.05; \omega_3 = 0.95$, they report $[D] = \begin{bmatrix} 8.9 & -1.6 \\ -8.9 & 203.1 \end{bmatrix} \times 10^{-11}$ m^2 s^{-1}. It is to be emphasized that the values of the Fick diffusivity matrix depending on the component numbering. For the same compositions, if the numbering is chosen as cyclohexane(1)/toluene(2)/polystyrene(3), the values of the Fick matrix can be re-calculated, using the basis of the data on the partial specific volumes provided in Table IV of Cussler and Lightfoot,[35] we obtain $[D] = \begin{bmatrix} 212 & 8.9 \\ -235.8 & -3.26 \end{bmatrix} \times 10^{-11}$ m^2 s^{-1}. In order to understand the large negative value of D_{21}, we estimated the matrix of thermodynamic factors for cyclohexane(1)/toluene(2)/polystyrene(3), using F-H parameters $\chi_{12} = 0.476; \chi_{13} = 0.51; \chi_{23} = 0.3548$, we obtain $[\Gamma] = \begin{bmatrix} 0.93 & -0.03 \\ -0.877 & 0.054 \end{bmatrix}$. The large negative value of Γ_{21} is the main cause of the large negative value of D_{21}.

4.7 List of Tables for Diffusion in polymer solutions

Table S5. Concentration measures and inter-relationships.

Concentration measure	units	Inter-relation, constraint
x_i, mole fraction of species *i*	-	$x_i = \frac{c_i}{c_t} = \frac{\frac{\omega_i}{M_i}}{\sum_{i=1}^{n}\frac{\omega_i}{M_i}} = \frac{\omega_i}{M_i}\overline{M}; \sum_{i=1}^{n} x_i = 1$
ω_i, mole fraction of species *i*	-	$\omega_i = \frac{\rho_i}{\rho_t} = \frac{x_i M_i}{\sum_{i=1}^{n} x_i M_i} = \frac{x_i M_i}{\overline{M}}; \sum_{i=1}^{n} \omega_i = 1$
c_i, molar density of species *i*	mol m^{-3}	$c_i = \frac{\rho_i}{M_i}; \sum_{i=1}^{n} c_i = c_t = \text{mixture molar density} = \frac{1}{\overline{V}}$
ρ_i, mass density of species *i*	kg m^{-3}	$\rho_i = c_i M_i; \sum_{i=1}^{n} \rho_i = \rho_t = \text{mixture mass density}$
M_i, molar mass of species *i*	kg mol^{-1}	$\overline{M} = \sum_{i=1}^{n} x_i M_i = \text{mean molar mass of mixture}$
$\overline{V_i}$, partial molar volume of *i*	m^3 mol^{-1}	$\overline{V} = \sum_{i=1}^{n} x_i \overline{V_i} = \frac{1}{c_t} = \text{mean molar volume of mixture}$
ϕ_i, volume fraction of species *i*	-	$\phi_i = c_i \overline{V_i} = \frac{\frac{\omega_i}{\rho_i}}{\sum_{i=1}^{n}\frac{\omega_i}{\rho_i}}$

4.8 List of Figures for Diffusion in polymer solutions

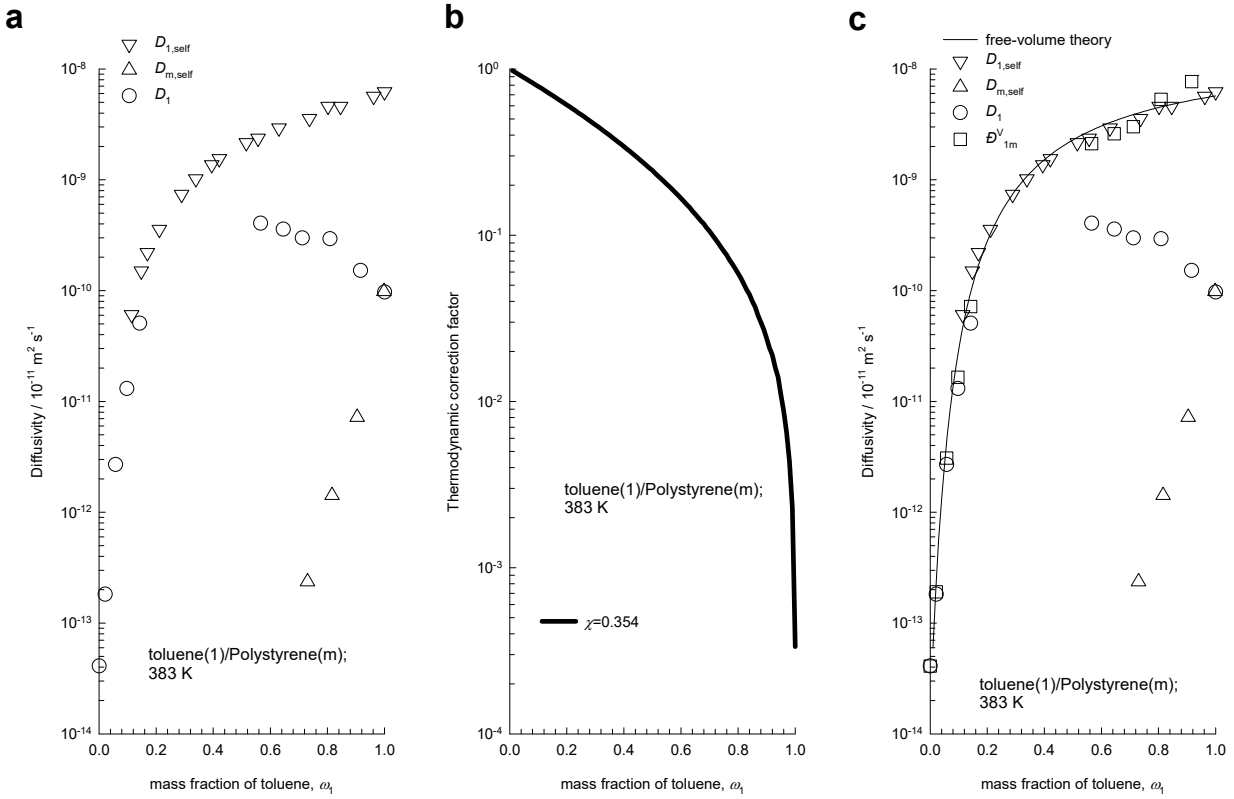

Figure S5. (a) Experimental data as reported in Figure 6 of Zielinski[28] for the self-diffusivities of toluene (1), and polystyrene (m) in polystyrene at 383 K as a function of the mass fraction of toluene. Also shown are the data for the Fick (mutual) diffusivity, D_1. (b) Calculations of the thermodynamic correction factor, $\left(\frac{\rho_1}{RT}\frac{\partial \mu_1}{\partial \rho_1}\right)$, taking $\chi = 0.354$. (c) Comparison of the M-S diffusivity, calculated using $Đ^V_{1m} = D_1 \Big/ \left(\frac{\rho_1}{RT}\frac{\partial \mu_1}{\partial \rho_1}\right)$, with D_1, $D_{1,\text{self}}$, and $D_{2,\text{self}}$. The continuous solid line is the estimation of the self-diffusivity using the free-volume theory.

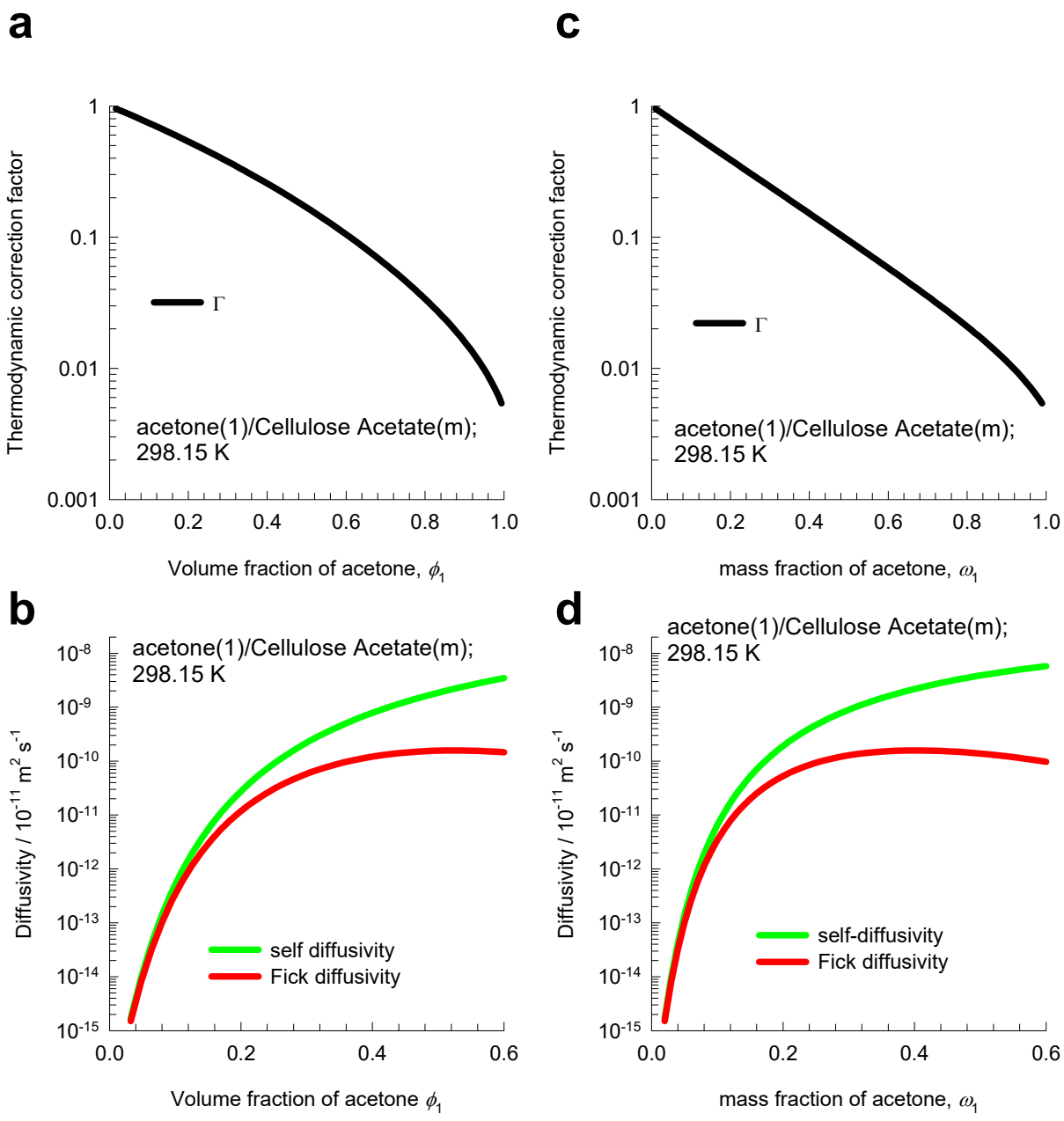

Figure S6. Calculations for (a, c) thermodynamic correction factor, $\Gamma = \dfrac{\partial \ln a_1}{\partial \ln \phi_1}$, (b, d) Fick diffusivity, $D_1 = Đ_{1m}^{V} \dfrac{\partial \ln a_1}{\partial \ln \phi_1}$, and self-diffusivity, $D_{1,self}$, for acetone (1) in cellulose acetate (m) at T = 298.15 K. The x-axes are (a, b) volume fractions, and (c, d) mass fractions. The input data are taken from the Verros and Malamataris.[29]

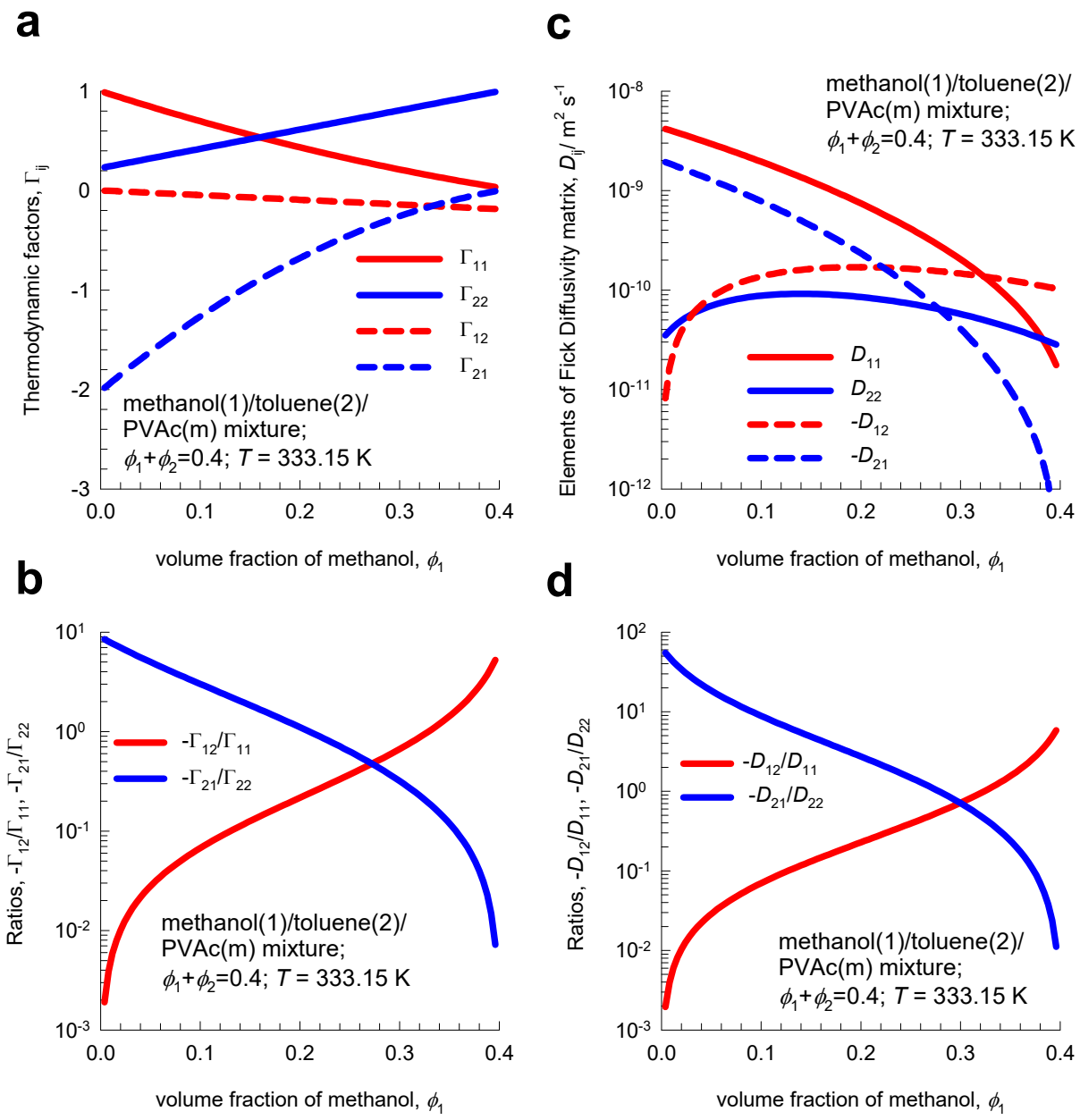

Figure S7. (a, b) Calculations of thermodynamic correction factors for methanol (1)/toluene (2)/poly(vinylacetate)(m) at T = 333.15 K.. (c, d) Calculations of elements of the Fick diffusivity matrix $[D]$. The calculations are based on the predictions of the self-diffusivities using the free-volume parameters provided in Table 1 of Zielinski and Hanley,[34] along with the Flory-Huggins parameters also provided in page 6 of their paper: $\chi_{12} = 1; \chi_{1m} = 1.19; \chi_{2m} = 0.78$.

5 Modelling the immersion precipitation process

In the immersion precipitation process for preparation of asymmetric polymeric membranes, a thin layer of casting film of solvent (2) /polymer (3) mixture, placed on a support layer, is brought into contact with a non-solvent (1) in a coagulation bath; see schematic in Figure S8. The non-solvent diffuses into the casting polymer film, causing the precipitation of the polymer. The immersion precipitation process for preparation of polymer membranes is controlled by molecular diffusion and occurs close to composition regions in which the ternary anti-solvent/solvent/polymer solutions is partially miscible. For detailed background on the physico-chemical phenomena involved in the immersion precipitation process, along with the modelling aspects, the reader is referred to the pioneering works of Strathmann and Kock,[36] Radovanovic et al.,[37, 38] Reuvers et al.,[39, 40] van den Berg and Smolders,[41] and Tsay and McHugh.[42] Comprehensive surveys of the literature on this subject are provided by van de Witte et al.,[43] Guillen et al.,[44] and Wang and Lai.[45]

The phase diagram for diffusion controlled immersion precipitation process is illustrated in Figure S9 for the ternary mixture consisting of water (non-solvent, component 1), acetone (solvent, component 2) and cellulose acetate (polymer = CA = m, component 3); the ternary phase diagram is constructed on the basis of the volume fractions. Two different subscripts are used for the polymer, m and 3. We shall use both these interchangeably. The binodal and spinodal curves for this ternary mixture are calculated on the basis on the Flory-Huggins equations that relate the component activities to volume fractions, ϕ_i .[46, 47] The binodal curve for this ternary mixture defines the limits of phase miscibility. The coagulation bath usually contains non-solvent (1), almost exclusively or to a predominant extent. The compositions at the interface between the polymer casting film and the coagulation bath lie at either ends of the tie-line, at compositions indicated by A* and CB*, respectively. Put another way, we have a concentration jump at the interface between the casting film and the coagulation bath. Usually, CB* is practically free

of polymer. The composition A*, is significantly richer in the polymer (CA), as compared to CB*. The spinodal curve defines the limit of phase stability, and along the spinodal curve, the condition $|\Gamma| = 0$ must be satisfied, i.e. we must have $\Gamma_{11}\Gamma_{22} = \Gamma_{12}\Gamma_{21}$, the product of the off-diagonal elements is equal in magnitude to the product of the diagonal elements.[14, 48] This situation implies a significant degree of thermodynamic coupling.

As illustration, the transient equilibration trajectory when a 10% solution of Cellulose Acetate (CA) in acetone (indicated by A in Figure S9) is immersed in the coagulation bath is indicated by the blue line connecting A and A*. With increasing immersion contact times, the compositions within the polymer casting film will get progressively richer in water, and poorer in acetone; this is clearly elucidated by Tsay and McHugh[42] and van de Witte et al.[43] Consequently, the equilibration trajectories get progressively closer to the binodal curve. Figure S10 plots the progression in the equilibration trajectories A-A*, B-B*, and C-C* with increasing immersion times; these plots are analogous to the trajectories plotted in Figure 5 of Tsay and McHugh[42] for immersion times of 0.24 s, 10 s, and 24 s. Particularly noteworthy is that the trajectory C-C* has penetrated into the metastable region between the binodal and spinodal curves. This foray into the metastable region causes precipitation of polymer in the casting film.

Detailed numerical modelling of the equilibration trajectories, using the Bearman frictional formulation, are available in the papers of Radovanovic et al.,[37, 38] Reuvers et al.,[39, 40] and Tsay and McHugh.[42] In this article, we set ourselves a different objective. We aim to show that the foray into the metastable regions, an inherent characteristic of immersion precipitation, is essentially engendered the thermodynamic correction factors $\Gamma_{ij} = \frac{\phi_i}{\phi_j}\frac{\partial \ln a_i}{\partial \ln \phi_j}$ that exert strong influences on the driving forces for diffusion.

Modelling the immersion precipitation process

For the system water (1)/acetone (2)/cellulose acetate (= CA = 3), Figure S11a shows calculations of the elements of the matrix of thermodynamic factors $[\Gamma]$ for compositions along a straight line connecting A and A* in Figure S10. Particularly noteworthy are the large negative values of Γ_{21}.

The self-diffusivities for water and acetone are estimated from eq (S97) using with free-volume parameters provided in Table 1 of Altinkaya and Ozbas.[49]

Rather than ignoring 1-2 friction, the M-S diffusivity $Đ_{12}^{V} = \frac{Đ_{21}^{V}}{\overline{V_1}}\overline{V_2}$ quantifying 1-2 friction is estimated using the following step-by-step procedure.

The experimental data of the Fick diffusivity for water(1)/acetone(2) pair diffusivity D_{12} as reported by Grossmann and Winkelmann[50] is used to determine the M-S diffusivity $Đ_{12}$ by correcting for the thermodynamic factor $Đ_{12} = \frac{D_{12}}{\Gamma}$; the thermodynamic factor is determined from the NRTL equation, with parameters $\tau_{12} = 2.09542$; $\tau_{12} = -0.6652$; $\alpha_{12} = 0.2$; the calculation details are provided in Figure S7, and Table 5 of Krishna.[14]

The variation of the M-S diffusivity $Đ_{12}$ with mole fraction of water, is described adequately by the Vignes interpolation formula[11, 12]

$$Đ_{12} = \left(Đ_{12}^{x_1 \to 1}\right)^{x_1} \left(Đ_{12}^{x_2 \to 1}\right)^{x_2} \tag{S98}$$

In eq (S98) the infinite-dilution values of the M-S diffusivities are

$$\begin{aligned} Đ_{12}^{x_1 \to 1} &= 1 \times 10^{-9} \text{ m}^2 \text{ s}^{-1} \\ Đ_{12}^{x_2 \to 1} &= 5.3 \times 10^{-9} \text{ m}^2 \text{ s}^{-1} \end{aligned} \tag{S99}$$

For use in eqs (S89), and (S90), the M-S diffusivity $Đ_{12}^{V} = \frac{Đ_{12}\overline{V_2}}{\overline{V}} = \frac{Đ_{21}^{V}}{\overline{V_1}}\overline{V_2}$ $Đ_{12}$ is calculated from eq (S98) using the interpolation formula for the binary water(1)/acetone(2) pair on a polymer-free basis. In other words, the mole fractions x_1 is calculated for the effective volume fraction of water (component 1) in the binary pair in the ternary mixture $\frac{\phi_1}{\phi_1 + \phi_2} = \frac{\phi_1}{1 - \phi_3}$

Figure S11b shows calculations of the Fick diffusivity matrix $[D]$ using a combination of eqs (S89), (S90), (S96), (S97), (S98), and (S99). Due to the significantly higher mobility of water than acetone, $D_{11} >> D_{22}$. The variation of the four elements of $[D]$ with the volume fraction of CA, shows approximately the same trends the corresponding elements of the matrix of thermodynamic factors $[\Gamma]$. The large negative value of the off-diagonal element D_{21} is largely attributable to the corresponding negative off-diagonal element Γ_{21}. The flux of acetone (2) is strongly influenced by the driving force for transfer of water (1).

5.1 A simplified analytic model for transient equilibration

In order to demonstrate the foray into the meta-stable region is engendered by the thermodynamic correction factors $\Gamma_{ij} = \frac{\phi_i}{\phi_j}\frac{\partial \ln a_i}{\partial \ln \phi_j}$, we adopt the simplified analytical solution to the immersion precipitation process, as presented by Tsay and McHugh.[51] For convenience of the readers, the model equations have been presented below, albeit using a slightly different nomenclature than in the original article by Tsay and McHugh.[51]

The following set of assumptions are made in the model development.

(i) The diffusion is essentially *z*-directional; see schematic in Figure S12. The position $z = 0$, corresponds to the position of the interface at start of the equilibration process. The adjoining immiscible phases, coagulation bath and polymer casting film are both considered to be semi-infinite. At the position $z = +\infty$ the composition corresponds to that of the bulk coagulation bath that is time-invariant. At the position $z = -\infty$ the composition corresponds to that of the polymer casting film that is contact with the support layer; this composition is also time-invariant.

(ii) At any time *t*, during the immersion precipitation process, we have thermodynamic equilibrium at the interface between the two-immiscible phases, at compositions A* and CB*.

Due to finite interphase diffusion, the position of the interface will be altered to satisfy the jump balance condition at the interface; this is discussed in detail below.

The assumption of two semi-infinite reservoirs allows the derivation of simple analytical solutions. However, this assumption also implies that the analytical solution can only be applied to represent the trajectories being followed for short contact times, say of the order of 1 s. Consequently, the A-A*, B-B*, and C-C* trajectories in Figure S10 need to be analyzed by choosing different initial compositions in the polymer casting film (A, B, C) and in the coagulation bath; each trajectory being allowed to progress for relatively short contact times of about 1 s.

The transient ternary diffusion within the polymer casting film is described by a set of *two independent* coupled partial differential equations

$$\frac{\partial\begin{pmatrix}\phi_1\\ \phi_2\end{pmatrix}}{\partial t} = -\frac{\partial\begin{pmatrix}J_1^V\\ J_2^V\end{pmatrix}}{\partial z} \qquad \text{(S100)}$$
$$\phi_3 = 1-\phi_1-\phi_2$$

The volumetric fluxes, J_i^V with respect to the volume average reference velocity is particularly convenient for polymeric solutions because the partial molar volumes are practically composition independent. The volumetric fluxes sum to zero. $J_1^V + J_2^V + J_3^V = 0$. The two independent fluxes J_i^V for non-solvent and solvent are described by eqs (S89), and (S90) as summarized below

$$\begin{pmatrix}J_1^V\\ J_2^V\end{pmatrix} = -[D]\frac{\partial}{\partial z}\begin{pmatrix}\phi_1\\ \phi_2\end{pmatrix};\quad [D]=[\Lambda][\Gamma]$$

$$[\Lambda]=[B]^{-1};\quad [B]=\begin{bmatrix}\dfrac{\phi_1}{Đ_{1m}^V}+\dfrac{\phi_2}{Đ_{12}^V}+\dfrac{\phi_m}{Đ_{1m}^V} & -\phi_1\left(\dfrac{1}{Đ_{12}^V}-\dfrac{1}{Đ_{1m}^V}\right)\\ -\phi_2\left(\dfrac{1}{Đ_{21}^V}-\dfrac{1}{Đ_{2m}^V}\right) & \dfrac{\phi_1}{Đ_{21}^V}+\dfrac{\phi_2}{Đ_{2m}^V}+\dfrac{\phi_m}{Đ_{2m}^V}\end{bmatrix}; \qquad \text{(S101)}$$

$$[\Gamma]=\begin{bmatrix}\phi_1\dfrac{\partial \ln a_1}{\partial \phi_1} & \phi_1\dfrac{\partial \ln a_1}{\partial \phi_2}\\ \phi_2\dfrac{\partial \ln a_2}{\partial \phi_1} & \phi_2\dfrac{\partial \ln a_2}{\partial \phi_2}\end{bmatrix}$$

Modelling the immersion precipitation process

The Fick diffusivity matrix $[D]$ is estimated using a combination of eqs (S89), (S90), (S96), (S97), (S98), and (S99). Combining eqs (S100), (S101), and (S102) we obtain

$$\frac{\partial\begin{pmatrix}\phi_1\\ \phi_2\end{pmatrix}}{\partial t}=[D]\frac{\partial^2\begin{pmatrix}\phi_1\\ \phi_2\end{pmatrix}}{\partial z^2};\qquad \phi_3=1-\phi_1-\phi_2 \tag{S102}$$

Commonly, the coagulation bath consists of a binary mixture of non-solvent(1) and solvent(2). The corresponding relation for the transient diffusion process is described by

$$\begin{aligned}&\frac{\partial\phi_{1b}}{\partial t}=-\frac{\partial J_{1b}^V}{\partial z};\quad \phi_{2b}=1-\phi_{1b}\\ &J_{1b}^V=-D_b\frac{\partial\phi_{1b}}{\partial z};\quad J_{2b}^V=-J_{1b}^V\\ &\frac{\partial\phi_{1b}}{\partial t}=D_b\frac{\partial^2\phi_{1b}}{\partial z^2}\end{aligned} \tag{S103}$$

The subscript *b* in eq (S103) refers to the coagulation bath. The symbol D_b in eq (S103) represents the Fick diffusivity in the binary aqueous solution in the coagulation bath. For water/acetone mixtures in the coagulation bath, the Fick diffusivity D_b is estimated as a function of the composition by using the combination of (S98), and (S99), along with calculation of the thermodynamic correction factors using the NRTL equation. For water/DMF mixtures in the coagulation bath, the Fick diffusivity D_b is estimated as a function of the composition by using the combination of eq (S98) and (S118) (see later section, along with calculation of the thermodynamic correction factors using the NRTL equation).

The initial conditions for eqs (S102), and (S103) are

$$\begin{aligned}&z\ge 0,\quad t=0,\quad \begin{pmatrix}\phi_1(z,0)\\ \phi_2(z,0)\end{pmatrix}=\begin{pmatrix}\phi_{10}\\ \phi_{20}\end{pmatrix}\\ &z\le 0,\quad t=0,\quad \phi_{1b}(z,0)=\phi_{1b0}\end{aligned} \tag{S104}$$

where ϕ_{i0} and ϕ_{1b0} are the initial compositions of the polymer casting film and bath, respectively

The boundary conditions are

$$z=-\infty, \quad t\geq 0, \quad \begin{pmatrix}\phi_1(-\infty,t)\\ \phi_2(-\infty,t)\end{pmatrix}=\begin{pmatrix}\phi_{10}\\ \phi_{20}\end{pmatrix}$$
$$z=+\infty, \quad t\geq 0, \quad \phi_{1b}(+\infty,t)=\phi_{1b0} \tag{S105}$$

An analytic solution for the transient volume fractions in bath is obtained if the Fick diffusivity D_b is assumed to be composition independent; see Crank[52]

$$\phi_{1b}(z,t)=\phi_{1b0}+\frac{erfc\left[\dfrac{z}{\sqrt{4D_bt}}\right]}{erfc\left[\dfrac{r}{\sqrt{4D_b}}\right]}\left(\phi_{1bI}-\phi_{1b0}\right) \tag{S106}$$

The corresponding analytic expression for the volume fractions in the polymer casting film are also derivable, if the Fick diffusivity matrix $[D]=[\Lambda][\Gamma]$ is also assumed to be composition independent; see Taylor and Krishna.[2] In all the calculations presented in this article, the Fick $[D]$ is evaluated using eq (S101) at the average volume fractions $\frac{1}{2}\begin{pmatrix}\phi_{10}+\phi_{1I}\\ \phi_{20}+\phi_{2I}\end{pmatrix}$. The transient volume fractions in the polymer film can be written 2 × 2 dimensional matrix generalization of eq (S106) (see Taylor and Krishna[2] for further theoretical background on matrix generalization strategies):

$$\begin{pmatrix}\phi_1(z,t)\\ \phi_2(z,t)\end{pmatrix}=\begin{pmatrix}\phi_{10}\\ \phi_{20}\end{pmatrix}+[Q]\begin{pmatrix}\phi_{1I}-\phi_{10}\\ \phi_{2I}-\phi_{20}\end{pmatrix}$$
$$[Q]=\left[erfc\left(-\frac{z}{\sqrt{4t}}[D]^{-1/2}\right)\right]\left[erfc\left(-\frac{r}{2}[D]^{-1/2}\right)\right]^{-1} \tag{S107}$$

The Sylvester theorem, detailed in Appendix A of Taylor and Krishna,[2] is required for explicit evaluation of the four elements of the 2 × 2 dimensional square matrix $[Q]$. For the case of distinct eigenvalues, λ_1 and λ_2 of the 2 × 2 dimensional square matrix $[D]$, the Sylvester theorem yields

Modelling the immersion precipitation process

$$[Q]=\frac{f(\lambda_1)\left[[D]-\lambda_2[I]\right]}{(\lambda_1-\lambda_2)}+\frac{f(\lambda_2)\left[[D]-\lambda_1[I]\right]}{(\lambda_2-\lambda_1)}$$
$$f(z,t,\lambda_i)=\frac{erfc\left[\frac{-z}{\sqrt{4\lambda_i t}}\right]}{erfc\left[\frac{-r}{\sqrt{4\lambda_i}}\right]} \qquad \text{(S108)}$$

In eq (S108), $[I]$ is the identity matrix with elements δ_{ik}, the Kronecker delta. The calculations of the equilibration trajectories in the polymer casting film, $\begin{pmatrix}\phi_1(z,t)\\ \phi_2(z,t)\end{pmatrix}$, using eqs (S107), and (S108) are easily implemented in MathCad 15.[1]

Due to interchange of non-solvent and solvent between the polymer casting film and the bath, the position of the interface will move with time. At the moving boundary, the boundary conditions are

$$\begin{pmatrix}\phi_1(\varepsilon(t),t)\\ \phi_2(\varepsilon(t),t)\end{pmatrix}=\begin{pmatrix}\phi_{1I}\\ \phi_{2I}\end{pmatrix};\quad \phi_{3I}=1-\phi_{1I}-\phi_{2I}$$
$$\phi_{1b}(\varepsilon(t),t)=\phi_{1bI}=1-\phi_{2bI} \qquad \text{(S109)}$$

In eq (S109), $\varepsilon(t)=r\sqrt{t}$ is the position of the moving interface (see schematic in Figure S12); r is a constant with units of m $s^{-1/2}$, that is determinable from the continuity of component fluxes at either side of the moving interface

$$J_i^V\Big|_{z=\varepsilon(t)}-J_{ib}^V\Big|_{z=\varepsilon(t)}=(\phi_{iI}-\phi_{ibI})\frac{d\varepsilon(t)}{dt};\quad i=1,2$$
$$\frac{d\varepsilon(t)}{dt}=\frac{dr\sqrt{t}}{dt}=\frac{r}{2\sqrt{t}} \qquad \text{(S110)}$$
$$J_i^V\Big|_{z=\varepsilon(t)}-J_{ib}^V\Big|_{z=\varepsilon(t)}=(\phi_{iI}-\phi_{ibI})\frac{r}{2\sqrt{t}};\quad i=1,2$$

The volume fractions ϕ_{iI} and ϕ_{1bI} are determined by the thermodynamic equilibrium constraints

$$\ln(a_{1I})=\ln(a_{1bI});\quad \ln(a_{2I})=\ln(a_{2bI}) \qquad \text{(S111)}$$

The natural logarithm of the component activities are described by eqs (S49), and (S50); note that since the coagulation bath is a polymer-free aqueous solution, eq (S50) is the appropriate expression to be used for calculation of $\ln\left(a_{ibI}\right)$.

The volume fractions at the (moving) interface between the casting film and the coagulation bath, $\begin{pmatrix}\phi_{1I}\\ \phi_{2I}\end{pmatrix}$; $\phi_{3I}=1-\phi_{1I}-\phi_{2I}$, must satisfy the conditions of thermodynamic equilibrium, eq (S111), along $\phi_{1b}(\varepsilon(t),t)=\phi_{1bI}=1-\phi_{2bI}$ with the jump-balance conditions for the interfacial fluxes at the moving interface, eq (S109). Essentially, we have a set of four independent equations in order to determine the four independent unknowns $r,\phi_{1I},\phi_{2I},\phi_{1bI}$. These four independent variables $r,\phi_{1I},\phi_{2I},\phi_{1bI}$ are time-invariant. In order to prove this, we present below the detailed derivations.

Noting that $\frac{\partial erf(z)}{\partial z}=\frac{2}{\sqrt{\pi}}\exp\left(-z^2\right)=-\frac{\partial erfc(z)}{\partial z}$ $\frac{\partial erfc\left[\frac{z}{\sqrt{4\lambda_i t}}\right]}{\partial z}=-\frac{2}{\sqrt{\pi}}\frac{1}{\sqrt{4\lambda_i t}}\exp\left(-\frac{z^2}{4\lambda_i t}\right)=-\frac{\partial erfc\left[-\frac{z}{\sqrt{4\lambda_i t}}\right]}{\partial z}$, and differentiating the composition profile for the volume fraction in coagulation bath, eq (S106), allows the determination of the interfacial fluxes

$$\frac{\partial \phi_{1b}(z,t)}{\partial z} = -\frac{2}{\sqrt{\pi}} \frac{1}{\sqrt{4D_b t}} \frac{\exp\left(-\frac{z^2}{4D_b t}\right)}{erfc\left[\frac{r}{\sqrt{4D_b}}\right]} \left(\phi_{1bI} - \phi_{1b0}\right)$$

$$J_{1b}^{V}\Big|_{z=\varepsilon(t)} = -D_b \frac{d\phi_{1b}(z,t)}{dz}\Big|_{z=\varepsilon(t)} = D_b \frac{\frac{2}{\sqrt{\pi}} \frac{1}{\sqrt{4D_b t}} \exp\left(\frac{-r^2}{4D_b}\right)}{erfc\left(\frac{r}{\sqrt{4D_b}}\right)} \left(\phi_{1bI} - \phi_{1b0}\right) \tag{S112}$$

$$\sqrt{\pi t} J_{1b}^{V}\Big|_{z=\varepsilon(t)} = \frac{D_b}{\sqrt{D_b}} \frac{\exp\left(\frac{-r^2}{4D_b}\right)}{erfc\left(\frac{r}{\sqrt{4D_b}}\right)} \left(\phi_{1bI} - \phi_{1b0}\right)$$

$$\sqrt{\pi t} J_{2b}^{V}\Big|_{z=\varepsilon(t)} = -\sqrt{\pi t} J_{1b}^{V}\Big|_{z=\varepsilon(t)} = -\frac{D_b}{\sqrt{D_b}} \frac{\exp\left(\frac{-r^2}{4D_b}\right)}{erfc\left(\frac{r}{\sqrt{4D_b}}\right)} \left(\phi_{1bI} - \phi_{1b0}\right)$$

The corresponding expressions for the interfacial fluxes in the polymer casting film are written analogously as matrix generalization of eq (S112)

$$\begin{pmatrix} J_1^V \\ J_2^V \end{pmatrix}\Big|_{z=\varepsilon(t)} = -[D] \frac{\partial \begin{pmatrix} \phi_1(z,t) \\ \phi_2(z,t) \end{pmatrix}}{\partial z}\Bigg|_{z=\varepsilon(t)}$$

$$\sqrt{\pi t} \begin{pmatrix} J_1^V \\ J_2^V \end{pmatrix}\Big|_{z=\varepsilon(t)} = -[D][Q_I] \begin{pmatrix} \phi_{1I} - \phi_{10} \\ \phi_{2I} - \phi_{20} \end{pmatrix} \tag{S113}$$

$$[Q_I] = [D]^{-1/2} \left[\exp\left(\frac{-r^2}{4}[D]^{-1}\right)\right] \left[erfc\left(-\frac{r}{2}[D]^{-1/2}\right)\right]^{-1}$$

In eq (S113), the Sylvester theorem is required for explicit evaluation of the four elements of the 2 × 2 dimensional square matrix $[Q_I]$. For the case of distinct eigenvalues, λ_1 and λ_2 of the 2 × 2 dimensional square matrix $[D]$, the Sylvester theorem yields

$$[Q_I] = \frac{f(\lambda_1)\left[[D]-\lambda_2[I]\right]}{(\lambda_1-\lambda_2)} + \frac{f(\lambda_2)\left[[D]-\lambda_1[I]\right]}{(\lambda_2-\lambda_1)}$$

$$f(z,t,\lambda_i) = \frac{1}{\sqrt{\lambda_i}} \frac{\exp\left(-\frac{r^2}{4\lambda_i}\right)}{erfc\left(\frac{-r}{\sqrt{4\lambda_i}}\right)} \tag{S114}$$

Combining eqs (S109), (S112), and (S113), we get

$$\begin{pmatrix}\phi_{1I}-\phi_{1bI}\\ \phi_{2I}-\phi_{2bI}\end{pmatrix}\frac{r}{2\sqrt{t}}\sqrt{\pi t} = \sqrt{\pi t}\begin{pmatrix}J_1^V\\ J_2^V\end{pmatrix}\Bigg|_{z=\varepsilon(t)} - \sqrt{\pi t}\begin{pmatrix}J_{1b}^V\\ J_{2b}^V\end{pmatrix}\Bigg|_{z=\varepsilon(t)}$$

$$\begin{pmatrix}\phi_{1I}-\phi_{1bI}\\ \phi_{2I}-\phi_{2bI}\end{pmatrix}\frac{r\sqrt{\pi}}{2} = -[D][Q_I]\begin{pmatrix}\phi_{1I}-\phi_{10}\\ \phi_{2I}-\phi_{20}\end{pmatrix} - \frac{D_b}{\sqrt{D_b}}\frac{\exp\left(\frac{-r^2}{4D_b}\right)}{erfc\left(\frac{r}{\sqrt{4D_b}}\right)}\begin{pmatrix}\phi_{1bI}-\phi_{1b0}\\ -(\phi_{1bI}-\phi_{1b0})\end{pmatrix} \tag{S115}$$

It is easy to see that eq (S115), which is precisely equivalent to equations A16 and A17 of Tsay and McHugh,[51] is time-invariant. In the simulation results presented in this article the set of jump balance conditions (eq (S115)), in combination with the conditions of thermodynamic equilibrium (eq (S111)), are solved using the Given-Find solve block of MathCad 15[1] in order to determine the four independent unknowns $r,\phi_{1I},\phi_{2I},\phi_{1bI}$. Since the compositions at each end of the tie-line $\phi_{1I},\phi_{2I},\phi_{1bI}$ are not initially known for a given set of initial conditions, a simple head-to-tail iteration procedure is employed. Firstly, the volume fraction ϕ_{1bI} of CB*, that lies on the binodal curve is assumed. The compositions at the other end of the tie-line must be in equilibrium, and these are determined by solving the set of two equations (S133) describing thermodynamic equilibrium. The Fick matrix $[D]$ is then evaluated using a combination of eqs (S89), (S90), (S96), (S97), (S98) and (S99) at the average volume fractions $\frac{1}{2}\begin{pmatrix}\phi_{10}+\phi_{1I}\\ \phi_{20}+\phi_{2I}\end{pmatrix}$. With this information, and an initial guess value for *r*, the set of four non-linear eqs (S111) and (S115) are solved to obtain updated values of $r,\phi_{1I},\phi_{2I},\phi_{1bI}$; these are used to obtain new

estimates of the Fick matrix $[D]$. The head-to-tail iteration procedure usually converges rapidly in about 3-4 steps. Generally speaking, the casting film shrinks in thickness, and the value of *r* is negative.

The simulations for the immersion precipitation process that are presented in the subsequent sections are most conveniently presented in terms of the dimensionless distance coordinate $\eta \equiv \frac{z}{\sqrt{4D_{ref}t}}$ where the chosen reference velocity $D_{ref} = 1\times10^{-9}$ m^2 s^{-1}. Expressed in terms of the dimensionless distance coordinate, the volume fraction profiles in the polymer casting film are

$$\begin{pmatrix}\phi_1(\eta)\\ \phi_2(\eta)\end{pmatrix} = \begin{pmatrix}\phi_{10}\\ \phi_{20}\end{pmatrix} + [Q]\begin{pmatrix}\phi_{1I}-\phi_{10}\\ \phi_{2I}-\phi_{20}\end{pmatrix};$$
$$[Q] = \frac{f(\lambda_1)\left[[D]-\lambda_2[I]\right]}{(\lambda_1-\lambda_2)} + \frac{f(\lambda_2)\left[[D]-\lambda_1[I]\right]}{(\lambda_2-\lambda_1)}$$
$$f(z,t,\lambda_i) = \frac{erfc\left[-\eta\sqrt{\frac{D_{ref}}{\lambda_i}}\right]}{erfc\left[\frac{-r}{\sqrt{4D_{ref}}}\sqrt{\frac{D_{ref}}{\lambda_i}}\right]} \qquad \text{(S116)}$$

The corresponding profiles in the coagulation bath are

$$\phi_{1b}(\eta) = \phi_{1b0} + \frac{erfc\left[\eta\sqrt{\frac{D_{ref}}{D_b}}\right]}{erfc\left[\frac{r}{\sqrt{4D_{ref}}}\sqrt{\frac{D_{ref}}{D_b}}\right]}(\phi_{1bI}-\phi_{1b0}) \qquad \text{(S117)}$$

5.2 Uphill diffusion in water/acetone/CA solutions

We first consider transient diffusion of water(1)/acetone(2)/CA(3) in which the initial volume fractions in the casting film and coagulation bath are, respectively, $\begin{pmatrix}\phi_{10}\\ \phi_{20}\end{pmatrix} = \begin{pmatrix}0\\ 0.9\end{pmatrix}$; $\begin{pmatrix}\phi_{1b0}\\ \phi_{2b0}\end{pmatrix} = \begin{pmatrix}1\\ 0\end{pmatrix}$; see Figure S13a. The F-H and diffusivity input data for the calculations are specified in Table S6.

The set of four non-linear eqs (S111) and (S115) are solved using the Given-Find solve block of MathCad 15;[1] the values of the volume fractions at either sides of the interface, A* and CB* are determined as $\begin{pmatrix}\phi_{1I}\\ \phi_{2I}\end{pmatrix}=\begin{pmatrix}0.2181\\ 0.34308\end{pmatrix}$; $\begin{pmatrix}\phi_{1bI}\\ \phi_{2bI}\end{pmatrix}=\begin{pmatrix}0.75432\\ 0.24568\end{pmatrix}$. The value of $\frac{r}{\sqrt{4D_{ref}}}=-7.48505\times10^{-3}$ is negative because of shrinkage of the polymer casting film.

For water/acetone mixtures in the coagulation bath, the Fick diffusivity D_b is evaluated as a function of the composition by using the combination of (S98) and (S99). The Fick diffusivity matrix $[D]$ is estimated using a combination of eqs (S89), (S90), (S96), (S97), (S98) and (S99). Evaluated at the arithmetic average volume fractions between the initial and final equilibrated compositions, $\frac{1}{2}\begin{pmatrix}\phi_{10}+\phi_{1I}\\ \phi_{2I}+\phi_{2I}\end{pmatrix}$, the elements of the matrix of thermodynamic factors, and the Fick diffusivity matrix are:

$[\Gamma]=\begin{bmatrix}0.39141 & 0.01964\\ -0.84517 & 0.11602\end{bmatrix}$; $[D]=\begin{bmatrix}1.59603 & 0.0816\\ -1.1073 & -0.0232\end{bmatrix}\times10^{-9}\,\mathrm{m^2s^{-1}}$. The large negative value of D_{21} is directly attributable to the corresponding negative value of Γ_{21}.

For convenience of the readers, all the input parameters, along with the values of $[\Gamma]$ and $[D]$ are also summarized in Figure S13

The transient equilibration trajectory A-A* is curvilinear; see Figure S13a in which the equilibration trajectories are plotted both in binary and ternary composition spaces. No foray into the meta-stable region is experienced. The calculated composition trajectory is comparable to the numerical simulation results as presented in Figure 5 of Tsay and McHugh[42] for immersion time of 0.24 s.

Figure S13b show the transient approach to equilibration, in which the *x*-axis is the dimensionless distance coordinate $\eta=\frac{z}{\sqrt{4D_{ref}t}}$, where the reference value of the diffusivity is $D_{ref}=1\times10^{-9}\ \mathrm{m^2\ s^{-1}}$. Particularly noteworthy is that the volume fraction of the polymer CA near the surface of the casting

film are significantly higher than in the base of the casting film, $z \approx 0$. This implies that the polymer distributes asymmetrically across the membrane thickness.

As the immersion time increases, the composition in the polymer casting film will become richer in water, but more impoverished in the solvent acetone. Conversely, the coagulation bath will get progressively richer in acetone and poorer in water. In our simplified approach, we model the transient equilibration trajectory by choosing the initial compositions of the casting film and coagulation baths for as $\begin{pmatrix}\phi_{10}\\ \phi_{20}\end{pmatrix}=\begin{pmatrix}0.11\\ 0.8\end{pmatrix}$; $\begin{pmatrix}\phi_{1b0}\\ \phi_{2b0}\end{pmatrix}=\begin{pmatrix}0.92\\ 0.08\end{pmatrix}$, and $\begin{pmatrix}\phi_{10}\\ \phi_{20}\end{pmatrix}=\begin{pmatrix}0.28\\ 0.63\end{pmatrix}$; $\begin{pmatrix}\phi_{1b0}\\ \phi_{2b0}\end{pmatrix}=\begin{pmatrix}0.75\\ 0.25\end{pmatrix}$ for B, and C, respectively.

Let us analyze the B-B* trajectory in which the initial volume fractions in casting film and coagulation bath are chosen $\begin{pmatrix}\phi_{10}\\ \phi_{20}\end{pmatrix}=\begin{pmatrix}0.11\\ 0.8\end{pmatrix}$; $\begin{pmatrix}\phi_{1b0}\\ \phi_{2b0}\end{pmatrix}=\begin{pmatrix}0.92\\ 0.08\end{pmatrix}$; see Figure S14.

The set of four non-linear eqs (S111) and (S115) are solved using the Given-Find solve block of MathCad 15;[1] the values of the volume fractions at either sides of the interface, B* and CB* are determined as $\begin{pmatrix}\phi_{1I}\\ \phi_{2I}\end{pmatrix}=\begin{pmatrix}0.23067\\ 0.40421\end{pmatrix}$; $\begin{pmatrix}\phi_{1bI}\\ \phi_{2bI}\end{pmatrix}=\begin{pmatrix}0.71629\\ 0.28371\end{pmatrix}$. The value of $\frac{r}{\sqrt{4D_{ref}}}=$ -0.05545 is negative because of shrinkage of the polymer casting film.

Evaluated at the arithmetic average volume fractions between the initial and final equilibrated compositions, $\frac{1}{2}\begin{pmatrix}\phi_{10}+\phi_{1I}\\ \phi_{2I}+\phi_{2I}\end{pmatrix}$, the elements of the matrix of thermodynamic factors, and the Fick diffusivity matrix are: $[\Gamma]=\begin{bmatrix}0.29527 & -0.01645\\ -0.81379 & 0.24899\end{bmatrix}$; $[D]=\begin{bmatrix}1.04718 & -0.05711\\ -0.78251 & 0.07094\end{bmatrix}\times 10^{-9}\,\mathrm{m^2 s^{-1}}$.

Noteworthy are the large negative values of both off-diagonal elements Γ_{12}, and Γ_{21}. Both off-diagonal elements D_{12} and D_{21} are negative, because of the corresponding negative values of Γ_{12}, and Γ_{21}.

We note that the B-B* is also curvilinear but no foray into the metastable region is observed; see Figure S14a. The curvilinear trajectories are directly attributable to the off-diagonal contributions of D_{12} and D_{21} that cause strong coupled diffusion phenomena.

The volume fractions of the three components are plotted in Figure S14b as function of the dimensionless distance coordinate $\frac{z}{\sqrt{4D_{ref}t}}$. There is a significantly higher volume fraction of the polymer near the surface of the casting film, $z \approx 0$. This implies that the polymer distributes asymmetrically across the membrane thickness.

Let us analyze the C-C* trajectory in which the initial volume fractions in casting film are chosen as $\begin{pmatrix}\phi_{10}\\ \phi_{20}\end{pmatrix}=\begin{pmatrix}0.28\\ 0.63\end{pmatrix}$; $\begin{pmatrix}\phi_{1b0}\\ \phi_{2b0}\end{pmatrix}=\begin{pmatrix}0.75\\ 0.25\end{pmatrix}$; see Figure S15.

The set of four non-linear (S111) and (S115) are solved using the Given-Find solve block of MathCad 15;[1] the values of the volume fractions at either sides of the interface, C* and CB* are determined as $\begin{pmatrix}\phi_{1I}\\ \phi_{2I}\end{pmatrix}=\begin{pmatrix}0.24596\\ 0.46422\end{pmatrix}$; $\begin{pmatrix}\phi_{1bI}\\ \phi_{2bI}\end{pmatrix}=\begin{pmatrix}0.6753\\ 0.3247\end{pmatrix}$. The value of $\frac{r}{\sqrt{4D_{ref}}}$ = -0.05476; $r=-3.46302\times10^{-6}$ is negative because of shrinkage of the polymer casting film.

Evaluated at the arithmetic average volume fractions between the initial and final equilibrated compositions, $\frac{1}{2}\begin{pmatrix}\phi_{10}+\phi_{1I}\\ \phi_{2I}+\phi_{2I}\end{pmatrix}$, the elements of the matrix of thermodynamic factors, and the Fick diffusivity matrix are: $[\Gamma]=\begin{bmatrix}0.15393 & -0.08279\\ -0.53829 & 0.49255\end{bmatrix}$; $[D]=\begin{bmatrix}0.46829 & -0.25204\\ -0.36327 & 0.21014\end{bmatrix}\times10^{-9}\,\mathrm{m^2s^{-1}}$. Noteworthy is the large negative value of both off-diagonal elements Γ_{12}, and Γ_{21}. Both off-diagonal elements D_{12} and D_{21} are negative, because of the corresponding negative values of Γ_{12}, and Γ_{21}.

We note that the C-C* is strongly curvilinear and has penetrated into the metastable region; see Figure S15a. The curvilinear trajectories are directly attributable to the off-diagonal contributions of D_{12} and D_{21} that cause strong coupled diffusion phenomena.

The volume fractions of the three components are plotted in Figure S15b as function of the dimensionless distance coordinate $\frac{z}{\sqrt{4D_{ref}t}}$. There is a significantly higher volume fraction of the

polymer near the surface of the casting film, $z \approx 0$. This implies that the polymer distributes asymmetrically across the membrane thickness. Also noteworthy is that the volume fraction of water shows a pronounced overshoot at $\frac{z}{\sqrt{4D_{ref}t}} \approx -0.2$; this overshoot signifies uphill diffusion.[14, 15, 53] The overshoot in water is a direct result of coupled diffusion phenomena, as explained in earlier works.[14, 15, 53] Figure S15c compares the transient volume fractions of water with the corresponding activities; the transient activity profiles show no overshoot, confirming that the diffusion is only uphill if gauged in terms of volume fraction; the transport is down the activity hill.

In order to demonstrate that the forays into the metastable region between the binodal and spinodal curves is engendered by thermodynamic coupling effects, we also calculated the equilibration trajectories in which the thermodynamic corrections are ignored by invoking the assumption $\Gamma_{ij} = \delta_{ij}$, the Kronecker delta. The corresponding equilibration trajectories are indicated by the dashed lines in Figure S15a. In this simplified scenario, no forays into the metastable region is observed. Indeed, the equilibration trajectory tends to veer *away* from the binodal curve in its approach to C*. The inescapable conclusion is that the influence of the thermodynamic correction factors is to draw the trajectories into the metastable region, leading eventually to polymer precipitation.

5.3 Uphill diffusion in water/DMF/PVDF solutions

For the ternary system water (non-solvent, component 1), dimethyl formamide (DMF, solvent, component 2) and poly(vinylidene fluoride) (PVDF = polymer = m, component 3), the binodal and spinodal curves are shown in Figure S16.

Let us analyze the A-A* trajectory using our simplified model in which the initial volume fractions in polymer casting film and coagulation bath are chosen, respectively, as $\begin{pmatrix} \phi_{10} \\ \phi_{20} \end{pmatrix} = \begin{pmatrix} 0 \\ 0.65 \end{pmatrix}$; $\begin{pmatrix} \phi_{1b0} \\ \phi_{2b0} \end{pmatrix} = \begin{pmatrix} 0.4 \\ 0.6 \end{pmatrix}$; see Figure S16.

Rather than ignoring 1-2 friction, the M-S diffusivity $Đ_{12}^{V} = \frac{Đ_{21}^{V}}{\overline{V_1}}\overline{V_2}$ quantifying 1-2 friction is estimated using the following step-by-step procedure. The experimental data of the Fick diffusivity for water(1)/DMF(2) pair diffusivity D_{12} as reported by Chen et al.[54] is used to determine the M-S diffusivity $Đ_{12}$ by correcting for the thermodynamic factor $Đ_{12} = \frac{D_{12}}{\Gamma}$; the thermodynamic factor is determined from the NRTL equation, with parameters $\tau_{12} = 0.18973$; $\tau_{12} = -0.10798$; $\alpha_{12} = 0.277$. The variation of the M-S diffusivity $Đ_{12}$ with mole fraction of water, is described adequately by the Vignes interpolation formula, [11, 12] eq (S34), in which the infinite-dilution values of the M-S diffusivities are

$$\begin{aligned} Đ_{12}^{x_1 \to 1} &= 1 \times 10^{-9} \text{ m}^2 \text{ s}^{-1} \\ Đ_{12}^{x_2 \to 1} &= 2.5 \times 10^{-9} \text{ m}^2 \text{ s}^{-1} \end{aligned} \tag{S118}$$

For use in eqs (S89), and (S90), the M-S diffusivity $Đ_{12}^{V} = \frac{Đ_{12}\overline{V_2}}{\overline{V}} = \frac{Đ_{21}^{V}}{\overline{V_1}}\overline{V_2}$ $Đ_{12}$ is calculated from eq (S34) using the interpolation formula for the binary water(1)/DMF(2) pair on a polymer-free basis. In other words, the mole fractions x_1 is calculated for the effective volume fraction of water (component 1) in the binary pair in the ternary mixture $\frac{\phi_1}{\phi_1 + \phi_2} = \frac{\phi_1}{1 - \phi_3}$.

For water/DMF mixtures in the coagulation bath, the Fick diffusivity D_b is estimated as a function of the composition by using the combination of (S98), and (S118), along with calculation of the thermodynamic correction factors using the NRTL equation. The Fick diffusivity matrix $[D]$ is estimated using a combination of eqs (S89), (S90), (S96), (S97), (S98), and (S118).

The set of four non-linear eqs (S111) and (S115) are solved using the Given-Find solve block of MathCad 15;[1] the values of the volume fractions at either sides of the interface, A* and CB* are determined as $\begin{pmatrix} \phi_{1I} \\ \phi_{2I} \end{pmatrix} = \begin{pmatrix} 0.0609 \\ 0.23075 \end{pmatrix}$; $\begin{pmatrix} \phi_{1bI} \\ \phi_{2bI} \end{pmatrix} = \begin{pmatrix} 0.29701 \\ 0.70299 \end{pmatrix}$.

Evaluated at the arithmetic average volume fractions between the initial and final equilibrated compositions, $\frac{1}{2}\begin{pmatrix}\phi_{10}+\phi_{1I}\\ \phi_{2I}+\phi_{2I}\end{pmatrix}$, the elements of the matrix of thermodynamic factors, and the Fick diffusivity matrix are: $[\Gamma]=\begin{bmatrix}0.81984 & -0.04225\\ -2.92545 & 0.42313\end{bmatrix}$; $[D]=\begin{bmatrix}3.23211 & -0.16621\\ -1.49605 & 0.08997\end{bmatrix}\times 10^{-9}\,\mathrm{m^2 s^{-1}}$. Noteworthy is the large negative value of both off-diagonal elements Γ_{12}, and Γ_{21}. Both off-diagonal elements D_{12} and D_{21} are negative, because of the corresponding negative values of Γ_{12}, and Γ_{21}.

We note that the A-A* is strongly curvilinear and has penetrated into the metastable region; see Figure S16a. The curvilinear trajectories are directly attributable to the off-diagonal contributions of D_{12} and D_{21} that cause strong coupled diffusion phenomena.

The volume fractions of the three components are plotted in Figure S16b as function of the dimensionless distance coordinate $\frac{z}{\sqrt{4D_{ref}t}}$. There is a significantly higher volume fraction of the polymer near the surface of the casting film, $z\approx 0$. Also noteworthy is that the volume fraction of water (1) shows a pronounced overshoot at $\frac{z}{\sqrt{4D_{ref}t}}\approx -0.1$; this overshoot signifies uphill diffusion.[14, 15, 53] The overshoot in water is a direct result of coupled diffusion phenomena, as explained in earlier works.[14, 15, 53]

5.4 Uphill diffusion in water/NMP/PSF solutions

For the ternary system water (non-solvent, component 1), N-methyl-2-pyrrolidone (NMP) (solvent, component 2) and polysulfone (PSF = polymer, component m= 3). The binodal and spinodal curves are shown in Figure S17.

Modelling the immersion precipitation process

Let us analyze the A-A* trajectory using our simplified model in which the initial volume fractions in polymer casting film and coagulation bath are chosen, respectively as $\begin{pmatrix}\phi_{10}\\ \phi_{20}\end{pmatrix}=\begin{pmatrix}0\\ 0.7\end{pmatrix}$; $\begin{pmatrix}\phi_{1b0}\\ \phi_{2b0}\end{pmatrix}=\begin{pmatrix}0.3\\ 0.7\end{pmatrix}$; see Figure S17.

Rather than ignoring 1-2 friction, the M-S diffusivity $Đ_{12}^{V}=\frac{Đ_{21}^{V}}{\overline{V_1}}\overline{V_2}$ quantifying 1-2 friction is estimated using the experimental data of the Fick diffusivity for water(1)/NMP(2) pair diffusivity D_{12} as reported by Tkacik and Zeman.[55] From this data the M-S diffusivity and both taken to be composition independent, both values being equal to $0.73\times10^{-9}\,\mathrm{m^2s^{-1}}$. For water/NMP mixtures in the coagulation bath, the Fick diffusivity $D_b=0.73\times10^{-9}\,\mathrm{m^2s^{-1}}$

The set of four non-linear eqs (S111) and (S115) are solved using the Given-Find solve block of MathCad 15;[1] the values of the volume fractions at either sides of the interface, A* and CB* are determined as $\begin{pmatrix}\phi_{1I}\\ \phi_{2I}\end{pmatrix}=\begin{pmatrix}0.01623\\ 0.23293\end{pmatrix}$; $\begin{pmatrix}\phi_{1bI}\\ \phi_{2bI}\end{pmatrix}=\begin{pmatrix}0.25625\\ 0.74375\end{pmatrix}$.

The value of $\frac{r}{\sqrt{4D_{ref}}}=$ -0.0148; $r=$ -9.35997×10^{-7} is negative because of shrinkage of the polymer casting film.

Evaluated at the arithmetic average volume fractions between the initial and final equilibrated compositions, $\frac{1}{2}\begin{pmatrix}\phi_{10}+\phi_{1I}\\ \phi_{2I}+\phi_{2I}\end{pmatrix}$, the elements of the matrix of thermodynamic factors, and the Fick diffusivity matrix are: $[\Gamma]=\begin{bmatrix}0.93085 & -0.01965\\ -5.36896 & 0.46328\end{bmatrix}$; $[D]=\begin{bmatrix}1.39456 & -0.02938\\ -0.6735 & 0.01775\end{bmatrix}\times10^{-9}\,\mathrm{m^2s^{-1}}$.

Noteworthy is the large negative value of both off-diagonal elements Γ_{12}, and Γ_{21}. Both off-diagonal elements D_{12} and D_{21} are negative, because of the corresponding negative values of Γ_{12}, and Γ_{21}.

We note that the A-A* trajectory is strongly curvilinear and has penetrated into the metastable region; see Figure S17a. The curvilinear trajectories are directly attributable to the off-diagonal contributions of D_{12} and D_{21} that cause strong coupled diffusion phenomena.

The volume fractions of the three components are plotted in Figure S17b as function of the dimensionless distance coordinate $\frac{z}{\sqrt{4D_{ref}t}}$. There is a significantly higher volume fraction of the polymer near the surface of the casting film, $z \approx 0$. Also noteworthy is that the volume fraction of water (1) shows a pronounced overshoot at $\frac{z}{\sqrt{4D_{ref}t}} \approx -0.1$; this overshoot signifies uphill diffusion.[14, 15, 53] The overshoot in water is a direct result of coupled diffusion phenomena, as explained in earlier works.[14, 15, 53]

In order to demonstrate that the forays into the metastable region between the binodal and spinodal curves is engendered by thermodynamic coupling effects, we also calculated the equilibration trajectories in which the thermodynamic corrections are ignored, by invoking the assumption $\Gamma_{ij} = \delta_{ij}$, the Kronecker delta. The corresponding equilibration trajectories are indicated by the dashed lines in Figure S17a. In this simplified scenario, no forays into the metastable region is observed. The inescapable conclusion is that the influence of the thermodynamic correction factors is to draw the trajectories into the metastable region, leading eventually to polymer precipitation.

5.5 Uphill diffusion in water/NMP/PEI solutions

For the ternary system water (non-solvent, component 1), N-methyl-2-pyrrolidone (NMP) (solvent, component 2) and polyetherimide (PEI = polymer, component m = 3). The binodal and spinodal curves are shown in Figure S18.

Modelling the immersion precipitation process

Let us analyze the A-A* trajectory using our simplified model in which the initial volume fractions in polymer casting film and coagulation bath are chosen, respectively as $\begin{pmatrix}\phi_{10}\\ \phi_{20}\end{pmatrix}=\begin{pmatrix}0\\ 0.65\end{pmatrix}$; $\begin{pmatrix}\phi_{1b0}\\ \phi_{2b0}\end{pmatrix}=\begin{pmatrix}0.35\\ 0.65\end{pmatrix}$; see Figure S18.

Rather than ignoring 1-2 friction, the M-S diffusivity $Đ_{12}^{V}=\frac{Đ_{21}^{V}}{\overline{V_1}}\overline{V_2}$ quantifying 1-2 friction is estimated using the experimental data of the Fick diffusivity for water(1)/NMP(2) pair diffusivity D_{12} as reported by Tkacik and Zeman.[55] From this data the M-S diffusivity and both taken to be composition independent, both values being equal to $0.73\times10^{-9}\,\mathrm{m^2s^{-1}}$. For water/NMP mixtures in the coagulation bath, the Fick diffusivity $D_b=0.73\times10^{-9}\,\mathrm{m^2s^{-1}}$

The set of four non-linear (S111) and (S115) are solved using the Given-Find solve block of MathCad 15;[1] the values of the volume fractions at either sides of the interface, A* and CB* are determined as $\begin{pmatrix}\phi_{1I}\\ \phi_{2I}\end{pmatrix}=\begin{pmatrix}0.08883\\ 0.36142\end{pmatrix}$; $\begin{pmatrix}\phi_{1bI}\\ \phi_{2bI}\end{pmatrix}=\begin{pmatrix}0.2491\\ 0.7509\end{pmatrix}$.

Evaluated at the arithmetic average volume fractions between the initial and final equilibrated compositions, $\frac{1}{2}\begin{pmatrix}\phi_{10}+\phi_{1I}\\ \phi_{2I}+\phi_{2I}\end{pmatrix}$, the elements of the matrix of thermodynamic factors, and the Fick diffusivity matrix are: $[\Gamma]=\begin{bmatrix}0.75052 & -0.03616\\ -3.08371 & 0.33542\end{bmatrix}$; $[D]=\begin{bmatrix}1.22949 & -0.05916\\ -0.64793 & 0.03233\end{bmatrix}\times10^{-9}\,\mathrm{m^2s^{-1}}$.

Noteworthy is the large negative value of both off-diagonal elements Γ_{12}, and Γ_{21}. Both off-diagonal elements D_{12} and D_{21} are negative, because of the corresponding negative values of Γ_{12}, and Γ_{21}.

We note that the A-A* trajectory is strongly curvilinear and has penetrated into the metastable region; see Figure S18a. The curvilinear trajectories are directly attributable to the off-diagonal contributions of D_{12} and D_{21} that cause strong coupled diffusion phenomena.

Modelling the immersion precipitation process

The volume fractions of the three components are plotted in Figure S18b as function of the dimensionless distance coordinate $\frac{z}{\sqrt{4D_{ref}t}}$. There is a significantly higher volume fraction of the polymer near the surface of the casting film, $z \approx 0$. Also noteworthy is that the volume fraction of water (1) shows a slight overshoot at $\frac{z}{\sqrt{4D_{ref}t}} \approx -0.02$; this overshoot signifies uphill diffusion.[14, 15, 53] The overshoot in water is a direct result of coupled diffusion phenomena, as explained in earlier works.[14, 15, 53]

5.6 List of Tables for Modelling the immersion precipitation process

Table S6. Flory-Huggins and diffusivity parameters for penetrants water (anti-solvent, component 1) and acetone (solvent, Component 2) in cellulose acetate (CA) (polymer, indicated by subscript m=3) at T = 298.15 K. The Flory-Huggins parameters are taken from Altena and Smolders.[56] The self-diffusivities for water (1)/acetone(2)/CA(m=3) are estimated using the free-volume parameters as reported in Table 1 of Altinkaya and Ozbas,[49] and Table 3.3 of the MS thesis of Yip,[57] that is available online. The values are reproduced below for ready reference.

Parameter	Units	Values
ρ_1, ρ_2, ρ_3	kg m^{-3}	1000, 790, 1310
M_1, M_2, M_3	g mol^{-1}	18, 58.08, 307000
$\overline{V_1}, \overline{V_2}, \overline{V_m}$	cm^3 mol^{-1}	18, 73.92, 30532
$\chi_{12} = a + b(u_2) + c(u_2)^2 + d(u_2)^3 + e(u_2)^4; \quad u_2 = \frac{\phi_2}{\phi_1 + \phi_2}$ $a = 1.1; b = -0.42; c = 4.09; d = -6.7; e = 4.28;$ $\chi_{1m} = 1.4; \chi_{2m} = 0.45;$		
V_1^*, V_2^*, V_3^*	cm^3 g^{-1}	1.071, 0.943, 2.67
$D_{1,self,0}, D_{2,self,0}$	10^{-8}m^2 s^{-1}	8.55, 3.6
E	J mol^{-1}	0
$\frac{K_{11}}{\gamma}, \frac{K_{12}}{\gamma}, \frac{K_{13}}{\gamma}$	cm^3 g^{-1} K^{-1}	0.00218, 0.00186, 0.000364
$K_{21} - T_{g1}, K_{22} - T_{g2}, K_{23} - T_{g3}$	K	−152.29, −53.33, −240
ξ_{13}, ξ_{23}	dimensionless	0.0943, 0.268

Table S7. Flory-Huggins and diffusivity parameters for penetrants water (anti-solvent, component 1) and DMF (solvent, Component 2) in PVDF (poly(vinylidene) fluoride), indicated by subscript m=3) at T = 298.15 K. The Flory-Huggins parameters are taken from Yip,[57] and Matsuyama et al.[58] The self-diffusivities are estimated using the free-volume parameters as reported in Table 3.3 of the MS thesis of Yip,[57] that is available online. The values are reproduced below for ready reference.

Parameter	Units	Values
ρ_1, ρ_2, ρ_3	kg m^{-3}	1000, 944.3, 1739
M_1, M_2, M_3	g mol^{-1}	18, 73.09, 534000
$\overline{V_1}, \overline{V_2}, \overline{V_m}$	cm^3 mol^{-1}	18, 77.4, 307000
$\chi_{12} = a + b(u_2) + c(u_2)^2 + d(u_2)^3 + e(u_2)^4$; $u_2 = \frac{\phi_2}{\phi_1 + \phi_2}$ $a = 0.5; b = 0.04; c = 0.8; d = -1.2; e = 0.8;$ $\chi_{1m} = 2.09; \chi_{2m} = 0.43;$		
V_1^*, V_2^*, V_3^*	cm^3 g^{-1}	1.071, 0.926, 0.565
$D_{1,self,0}, D_{2,self,0}$	10^{-8}m^2 s^{-1}	8.55, 8.48
E	J mol^{-1}	0
$\frac{K_{11}}{\gamma}, \frac{K_{12}}{\gamma}, \frac{K_{13}}{\gamma}$	cm^3 g^{-1} K^{-1}	0.00218, 0.000976, 0.000273
$K_{21} - T_{g1}, K_{22} - T_{g2}, K_{23} - T_{g3}$	K	–152.29, –43.8, –127
ξ_{13}, ξ_{23}	dimensionless	0.313, 1.1

Table S8. Flory-Huggins and diffusivity parameters for penetrants water (anti-solvent, component 1) and NMP (solvent, Component 2) in PSF (polysulfone, indicated by subscript m=3) at T = 298.15 K. The Flory-Huggins parameters are taken from Yip,[57] and Kim et al.[59] The self-diffusivities are estimated using the free-volume parameters as reported in Table 3.3 of the MS thesis of Yip,[57] that is available online. The values are reproduced below for ready reference.

Parameter	Units	Values
ρ_1, ρ_2, ρ_3	kg m^{-3}	1000, 1030, 1240
M_1, M_2, M_3	g mol^{-1}	18, 99.1, 20270
$\overline{V_1}, \overline{V_2}, \overline{V_m}$	cm^3 mol^{-1}	18, 96.2, 16347
$\chi_{12} = a + b(u_2) + c(u_2)^2 + d(u_2)^3 + e(u_2)^4; \quad u_2 = \frac{\phi_2}{\phi_1 + \phi_2}$ $a = 0.785; b = 0.665; c = 0; d = 0; e = 0;$ $\chi_{1m} = 3.7; \chi_{2m} = 0.24;$		
V_1^*, V_2^*, V_3^*	cm^3 g^{-1}	1.071, 0.841, 0.733
$D_{1,self,0}, D_{2,self,0}$	10^{-8}m^2 s^{-1}	8.55, 3.137
E	J mol^{-1}	0
$\frac{K_{11}}{\gamma}, \frac{K_{12}}{\gamma}, \frac{K_{13}}{\gamma}$	cm^3 g^{-1} K^{-1}	0.00218, 0.000963, 0.00043
$K_{21} - T_{g1}, K_{22} - T_{g2}, K_{23} - T_{g3}$	K	–152.29, –48.496, –410
ξ_{13}, ξ_{23}	dimensionless	0.097, 0.4194

Table S9. Flory-Huggins and diffusivity parameters for penetrants water (anti-solvent, component 1) and NMP (solvent, Component 2) in PEI (polyetherimide), indicated by subscript m=3) at T = 298.15 K. The Flory-Huggins parameters are taken from Yip,[57] Kim et al.,[59] and Fernandes et al.[60] The self-diffusivities are estimated using the free-volume parameters as reported in Table 3.3 of the MS thesis of Yip,[57] that is available online. The values are reproduced below for ready reference.

Parameter	Units	Values
ρ_1, ρ_2, ρ_3	kg m^{-3}	1000,1030,1270
M_1, M_2, M_3	g mol^{-1}	18, 99.1, 22400
$\overline{V_1}, \overline{V_2}, \overline{V_m}$	cm^3 mol^{-1}	18, 96.2, 17638
$\chi_{12} = a + b(u_2) + c(u_2)^2 + d(u_2)^3 + e(u_2)^4$; $u_2 = \frac{\phi_2}{\phi_1 + \phi_2}$ $a = 0.785; b = 0.665; c = 0; d = 0; e = 0;$ $\chi_{1m} = 2.1; \chi_{2m} = 0.507;$		
V_1^*, V_2^*, V_3^*	cm^3 g^{-1}	1.071, 0.841, 0.663
$D_{1,self,0}, D_{2,self,0}$	10^{-8}m^2 s^{-1}	8.55, 3.137
E	J mol^{-1}	0
$\frac{K_{11}}{\gamma}, \frac{K_{12}}{\gamma}, \frac{K_{13}}{\gamma}$	cm^3 g^{-1} K^{-1}	0.00218, 0.000963, 0.000452
$K_{21} - T_{g1}, K_{22} - T_{g2}, K_{23} - T_{g3}$	K	–152.29, –48.496, –443
ξ_{13}, ξ_{23}	dimensionless	0.0909, 0.393

5.7 List of Figures for Modelling the immersion precipitation process

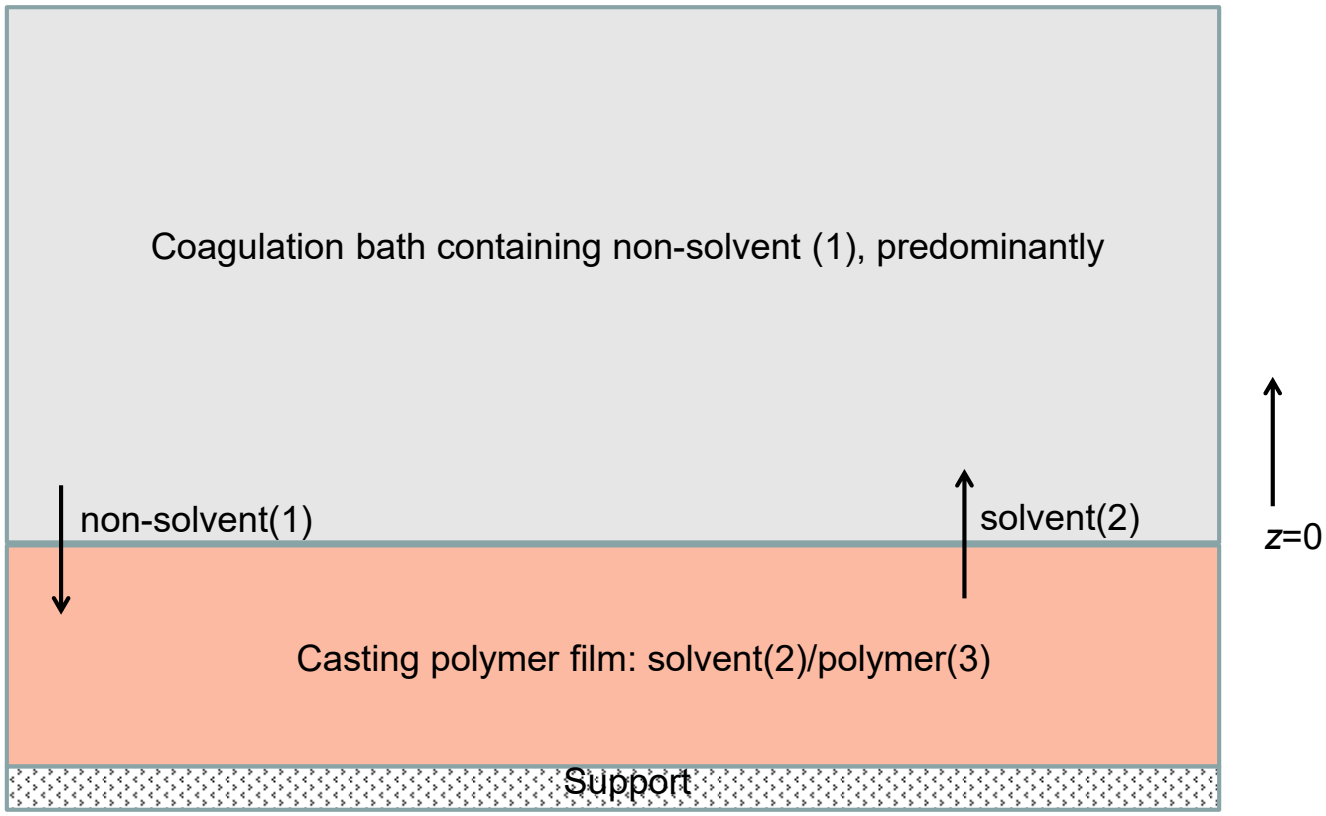

Figure S8. Schematic of the configuration used to model the immersion precipitation process.

Modelling the immersion precipitation process

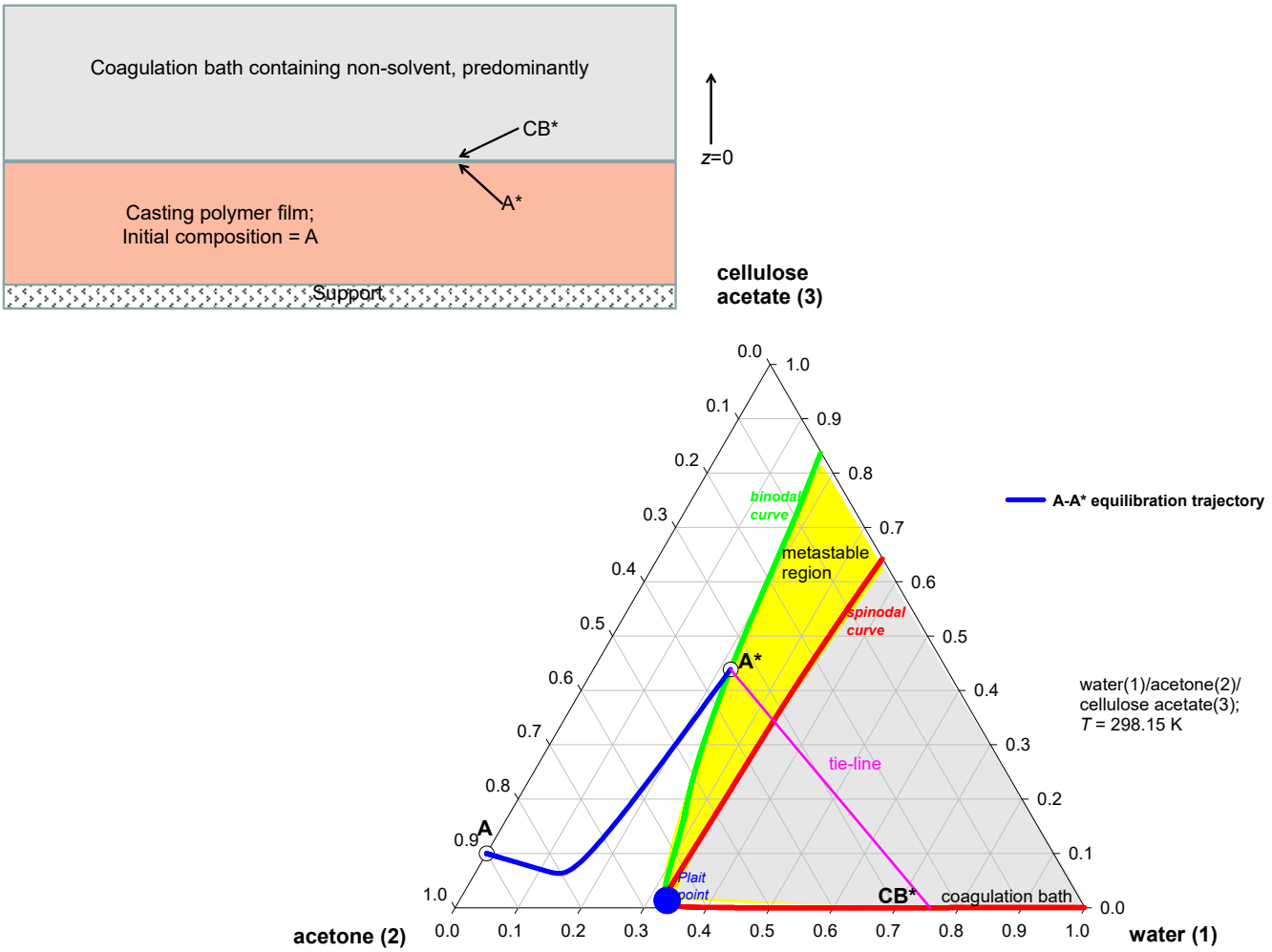

Figure S9. Transient equilibration trajectory A-A* during the immersion precipitation process for membrane preparation; adapted from the Figure 5 of Tsay and McHugh for an immersion time of 0.24 s.[42] A 10% solution of Cellulose Acetate (CA) in acetone is immersed in a coagulation bath of pure water. The equilibration trajectory A-A* was determined from our simulations (described in detail in this article).

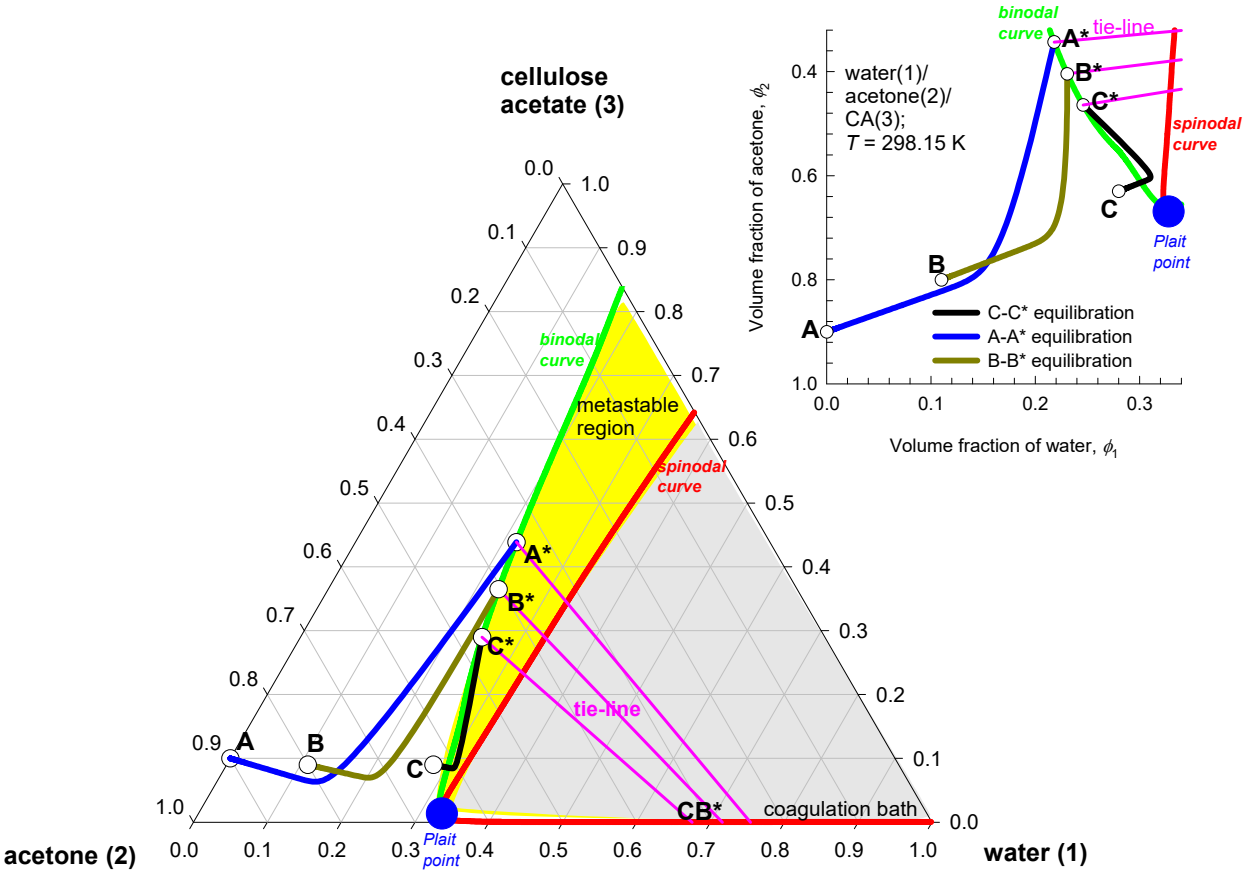

Figure S10. Transient equilibration trajectories A-A*, B-B*, and C-C* during the immersion precipitation process for membrane preparation with increasing immersion times. These trajectories were determined from our simulations (described in detail in this article) using the starting compositions A, B, and C in the polymer casting film for three different, increasing, immersion times ranging from 0.24 s, 10 s, and 24 s, as presented in Figure 5 of Tsay and McHugh.[42]

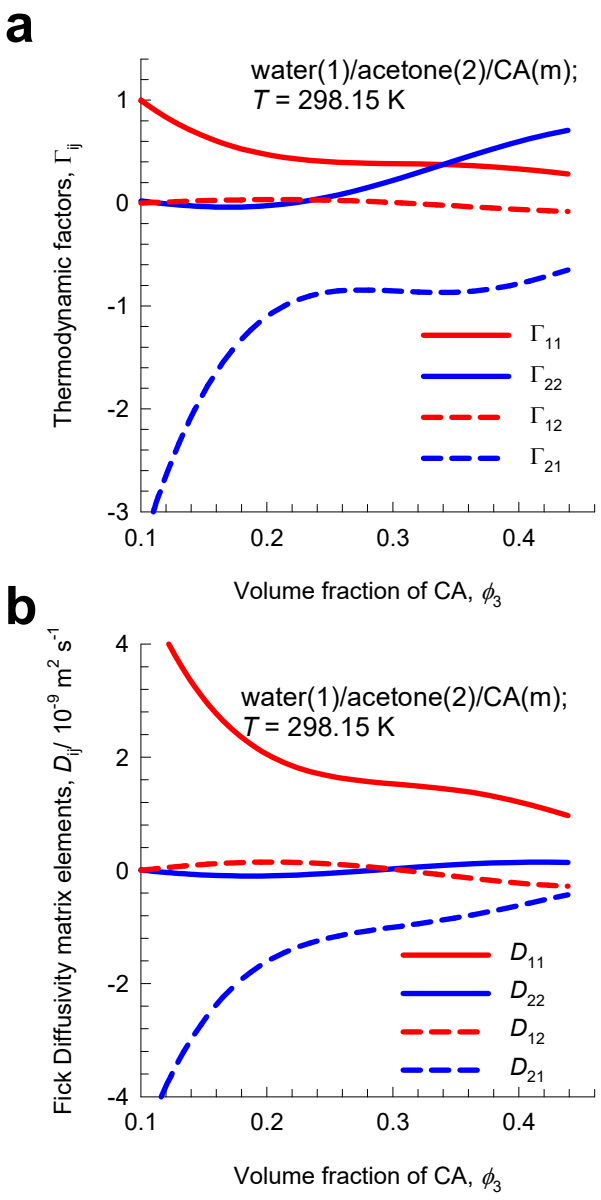

Figure S11. Calculations for (a) matrix of thermodynamic correction factors, $[\Gamma]$, and (b) Elements of the Fick diffusivity matrix $[D]$, for water(1)/acetone(2)/CA(m) at T = 298.15 K. The input data for the calculations are specified in Table S6.

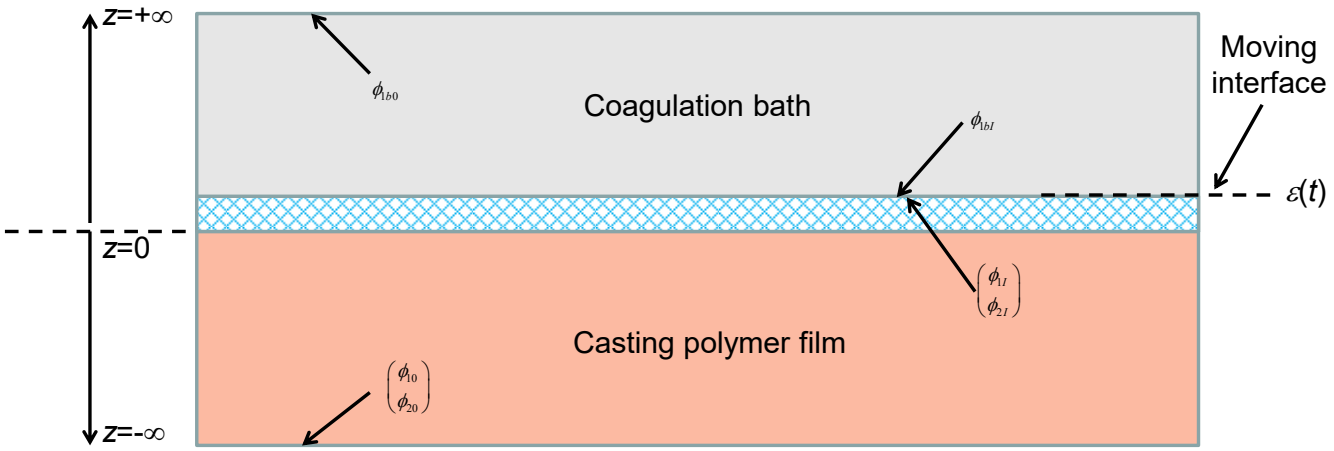

Figure S12. Schematic of the configuration used to model the immersion precipitation process.

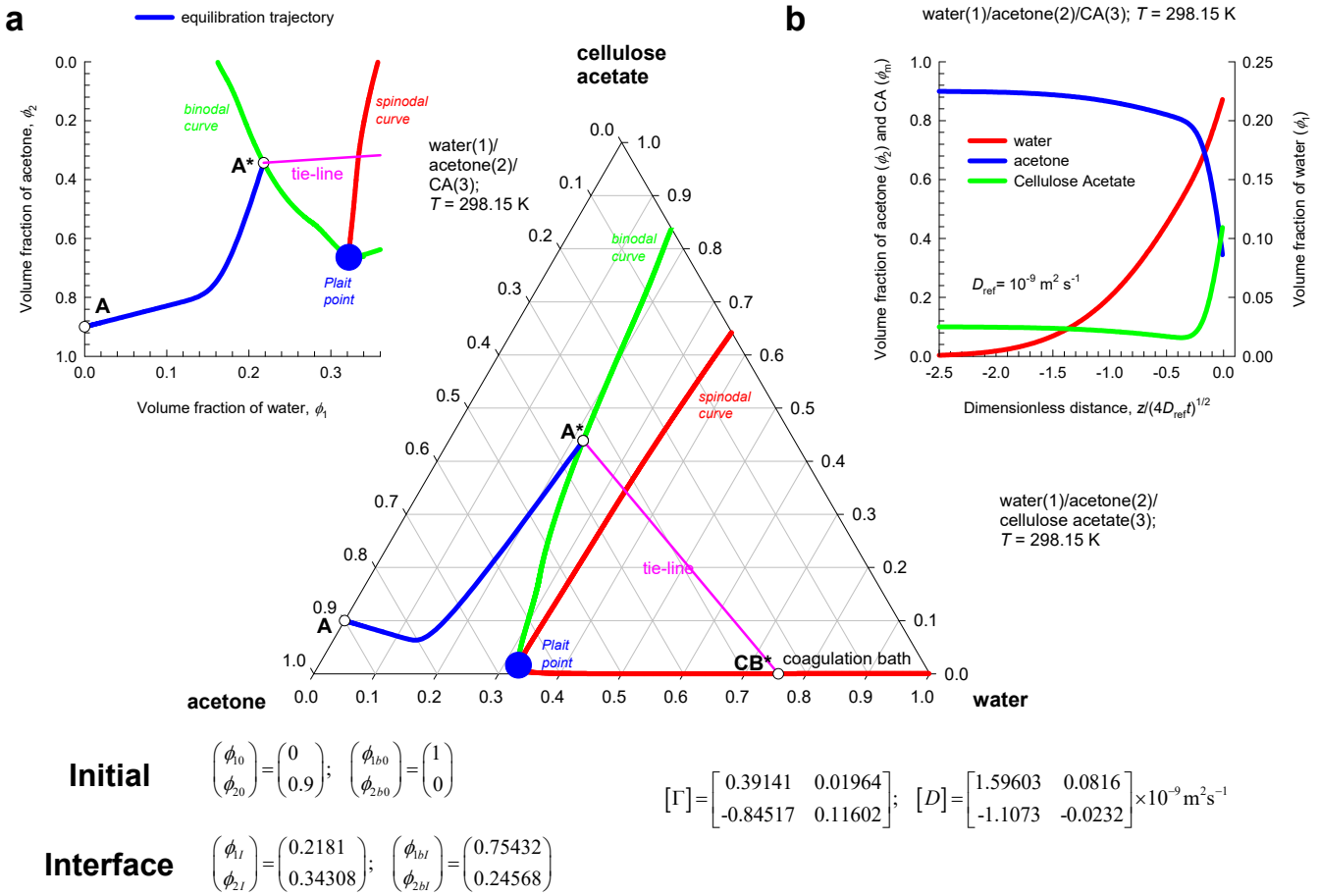

Initial $\begin{pmatrix}\phi_{10}\\ \phi_{20}\end{pmatrix}=\begin{pmatrix}0\\ 0.9\end{pmatrix}$; $\begin{pmatrix}\phi_{1b0}\\ \phi_{2b0}\end{pmatrix}=\begin{pmatrix}1\\ 0\end{pmatrix}$

Interface $\begin{pmatrix}\phi_{1I}\\ \phi_{2I}\end{pmatrix}=\begin{pmatrix}0.2181\\ 0.34308\end{pmatrix}$; $\begin{pmatrix}\phi_{1bI}\\ \phi_{2bI}\end{pmatrix}=\begin{pmatrix}0.75432\\ 0.24568\end{pmatrix}$

$$[\Gamma]=\begin{bmatrix}0.39141 & 0.01964\\ -0.84517 & 0.11602\end{bmatrix};\quad [D]=\begin{bmatrix}1.59603 & 0.0816\\ -1.1073 & -0.0232\end{bmatrix}\times 10^{-9}\,\mathrm{m^2 s^{-1}}$$

Figure S13. (a) Transient equilibration trajectory in a ternary system consisting of water (non-solvent, component 1), acetone (solvent, component 2) and cellulose acetate (polymer = m, component 3). The A-A* equilibration trajectory is indicated by the blue line in binary and ternary composition space. (b) Transient volume fraction profiles in the slab, as function of the dimensionless distance coordinate $\frac{z}{\sqrt{4D_{ref}t}}$. The Flory-Huggins parameters and diffusivity data are provided in Table S6.

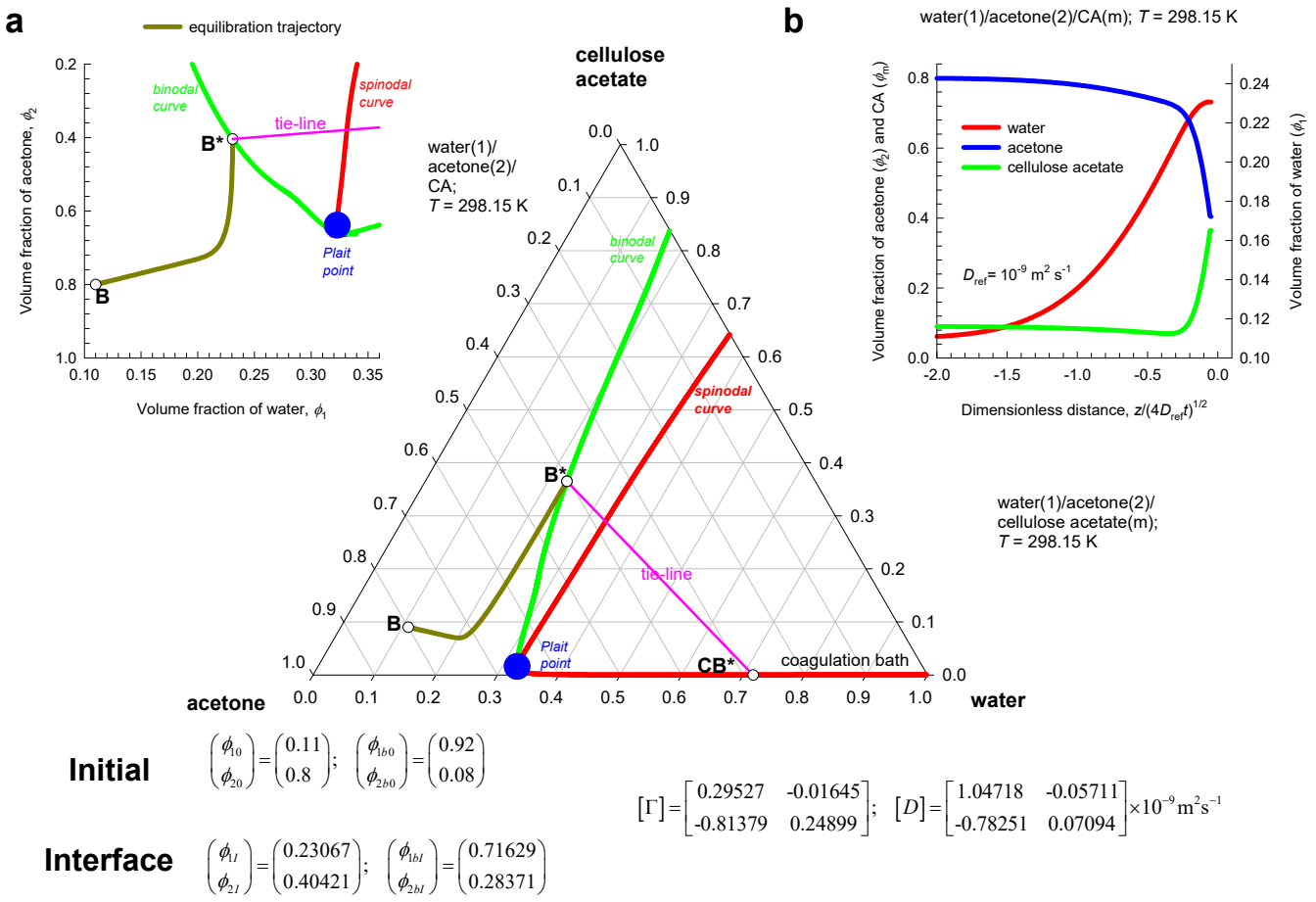

Figure S14. (a) Transient equilibration trajectory in a ternary system consisting of water (non-solvent, component 1), acetone (solvent, component 2) and cellulose acetate (polymer = m, component 3). The B-B* equilibration trajectory is indicated by the blue line in binary and ternary composition space. (b) Transient volume fraction profiles in the slab, as function of the dimensionless distance coordinate $\frac{z}{\sqrt{4D_{ref}t}}$. The Flory-Huggins parameters and diffusivity data are provided in Table S6.

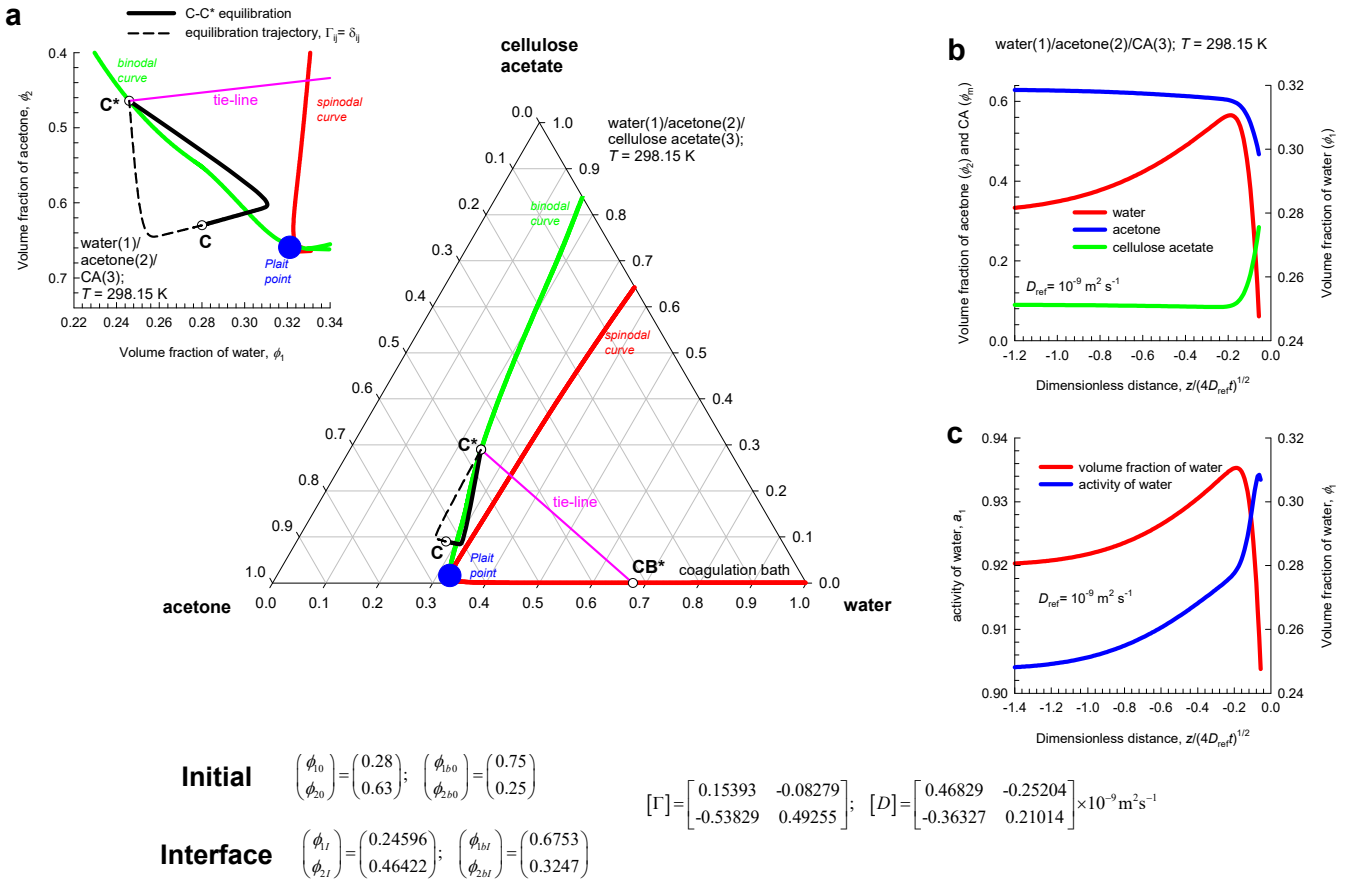

Figure S15. (a) Transient equilibration trajectory in a ternary system consisting of water (non-solvent, component 1), acetone (solvent, component 2) and cellulose acetate (polymer = m, component 3). The C-C* equilibration trajectory is indicated by the blue line in binary and ternary composition space. The dashed lines represent simulation results for which thermodynamic coupling effects are considered to be negligible. (b) Transient volume fraction profiles in the slab, as function of the dimensionless distance coordinate $\frac{z}{\sqrt{4D_{ref}t}}$. (c) Comparing the transient volume fractions of water with the corresponding activities. The Flory-Huggins parameters and diffusivity data are provided in Table S6.

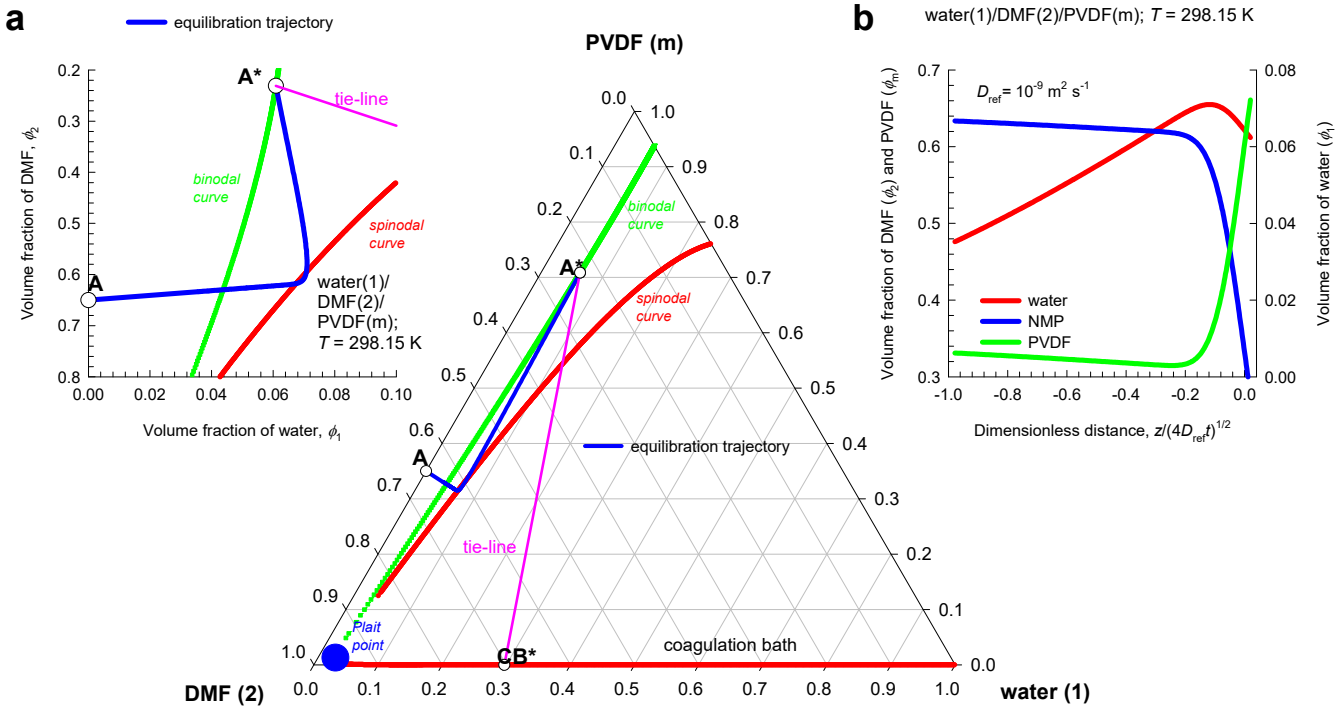

Initial $\begin{pmatrix}\phi_{10}\\ \phi_{20}\end{pmatrix}=\begin{pmatrix}0\\ 0.65\end{pmatrix}$; $\begin{pmatrix}\phi_{1b0}\\ \phi_{2b0}\end{pmatrix}=\begin{pmatrix}0.4\\ 0.6\end{pmatrix}$

$$[\Gamma]=\begin{bmatrix}0.81984 & -0.04225\\ -2.92545 & 0.42313\end{bmatrix};\quad [D]=\begin{bmatrix}3.23211 & -0.16621\\ -1.49605 & 0.08997\end{bmatrix}\times 10^{-9}\,\mathrm{m^2 s^{-1}}$$

Interface $\begin{pmatrix}\phi_{1I}\\ \phi_{2I}\end{pmatrix}=\begin{pmatrix}0.0609\\ 0.23075\end{pmatrix}$; $\begin{pmatrix}\phi_{1bI}\\ \phi_{2bI}\end{pmatrix}=\begin{pmatrix}0.29701\\ 0.70299\end{pmatrix}$

Figure S16. (a) Transient equilibration trajectory in a ternary system consisting of water (non-solvent, component 1), DMF (solvent, component 2) and PVDF (polymer = m, component 3). The A-A* equilibration trajectory is indicated by the blue line in binary and ternary composition space. (b) Transient volume fraction profiles in the slab, as function of the dimensionless distance coordinate $\frac{z}{\sqrt{4D_{ref}t}}$. The Flory-Huggins parameters and diffusivity data are provided in Table S7.

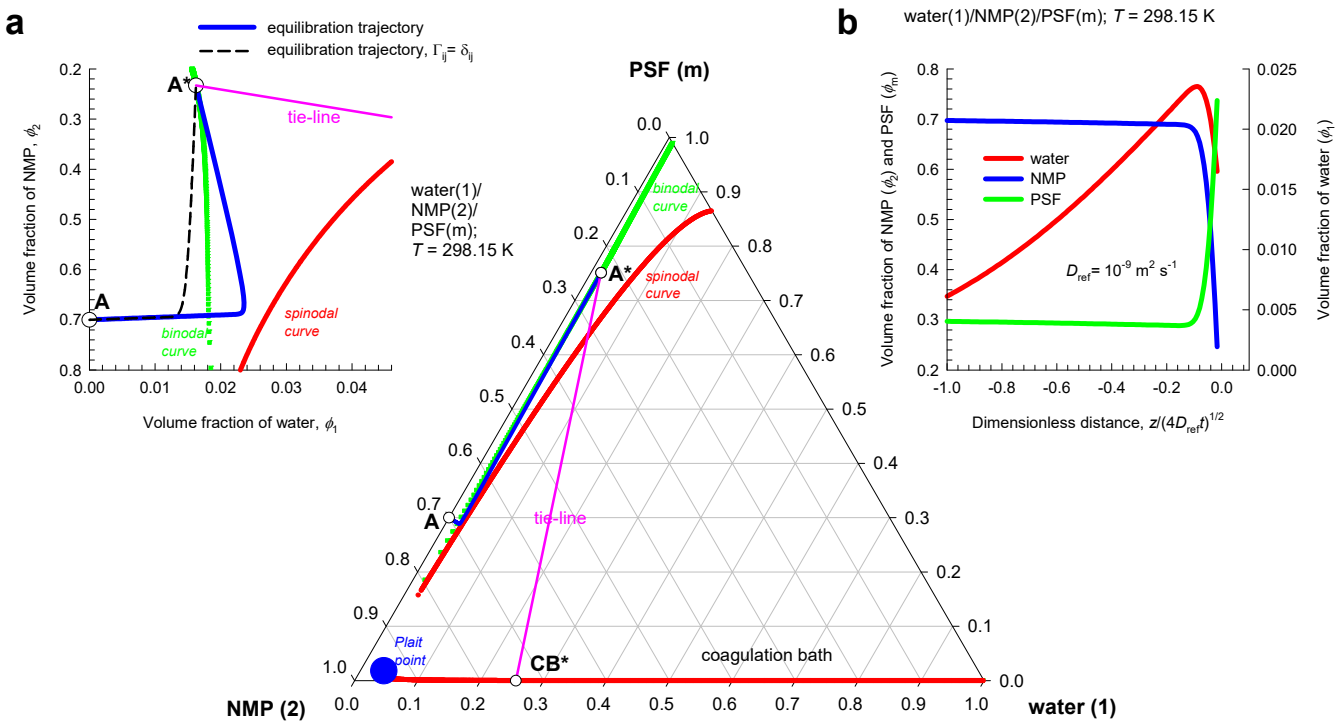

Initial $\begin{pmatrix}\phi_{10}\\ \phi_{20}\end{pmatrix}=\begin{pmatrix}0\\ 0.7\end{pmatrix}$; $\begin{pmatrix}\phi_{1b0}\\ \phi_{2b0}\end{pmatrix}=\begin{pmatrix}0.3\\ 0.7\end{pmatrix}$

Interface $\begin{pmatrix}\phi_{1I}\\ \phi_{2I}\end{pmatrix}=\begin{pmatrix}0.01623\\ 0.23293\end{pmatrix}$; $\begin{pmatrix}\phi_{1bI}\\ \phi_{2bI}\end{pmatrix}=\begin{pmatrix}0.25625\\ 0.74375\end{pmatrix}$

$$[\Gamma]=\begin{bmatrix}0.93085 & -0.01965\\ -5.36896 & 0.46328\end{bmatrix};\quad [D]=\begin{bmatrix}1.39456 & -0.02938\\ -0.6735 & 0.01775\end{bmatrix}\times 10^{-9}\,\mathrm{m^2 s^{-1}}$$

Figure S17. (a) Transient equilibration trajectory in a ternary system consisting of water (non-solvent, component 1), N-methyl-2-pyrrolidone (NMP) (solvent, component 2) and polysulfone (PSF = polymer, component 3). The A-A* equilibration trajectory is indicated by the blue line in binary and ternary composition space. (b) Transient volume fraction profiles in the slab, as function of the dimensionless distance coordinate $\frac{z}{\sqrt{4D_{ref}t}}$. The Flory-Huggins parameters and diffusivity data are provided in Table S8.

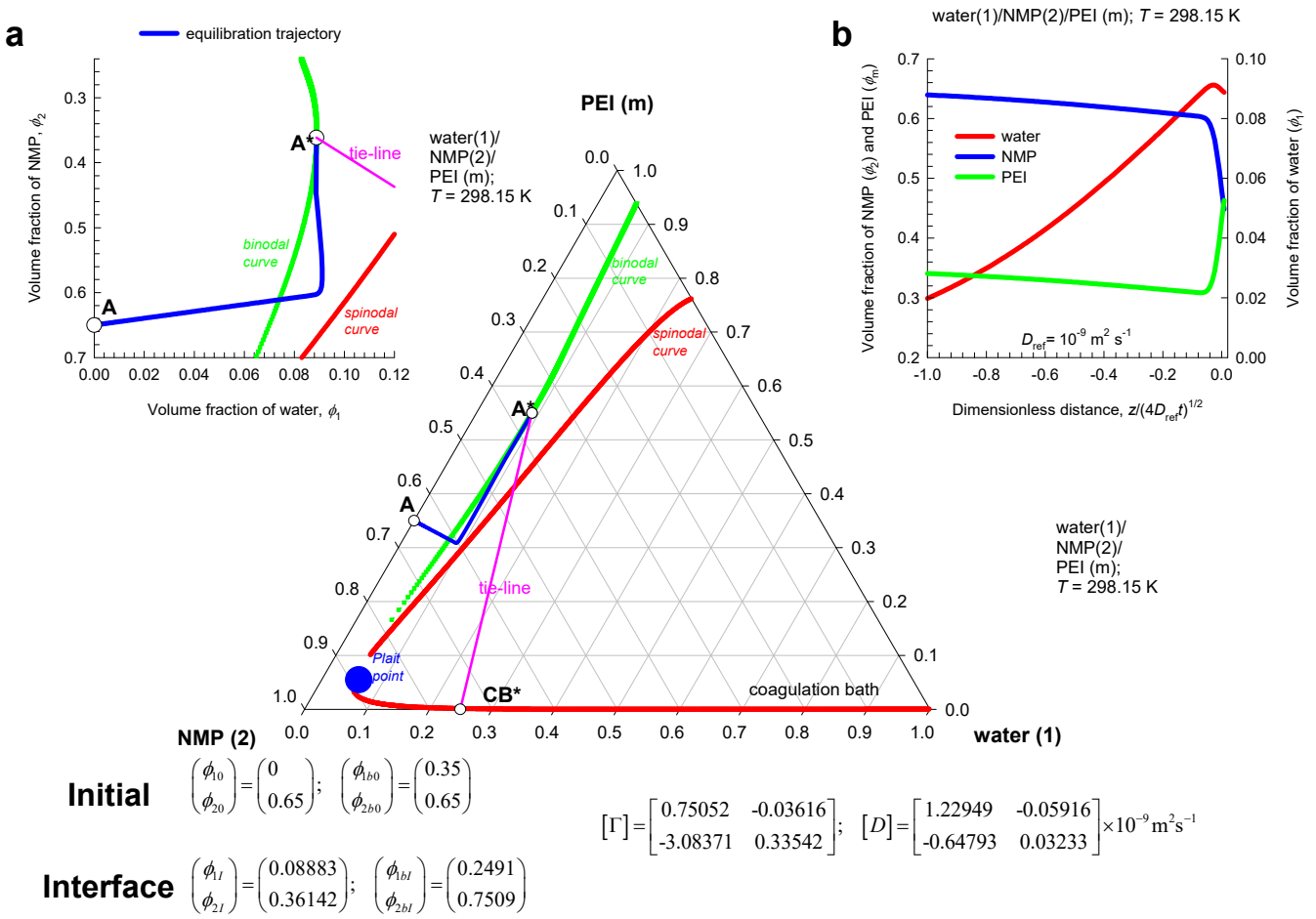

Figure S18. (a) Transient equilibration trajectory in a ternary system consisting of water (non-solvent, component 1), N-methyl-2-pyrrolidone (NMP) (solvent, component 2) and poly(etherimide) (= PEI = polymer = m, component 3). The A-A& equilibration trajectory is indicated by the blue line in binary and ternary composition space. (b) Transient volume fraction profiles in the slab, as function of the dimensionless distance coordinate $\frac{z}{\sqrt{4D_{ref}t}}$. The Flory-Huggins parameters and diffusivity data are provided in Table S9.

6 Emulsification in partially miscible ternary liquid mixtures

Miller[61] wrote "If the two bulk liquids are not initially at equilibrium, it is conceivable that dynamic processes such as diffusion could produce emulsification when the two liquids are brought into contact without stirring." The aniseed-based alcoholic beverage Ouzo consists of a three component mixture of ethanol (≈ 45 vol%), water (55 vol%) and an essential oil called trans-anethol (≈ 0.1%).[62] The addition of five volumes of water to one volume of Ouzo causes the drink to appear milky white.[62] Vitale and Katz[63] have coined the generic term "Ouzo effect" to describe such a process of creating meta-stable liquid-liquid dispersions. Since no input of mechanical energy is involved, this offers an energy-efficient method of producing nanospheres and nanoparticles.[64]

Essential to the formation of meta-stable dispersions is the requirement that the composition trajectories during equilibration enter the meta-stable region in the liquid-liquid phase equilibrium diagram. In the paper by Ruschak and Miller,[65] the necessary conditions for spontaneous emulsification are derived in terms of diffusion equilibration composition trajectories that must necessarily enter the meta-stable regions. Ruschak and Miller[65] adopted the Fickian formulation in which the diffusion flux of each species i, J_i, with respect to the molar average mixture velocity, is considered to be linearly dependent on its own composition gradient

$$J_i = -c_t D_i \frac{dx_i}{dz}; \quad i = 1,2,3 \tag{S119}$$

in which all the component diffusivities in the ternary mixture are equal to one another, i.e. $D_1 = D_2 = D_3 = D$. Only two of the eqs (S119) are independent because the mole fraction gradients sum to zero

$$\frac{dx_1}{dz} + \frac{dx_2}{dz} + \frac{dx_3}{dz} = 0 \tag{S120}$$

and the diffusion fluxes also sum to zero

$$J_1 + J_2 + J_3 = 0 \tag{S121}$$

As illustration, Figure S19 shows the phase diagram for the partially miscible water(1)/ethanol(2)/benzene(3) mixtures at 298 K. Bring pure water (indicated by A) into contact with a 50/50 ethanol/benzene mixture (indicated by B) results in a mixture composition that ends up in the two-phase region of the phase diagram (indicated by M). This mixture will separate into two liquid phases of compositions A* and B* that lie on the binodal curve, are at either ends of the tie-line. The phase A will equilibrate to the composition A*, while phase B will equilibrate to B*. Using the model of Ruschak and Miller,[65] wherein all the component diffusivities in the ternary mixture are equal to one another, i.e. $D_1 = D_2 = D_3 = D$, the diffusion equilibration trajectories A-A*, and B-B* will both be straight lines in ternary composition space. We note that the A-A* equilibration lies in the meta-stable region between the binodal and spinodal curves. This foray into the metastable region is a necessary condition for emulsification to occur.

The primary objective of this article is to show that the diffusional equilibration trajectories will be generally curvilinear and forays into meta-stable regions will occur for scenarios in which the Ruschak-Miller analysis do not anticipate. For this purpose, we develop an analytic solution to the transient equilibration for calculating the A-A*, and B-B* trajectories using the Maxwell-Stefan formulation that includes the strong influences of thermodynamic coupling engendered by $\Gamma_{ij} = \delta_{ij} + x_i \dfrac{\partial \ln \gamma_i}{\partial x_j}$; $\quad i, j = 1, 2 \ldots n-1$ in either fluid phase, A and B.

6.1 A simplified analytic model for transient equilibration

Below we generalize the analytic solutions presented in the works of Ruschak and Miller,[65] Jackson,[66] and Tsay and McHugh.[51]

The following set of assumptions are made in the model development; see schematic in Figure S20.

(iii) The diffusion is essentially z-directional. The position $z = 0$, corresponds to the position of the interface at start of the equilibration process. The adjoining immiscible phases A and B of

ternary liquid mixtures, of two different compositions, expressed in mole fractions, are both considered to be semi-infinite. At the position $z = -\infty$ the composition corresponds to that of the liquid mixture in phase B. At the position $z = +\infty$ the composition corresponds to that of the liquid mixture in phase A. These compositions are time-invariant.

(iv) At any time *t*, during the inter-diffusion process, we have thermodynamic equilibrium between the two-immiscible phases, at compositions A* and B*. Due to finite interphase diffusion, the position of the interface will be altered to satisfy the jump balance condition at the interface.

This assumption of two semi-infinite reservoirs allows the derivation of simple analytical solutions. However, this assumption also implies that the analytical solution can only be applied to represent the trajectories being followed for relatively short contact times.

The transient ternary diffusion within the phase A is described by a set of *two independent* coupled partial differential equations

$$c_{tA}\frac{\partial\begin{pmatrix}x_{1A}\\x_{2A}\end{pmatrix}}{\partial t} = -\frac{\partial\begin{pmatrix}J_{1A}\\J_{2A}\end{pmatrix}}{\partial z} \qquad \text{(S122)}$$

$$x_{3A} = 1 - x_{1A} - x_{2A}$$

The molar fluxes, J_{iA} are defined with respect to the molar average reference velocity, *u*. The molar fluxes sum to zero $J_{1A} + J_{2A} + J_{3A} = 0$. The two independent fluxes J_{1A}, J_{2A} are described by

$$\begin{pmatrix}J_{1A}\\J_{2A}\end{pmatrix} = -c_{tA}\left[D_A\right]\frac{\partial}{\partial z}\begin{pmatrix}x_{1A}\\x_{2A}\end{pmatrix} \qquad \text{(S123)}$$

In eq (S123), c_{tA} is the total molar concentration of the ternary liquid mixture in phase A.

Combining eqs (S122), and (S123) we obtain

$$\frac{\partial\begin{pmatrix}x_{1A}\\x_{2A}\end{pmatrix}}{\partial t} = \left[D_A\right]\frac{\partial^2\begin{pmatrix}x_{1A}\\x_{2A}\end{pmatrix}}{\partial z^2}; \qquad \text{(S124)}$$

The corresponding relation for the transient diffusion process in the ternary liquid mixture in phase B is described by

$$\frac{\partial\begin{pmatrix} x_{1B} \\ x_{2B} \end{pmatrix}}{\partial t} = [D_B]\frac{\partial^2\begin{pmatrix} x_{1B} \\ x_{2B} \end{pmatrix}}{\partial z^2}; \tag{S125}$$

The initial conditions for eqs (S124), and (S125) are

$$\begin{aligned} &z \geq 0, \quad t = 0, \quad \begin{pmatrix} x_{1A}(z,0) \\ x_{2A}(z,0) \end{pmatrix} = \begin{pmatrix} x_{1A0} \\ x_{2A0} \end{pmatrix} \\ &z \leq 0, \quad t = 0, \quad \begin{pmatrix} x_{1B}(-z,0) \\ x_{2B}(-z,0) \end{pmatrix} = \begin{pmatrix} x_{1B0} \\ x_{2B0} \end{pmatrix} \end{aligned} \tag{S126}$$

where x_{iA0} and x_{iB0} are the initial compositions of the liquid phases A and B, respectively

The boundary conditions are

$$\begin{aligned} &z = \infty, \quad t \geq 0, \quad \begin{pmatrix} x_{1A}(\infty,t) \\ x_{2A}(\infty,t) \end{pmatrix} = \begin{pmatrix} x_{1A0} \\ x_{2A0} \end{pmatrix} \\ &z = -\infty, \quad t \geq 0, \quad \begin{pmatrix} x_{1B}(-\infty,t) \\ x_{2B}(-\infty,t) \end{pmatrix} = \begin{pmatrix} x_{1B0} \\ x_{2B0} \end{pmatrix} \end{aligned} \tag{S127}$$

Analytic solutions for the transient mole fractions in phases A, and B are obtained if the Fick diffusivity matrices $[D_A]$, and $[D_B]$ are assumed to be composition independent; see Crank[52] and Taylor and Krishna.[2] In practice, the Fick diffusivity matrices $[D_A]$, and $[D_B]$ are evaluated using eq (S30) at the average mole fractions $\frac{1}{2}\begin{pmatrix} x_{1A0}+x_{1AI} \\ x_{2A0}+x_{2AI} \end{pmatrix}$, and $\frac{1}{2}\begin{pmatrix} x_{1B0}+x_{1BI} \\ x_{2B0}+x_{2BI} \end{pmatrix}$, respectively. For phase A, the composition profile can be written in 2 dimensional matrix notation as

$$\begin{pmatrix} x_{1A}(z,t) \\ x_{2A}(z,t) \end{pmatrix} = \begin{pmatrix} x_{1A0} \\ x_{2A0} \end{pmatrix} + [Q_A]\begin{pmatrix} x_{1AI}-x_{1A0} \\ x_{2AI}-x_{2A0} \end{pmatrix}; \quad [Q_A] = \left[erfc\left(\frac{z[D_A]^{-1/2}}{\sqrt{4t}} \right) \right] \left[erfc\left(\frac{r}{2}[D_A]^{-1/2} \right) \right]^{-1} \tag{S128}$$

The Sylvester theorem, detailed in Appendix A of Taylor and Krishna,[2] is required for explicit evaluation of the four elements of the 2 × 2 dimensional square matrix $[Q_A]$. For the case of distinct eigenvalues, λ_{1A} and λ_{2A} of the 2 × 2 dimensional square matrix $[D_A]$, the Sylvester theorem yields

$$[Q_A] = \frac{f(\lambda_{1A})\left[[D_A] - \lambda_{2A}[I]\right]}{(\lambda_{1A} - \lambda_{2A})} + \frac{f(\lambda_{2A})\left[[D_A] - \lambda_{1A}[I]\right]}{(\lambda_{2A} - \lambda_{1A})}$$
$$f(z,t,\lambda_{iA}) = \frac{erfc\left(\frac{z}{\sqrt{4\lambda_{iA}t}}\right)}{erfc\left(\frac{r}{\sqrt{4\lambda_{iA}}}\right)} \qquad \text{(S129)}$$

In eq (S129), $[I]$ is the identity matrix with elements δ_{ik}, the Kronecker delta. The calculations of the equilibration trajectories are easily implemented in MathCad 15.[1]

Analogously for phase B, we write

$$\begin{pmatrix} x_{1B}(z,t) \\ x_{2B}(z,t) \end{pmatrix} = \begin{pmatrix} x_{1B0} \\ x_{2B0} \end{pmatrix} + [Q_B]\begin{pmatrix} x_{1BI} - x_{1B0} \\ x_{2BI} - x_{2B0} \end{pmatrix}; \quad [Q_B] = \left[erfc\left(\frac{-z[D_A]^{-1/2}}{\sqrt{4t}} \right) \right] \left[erfc\left(\frac{-r}{2}[D_A]^{-1/2} \right) \right]^{-1}$$

$$[Q_B] = \frac{f(\lambda_{1B})\left[[D_B] - \lambda_{2B}[I]\right]}{(\lambda_{1B} - \lambda_{2B})} + \frac{f(\lambda_{2B})\left[[D_B] - \lambda_{1B}[I]\right]}{(\lambda_{2B} - \lambda_{1B})}$$
$$f(z,t,\lambda_{iB}) = \frac{erfc\left(\frac{-z}{\sqrt{4\lambda_{iB}t}}\right)}{erfc\left(\frac{-r}{\sqrt{4\lambda_{iB}}}\right)} \qquad \text{(S130)}$$

Due to interchange of components 1, 2, and 3 between the phases A and B, the position of the liquid/liquid interface will move with time. At the moving boundary, the boundary conditions are

$$\begin{pmatrix} x_{1A}(\varepsilon(t),t) \\ x_{2A}(\varepsilon(t),t) \end{pmatrix} = \begin{pmatrix} x_{1AI} \\ x_{2AI} \end{pmatrix}; \quad x_{3AI} = 1 - x_{1AI} - x_{2AI}$$
$$\begin{pmatrix} x_{1B}(\varepsilon(t),t) \\ x_{2B}(\varepsilon(t),t) \end{pmatrix} = \begin{pmatrix} x_{1BI} \\ x_{2BI} \end{pmatrix}; \quad x_{3BI} = 1 - x_{1BI} - x_{2BI} \qquad \text{(S131)}$$

In eq (S131), $\varepsilon(t) = r\sqrt{t}$ is the position of the moving interface; r is a constant that is determinable from the continuity of component molar fluxes at either side of the moving interface

$$J_{iA}\big|_{z=\varepsilon(t)} - J_{iB}\big|_{z=\varepsilon(t)} = \left(c_{tAI}x_{iAI} - c_{tBI}x_{ibI}\right)\frac{d\varepsilon(t)}{dt};\quad i=1,2$$
$$\frac{d\varepsilon(t)}{dt} = \frac{dr\sqrt{t}}{dt} = \frac{r}{2\sqrt{t}} \tag{S132}$$
$$J_{iA}\big|_{z=\varepsilon(t)} - J_{iB}\big|_{z=\varepsilon(t)} = \left(c_{tAI}x_{iAI} - c_{tBI}x_{ibI}\right)\frac{r}{2\sqrt{t}};\quad i=1,2$$

In eq (S132), c_{tAI}, and c_{tBI} are the total molar concentrations of the ternary liquid mixtures at the interface in phases A, and B, respectively.

The mole fractions at the interface layer x_{iAI} and x_{iBI} are determined by the thermodynamic equilibrium constraint requiring that the component activities be equal in either fluid phase

$$a_{iAI} = a_{iBI};\quad i=1,2,3 \tag{S133}$$

The component activities are determinable from phase equilibrium models such as the NRTL, UNIQUAC, or an equation of state.

The mole fractions at the (moving) interface between the casting film and the coagulation bath, x_{iAI}, x_{iBI}, must satisfy the conditions of thermodynamic equilibrium, eq (S133), along with the jump-balance conditions for the interfacial fluxes at the moving interface, eq (S132). Essentially, we have a set of five independent equations in order to determine the five independent unknowns $r, x_{1AI}, x_{2AI}, x_{1BI}, x_{2BI}$; these five independent variables are time-invariant. In order to prove this, we present below the detailed derivations.

Noting that $\dfrac{\partial erf(z)}{\partial z} = \dfrac{2}{\sqrt{\pi}}\exp\left(-z^2\right) = -\dfrac{\partial erfc(z)}{\partial z}$

$$\frac{\partial erfc\left[\dfrac{z}{\sqrt{4\lambda_i t}}\right]}{\partial z} = -\frac{2}{\sqrt{\pi}}\frac{1}{\sqrt{4\lambda_i t}}\exp\left(-\frac{z^2}{4\lambda_i t}\right) = -\frac{\partial erfc\left[-\dfrac{z}{\sqrt{4\lambda_i t}}\right]}{\partial z}$$

, and differentiating the composition profiles for phases A, and B, eqs (S128), and (S130), allows the determination of the interfacial fluxes

$$\left.\begin{pmatrix} J_{1A} \\ J_{2A} \end{pmatrix}\right|_{z=\varepsilon(t)} = -c_{tA}\left[D_A\right]\left.\frac{\partial\begin{pmatrix} x_{1A}(z,t) \\ x_{2A}(z,t) \end{pmatrix}}{\partial z}\right|_{z=\varepsilon(t)} \quad ;$$

$$\left.\sqrt{\pi t}\begin{pmatrix} J_{1A} \\ J_{2A} \end{pmatrix}\right|_{z=\varepsilon(t)} = c_{tA}\left[D_A\right]\left[Q_{AI}\right]\begin{pmatrix} x_{1AI}-x_{1A0} \\ x_{2AI}-x_{2A0} \end{pmatrix} \tag{S134}$$

$$\left[Q_{AI}\right] = \left[D_A\right]^{-1/2}\left[\exp\left(\frac{-r^2}{4}\left[D_A\right]^{-1}\right)\right]\left[erfc\left(\frac{r}{2}\left[D_A\right]^{-1/2}\right)\right]^{-1}$$

In eq (S134), the Sylvester theorem is required for explicit evaluation of the four elements of the 2 × 2 dimensional square matrix $\left[Q_{AI}\right]$. For the case of distinct eigenvalues, λ_{1A} and λ_{2A} of the 2 × 2 dimensional square matrix $\left[D_A\right]$, the Sylvester theorem yields

$$\left[Q_{AI}\right] = \frac{f\left(\lambda_{1A}\right)\left[\left[D_A\right]-\lambda_{2A}\left[I\right]\right]}{\left(\lambda_{1A}-\lambda_{2A}\right)} + \frac{f\left(\lambda_{2A}\right)\left[\left[D_A\right]-\lambda_{1A}\left[I\right]\right]}{\left(\lambda_{2A}-\lambda_{1A}\right)}$$

$$f\left(z,t,\lambda_{iA}\right) = \frac{1}{\sqrt{\lambda_{iA}}}\frac{\exp\left(-\frac{r^2}{4\lambda_{iA}}\right)}{erfc\left(\frac{r}{\sqrt{4\lambda_{iA}}}\right)} \tag{S135}$$

The corresponding expressions for the interfacial fluxes in the phase B are written analogously

$$\left.\begin{pmatrix} J_{1B} \\ J_{2B} \end{pmatrix}\right|_{z=\varepsilon(t)} = -c_{tB}\left[D_B\right]\left.\frac{\partial\begin{pmatrix} x_{1B}(z,t) \\ x_{2B}(z,t) \end{pmatrix}}{\partial z}\right|_{z=\varepsilon(t)}$$

$$\left.\sqrt{\pi t}\begin{pmatrix} J_{1B} \\ J_{2B} \end{pmatrix}\right|_{z=\varepsilon(t)} = -c_{tB}\left[D_B\right]\left[Q_{BI}\right]\begin{pmatrix} x_{1BI}-x_{1B0} \\ x_{2BI}-x_{2B0} \end{pmatrix};$$

$$\left[Q_{BI}\right] = \left[D_B\right]^{-1/2}\left[\exp\left(\frac{-r^2}{4}\left[D_B\right]^{-1}\right)\right]\left[erfc\left(\frac{-r}{2}\left[D_B\right]^{-1/2}\right)\right]^{-1} \tag{S136}$$

$$\left[Q_{BI}\right] = \frac{f\left(\lambda_{1B}\right)\left[\left[D_B\right]-\lambda_{2B}\left[I\right]\right]}{\left(\lambda_{1B}-\lambda_{2B}\right)} + \frac{f\left(\lambda_{2B}\right)\left[\left[D_B\right]-\lambda_{1B}\left[I\right]\right]}{\left(\lambda_{2B}-\lambda_{1B}\right)};$$

$$f\left(z,t,\lambda_{iB}\right) = \frac{1}{\sqrt{\lambda_{iB}}}\frac{\exp\left(-\frac{r^2}{4\lambda_{iB}}\right)}{erfc\left(\frac{-r}{\sqrt{4\lambda_{iB}}}\right)}$$

Combining eqs (S132), (S134), and (S136) we get

$$\begin{pmatrix} c_{tAI}x_{1AI}-c_{tBI}x_{1bI} \\ c_{tAI}x_{2AI}-c_{tBI}x_{2bI} \end{pmatrix}\frac{r}{2\sqrt{t}}\sqrt{\pi t} = \sqrt{\pi t}\left.\begin{pmatrix} J_{1A} \\ J_{2A} \end{pmatrix}\right|_{z=\varepsilon(t)} - \sqrt{\pi t}\left.\begin{pmatrix} J_{1B} \\ J_{2B} \end{pmatrix}\right|_{z=\varepsilon(t)}$$

$$\begin{pmatrix} c_{tAI}x_{1AI}-c_{tBI}x_{1bI} \\ c_{tAI}x_{2AI}-c_{tBI}x_{2bI} \end{pmatrix}\frac{r\sqrt{\pi}}{2} = c_{tA}\left[D_A\right]\left[Q_{AI}\right]\begin{pmatrix} x_{1AI}-x_{1A0} \\ x_{2AI}-x_{2A0} \end{pmatrix} + c_{tB}\left[D_B\right]\left[Q_{BI}\right]\begin{pmatrix} x_{1BI}-x_{1B0} \\ x_{2BI}-x_{2B0} \end{pmatrix} \tag{S137}$$

It is easy to see that eq (S137) is time-invariant. In the simulation results presented in this article the set of jump balance conditions (eq (S137)), in combination with the conditions of thermodynamic equilibrium (eq (S133)), are solved using the Given-Find solve block of MathCad 15[1] in order to determine the five independent unknowns $r, x_{1AI}, x_{2AI}, x_{1BI}, x_{2BI}$. Since the compositions at each end of the tie-line $x_{1AI}, x_{2AI}, x_{1BI}, x_{2BI}$ are not initially known for a given set of initial conditions, a simple head-to-tail iteration procedure is employed. Firstly, the mole fractions x_{1BI}, x_{2BI} of B*, that lies on the binodal curve are assumed. The compositions at the other end of the tie-line must be in equilibrium, and these are determined by solving the set eqs (S133) describing thermodynamic equilibrium. The Fick diffusivity matrices $\left[D_A\right]$, and $\left[D_B\right]$ are then evaluated using eq (S30) at the arithmetic average mole

fractions $\frac{1}{2}\begin{pmatrix} x_{1A0}+x_{1AI} \\ x_{2A0}+x_{2AI} \end{pmatrix}$, and $\frac{1}{2}\begin{pmatrix} x_{1B0}+x_{1BI} \\ x_{2B0}+x_{2BI} \end{pmatrix}$, respectively. With this information, and an initial guess value for r, the set of five non-linear eqs (S137) and (S133) are solved to obtain updated values of $r, x_{1AI}, x_{2AI}, x_{1BI}, x_{2BI}$; these are used to obtain new estimates of the Fick diffusivity matrices $[D_A]$, and $[D_B]$. The head-to-tail iteration procedure usually converges rapidly in about 3-4 steps.

The simulations illustrating diffusional forays into meta-stable regions that are presented in the subsequent sections are most convenient presented in terms of the dimensionless distance coordinate $\eta \equiv \frac{z}{\sqrt{4D_{ref}t}}$ where the chosen reference velocity $D_{ref} = 1\times10^{-9}$ m^2 s^{-1}. Expressed in terms of the dimensionless distance coordinate, the mole fraction profiles in phase A are

$$\begin{pmatrix} x_{1A}(\eta) \\ x_{2A}(\eta) \end{pmatrix} = \begin{pmatrix} x_{1A0} \\ x_{2A0} \end{pmatrix} + [Q_A]\begin{pmatrix} x_{1AI}-x_{1A0} \\ x_{2AI}-x_{2A0} \end{pmatrix};$$
$$[Q_A] = \left[erfc\left(\eta\sqrt{D_{ref}}[D_A]^{-1/2}\right)\right]\left[erfc\left(\frac{r}{\sqrt{4D_{ref}}}\sqrt{D_{ref}}[D_A]^{-1/2}\right)\right]^{-1} \quad \text{(S138)}$$

The corresponding mole fraction profiles in phase B are

$$\begin{pmatrix} x_{1B}(z,t) \\ x_{2B}(z,t) \end{pmatrix} = \begin{pmatrix} x_{1B0} \\ x_{2B0} \end{pmatrix} + [Q_B]\begin{pmatrix} x_{1BI}-x_{1B0} \\ x_{2BI}-x_{2B0} \end{pmatrix};$$
$$[Q_B] = \left[erfc\left(-\eta\sqrt{D_{ref}}[D_B]^{-1/2}\right)\right]\left[erfc\left(\frac{-r}{\sqrt{4D_{ref}}}\sqrt{D_{ref}}[D_B]^{-1/2}\right)\right]^{-1} \quad \text{(S139)}$$

The Sylvester theorem, detailed in Appendix A of Taylor and Krishna,[2] is required for explicit evaluation of the four elements of the 2 × 2 dimensional square matrices $[Q_A]$, and $[Q_B]$; see eqs (S129), and (S130).

If the interface is considered to be stationary, eqs (S138), and (S139) simplify to yield

$$\begin{pmatrix} x_{1A}(\eta) \\ x_{2A}(\eta) \end{pmatrix} = \begin{pmatrix} x_{1A0} \\ x_{2A0} \end{pmatrix} + [Q_A] \begin{pmatrix} x_{1AI} - x_{1A0} \\ x_{2AI} - x_{2A0} \end{pmatrix}; \quad [Q_A] = \left[erfc\left(\eta \sqrt{D_{ref}} [D_A]^{-1/2} \right) \right]$$
$$\begin{pmatrix} x_{1B}(\eta) \\ x_{2B}(\eta) \end{pmatrix} = \begin{pmatrix} x_{1B0} \\ x_{2B0} \end{pmatrix} + [Q_B] \begin{pmatrix} x_{1BI} - x_{1B0} \\ x_{2BI} - x_{2B0} \end{pmatrix}; \quad [Q_B] = \left[erfc\left(-\eta \sqrt{D_{ref}} [D_B]^{-1/2} \right) \right] \tag{S140}$$

A further special scenario emerges when the two phases A and B are entirely miscible; in this scenario, the transient equilibration process of two miscible ternary liquid mixtures A and B, of different initial compositions will equilibrate following the following set of equations

$$\begin{pmatrix} x_{1A}(\eta) \\ x_{2A}(\eta) \end{pmatrix} = \begin{pmatrix} x_{1A0} \\ x_{2A0} \end{pmatrix} + [Q_A] \begin{pmatrix} x_{1I} - x_{1A0} \\ x_{2I} - x_{2A0} \end{pmatrix}; \quad [Q_A] = \left[erfc\left(\eta \sqrt{D_{ref}} [D_A]^{-1/2} \right) \right]$$
$$\begin{pmatrix} x_{1B}(\eta) \\ x_{2B}(\eta) \end{pmatrix} = \begin{pmatrix} x_{1B0} \\ x_{2B0} \end{pmatrix} + [Q_B] \begin{pmatrix} x_{1I} - x_{1B0} \\ x_{2I} - x_{2B0} \end{pmatrix}; \quad [Q_B] = \left[erfc\left(-\eta \sqrt{D_{ref}} [D_B]^{-1/2} \right) \right] \tag{S141}$$
$$x_{1I} = \frac{x_{1A0} + x_{1B0}}{2}; \quad x_{2I} = \frac{x_{2A0} + x_{2B0}}{2}$$

Equation (S141) implies that the final equilibrated composition is the arithmetic average of the initial compositions of the two mixtures A, and B.

6.2 Uphill diffusion in partially miscible glycerol/acetone/water mixtures

The experimental data (indicated by the white circles) for transient equilibration of glycerol-rich and acetone-rich phases of the glycerol/acetone/water mixture were measured in a stirred Lewis cell by Krishna et al.;[67] see Figure S21. The initial compositions in the acetone-rich phase (A) and glycerol-rich phase (B) are $\begin{pmatrix} x_{1A0} \\ x_{2A0} \end{pmatrix} = \begin{pmatrix} 0 \\ 0.77 \end{pmatrix}$; $\begin{pmatrix} x_{1B0} \\ x_{2B0} \end{pmatrix} = \begin{pmatrix} 0.85 \\ 0 \end{pmatrix}$. The composition of the A-B mixture lies in the two phase region, and therefore will separate into two liquid phases with compositions A* and B*, at either end of the tie-line. The experimentally determined values of the final equilibrated compositions at either side of the interface, A* and B*, are $\begin{pmatrix} x_{1AI} \\ x_{2AI} \end{pmatrix} = \begin{pmatrix} 0.042 \\ 0.894 \end{pmatrix}$; $\begin{pmatrix} x_{1BI} \\ x_{2BI} \end{pmatrix} = \begin{pmatrix} 0.539414 \\ 0.161496 \end{pmatrix}$. The transient equilibration trajectories in phases A, and B in the Lewis stirred cell will be modeled assuming that each

of the phases is semi-infinite in either direction of the interface, that remains stationary during the equilibration process. With these set of assumptions, the equilibration trajectories are described by eq (S140).

For calculation of the transient equilibration trajectories, the Fick diffusivity matrices $[D_A]$, and $[D_B]$ are evaluated using eq (S45), wherein the scalar diffusivity $|\Lambda|^{1/2}$ is calculated from $|\Lambda|^{1/2} = (D_{1,self})^{x_1} (D_{2,self})^{x_2} (D_{3,self})^{x_3}$, taking $D_{1,\mathrm{self}} = 0.01$, $D_{2,\mathrm{self}} = 3.2$, $D_{3,\mathrm{self}} = 0.5$ with units 10^{-9} m^2 s^{-1}; the accuracy of this estimation procedure has been firmly established in our previous works.[14, 15, 48]

Evaluated at the arithmetic average mole fractions $\frac{1}{2}\begin{pmatrix} x_{1A0} + x_{1AI} \\ x_{2A0} + x_{2AI} \end{pmatrix}$, and $\frac{1}{2}\begin{pmatrix} x_{1B0} + x_{1BI} \\ x_{2B0} + x_{2BI} \end{pmatrix}$, the matrices of thermodynamic correction factors, and the Fick diffusivity matrices are

$$[\Gamma_A] = \begin{bmatrix} 1.064438 & 0.177947 \\ 0.956407 & 0.766246 \end{bmatrix}; \quad [D_A] = \begin{bmatrix} 2.296962 & 0.383994 \\ 2.06384 & 1.653491 \end{bmatrix} \times 10^{-9}\,\mathrm{m^2 s^{-1}} \text{ and}$$

$$[\Gamma_B] = \begin{bmatrix} 2.174183 & 1.17946 \\ 0.020901 & 0.692517 \end{bmatrix}; \quad [D_B] = \begin{bmatrix} 8.338294 & 4.523394 \\ 0.080158 & 2.6559 \end{bmatrix} \times 10^{-11}\,\mathrm{m^2 s^{-1}}.$$ Particularly noteworthy are the large magnitudes of the off-diagonal elements of the Fick diffusivity matrices, that are directly attributable to the corresponding large off-diagonal elements of the matrices of thermodynamic correction factors.

The calculated equilibration trajectories are indicated by the blue lines in Figure S21; these are both curvilinear in shape and in good agreement with the measured experimental data.

In order to demonstrate that the curvilinear equilibration trajectories may enter the meta-stable regions between the binodal and spinodal curve, we choose a different set of starting compositions for the acetone-rich phase (A) and glycerol-rich phase (B) as $\begin{pmatrix} x_{1A0} \\ x_{2A0} \end{pmatrix} = \begin{pmatrix} 0 \\ 0.6 \end{pmatrix}$; $\begin{pmatrix} x_{1B0} \\ x_{2B0} \end{pmatrix} = \begin{pmatrix} 0.9 \\ 0.1 \end{pmatrix}$; see Figure S22. The composition of the A-B mixture lies in the two phase region, and therefore will separate into two liquid phases with compositions A* and B*, at either end of the tie-line. Using the head-to-tail iteration

procedure, outlined in the foregoing section, the final converged values of the mole fractions at either sides of the interface, A* and B* are determined as $\begin{pmatrix} x_{1AI} \\ x_{2AI} \end{pmatrix} = \begin{pmatrix} 0.076941 \\ 0.58913 \end{pmatrix}$; $\begin{pmatrix} x_{1BI} \\ x_{2BI} \end{pmatrix} = \begin{pmatrix} 0.203211 \\ 0.307942 \end{pmatrix}$.

Evaluated at the arithmetic average mole fractions $\frac{1}{2}\begin{pmatrix} x_{1A0} + x_{1AI} \\ x_{2A0} + x_{2AI} \end{pmatrix}$, and $\frac{1}{2}\begin{pmatrix} x_{1B0} + x_{1BI} \\ x_{2B0} + x_{2BI} \end{pmatrix}$, the matrices of thermodynamic correction factors, and the Fick diffusivity matrices are

$$[\Gamma_A] = \begin{bmatrix} 1.162681 & 0.248166 \\ 1.251188 & 0.570727 \end{bmatrix}; \quad [D_A] = \begin{bmatrix} 1.507982 & 0.321868 \\ 1.622774 & 0.740226 \end{bmatrix} \times 10^{-9}\,\mathrm{m^2 s^{-1}} \text{ and}$$

$$[\Gamma_B] = \begin{bmatrix} 2.153468 & 1.428097 \\ 0.124265 & 0.365738 \end{bmatrix}; \quad [D_B] = \begin{bmatrix} 18.171242 & 12.050468 \\ 1.048567 & 3.086145 \end{bmatrix} \times 10^{-11}\,\mathrm{m^2 s^{-1}}.$$

Particularly noteworthy are the relatively large magnitudes of the off-diagonal elements of the Fick diffusivity matrices, that are directly attributable to the corresponding large off-diagonal elements of the matrices of thermodynamic correction factors.

The equilibration trajectories A-A* and B-B*, calculated using eqs (S138), and (S139), are indicated by the solid blue lines in Figure S22a. We note that the B-B* trajectory exhibits a foray into the meta-stable region; this foray could result in emulsion formation. For the glycerol-rich phase, the mole fractions of the three components are plotted in Figure S22b as function of the dimensionless distance coordinate $\frac{z}{\sqrt{4D_{ref}t}}$. We note that acetone experiences a pronounced undershoot during the transient equilibration process; this undershoot signifies uphill diffusion[14, 15, 53] that is engendered by thermodynamic coupling effects.

Diffusional forays are also possible if mixture of two ternary liquid mixtures of compositions A and B lies in the homogeneous region of the phase equilibrium diagram, close to the binodal curve. In order to demonstrate this, we choose a different set of starting compositions for the acetone-rich phase (A) and

glycerol-rich phase (B) as $\begin{pmatrix} x_{1A0} \\ x_{2A0} \end{pmatrix} = \begin{pmatrix} 0 \\ 0.3 \end{pmatrix}$; $\begin{pmatrix} x_{1B0} \\ x_{2B0} \end{pmatrix} = \begin{pmatrix} 1 \\ 0 \end{pmatrix}$; see Figure S23. The composition of the A-B mixture, A*= B* = $\begin{pmatrix} x_{1I} \\ x_{2I} \end{pmatrix} = \begin{pmatrix} \frac{x_{1A0} + x_{1B0}}{2} \\ \frac{x_{2A0} + x_{2B0}}{2} \end{pmatrix} = \begin{pmatrix} 0.5 \\ 0.15 \end{pmatrix}$ lies in the homogeneous single phase region.

Evaluated at the arithmetic average mole fractions $\frac{1}{2}\begin{pmatrix} x_{1A0} + x_{1I} \\ x_{2A0} + x_{2I} \end{pmatrix}$, and $\frac{1}{2}\begin{pmatrix} x_{1B0} + x_{1I} \\ x_{2B0} + x_{2I} \end{pmatrix}$, the matrices of thermodynamic correction factors, and the Fick diffusivity matrices are

$$\left[\Gamma_A\right] = \begin{bmatrix} 2.02215 & 0.964119 \\ 0.41644 & 0.421514 \end{bmatrix}; \quad \left[D_A\right] = \begin{bmatrix} 0.57734 & 0.275264 \\ 0.118897 & 0.120346 \end{bmatrix} \times 10^{-9}\,\mathrm{m^2 s^{-1}} \text{ and}$$

$$\left[\Gamma_B\right] = \begin{bmatrix} 2.010421 & 1.070186 \\ 4.788247\times10^{-3} & 0.706486 \end{bmatrix}; \quad \left[D_B\right] = \begin{bmatrix} 6.144592 & 3.270885 \\ 0.014635 & 2.159282 \end{bmatrix} \times 10^{-11}\,\mathrm{m^2 s^{-1}}.$$

Particularly noteworthy are the relatively large magnitudes of the off-diagonal elements of the Fick diffusivity matrices, that are directly attributable to the corresponding large off-diagonal elements of the matrices of thermodynamic correction factors.

The equilibration trajectories A-A* and B-B* calculated using eq (S141) are indicated by the solid blue lines. We note that the A-A* trajectory exhibits a foray into the meta-stable region (cf. Figure S23); this foray could result in emulsion formation.

If thermodynamic coupling effects are completely ignored by invoking the assumption $\Gamma_{ij} = \delta_{ij}$, the Kronecker delta, the equilibration trajectories (shown by the dotted lines) do not exhibit any foray into the meta-stable region.

6.3 Uphill diffusion in water(1)/chloroform(2)/acetic acid(3) mixtures

For water(1)/chloroform(2)/acetic-acid(3) mixtures we demonstrate that the curvilinear equilibration trajectories may enter the meta-stable regions between the binodal and spinodal curve. The initial starting compositions for the water-rich phase (A) and chloroform-rich phase (B) are

$\begin{pmatrix} x_{1A0} \\ x_{2A0} \end{pmatrix} = \begin{pmatrix} 0.56 \\ 0 \end{pmatrix}$; $\begin{pmatrix} x_{1B0} \\ x_{2B0} \end{pmatrix} = \begin{pmatrix} 0.05 \\ 0.95 \end{pmatrix}$; see Figure S24. The composition of the A-B mixture lies in the two phase region, and therefore will separate into two liquid phases with compositions A* and B*, at either end of the tie-line. For calculation of the transient equilibration trajectories, the Fick diffusivity matrices $[D_A]$, and $[D_B]$ are evaluated using eq (S45), wherein the scalar diffusivity $|\Lambda|^{1/2}$ is calculated from $|\Lambda|^{1/2} = (D_{1,self})^{x_1} (D_{2,self})^{x_2} (D_{3,self})^{x_3}$, taking $D_{1,\text{self}}$= 0.4, $D_{2,\text{self}}$= 0.8, $D_{3,\text{self}}$= 1.1 with units 10^{-9} m^2 s^{-1}; the accuracy of this estimation procedure has been firmly established in our previous works.[14, 15, 48]

Using the head-to-tail iteration procedure for the moving interface solution, outlined in a foregoing section, the final converged values of the mole fractions at either sides of the interface, A* and B* are determined as $\begin{pmatrix} x_{1AI} \\ x_{2AI} \end{pmatrix} = \begin{pmatrix} 0.5557304 \\ 0.10821082 \end{pmatrix}$; $\begin{pmatrix} x_{1BI} \\ x_{2BI} \end{pmatrix} = \begin{pmatrix} 0.31227988 \\ 0.31941605 \end{pmatrix}$.

Evaluated at the arithmetic average mole fractions $\frac{1}{2}\begin{pmatrix} x_{1A0} + x_{1AI} \\ x_{2A0} + x_{2AI} \end{pmatrix}$, and $\frac{1}{2}\begin{pmatrix} x_{1B0} + x_{1BI} \\ x_{2B0} + x_{2BI} \end{pmatrix}$, the matrices of thermodynamic correction factors, and the Fick diffusivity matrices are

$$[\Gamma_A] = \begin{bmatrix} 1.10052017 & 1.46264076 \\ 0.27788563 & 0.89132962 \end{bmatrix}; \quad [D_A] = \begin{bmatrix} 0.6767361 & 0.89941269 \\ 0.1708785 & 0.54809984 \end{bmatrix} \times 10^{-9}\,\text{m}^2\text{s}^{-1} \text{ and}$$

$$[\Gamma_B] = \begin{bmatrix} 0.95610059 & 0.60317132 \\ 0.79275008 & 0.76248396 \end{bmatrix}; \quad [D_B] = \begin{bmatrix} 0.71537497 & 0.45130572 \\ 0.59315262 & 0.57050686 \end{bmatrix} \times 10^{-9}\,\text{m}^2\text{s}^{-1}.$$

Particularly noteworthy are the relatively large magnitudes of the off-diagonal elements of the Fick diffusivity matrices, that are directly attributable to the corresponding large off-diagonal elements of the matrices of thermodynamic correction factors.

The equilibration trajectories A-A* and B-B*, calculated using eqs (S138), and (S139), are indicated by the solid blue lines in Figure S24. We note that the B-B* trajectory exhibits a foray into the meta-stable region; this foray could result in emulsion formation.

6.4 Uphill diffusion in water(1)/acetone(2)/ethylacetate(3) mixtures

For water(1)/acetone(2)/ethylacetate(3) mixtures we demonstrate that the curvilinear equilibration trajectories may enter the meta-stable regions between the binodal and spinodal curve. The initial starting compositions for the ethylacetate-rich phase (A) and water-rich phase (B) are $\begin{pmatrix} x_{1A0} \\ x_{2A0} \end{pmatrix} = \begin{pmatrix} 0.1 \\ 0 \end{pmatrix}$; $\begin{pmatrix} x_{1B0} \\ x_{2B0} \end{pmatrix} = \begin{pmatrix} 0.8 \\ 0.2 \end{pmatrix}$; see Figure S25a. The composition of the A-B mixture lies in the two phase region, and therefore will separate into two liquid phases with compositions A* and B*, at either end of the tie-line. For calculation of the transient equilibration trajectories, the Fick diffusivity matrices $[D_A]$, and $[D_B]$ are evaluated using eq (S45), wherein the scalar diffusivity $|\Lambda|^{1/2}$ is estimated using $|\Lambda|^{1/2} = \sqrt{\frac{Đ_{12} Đ_{13} Đ_{23}}{x_1 Đ_{23} + x_2 Đ_{13} + x_3 Đ_{12}}}$, wherein the infinite dilution M-S pair diffusivities are estimated using the Wilke-Change correlation.[14, 15, 48]

Using the head-to-tail iteration procedure for the moving interface solution, outlined in a foregoing section, the final converged values of the mole fractions at either sides of the interface, A* and B* are determined as $\begin{pmatrix} x_{1AI} \\ x_{2AI} \end{pmatrix} = \begin{pmatrix} 0.345783 \\ 0.304066 \end{pmatrix}$; $\begin{pmatrix} x_{1BI} \\ x_{2BI} \end{pmatrix} = \begin{pmatrix} 0.851566 \\ 0.112756 \end{pmatrix}$.

Evaluated at the arithmetic average mole fractions $\frac{1}{2}\begin{pmatrix} x_{1A0} + x_{1AI} \\ x_{2A0} + x_{2AI} \end{pmatrix}$, and $\frac{1}{2}\begin{pmatrix} x_{1B0} + x_{1BI} \\ x_{2B0} + x_{2BI} \end{pmatrix}$, the matrices of thermodynamic correction factors, and the Fick diffusivity matrices are

$$[\Gamma_A] = \begin{bmatrix} 0.32443 & -0.271489 \\ -0.042701 & 1.139018 \end{bmatrix}; \quad [D_A] = \begin{bmatrix} 0.798534 & -0.692396 \\ -0.129092 & 1.820496 \end{bmatrix} \times 10^{-9}\,\mathrm{m^2 s^{-1}} \text{ and}$$

$$[\Gamma_B] = \begin{bmatrix} -0.199831 & -0.610359 \\ 1.021323 & 1.561543 \end{bmatrix}; \quad [D_B] = \begin{bmatrix} -0.765409 & -1.473046 \\ 1.552319 & 2.386829 \end{bmatrix} \times 10^{-9}\,\mathrm{m^2 s^{-1}}.$$

Particularly noteworthy are the relatively large magnitudes of the off-diagonal elements of the Fick diffusivity matrices, that are directly attributable to the corresponding large off-diagonal elements of the matrices of thermodynamic correction factors.

Emulsification in partially miscible ternary liquid mixtures

The equilibration trajectories A-A* and B-B*, calculated using eqs (S138), and (S139), are indicated by the solid blue lines in Figure S25a. We note that the A-A* trajectory exhibits a foray into the meta-stable region; this foray could result in emulsion formation.

For the ethyl-acetate rich phase, the mole fractions of the three components are plotted in Figure S25b as function of the dimensionless distance coordinate $\frac{z}{\sqrt{4D_{ref}t}}$. We note that water experiences an undershoot during the transient equilibration process; this undershoot signifies uphill diffusion[14, 15, 53] that is engendered by thermodynamic coupling effects.

Diffusional forays are also possible if mixture of two ternary liquid mixtures of compositions A and B lies in the homogeneous region of the phase equilibrium diagram, close to the binodal curve. In order to demonstrate this, we choose a different set of starting compositions for the ethyl-acetate-rich phase (A) and water-rich phase (B) as $\begin{pmatrix} x_{1A0} \\ x_{2A0} \end{pmatrix} = \begin{pmatrix} 0.1 \\ 0 \end{pmatrix}$; $\begin{pmatrix} x_{1B0} \\ x_{2B0} \end{pmatrix} = \begin{pmatrix} 0.46 \\ 0.54 \end{pmatrix}$; see Figure S26. The composition of the A-B mixture, A*= B* = $\begin{pmatrix} x_{1I} \\ x_{2I} \end{pmatrix} = \begin{pmatrix} \frac{x_{1A0}+x_{1B0}}{2} \\ \frac{x_{2A0}+x_{2B0}}{2} \end{pmatrix} = \begin{pmatrix} 0.28 \\ 0.27 \end{pmatrix}$ lies in the homogeneous single phase region.

Evaluated at the arithmetic average mole fractions $\frac{1}{2}\begin{pmatrix} x_{1A0}+x_{1I} \\ x_{2A0}+x_{2I} \end{pmatrix}$, and $\frac{1}{2}\begin{pmatrix} x_{1B0}+x_{1I} \\ x_{2B0}+x_{2I} \end{pmatrix}$, the matrices of thermodynamic correction factors, and the Fick diffusivity matrices are

$$[\Gamma_A] = \begin{bmatrix} 0.405118 & -0.235514 \\ -0.060166 & 1.11633 \end{bmatrix}; \quad [D_A] = \begin{bmatrix} 0.805166 & -0.468081 \\ -0.11958 & 2.218687 \end{bmatrix} \times 10^{-9}\,\mathrm{m^2 s^{-1}} \text{ and}$$

$$[\Gamma_B] = \begin{bmatrix} 0.050634 & -0.464034 \\ 0.398981 & 1.417488 \end{bmatrix}; \quad [D_B] = \begin{bmatrix} 0.117665 & -1.07834 \\ 0.927167 & 3.294013 \end{bmatrix} \times 10^{-11}\,\mathrm{m^2 s^{-1}}.$$

Particularly noteworthy are the relatively large magnitudes of the off-diagonal elements of the Fick diffusivity matrices, that are directly attributable to the corresponding large off-diagonal elements of the matrices of thermodynamic correction factors.

The equilibration trajectories A-A* and B-B* calculated using eq (S141) are indicated by the solid blue lines. We note that the B-B* trajectory exhibits a foray into the meta-stable region (cf. Figure S26); this foray could result in emulsion formation.

If thermodynamic coupling effects are completely ignored by invoking the assumption $\Gamma_{ij} = \delta_{ij}$, the Kronecker delta, the equilibration trajectories (shown by the dotted lines) do not exhibit any foray into the meta-stable region.

6.5 Uphill diffusion in water(1)/ethanol (2)/ethylacetate(3) mixtures

For water(1)/ethanol(2)/ethylacetate(3) mixtures we demonstrate that the curvilinear equilibration trajectories may enter the meta-stable regions between the binodal and spinodal curve. The initial starting compositions for the water-rich phase (A) and ethylacetate-rich phase (B) are $\begin{pmatrix} x_{1A0} \\ x_{2A0} \end{pmatrix} = \begin{pmatrix} 0.85 \\ 0.15 \end{pmatrix}$; $\begin{pmatrix} x_{1B0} \\ x_{2B0} \end{pmatrix} = \begin{pmatrix} 0.1 \\ 0 \end{pmatrix}$; see Figure S27a. The composition of the A-B mixture lies in the two phase region, and therefore will separate into two liquid phases with compositions A* and B*, at either end of the tie-line. For calculation of the transient equilibration trajectories, the Fick diffusivity matrices $[D_A]$, and $[D_B]$ are evaluated using eq (S45), wherein the scalar diffusivity $|\Lambda|^{1/2}$ is assumed to have the value $|\Lambda|^{1/2} = 1\times10^{-9}\ \mathrm{m^2 s^{-1}}$.

Using the head-to-tail iteration procedure for the moving interface solution, outlined in a foregoing section, the final converged values of the mole fractions at either sides of the interface, A* and B* are determined as $\begin{pmatrix} x_{1AI} \\ x_{2AI} \end{pmatrix} = \begin{pmatrix} 0.801496 \\ 0.130168 \end{pmatrix}$; $\begin{pmatrix} x_{1BI} \\ x_{2BI} \end{pmatrix} = \begin{pmatrix} 0.605492 \\ 0.181393 \end{pmatrix}$.

Evaluated at the arithmetic average mole fractions $\frac{1}{2}\begin{pmatrix} x_{1A0} + x_{1AI} \\ x_{2A0} + x_{2AI} \end{pmatrix}$, and $\frac{1}{2}\begin{pmatrix} x_{1B0} + x_{1BI} \\ x_{2B0} + x_{2BI} \end{pmatrix}$, the Fick diffusivity matrices are

$$[D_A] = \begin{bmatrix} -0.528945 & -1.664652 \\ 1.213593 & 2.714187 \end{bmatrix} \times 10^{-9}\ \mathrm{m^2 s^{-1}} \text{ and}$$

$$[D_B] = \begin{bmatrix} 0.24995 & -1.051542 \\ -0.146769 & 1.913183 \end{bmatrix} \times 10^{-9}\,\mathrm{m^2 s^{-1}}.$$

Particularly noteworthy are the relatively large magnitudes of the off-diagonal elements of the Fick diffusivity matrices, that are directly attributable to the corresponding large off-diagonal elements of the matrices of thermodynamic correction factors.

The equilibration trajectories A-A* and B-B*, calculated using eqs (S138), and (S139), are indicated by the solid blue lines in Figure S27a. We note that the B-B* trajectory exhibits a foray into the meta-stable region; this foray could result in emulsion formation.

For the ethylacetate rich phase, the mole fractions of the three components are plotted in Figure S27b as function of the dimensionless distance coordinate $\frac{z}{\sqrt{4D_{ref}t}}$. We note that water experiences a slight undershoot during the transient equilibration process; this undershoot signifies uphill diffusion[14, 15, 53] that is engendered by thermodynamic coupling effects.

6.6 Uphill diffusion in water(1)/acetic-acid (2)/1-hexanol(3) mixtures

For water(1)/acetic-acid(2)/1-hexanol(3) mixtures we demonstrate that the curvilinear equilibration trajectories may enter the meta-stable regions between the binodal and spinodal curve. The initial starting compositions for the water-rich phase (A) and 1-hexanol-rich phase (B) are $\begin{pmatrix} x_{1A0} \\ x_{2A0} \end{pmatrix} = \begin{pmatrix} 0.8 \\ 0.2 \end{pmatrix}$; $\begin{pmatrix} x_{1B0} \\ x_{2B0} \end{pmatrix} = \begin{pmatrix} 0.1 \\ 0 \end{pmatrix}$; see Figure S28. The composition of the A-B mixture lies in the two phase region, and therefore will separate into two liquid phases with compositions A* and B*, at either end of the tie-line. For calculation of the transient equilibration trajectories, the Fick diffusivity matrices $[D_A]$, and $[D_B]$ are evaluated using eq (S45), wherein the scalar diffusivity $|\Lambda|^{1/2}$ is assumed to have the value $|\Lambda|^{1/2} = 1\times10^{-9}\ \mathrm{m^2 s^{-1}}$.

Emulsification in partially miscible ternary liquid mixtures

Using the head-to-tail iteration procedure for the moving interface solution, outlined in a foregoing section, the final converged values of the mole fractions at either sides of the interface, A* and B* are determined as $\begin{pmatrix} x_{1AI} \\ x_{2AI} \end{pmatrix} = \begin{pmatrix} 0.777853 \\ 0.183813 \end{pmatrix}$; $\begin{pmatrix} x_{1BI} \\ x_{2BI} \end{pmatrix} = \begin{pmatrix} 0.587665 \\ 0.253836 \end{pmatrix}$.

Evaluated at the arithmetic average mole fractions $\frac{1}{2}\begin{pmatrix} x_{1A0} + x_{1AI} \\ x_{2A0} + x_{2AI} \end{pmatrix}$, and $\frac{1}{2}\begin{pmatrix} x_{1B0} + x_{1BI} \\ x_{2B0} + x_{2BI} \end{pmatrix}$, the Fick diffusivity matrices are

$$[D_A] = \begin{bmatrix} -0.741926 & -1.423583 \\ 1.445324 & 2.305922 \end{bmatrix} \times 10^{-9}\,\mathrm{m^2 s^{-1}} \text{ and}$$

$$[D_B] = \begin{bmatrix} 0.630045 & -0.560827 \\ -0.203612 & 1.001456 \end{bmatrix} \times 10^{-9}\,\mathrm{m^2 s^{-1}}.$$

Particularly noteworthy are the relatively large magnitudes of the off-diagonal elements of the Fick diffusivity matrices, that are directly attributable to the corresponding large off-diagonal elements of the matrices of thermodynamic correction factors.

The equilibration trajectories A-A* and B-B*, calculated using eqs (S138), and (S139), are indicated by the solid blue lines in Figure S28. We note that the B-B* trajectory exhibits a foray into the meta-stable region; this foray could result in emulsion formation.

Diffusional forays are also possible if mixture of two ternary liquid mixtures of compositions A and B lies in the homogeneous region of the phase equilibrium diagram, close to the binodal curve. In order to demonstrate this, we choose a different set of starting compositions for the water-rich phase (A) and 1-hexanol-rich phase (B) as $\begin{pmatrix} x_{1A0} \\ x_{2A0} \end{pmatrix} = \begin{pmatrix} 0.15 \\ 0 \end{pmatrix}$; $\begin{pmatrix} x_{1B0} \\ x_{2B0} \end{pmatrix} = \begin{pmatrix} 0.62 \\ 0.38 \end{pmatrix}$; see Figure S29.

The composition of the A-B mixture, A*= B* = $\begin{pmatrix} x_{1I} \\ x_{2I} \end{pmatrix} = \begin{pmatrix} \frac{x_{1A0} + x_{1B0}}{2} \\ \frac{x_{2A0} + x_{2B0}}{2} \end{pmatrix} = \begin{pmatrix} 0.385 \\ 0.19 \end{pmatrix}$ lies in the homogeneous single phase region.

Evaluated at the arithmetic average mole fractions $\frac{1}{2}\begin{pmatrix} x_{1A0}+x_{1I} \\ x_{2A0}+x_{2I} \end{pmatrix}$, and $\frac{1}{2}\begin{pmatrix} x_{1B0}+x_{1I} \\ x_{2B0}+x_{2I} \end{pmatrix}$, the Fick diffusivity matrices are

$$[D_A] = \begin{bmatrix} 0.773471 & -0.430359 \\ -0.16503 & 0.956984 \end{bmatrix} \times 10^{-9}\,\mathrm{m^2 s^{-1}} \text{ and}$$

$$[D_B] = \begin{bmatrix} 0.140218 & -0.768897 \\ 0.078006 & 1.370439 \end{bmatrix} \times 10^{-9}\,\mathrm{m^2 s^{-1}}.$$

Particularly noteworthy are the relatively large magnitudes of the off-diagonal elements of the Fick diffusivity matrices, that are directly attributable to the corresponding large off-diagonal elements of the matrices of thermodynamic correction factors.

The equilibration trajectories A-A* and B-B* calculated using eq (S141) are indicated by the solid blue lines. We note that the A-A* trajectory exhibits a foray into the meta-stable region (cf. Figure S29); this foray could result in emulsion formation.

If thermodynamic coupling effects are completely ignored by invoking the assumption $\Gamma_{ij} = \delta_{ij}$, the Kronecker delta, the equilibration trajectories (shown by the dotted lines) do not exhibit any foray into the meta-stable region.

6.7 Uphill diffusion in water(1)/acetic-acid (2)/MTBE(3) mixtures

For water(1)/acetic-acid(2)/MTBE(3) mixtures we demonstrate that the curvilinear equilibration trajectories may enter the meta-stable regions between the binodal and spinodal curve. The initial starting compositions for the water-rich phase (A) and MTBE-rich phase (B) are $\begin{pmatrix} x_{1A0} \\ x_{2A0} \end{pmatrix} = \begin{pmatrix} 0.85 \\ 0.15 \end{pmatrix}$; $\begin{pmatrix} x_{1B0} \\ x_{2B0} \end{pmatrix} = \begin{pmatrix} 0.05 \\ 0 \end{pmatrix}$; see Figure S30a. The composition of the A-B mixture lies in the two phase region, and therefore will separate into two liquid phases with compositions A* and B*, at either end of the tie-line. For calculation of the transient equilibration trajectories, the Fick diffusivity

matrices $[D_A]$, and $[D_B]$ are evaluated using eq (S45), wherein the scalar diffusivity $|\Lambda|^{1/2}$ is assumed to have the value $|\Lambda|^{1/2} = 1\times10^{-9}$ m^{2}s^{-1}.

Using the head-to-tail iteration procedure for the moving interface solution, outlined in a foregoing section, the final converged values of the mole fractions at either sides of the interface, A* and B* are determined as $\begin{pmatrix} x_{1AI} \\ x_{2AI} \end{pmatrix} = \begin{pmatrix} 0.85090555 \\ 0.11244516 \end{pmatrix}$; $\begin{pmatrix} x_{1BI} \\ x_{2BI} \end{pmatrix} = \begin{pmatrix} 0.46928732 \\ 0.24612399 \end{pmatrix}$.

Evaluated at the arithmetic average mole fractions $\frac{1}{2}\begin{pmatrix} x_{1A0} + x_{1AI} \\ x_{2A0} + x_{2AI} \end{pmatrix}$, and $\frac{1}{2}\begin{pmatrix} x_{1B0} + x_{1BI} \\ x_{2B0} + x_{2BI} \end{pmatrix}$, the Fick diffusivity matrices are

$$[D_A] = \begin{bmatrix} -0.88449784 & -2.23493914 \\ 1.78233869 & 3.42983167 \end{bmatrix} \times 10^{-9}\,\mathrm{m^2 s^{-1}} \text{ and}$$

$$[D_B] = \begin{bmatrix} 0.2160129 & -0.85366825 \\ -0.20855647 & 1.84454786 \end{bmatrix} \times 10^{-9}\,\mathrm{m^2 s^{-1}}.$$

Particularly noteworthy are the relatively large magnitudes of the off-diagonal elements of the Fick diffusivity matrices, that are directly attributable to the corresponding large off-diagonal elements of the matrices of thermodynamic correction factors.

The equilibration trajectories A-A* and B-B*, calculated using eqs (S138), and (S139), are indicated by the solid blue lines in Figure S30a. We note that the B-B* trajectory exhibits a foray into the meta-stable region; this foray could result in emulsion formation.

For the MTBE rich phase, the mole fractions of the three components are plotted in Figure S30b as function of the dimensionless distance coordinate $\frac{z}{\sqrt{4D_{ref}t}}$. We note that water experiences a slight undershoot during the transient equilibration process; this undershoot signifies uphill diffusion[14, 15, 53] that is engendered by thermodynamic coupling effects.

6.8 Uphill diffusion in water(1)/ethanol (2)/cyclohexane(3) mixtures

For water(1)/ethanol(2)/cyclohexane(3) mixtures we shall demonstrate that diffusional forays are possible if mixture of two ternary liquid mixtures of A and B lies in the homogeneous region of the phase equilibrium diagram, close to the binodal curve. In order to demonstrate this, we choose the set of starting compositions for the ethanol-rich phase (A) and cyclohexane-rich phase (B) as $\begin{pmatrix} x_{1A0} \\ x_{2A0} \end{pmatrix} = \begin{pmatrix} 0.375 \\ 0.62 \end{pmatrix}$; $\begin{pmatrix} x_{1B0} \\ x_{2B0} \end{pmatrix} = \begin{pmatrix} 0 \\ 0.57 \end{pmatrix}$; see Figure S31a. The composition of the A-B mixture, A*= B* = $\begin{pmatrix} x_{1I} \\ x_{2I} \end{pmatrix} = \begin{pmatrix} \frac{x_{1A0} + x_{1B0}}{2} \\ \frac{x_{2A0} + x_{2B0}}{2} \end{pmatrix} = \begin{pmatrix} 0.1875 \\ 0.595 \end{pmatrix}$ lies in the homogeneous single phase region.

For calculation of the transient equilibration trajectories, the Fick diffusivity matrices $[D_A]$, and $[D_B]$ are evaluated using eq (S45), wherein the scalar diffusivity $|\Lambda|^{1/2}$ is estimated using $|\Lambda|^{1/2} = \sqrt{\frac{Đ_{12} Đ_{13} Đ_{23}}{x_1 Đ_{23} + x_2 Đ_{13} + x_3 Đ_{12}}}$, wherein the infinite dilution M-S pair diffusivities are estimated using the Wilke-Change correlation.[14, 15, 48]

Evaluated at the arithmetic average mole fractions $\frac{1}{2}\begin{pmatrix} x_{1A0} + x_{1I} \\ x_{2A0} + x_{2I} \end{pmatrix}$, and $\frac{1}{2}\begin{pmatrix} x_{1B0} + x_{1I} \\ x_{2B0} + x_{2I} \end{pmatrix}$, the matrices of thermodynamic correction factors, and the Fick diffusivity matrices are

$$[\Gamma_A] = \begin{bmatrix} 0.17271 & -0.42498 \\ -0.0155 & 0.74746 \end{bmatrix}; \quad [D_A] = \begin{bmatrix} 0.52899 & -1.30166 \\ -0.04747 & 2.28938 \end{bmatrix} \times 10^{-9}\,\mathrm{m^2 s^{-1}} \text{ and}$$

$$[\Gamma_B] = \begin{bmatrix} 0.59141 & -0.19602 \\ -0.70702 & 0.3644 \end{bmatrix}; \quad [D_B] = \begin{bmatrix} 1.70934 & -0.56656 \\ -2.04347 & 1.0532 \end{bmatrix} \times 10^{-11}\,\mathrm{m^2 s^{-1}}.$$

Particularly noteworthy are the relatively large magnitudes of the off-diagonal elements of the Fick diffusivity matrices, that are directly attributable to the corresponding large off-diagonal elements of the matrices of thermodynamic correction factors.

The equilibration trajectories A-A* and B-B* calculated using eq (S141) are indicated by the solid blue lines Figure S31a. We note that the B-B* trajectory exhibits a foray into the meta-stable region; this foray could result in emulsion formation.

The composition profiles of the three components are plotted in Figure S31b as function of the dimensionless distance coordinate $\frac{z}{\sqrt{4D_{ref}t}}$. We note that ethanol experiences a pronounced undershoot during the transient equilibration process. Concomitantly, cyclohexane displays a slight overshoot. The overshoot and undershoot phenomena signify uphill diffusion[14, 15, 53] that is engendered by thermodynamic coupling effects.

If thermodynamic coupling effects are completely ignored by invoking the assumption $\Gamma_{ij} = \delta_{ij}$, the Kronecker delta, the equilibration trajectories (shown by the dotted lines) do not exhibit any foray into the meta-stable region.

6.9 Uphill diffusion in water(1)/acetontrile(2)/toluene(3) mixtures

For water(1)/acetonitrile(2)/toluene(3) mixtures, the experiments of Califano and Mauri[68] demonstrate that the mixing of two liquids of different compositions can lead to forays into meta-stable regions and emulsion formation in either the water-rich or toluene-rich phases. Herein, we trace the origins of such diffusional forays to thermodynamic coupling effects. we demonstrate that forays into metastable regions

Consider the inter-diffusion between acetonitrile-rich phase (A) and water-rich phase (B) with initial compositions $\begin{pmatrix} x_{1A0} \\ x_{2A0} \end{pmatrix} = \begin{pmatrix} 0 \\ 0.63 \end{pmatrix}$; $\begin{pmatrix} x_{1B0} \\ x_{2B0} \end{pmatrix} = \begin{pmatrix} 0.24 \\ 0.76 \end{pmatrix}$; see Figure S32a. The composition of the A-B mixture, A*= B* = $\begin{pmatrix} x_{1I} \\ x_{2I} \end{pmatrix} = \begin{pmatrix} \frac{x_{1A0} + x_{1B0}}{2} \\ \frac{x_{2A0} + x_{2B0}}{2} \end{pmatrix} = \begin{pmatrix} 0.12 \\ 0.695 \end{pmatrix}$ lies in the homogeneous single phase region.

For calculation of the transient equilibration trajectories, the Fick diffusivity matrices $[D_A]$, and $[D_B]$ are evaluated using eq (S45), wherein the scalar diffusivity $|\Lambda|^{1/2}$ is assumed to have the value $|\Lambda|^{1/2} = 1\times10^{-9}\ \mathrm{m^2 s^{-1}}$. Evaluated at the arithmetic average mole fractions $\frac{1}{2}\begin{pmatrix} x_{1A0} + x_{1I} \\ x_{2A0} + x_{2I} \end{pmatrix}$, and $\frac{1}{2}\begin{pmatrix} x_{1B0} + x_{1I} \\ x_{2B0} + x_{2I} \end{pmatrix}$, the Fick diffusivity matrices are

$$[D_A] = \begin{bmatrix} 0.48838 & -0.20289 \\ -0.58745 & 0.79614 \end{bmatrix} \times 10^{-9}\,\mathrm{m^2 s^{-1}} \text{ and}$$

$$[D_B] = \begin{bmatrix} -0.01252 & -0.41202 \\ 0.50203 & 1.17708 \end{bmatrix} \times 10^{-9}\,\mathrm{m^2 s^{-1}}.$$

Particularly noteworthy are the relatively large magnitudes of the off-diagonal elements of the Fick diffusivity matrices, that are directly attributable to the corresponding large off-diagonal elements of the matrices of thermodynamic correction factors.

The equilibration trajectories A-A* and B-B* calculated using eq (S141) are indicated by the solid blue lines. We note that the B-B* trajectory exhibits a foray into the meta-stable region (cf. Figure S32a); this foray could result in emulsion formation. If thermodynamic coupling effects are completely ignored by invoking the assumption $\Gamma_{ij} = \delta_{ij}$, the Kronecker delta, the equilibration trajectories (shown by the dotted lines) do not exhibit any foray into the meta-stable region.

The composition profiles of the three components are plotted in Figure S32b as function of the dimensionless distance coordinate $\frac{z}{\sqrt{4D_{ref}t}}$. We note that water experiences a pronounced overshoot during the transient equilibration process. Acetonitrile displays both overshoot and undershoot phenomena. The overshoot and undershoot phenomena signify uphill diffusion[14, 15, 53] that is engendered by thermodynamic coupling effects.

Forays into meta-stable regions are also realized for a different set of compositions for the acetonitrile-rich phase (A) and water-rich phase (B) with initial compositions

$\begin{pmatrix} x_{1A0} \\ x_{2A0} \end{pmatrix} = \begin{pmatrix} 0 \\ 0.8 \end{pmatrix}$; $\begin{pmatrix} x_{1B0} \\ x_{2B0} \end{pmatrix} = \begin{pmatrix} 0.35 \\ 0.65 \end{pmatrix}$; see Figure S33a. The composition of the A-B mixture, A*= B* = $\begin{pmatrix} x_{1I} \\ x_{2I} \end{pmatrix} = \begin{pmatrix} \frac{x_{1A0} + x_{1B0}}{2} \\ \frac{x_{2A0} + x_{2B0}}{2} \end{pmatrix} = \begin{pmatrix} 0.175 \\ 0.725 \end{pmatrix}$ lies in the homogeneous single phase region.

Evaluated at the arithmetic average mole fractions $\frac{1}{2}\begin{pmatrix} x_{1A0} + x_{1I} \\ x_{2A0} + x_{2I} \end{pmatrix}$, and $\frac{1}{2}\begin{pmatrix} x_{1B0} + x_{1I} \\ x_{2B0} + x_{2I} \end{pmatrix}$, the Fick diffusivity matrices are

$$[D_A] = \begin{bmatrix} 0.39488 & -0.24774 \\ -0.1031 & 0.94395 \end{bmatrix} \times 10^{-9}\,\mathrm{m^2 s^{-1}} \text{ and}$$

$$[D_B] = \begin{bmatrix} -0.25967 & -0.51125 \\ 0.9391 & 1.35636 \end{bmatrix} \times 10^{-9}\,\mathrm{m^2 s^{-1}}.$$

Particularly noteworthy are the relatively large magnitudes of the off-diagonal elements of the Fick diffusivity matrices, that are directly attributable to the corresponding large off-diagonal elements of the matrices of thermodynamic correction factors.

The equilibration trajectories A-A* and B-B* calculated using eq (S141) are indicated by the solid blue lines. We note that the B-B* trajectory exhibits a foray into the meta-stable region (cf. Figure S33a); this foray could result in emulsion formation. If thermodynamic coupling effects are completely ignored by invoking the assumption $\Gamma_{ij} = \delta_{ij}$, the Kronecker delta, the equilibration trajectories (shown by the dotted lines) do not exhibit any foray into the meta-stable region.

The composition profiles of the three components are plotted in Figure S33b as function of the dimensionless distance coordinate $\frac{z}{\sqrt{4D_{ref}t}}$. We note that water experiences a pronounced overshoot during the transient equilibration process. Concomitantly, acetonitrile displays and undershoot phenomena. The overshoot and undershoot phenomena signify uphill diffusion[14, 15, 53] that is engendered by thermodynamic coupling effects.

6.10 List of Tables for Emulsification in partially miscible ternary liquid mixtures

Table S10. NRTL parameters for glyercol(1)/acetone(2)/water(3) at 298 K. These parameters are from Krishna et al.[8]

	$\tau_{ij} = A_{ij}/T$	$\tau_{ji} = A_{ji}/T$	$\alpha_{ij} = \alpha_{ji}$
	dimensionless	dimensionless	dimensionless
glycerol(1)/acetone(2)	0.868423	2.467651	0.2
glycerol(1)/water(3)	-1.293658	-1.520738	0.2
acetone(2)/water(3)	-0.665537	2.096477	0.2

Table S11. UNIQUAC parameters for water(1)/chloroform(2)/acetic-acid(3) at 298 K. These parameters are from Pertler.[69] These parameters needed re-adjustment in order to match the experimental solubility data of Othmer and Ku.[70] The following are the adjusted values used in the calculations.

	r_i	q_i
	dimensionless	dimensionless
water(1)	0.92	1.4
chloroform(2)	2.87	2.41
acetic-acid(3)	2.2024	2.072

	$\tau_{ij} = \exp(-A_{ij}/T)$	$\tau_{ji} = \exp(-A_{ji}/T)$
	dimensionless	dimensionless
water(1)/chloroform(2)	0.42845912	0.22867995
water(1)/acetic-acid(3)	1.27379861	1.31092921
chloroform(2)/acetic-acid(3)	1.38787923	0.885

Table S12. UNIQUAC parameters for water(1)/acetone(2)/ethylacetate(3) at 293 K. These parameters are from Pertler.[69]

	r_i	q_i
	dimensionless	dimensionless
water(1)	0.92	1.4
acetone(2)	2.5735	2.336
ethyl-acetate(3)	3.4786	3.116

	$\tau_{ij} = \exp(-A_{ij}/T)$	$\tau_{ji} = \exp(-A_{ji}/T)$
	dimensionless	dimensionless
water(1)/acetone(2)	1.327669	0.487929
water(1)/ethylacetate(3)	0.770478	0.253826
acetone(2)/ethyl-acetate(3)	1.307766	0.826986

Table S13. UNIQUAC parameters for water (1)/ethanol(2)/ethyl-acetate(3). These parameters are taken from Table 3 of Resa and Goenaga.[71]

	r_i	q_i
	dimensionless	dimensionless
water(1)	0.92	1.4
ethanol(2)	2.105	1.972
Ethyl acetate (3)	3.4786	3.116

	A_{ij}	A_{ji}
	K^{-1}	K^{-1}
Water(1)/ethanol(2)	-109.102	-137.836
water(1)/ethyl acetate(3)	176.158	320.83
Ethanol(2)/ Ethyl-acetate(3)	-355.791	390.218

Table S14. NRTL parameters for water(1)/acetic acid(2)/1-hexanol(3) at 298 K. These parameters are taken from Table 3 of Fahim et al.[72]

	$\tau_{ij} = \left(a_{ij}^0 + b_{ij}\left(T - 273.15\right)\right)/T$	$\tau_{ji} = \left(a_{ji}^0 + b_{ji}\left(T - 273.15\right)\right)/T$	$\alpha_{ij} = \alpha_{ji}$
	dimensionless	dimensionless	dimensionless
water(1)/acetic acid(2)	1.219886	-0.323559	0.2
water(1)/ 1-hexanol(3)	6.951283	-0.345447	0.2
Acetic acid (2)/ 1-hexanol(3)	-0.361647	0.990639	0.2

Table S15. NRTL parameters for water(1)/acetic acid(2)/MTBE (3) at 298.15 K. The parameters are from Zhang and Wang.[73]

	$\tau_{ij} = A_{ij}/T$	$\tau_{ji} = A_{ji}/T$	$\alpha_{ij} = \alpha_{ji}$
	dimensionless	dimensionless	dimensionless
water(1)/acetic acid (2)	0.354	-1.2151	0.47
water(1)/MTBE(3)	3.9737	1.2998	0.2
Acetic acid(2)/ MTBE(3)	-0.2774	-2.8068	0.37

Table S16. NRTL parameters for water(1)/ethanol(2)/cyclohexane (3) at 298 K. These parameters are from the DECHEMA Dortmund data bank, as reported in Table 1 of Springer et al.[74]

	τ_{ij}	τ_{ji}	$\alpha_{ij} = \alpha_{ji}$
	dimensionless	dimensionless	dimensionless
Water(1)/ethanol(2)	1.8707	0.0976	0.3475
water(1)/cyclohexane(3)	14.84	5.6653	0.21159
ethanol(2)/cyclohexane(3)	1.4786	2.408	0.46261

Table S17. NRTL parameters for water(1)/acetonitrile(2)/toluene (3) at 293.15 K. The parameters are from Di Cave and Mazzarotta.[75]

	τ_{ij}	τ_{ji}	$\alpha_{ij} = \alpha_{ji}$
	dimensionless	dimensionless	dimensionless
water(1)/acetonitrile (2)	1.60724	0.95391	0.3
water(1)/toluene(3)	4.48747	7.26421	0.2
Acetonitrile(2)/ toluene(3)	0.97552	-0.0199	0.3

6.11 List of Figures for Emulsification in partially miscible ternary liquid mixtures

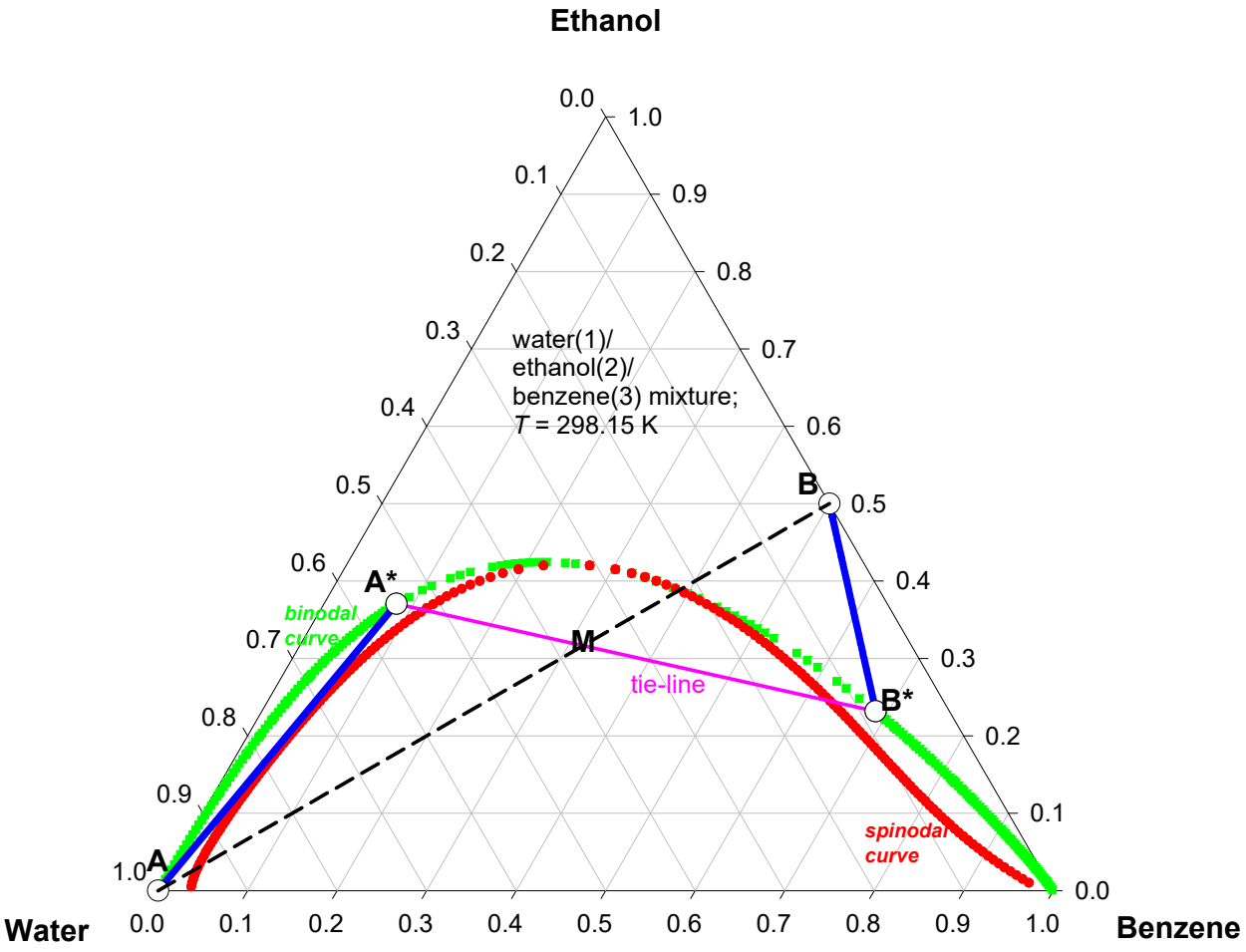

Figure S19. Transient equilibration trajectories A-A*, and B-B* for water(1)/ethanol(2)/benzene(3) mixture at 298 K, demonstrating forays into the metastable region in the water-rich region of the phase diagram.

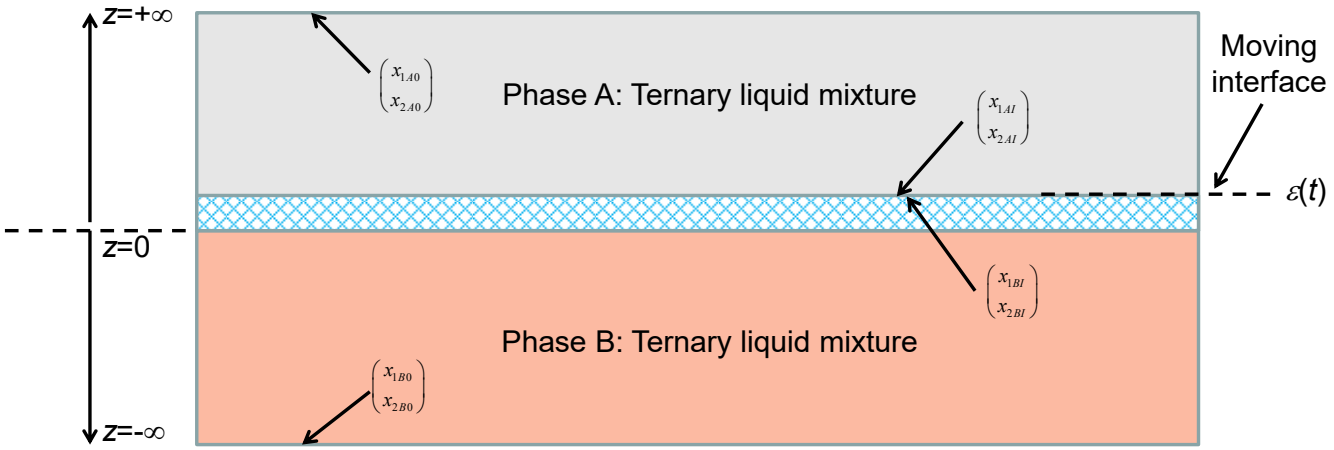

Figure S20. Schematic showing the chosen configuration for modeling transient equilibration between two phases A and B of partially miscible ternary liquid mixtures.

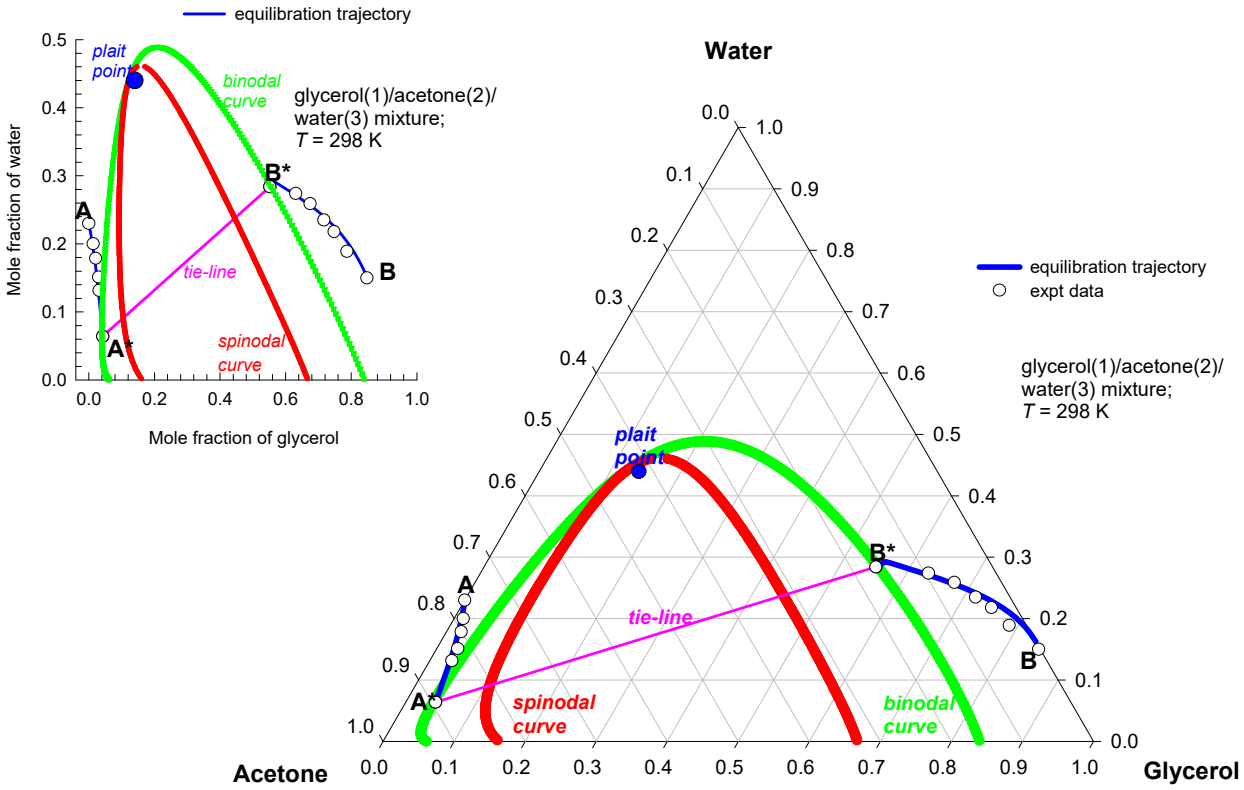

Figure S21. Transient equilibration trajectories for the system glycerol(1)/acetone(2)/water(3) mixtures at 298 K. The experimental data for the equilibration paths for glycerol(1)/acetone(2)/water(3) mixture measured in a stirred Lewis cell by Krishna et al.,[67] indicated by the symbols, are compared with the calculated equilibration trajectories, indicated by the solid blue lines. The phase equilibrium is determined from the NRTL parameters in Table S10.

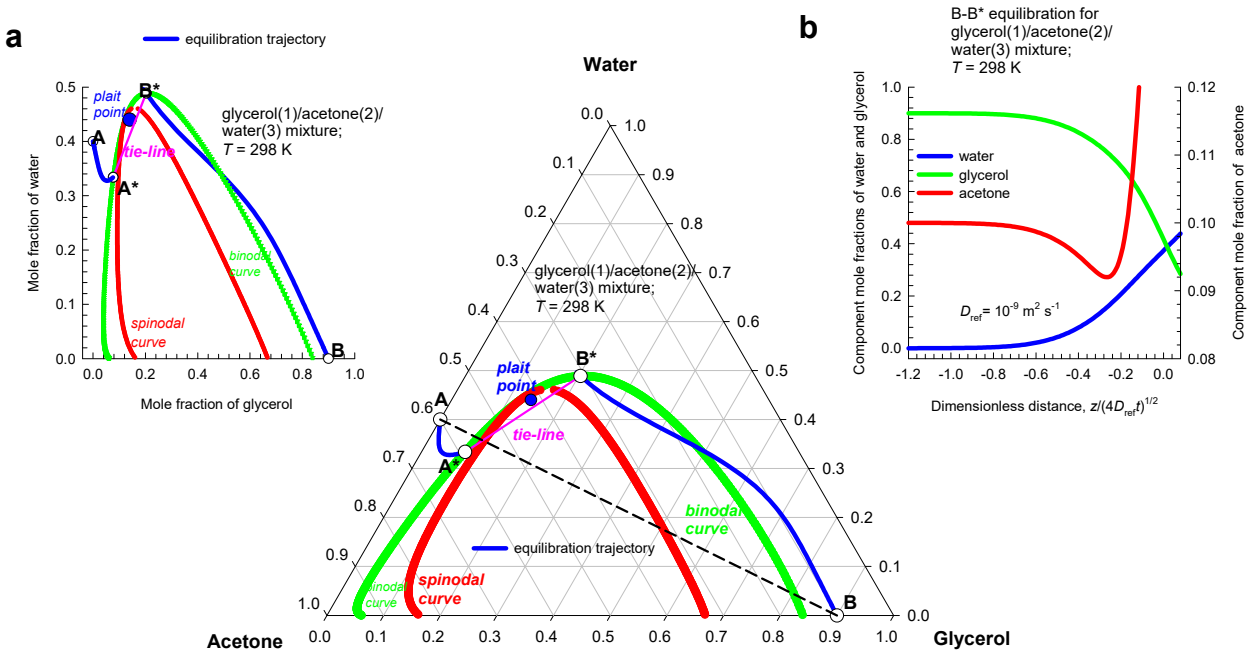

Figure S22. (a) Transient equilibration trajectories for glycerol(1)/acetone(2)/water(3) mixture at 298 K, demonstrating forays into the metastable region. (b) Transient composition profiles in glycerol-rich phase B plotted as function of the dimensionless distance coordinate $\frac{z}{\sqrt{4D_{ref}t}}$. The phase equilibrium is determined from the NRTL parameters in Table S10.

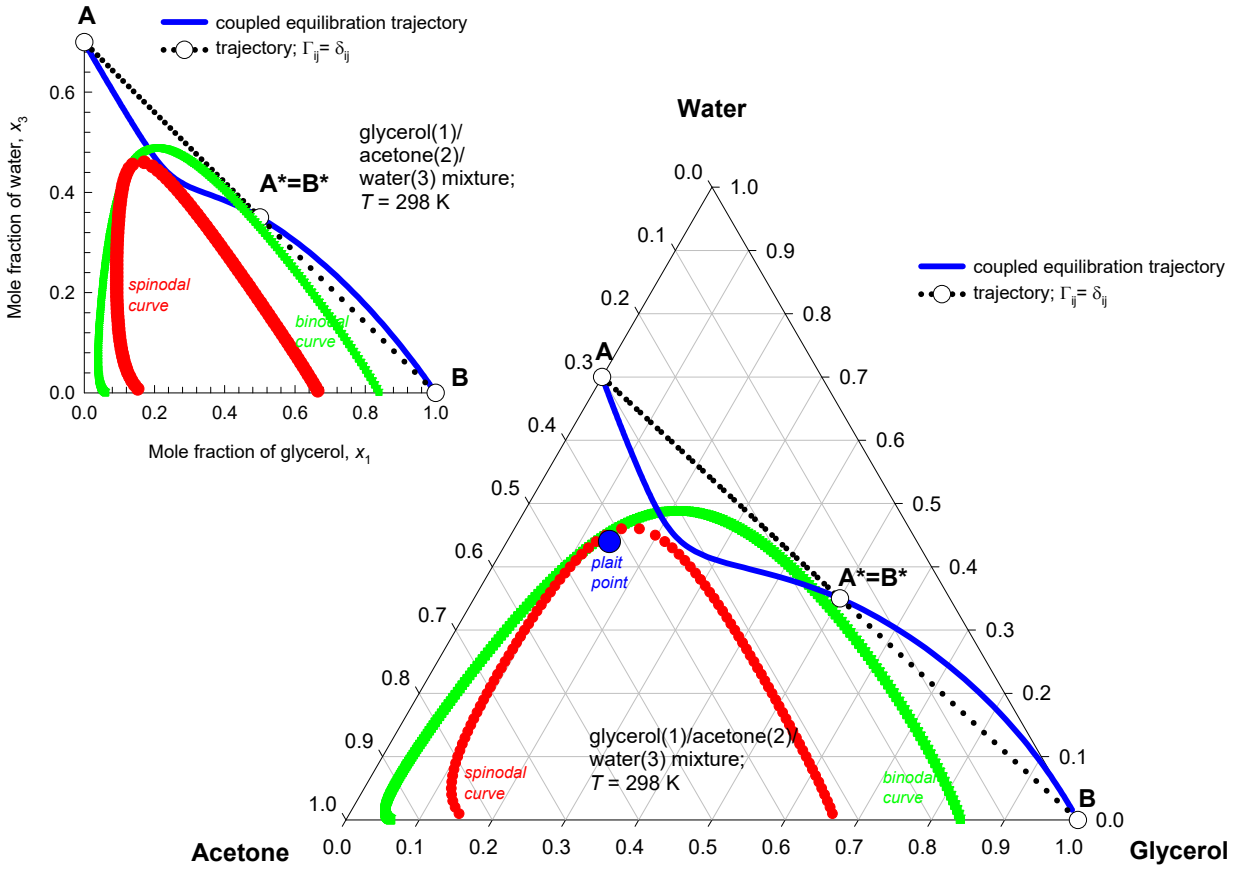

Figure S23. Transient equilibration trajectories followed during equilibration of homogenous mixtures of two different compositions for the system glycerol(1)/acetone(2)/water(3). The NRTL parameters for calculation of the phase equilibrium thermodynamics are provided in Table S10.

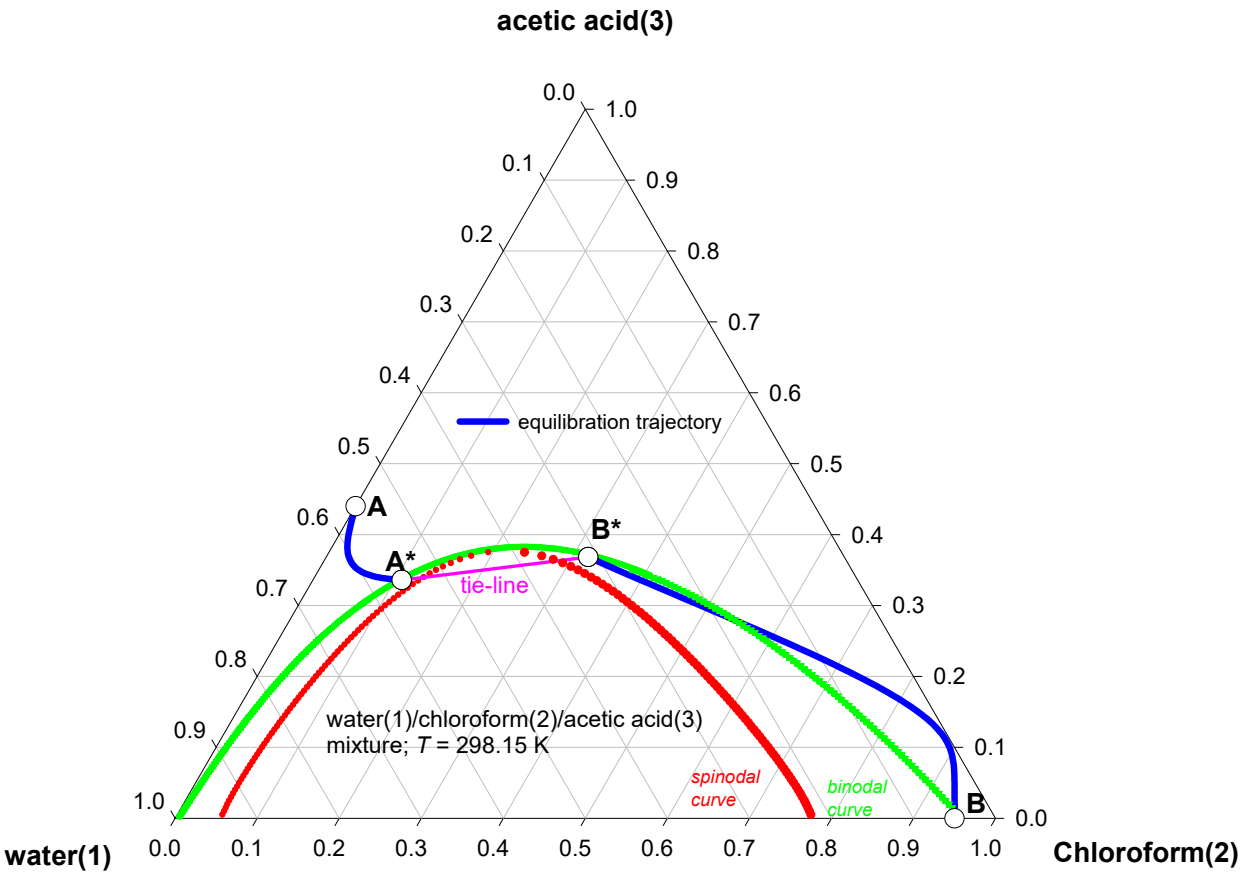

Figure S24. Transient equilibration trajectories for water(1)/chloroform(2)/acetic-acid(3) mixture at 298 K. The UNIQUAC parameters are provided in Table S11.

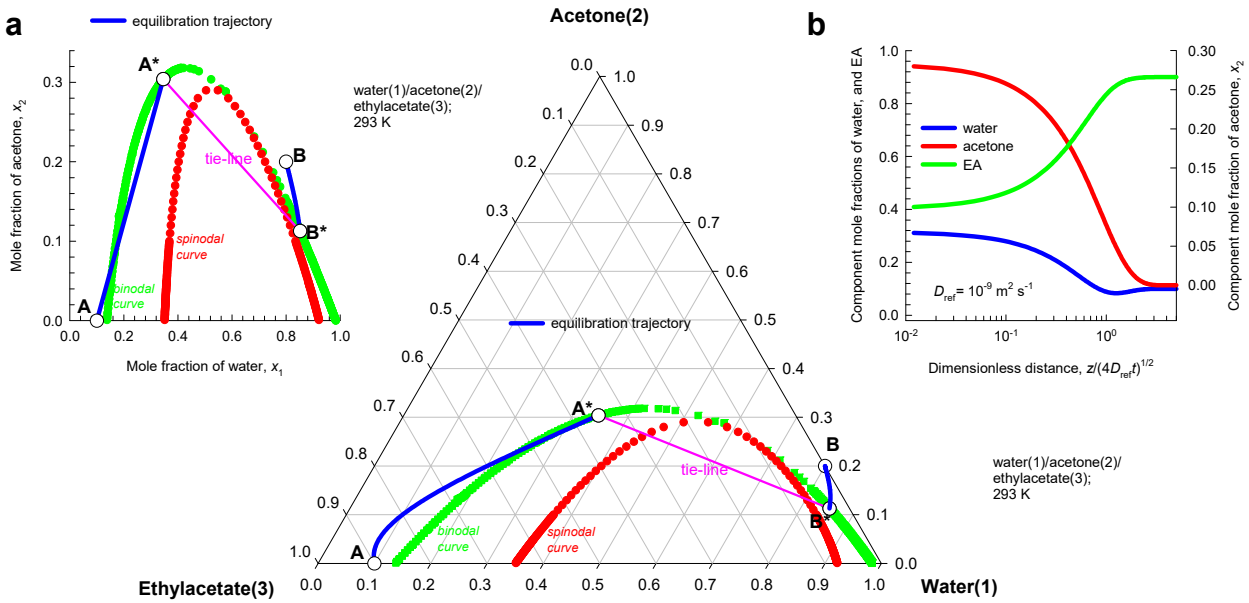

Figure S25. (a) Transient equilibration trajectories for water(1)/acetone(2)/ethyl-acetate(3) mixtures at 293 K. (b) Transient composition profiles in ethylacetate-rich phase B plotted as function of the dimensionless distance coordinate $\frac{z}{\sqrt{4D_{ref}t}}$. The UNIQUAC parameters for calculation of the phase equilibrium thermodynamics are provided in Table S12.

.

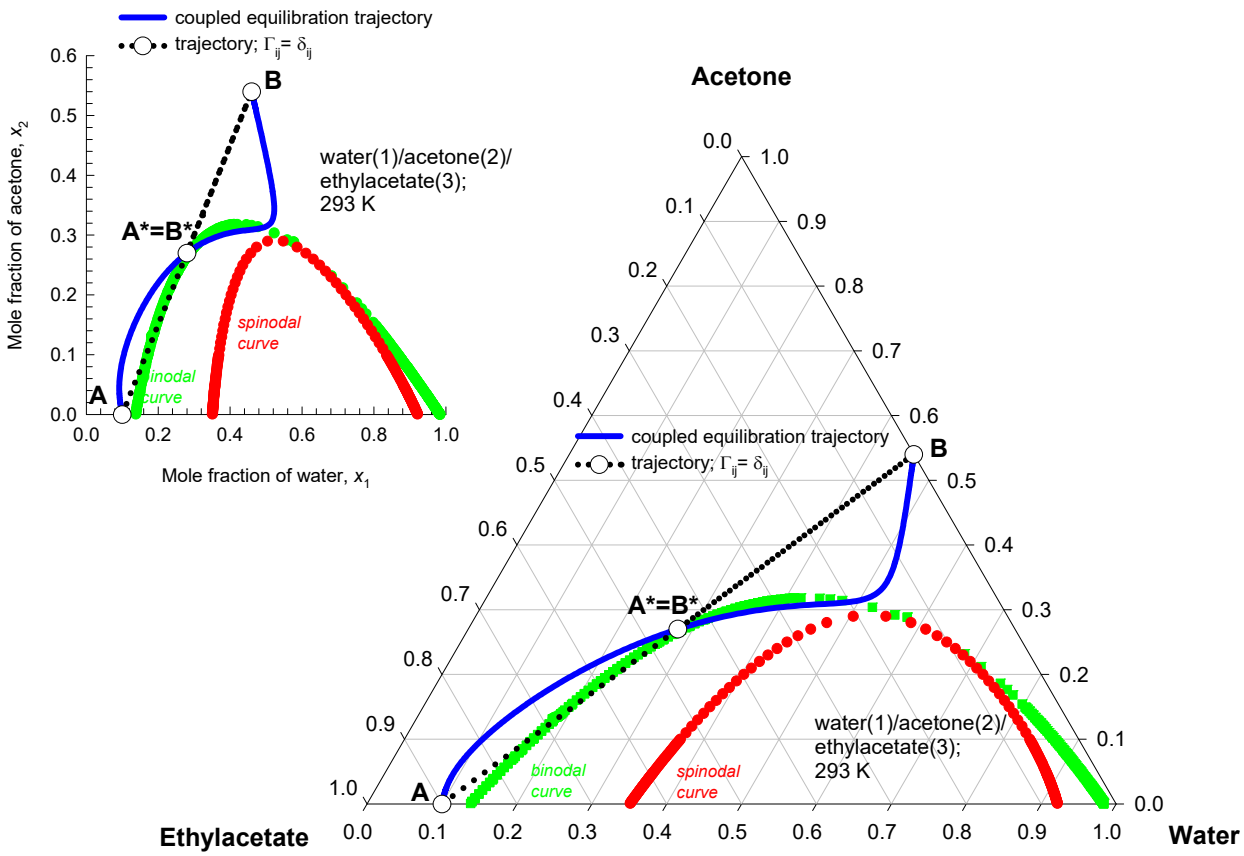

Figure S26. Transient equilibration trajectories followed during equilibration of homogenous mixtures of two different compositions for the system water(1)/acetone(2)/ethyl-acetate(3) mixture. The UNIQUAC parameters for calculation of the phase equilibrium thermodynamics are provided in Table S12.

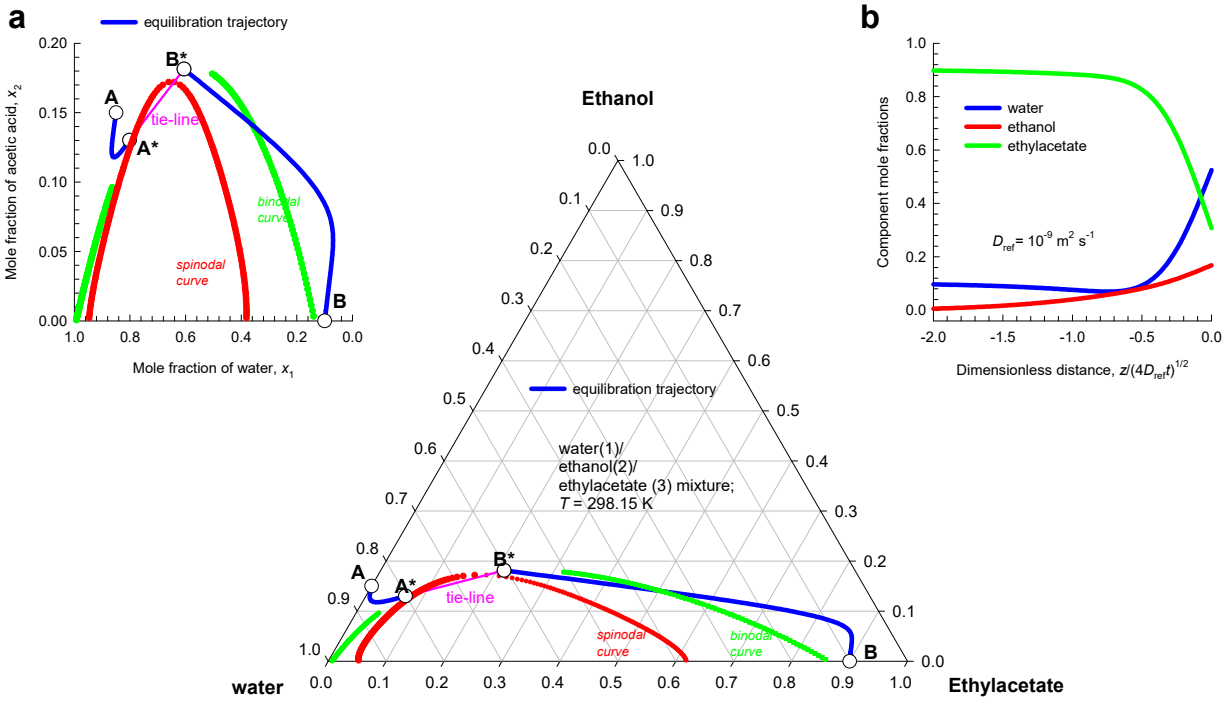

Figure S27. (a) Transient equilibration trajectories for the system water(1)/ethanol(2)/ethyl-acetate(3) at 298 K. (b) Transient composition profiles in ethylacetate-rich phase B plotted as function of the dimensionless distance coordinate $\frac{z}{\sqrt{4D_{ref}t}}$. The UNIQUAC parameters for calculation of the phase equilibrium thermodynamics are provided in Table S13.

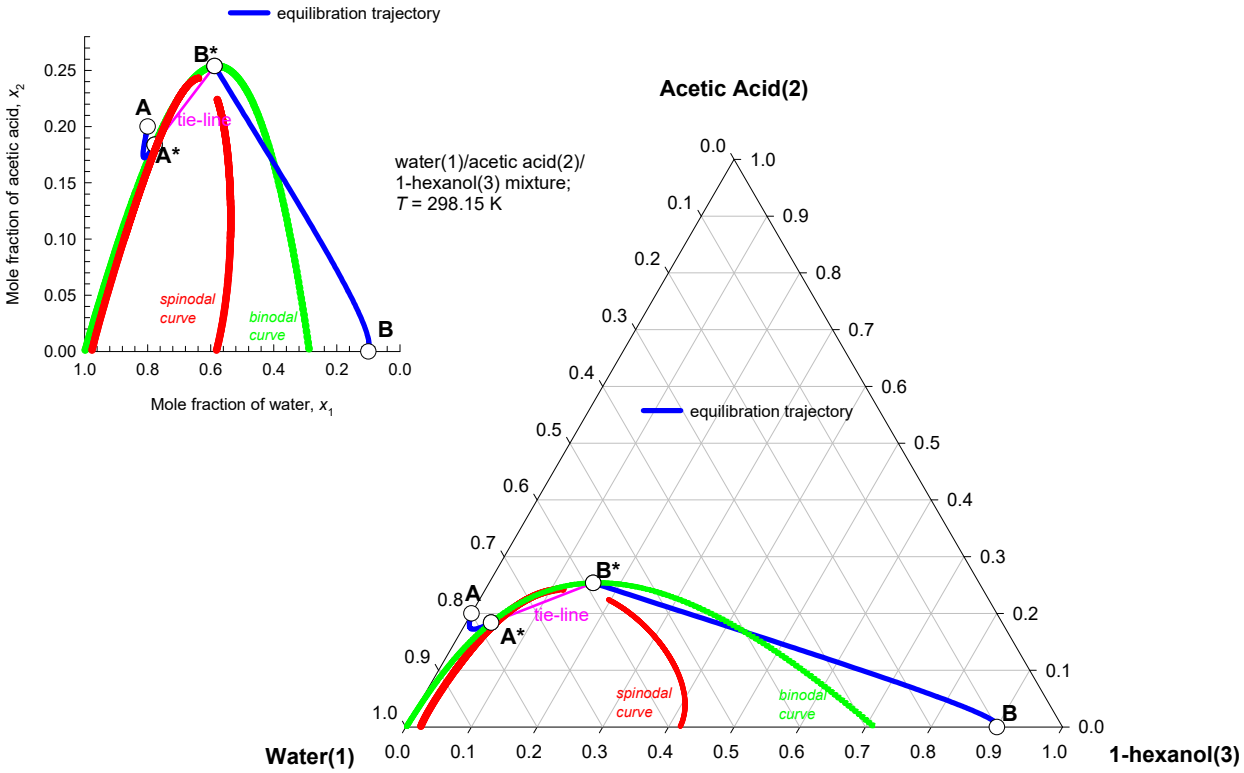

Figure S28. Transient equilibration trajectories for the system water(1)/acetic acid(2)/1-hexanol(3) at 298 K. The NRTL parameters for calculation of the phase equilibrium thermodynamics are provided in Table S14.

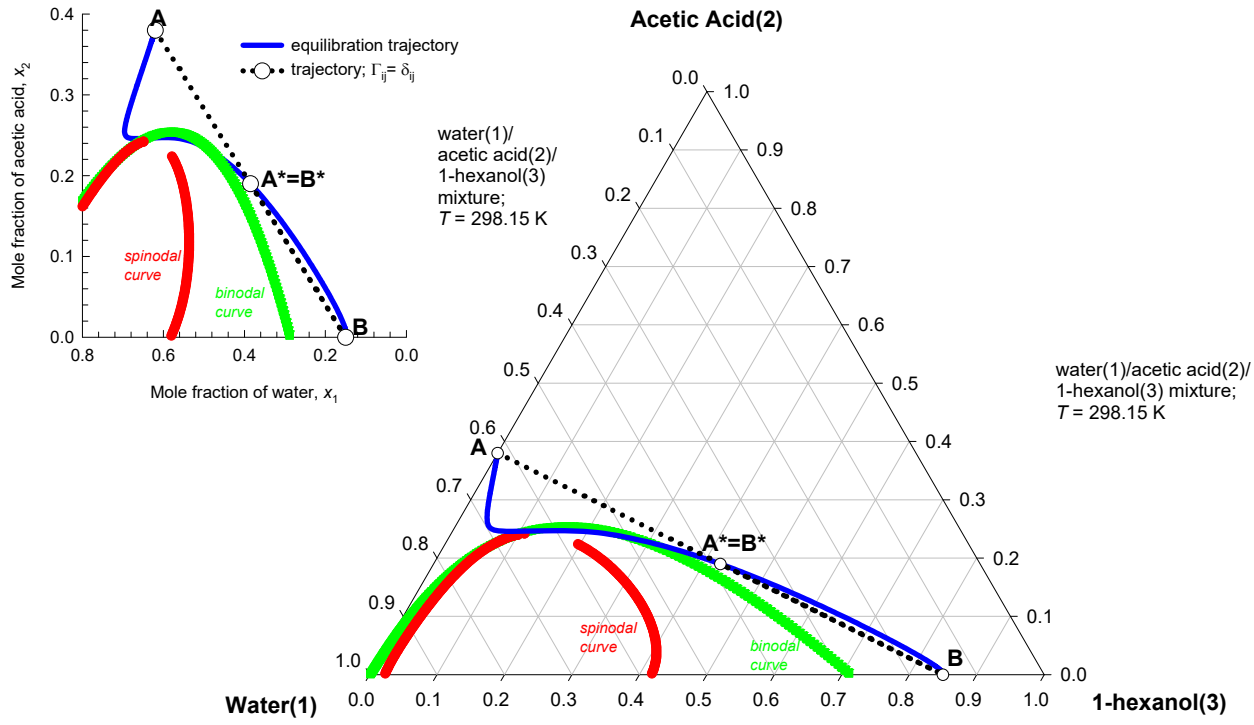

Figure S29. Transient equilibration trajectories followed during equilibration of homogenous mixtures of two different compositions for the system water(1)/acetic acid(2)/1-hexanol(3) at 298 K. The NRTL parameters for calculation of the phase equilibrium thermodynamics are provided in Table S14.

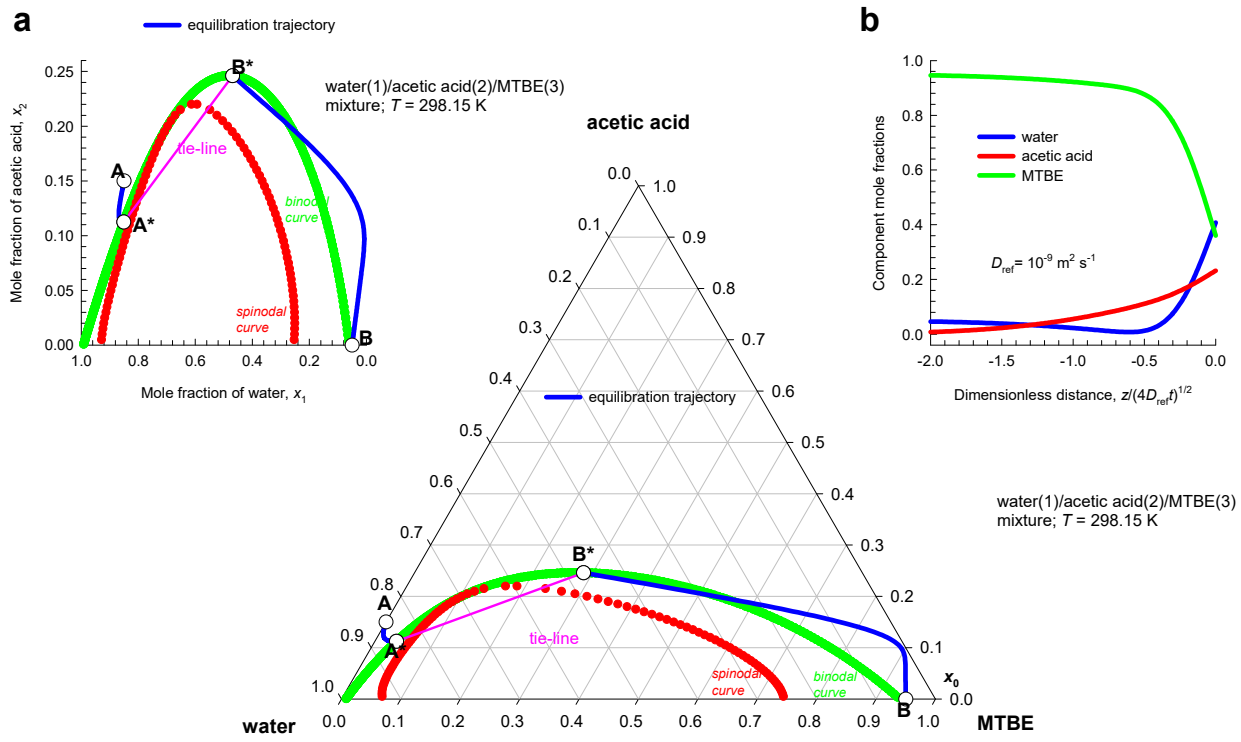

Figure S30. (a) Transient equilibration trajectories for the system water(1)/acetic-acid(2)/MTBE(3) at 298 K. (b) Transient composition profiles in MTBE-rich phase B, as function of the dimensionless distance coordinate $\frac{z}{\sqrt{4D_{ref}t}}$. The NRTL parameters for calculation of the phase equilibrium thermodynamics are provided in Table S15.

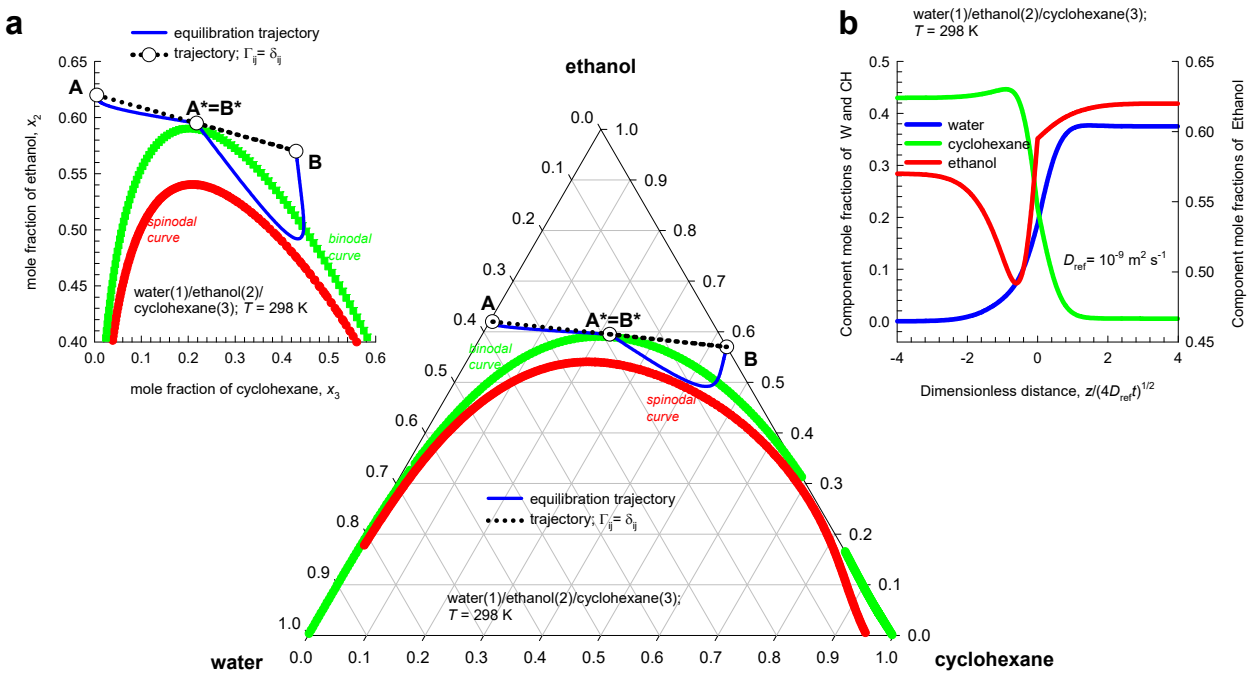

Figure S31. (a) Transient equilibration trajectories followed during equilibration of homogenous mixtures of two different compositions for the system water(1)/ethanol(2)/cyclohexane(3) at 298 K. (b) Transient composition profiles plotted as function of the dimensionless distance coordinate $\frac{z}{\sqrt{4D_{ref}t}}$.

The NRTL parameters for calculation of the phase equilibrium thermodynamics are provided in Table S16.

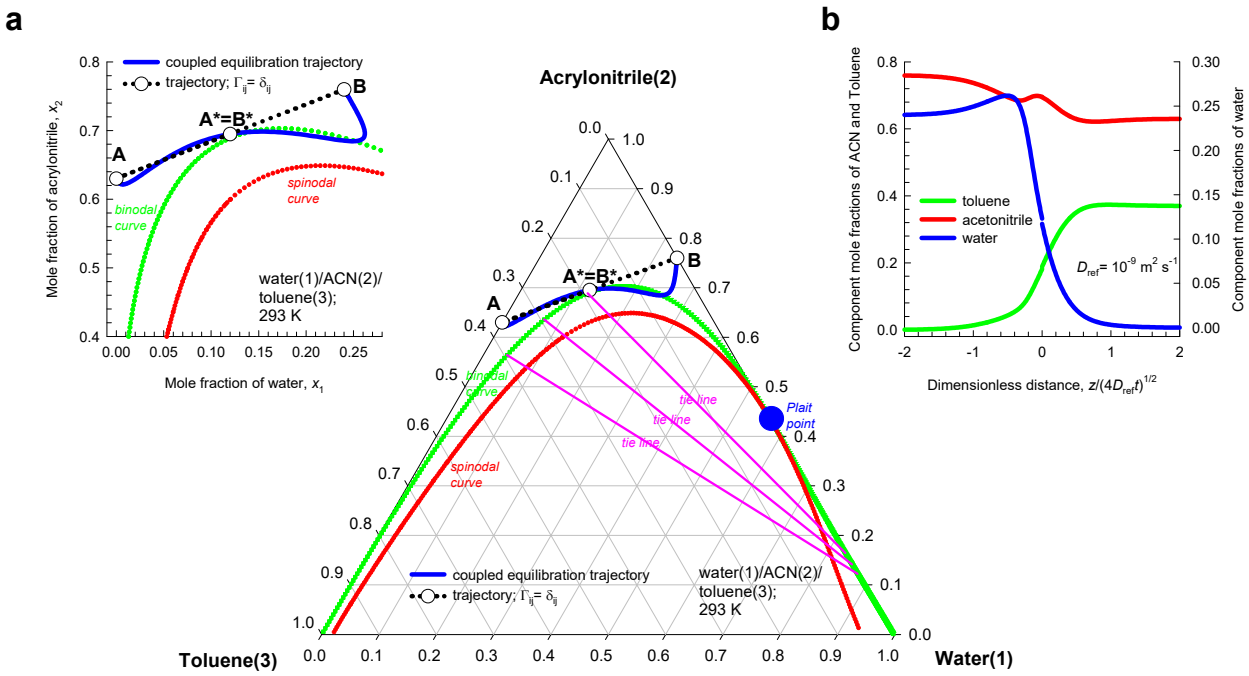

Figure S32. (a) Transient equilibration trajectories followed during equilibration of homogenous mixtures of two different compositions for the system water(1)/acetontrile(2)/toluene(3) at 293.15 K. (b) Transient composition profiles plotted as function of the dimensionless distance coordinate $\frac{z}{\sqrt{4D_{ref}t}}$.

The NRTL parameters for calculation of the phase equilibrium thermodynamics are provided in Table S17.

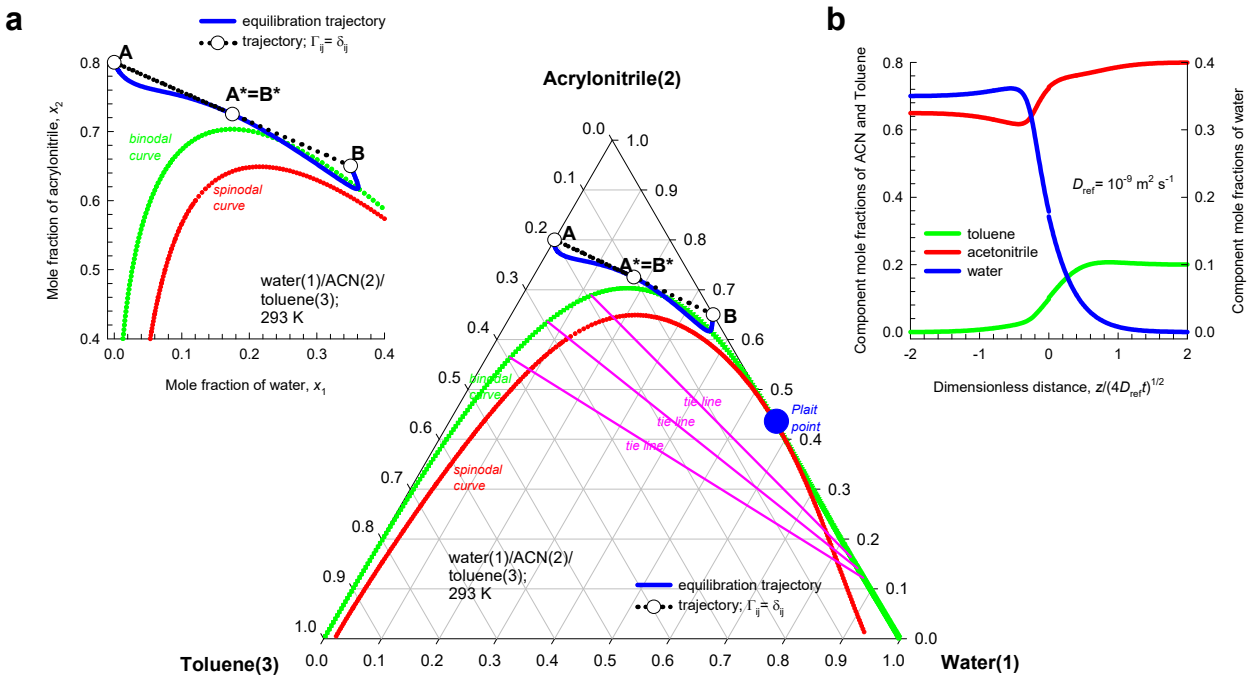

Figure S33. (a) Transient equilibration trajectories followed during equilibration of homogenous mixtures of two different compositions for the system water(1)/acetontrile(2)/toluene(3) at 293.15 K. (b) Transient composition profiles plotted as function of the dimensionless distance coordinate $\frac{z}{\sqrt{4D_{ref}t}}$.

The NRTL parameters for calculation of the phase equilibrium thermodynamics are provided in Table S17.

7 Nomenclature

Latin alphabet

a_i	component activity, dimensionless
$[B]$	matrix of inverse M-S coefficients, m^{-2} s
c_i	molar concentration of species *i*, mol m^{-3}
c_t	total molar concentration of mixture, mol m^{-3}
$Đ_{12}$	M-S exchange coefficient for binary mixture, m^2 s^{-1}
$Đ_{ij}$	M-S binary pair diffusivity, m^2 s^{-1}
$Đ_{ij}^V$	modified M-S diffusivity for binary penetrant pair *i*-*j*, m^2 s^{-1}
$Đ_{im}^V$	modified M-S diffusivity for penetrant *i* in polymer m, m^2 s^{-1}
$D_{i,self}$	self-diffusivity of species *i*, m^2 s^{-1}
D_{12}	Fick diffusivity for binary 1-2 mixture , m^2 s^{-1}
$[D]$	Fick diffusivity matrix, m^2 s^{-1}
$\lvert D \rvert$	Determinant of the Fick diffusivity matrix, m^4 s^{-2}
$\lvert D \rvert^{1/2}$	Square-root of determinant of $[D]$, m^2 s^{-1}
$[I]$	Identity matrix, dimensionless
j_i	mass diffusion flux of species *i* with respect to v, kg m^{-2} s^{-1}
J_i	molar diffusion flux of species *i* with respect to u, mol m^{-2} s^{-1}
J_i^V	volumetric diffusion fluxes with respect to u^V, mol m^{-2} s^{-1}
M_i	molar mass of species *i*, kg mol^{-1}
$\overline{M}$	mean molar mass of mixture, kg mol^{-1}

Nomenclature

n	number of species in the mixture, dimensionless
$[Q]$	two-dimensional square matrix, dimensionless
R	gas constant, 8.314 J mol^{-1} K^{-1}
t	time, s
T	absolute temperature, K
x_i	mole fraction of component *i* in bulk fluid phase, dimensionless
X_i	generalized composition variable, dimensionless
y_i	mole fraction of component *i* in bulk vapor phase, dimensionless
u	molar average mixture velocity, m s^{-1}
u^V	volume average mixture velocity, m s^{-1}
$u_2^L = \frac{\phi_2^L}{\phi_1^L + \phi_2^L}$	relative volume fractions in bulk liquid mixture, dimensionless
$u_2 = \frac{\phi_2}{\phi_1 + \phi_2}$	relative volume fractions in polymer phase, dimensionless
v	mass average mixture velocity, m s^{-1}
$\overline{V_i}$	partial molar volume of species *i,* m^3 mol^{-1}
$\overline{V}$	mean molar volume of mixture, m^3 mol^{-1}
z	direction coordinate, m

Greek alphabet

γ_i	activity coefficient of component *i*, dimensionless
$\varepsilon(t)$	position of moving boundary, m
δ_{ij}	Kronecker delta, dimensionless
Γ_{ij}	thermodynamic correction factors, dimensionless
$[\Gamma]$	matrix of thermodynamic factors, dimensionless

Nomenclature

$\lvert\Gamma\rvert^{1/2}$	Square-root of determinant of $[\Gamma]$, dimensionless
λ_i	eigenvalue of diffusivity matrix, $m^2\ s^{-1}$
$[\Lambda]=[B]^{-1}$	matrix of M-S diffusivities, $m^2\ s^{-1}$
$\lvert\Lambda\rvert^{1/2}$	Square-root of determinant of $[\Lambda]$, $m^2\ s^{-1}$
μ_i	molar chemical potential, J mol^{-1}
ϕ_i	volume fraction of penetrant *i* in polymer, dimensionless
ϕ_m	volume fraction of polymer, dimensionless
ϕ_i^L	volume fraction in bulk liquid mixture, dimensionless
ρ_i	mass density of component *i*, kg m^{-3}
χ	interaction parameter in Flory-Huggins model, dimensionless
ω_i	mass fraction of component *i*, dimensionless

Subscript

i	referring to component *i*
I	referring to the interface
m	refers to polymer
n	referring to component *n*
t	referring to total mixture

Superscript

mass	mass average reference velocity frame
V	volume average reference velocity frame

Nomenclature

Matrix notation

( )	column matrix
[ ]	square matrix

8 References

(1) PTC MathCad 15.0. http://www.ptc.com/, PTC Corporate Headquarters, Needham, 3 November 2015.

(2) Taylor, R.; Krishna, R. *Multicomponent mass transfer*. John Wiley: New York, 1993.

(3) Leahy-Dios, A.; Bou-Ali, M. M.; Platten, J. K.; Firoozabadi, A. Measurements of molecular and thermal diffusion coefficients in ternary mixtures. *J. Chem. Phys.* **2005**, *122*, 234502.

(4) Alimadadian, A.; Colver, C. P. A New Technique for the Measurement of Ternary Diffusion Coefficients in Liquid Systems. *Can. J. Chem. Eng.* **1976**, *54*, 208-213.

(5) Maxwell, J. C. On the dynamical theory of gases. *Phil. Trans. Roy. Soc.* **1866**, *157*, 49-88.

(6) Stefan, J. Über das Gleichgewicht und die Bewegung insbesondere die Diffusion von Gasgemengen. *Sitzber. Akad. Wiss. Wien.* **1871**, *63*, 63-124.

(7) Standart, G. L.; Taylor, R.; Krishna, R. The Maxwell-Stefan formulation of irreversible thermodynamics for simultaneous heat and mass transfer. *Chem. Eng. Commun.* **1979**, *3*, 277-289.

(8) Krishna, R.; Low, C. Y.; Newsham, D. M. T.; Olivera Fuentes, C. G.; Paybarah, A. Liquid Liquid Equilibrium in the System Glycerol Water Acetone at 25 ^{o}C. *Fluid Phase Equilib.* **1989**, *45*, 115-120.

(9) Krishna, R.; van Baten, J. M. Describing Diffusion in Fluid Mixtures at Elevated Pressures by Combining the Maxwell-Stefan Formulation with an Equation of State *Chem. Eng. Sci.* **2016**, *153*, 174-187.

(10) Tuan, D. Q.; Zollweg, J. A.; Rizvi, S. S. H. Concentration Dependence of the Diffusion Coefficient of Lipid in Supercritical Carbon Dioxide. *Ind. Eng. Chem. Res.* **1999**, *38*, 2787-2793.

(11) Krishna, R.; van Baten, J. M. The Darken relation for multicomponent diffusion in liquid mixtures of linear alkanes. An investigation using Molecular Dynamics (MD) simulations. *Ind. Eng. Chem. Res.* **2005**, *44*, 6939-6947.

(12) Krishna, R.; van Baten, J. M. Unified Maxwell-Stefan Description of Binary Mixture Diffusion in Micro- and Meso- Porous Materials. *Chem. Eng. Sci.* **2009**, *64*, 3159-3178.

(13) Wesselingh, J. A.; Bollen, A. M. Multicomponent diffusivities from the free volume theory. *Chem. Eng. Res. Des.* **1997**, *75*, 590-602.

(14) Krishna, R. Serpentine Diffusion Trajectories and the Ouzo Effect in Partially Miscible Ternary Liquid Mixtures. *Phys. Chem. Chem. Phys.* **2015**, *17*, 27428-27436.

(15) Krishna, R. Diffusing Uphill with James Clerk Maxwell and Josef Stefan. *Chem. Eng. Sci.* **2019**, *195*, 851-880. https://doi.org/10.1016/j.ces.2018.10.032.

(16) Wesselingh, J. A.; Krishna, R. *Mass transfer in multicomponent mixtures*. VSSD: Delft, 2000.

(17) Ribeiro, C. P.; Freeman, B. D. Sorption, Dilation, and Partial Molar Volumes of Carbon Dioxide and Ethane in Cross-Linked Poly(ethylene oxide). *Macromolecules* **2008**, *41*, 9458-9468.

(18) Ribeiro, C. P.; Freeman, B. D. Solubility and Partial Molar Volume of Carbon Dioxide and Ethane in Crosslinked Poly(ethylene oxide) Copolymer. *J. Polym. Sci.: Part B: Polym. Phys.* **2010**, *41*, 9458-9468.

(19) Mulder, M. H. V.; Franken, A. C. M.; Smolders, C. A. Preferential Sorpton versus Preferential Permeability in Pervaporation. *J. Membr. Sci.* **1985**, *22*, 155-178.

(20) Yang, T.-H.; Lue, S. J. Modeling Sorption Behavior for Ethanol/Water Mixtures in a Cross-linked Polydimethylsiloxane Membrane Using the Flory-Huggins Equation. *J. Macromol. Sci., Part B: Phys* **2013**, *52*, 1009-1029.

(21) Varady, M. J.; Pearl, T. P.; Stevenson, S. M.; Mantooth, B. A. Decontamination of VX from Silicone: Characterization of Multicomponent Diffusion Effects. *Ind. Eng. Chem. Res.* **2016**, *55*, 3139-3149.

(22) Vrentas, J. S.; Duda, J. L. Molecular diffusion in polymer solutions. *A.I.Ch.E.J.* **1979**, *25*, 1-24.

(23) Price, P. E.; Romdhane, I. H. Multicomponent Diffusion Theory and Its Applications to Polymer-Solvent Systems. *A.I.Ch.E.J.* **2003**, *49*, 309-322.

(24) Bearman, R. J. On the Molecular Basis of some Current Theories of Diffusion. *J. Phys. Chem.* **1961**, *65*, 1961-1968.

(25) Wesselingh, J. A.; Bollen, A. M. Multicomponent Diffusivities from the Free Volume Theory. *Trans. Inst. Chem. Eng.* **1997**, *75, Part A*, 590-602.

(26) Wilke, C. R.; Chang, P. Correlation of Diffusion Coefficients in Dilute Solutions. *A.I.Ch.E.J.* **1955**, *1*, 264-270.

(27) Reid, R.C.; Prausnitz, J. M.; Poling, B. E. *The Properties of Gases and Liquids*. 4th Edition, McGraw-Hill: New York, 1986.

(28) Zielinski, J. M. A Friction Factor Analysis of the Coupling between Polymer/Solvent Self- and Mutual-Diffusion: Pol ystyrene/Toluene. *J. Polym. Sci.: Part B: Polym. Phys.* **1996**, *24*, 2759-2766.

(29) Verros, G. D.; Malamataris, N. A. Estimation of Diffusion Coefficients in Acetone-Cellulose Acetate Solutions. *Ind. Eng. Chem. Res.* **1999**, *38*, 3572-3580.

(30) Alsoy, S.; Duda, J. L. Modeling of Multicomponent Drying of Polymer Films. *A.I.Ch.E.J.* **1999**, *45*, 896-905.

(31) Brun, J.-P.; Larchet, C.; Melet, R.; Bulvestre, G. Modelling of the Pervaporation of Binary Mixtures through Moderately Swelling, Non-Reacting Membranes. *J. Membr. Sci.* **1985**, *23*, 257-283.

(32) Ribeiro, C. P.; Freeman, B. D.; Paul, D. R. Modeling of Multicomponent Mass Transfer across Polymer Films using a Thermodynamically Consistent Formulation of the Maxwell-Stefan Equations in terms of Volume Fractions. *Polymer* **2011**, *52*, 3970-3983.

(33) Vrentas, J. S.; Vrentas, C. M. Restrictions on Friction Coefficients for Binary and Ternary Diffusion. *Ind. Eng. Chem. Res.* **2007**, *46*, 3422-3428.

(34) Zielinski, J. M.; Hanley, B. F. Practical Friction-Based Approach to Modeling Multicomponent Diffusion. *A.I.Ch.E.J.* **1999**, *45*, 1-12.

(35) Cussler, E. L.; Lightfoot, E. N. Multicomponent Diffusion Involving High Polymers. I. Diffusion of Monodisperse Polystyrene in Mixed Solvents. *J. Phys. Chem.* **1965**, *69*, 1135-1144.

(36) Strathmann, H.; Kock, K. The Formation Mechanism of Phase Inversion Membranes. *Desalination* **1977**, *21*, 2411-2255.

(37) Radovanovic, P.; Thiel, S. W.; Hwang, S.-T. Formation of asymmetric polysulfone membranes by immersion precipitation. Part I. Modelling mass transport during gelation. *J. Membr. Sci.* **1992**, *65*, 213-229.

(38) Radovanovic, P.; Thiel, S. W.; Hwang, S.-T. Formation of asymmetric polysulfone membranes by immersion precipitation. Part II. The effects of casting solution and gelation bath compositions on membrane
structure and skin formation. *J. Membr. Sci.* **1992**, *65*, 231-246.

(39) Reuvers, A. J.; van den Berg, J. W. A.; Smolders, C. A. Formation of membranes by means of immersion precipitation Part II. The mechanism of formation of membranes prepared from the system cellulose acetate - acetone - water. *J. Membr. Sci.* **1987**, *34*, 45-65.

(40) Reuvers, A. J.; Smolders, C. A. Formation of membranes by means of immersion precipitation Part II. The mechanism of formation of membranes prepared from the system cellulose acetate - acetone - water. *J. Membr. Sci.* **1987**, *34*, 67-86.

(41) van den Berg, G. B.; Smolders, C. A. Diffusional phenomena in membrane separation processes. *J. Membr. Sci.* **1992**, *73*, 103-118.

(42) Tsay, C. S.; McHugh, A. J. Mass Transfer Modeling of Asymmetric Membrane Formation by Phase Inversion. *J. Polym. Sci.: Part B: Polym. Phys.* **1990**, *28*, 1327-1365.

(43) van de Witte, P.; Dijkstra, P. J.; van den Berg, J. W. A.; Feijen, J. Phase separation processes in polymer solutions in relation to membrane formation. *J. Membr. Sci.* **1996**, *117*, 1-31.

(44) Guillen, G. R.; Yinjin Pan, Y.; Li, M.; Hoek, E. V. Preparation and Characterization of Membranes Formed by Nonsolvent Induced Phase Separation: A Review. *Ind. Eng. Chem. Res.* **2011**, *50*, 3798-3817.

(45) Wang, D.-M.; Lai, J.-Y. Recent advances in preparation and morphology control of polymeric membranes formed by nonsolvent induced phase separation. *Curr. Opin. Chem. Eng.* **2013**, *2*, 229-237.

(46) Krishna, R. Describing Mixture Permeation across Polymeric Membranes by a Combination of Maxwell-Stefan and Flory-Huggins Models. *Polymer* **2016**, *103*, 124-131.

(47) Krishna, R. Using the Maxwell-Stefan formulation for Highlighting the Influence of Interspecies (1-2) Friction on Binary Mixture Permeation across Microporous and Polymeric Membranes. *J. Membr. Sci.* **2017**, *540*, 261-276. https://doi.org/10.1016/j.memsci.2017.06.062.

(48) Krishna, R. Highlighting Diffusional Coupling Effects in Ternary Liquid Extraction and Comparisons with Distillation. *Ind. Eng. Chem. Res.* **2016**, *55*, 1053-1063.

(49) Altinkaya, S. A.; Ozbas, B. Modeling of Asymmetric Membrane Formation by Dry-casting Method. *J. Membr. Sci.* **2004**, *230*, 71-89.

(50) Grossmann, T.; Winkelmann, J. Ternary Diffusion Coefficients of Glycerol + Acetone + Water by Taylor Dispersion Measurements at 298.15 K. *J. Chem. Eng. Data* **2005**, *50*, 1396-1403.

(51) Tsay, C. S.; McHugh, A. J. An Improved Numerical Algorithm for Ternary Diffusion with a Moving Interface. *Chem. Eng. Sci.* **1991**, *46*, 1179-1187.

(52) Crank, J. *The Mathematics of Diffusion*. 2nd Edition, Clarendon Press: Oxford, 1975.

(53) Krishna, R. Uphill Diffusion in Multicomponent Mixtures. *Chem. Soc. Rev.* **2015**, *44*, 2812-2836.

(54) Materials for Separation Technologies: Energy and Emission Reduction Opportunities. U.S. Department of Energy, Energy Efficiency and Renewable Energy, 2005.

(55) Tkacik, G.; Zeman, L. Component Mobility Analysis in the Membrane-Forming System Water/N-methyl-2-pyrrolidone/Polyethersulfone. *J. Membr. Sci.* **1987**, *31*, 273-288.

(56) Altena, F. W.; Smolders, C. A. Calculation of Liquid-Liquid Phase Separation in a Ternary System of a Polymer in a Mixture of a Solvent and a Nonsolvent. *Macromolecules* **1982**, *15*, 1491-1497.

(57) Yip, Y.-L. *Modeling of dry-casting and non-solvent vapor induced phase separation*. Theses and Dissertations, Lehigh University, Lehigh, 2005. http://preserve.lehigh.edu/cgi/viewcontent.cgi?article=1888&context=etd

(58) Matsuyama, H.; Teramoto, M.; Nakatani, R.; Maki, T. Membrane Formation via Phase Separation Induced by Penetrationof Nonsolvent from Vapor Phase. I. Phase Diagram and Mass Transfer Process. *J. Appl. Polymer Sci.* **1999**, *74*, 159-170.

(59) Kim, J. Y.; Lee, H. K.; Baik, K. J.; Kim, S. C. Liquid–Liquid Phase Separation in Polysulfone/Solvent/Water Systems. *J. Appl. Polymer Sci.* **1997**, *65*, 2643-2653.

(60) Fernandes, G. R.; Pinto, J. C.; Nobrega, R. Modeling and Simulation of the Phase-Inversion Process During Membrane Preparation. *J. Appl. Polymer Sci.* **2001**, *82*, 3036-3051.

(61) Miller, C. A. Spontaneous Emulsification Produced by Diffusion - A Review. *Colloids Surf.* **1988**, *29*, 89-102.

(62) Sitnikova, N. L.; Sprik, R.; Wegdam, G.; Eiser, E. Spontaneously Formed trans-Anethol/Water/Alcohol Emulsions: Mechanism of Formation and Stability. *Langmuir* **2005**, *21*, 7083-7089.

(63) Vitale, S. A.; Katz, J. L. Liquid Droplet Dispersions Formed by Homogeneous Liquid-Liquid Nucleation: “The Ouzo Effect”. *Langmuir* **2003**, *19*, 4105-4110.

(64) Ganachaud, F.; Katz, J. L. Nanoparticles and Nanocapsules Created Using the Ouzo Effect: Spontaneous Emulsification as an Alternative to Ultrasonic and High-Shear Devices *ChemPhysChem* **2005**, *6*, 209-216.

(65) Ruschak, K. J.; Miller, C. A. Spontaneous Emulsification in Ternary Systems with Muss Transfer. *Ind. Eng. Chem., Fundam.* **1972**, *11*, 534-540.

(66) Jackson, R. Diffusion in Ternary Mixtures with and without Phase Boundaries. *Ind. Eng. Chem., Fundam.* **1977**, *16*, 304-306.

(67) Krishna, R.; Low, C. Y.; Newsham, D. M. T.; Olivera-Fuentes, C. G.; Standart, G. L. Ternary mass transfer in liquid-liquid extraction. *Chem. Eng. Sci.* **1985**, *40*, 893-903.

(68) Califano, F.; Mauri, R. Retardation of the Phase Segregation of Liquid Mixtures with a Critical Point of Miscibility. *A.I.Ch.E.J.* **2018**, *64*, 4047-4052.

(69) Pertler, M. *Die Mehrkomponenten-Diffuson in nicht vollständig mischbaren Flüssigkeiten*. Technische Universität München, München, 1996.

(70) Othmer, D. F.; Ku, P. L. Solubility Data for Ternary Liquid Systems. Acetic Acid and Formic Acid Distributed between Chloroform and Water. *J. Chem. Eng. Data* **1960**, *5*, 42-44.

(71) Resa, J. M.; Goenaga, J. M. Liquid-Liquid Equilibrium Diagrams of Ethanol + Water + (Ethyl Acetate or 1-Pentanol) at Several Temperatures. *J. Chem. Eng. Data* **2006**, *51*, 1300-1305.

(72) Fahim, M. A.; Al-Muhtaseb, S. A.; Al-Nashef, I. M. Liquid-Liquid Equilibria of the Ternary System Water + Acetic Acid + 1-Hexanol. *J. Chem. Eng. Data* **1997**, *42*, 183-186.

(73) Zhang, H.; Wang, T. Measurement and Correlation of Liquid-Liquid Equilibrium Data for Water + Acetic Acid + Methyl tert-Butyl Ether + NaCl. *J. Chem. Eng. Data* **2009**, *54*, 945-949.

(74) Springer, P. A. M.; Baur, R.; Krishna, R. Composition trajectories for heterogeneous azeotropic distillation in a bubble-cap tray column: Influence of mass transfer. *Chem. Eng. Res. Des.* **2003**, *81*, 413-426.

(75) Di Cave, S.; Mazzarotta, B. Liquid-Liquid Equilibria for Ternary Systems Formed by Acetonitrile, Water, and Aromatic Hydrocarbons. *J. Chem. Eng. Data* **1991**, *36*, 298-303.